DEVELOPMENT OF FLAX FIBER-REINFORCED POLYETHYLENE BIOCOMPOSITES BY INJECTION MOLDING

A Thesis Submitted to the College of Graduate Studies and Research

in Partial Fulfillment of the Requirements

for the Degree of Doctor of Philosophy

in the Department of Agricultural and Bioresource Engineering

University of Saskatchewan

Saskatoon, Canada

By

Xue Li

PERMISSION TO USE

In presenting this thesis in partial fulfillment of the requirements for a Postgraduate degree from the University of Saskatchewan, the author has agreed that the Libraries of this University may make it freely available for inspection. The author has further agreed that permission for copying of this thesis in any manner, in whole or in part, for scholarly purposes may be granted by the professor or professors who supervised the thesis work recorded here or, in their absence, by the Head of the Department or the Dean of the College in which the thesis work was done. It is understood that any copying or publication or use of this thesis or parts thereof for financial gain shall not be allowed without the author's written permission. It is also understood that due recognition shall be given to the author and to the University of Saskatchewan in any scholarly use which may be made of any material in this thesis.

Requests for permission to copy or to make other use of material in this thesis in whole or part should be addressed to:

Head of the Department of Agricultural and Bioresource Engineering
University of Saskatchewan
Saskatoon, Saskatchewan
Canada S7N 5A9

ABSTRACT

Flax fiber-reinforced plastic composites have attracted increasing interest because of the advantages of flax fibers, such as low density, relatively high toughness, high strength and stiffness, and biodegradability. Thus, oilseed flax fiber derived from flax straw, a renewable resource available in Western Canada, is recognized as a potential replacement for glass fiber in composites. Among plastics, polyethylene is a suitable material for use as a matrix in composites. However, there are not many studies in this area. Therefore, the main goal of this research was to develop flax fiber-polyethylene (PE) biocomposites via injection molding and investigate the effect of material properties and processing parameters on their properties.

Alkali, silane, potassium permanganate, sodium chlorite, and acrylic acid treatments were employed to flax fiber to decrease the hydrophilic of fiber and improve the adhesion between the fiber and the matrix. All chemically treated fiber-HDPE biocomposites had higher tensile strength and lower water absorption compared with non-chemically treated ones. Acrylic acid treatment of the fiber resulted in slight increase in its degradation temperature; using this treated fiber resulted in biocomposites with the best performance. Therefore, the morphological, chemical, and thermal properties of acrylic acid treated fiber were also studied.

Linear Low Density Polyethylene (LLDPE) and High Density Polyethylene (HDPE) were the main matrices investigated in this research. Showing a high tensile strength and similar water absorption, HDPE was used as the matrix in further research. Flax fiber with 98-99% purity was chosen as reinforcement since the flax shive mixed

with the fiber decreased the tensile and flexural properties but increased the water absorption of the biocomposite.

Acrylic acid-treated fiber-HDPE biocomposites had been developed through injection molding under different processing conditions. Increasing the fiber content of biocomposite increased its tensile and flexural strengths, especially flexural modulus, but its water absorption capacity also increased. It was possible to improve the mechanical properties of biocomposites and decrease the water absorption by adjusting injection temperature and pressure. Injection temperature had more influence on the quality of the biocomposite than injection pressure. Injection temperature lower than 195°C was recommended to achieve good composite quality.

Melts of HDPE and flax fiber-HDPE biocomposites were categorized as power-law fluids. Apparent viscosity, consistency coefficient, and flow behavior index of biocomposites were determined to study their flow behavior. The statistical relationship of these parameters with temperature and fiber content were modeled using the SAS and SPSS softwares. The injection filling time was related to the material rheological properties: biocomposites required longer filling time than pure HDPE. Low injection temperature also resulted in long filling time.

The thermal conductivity, thermal diffusivity, and specific heat of biocomposites containing 10, 20, and 30% fiber by mass were determined in the processing temperature range of 170 to 200°C. Fiber content showed a significant influence on the thermal properties of the biocomposites. The predicted minimum cooling time increased with the thickness of the molded material, mold temperature, and injection temperature, but it decreased with the ejection temperature.

ACKNOWLEDGEMENTS

I would like to express my heartfelt gratitude and appreciation to my supervisor, Dr. Lope G. Tabil, for his guidance, support, patience and encouragement during my graduate study. I would also like to acknowledge my co-supervisor Dr. Satya Panigrahi, for his generous support and scientific advices, as well as his understanding in every phase of this research.

Sincere thanks to other professors in my Graduate Advisory Committee, Drs. Ike Oguocha, Huiqing Guo, and Venkatesh Meda, for their time and valuable comments and suggestions for this thesis and through my whole Ph.D program studies. Thank you to Dr. Kurt Rosentrater for serving as external examiner of my Ph.D thesis.

Appreciation also goes to Bill Crerar, Toni Schleicher, Anthony Opoku, Louis Roth, faculty and staff in the Department of Agricultural and Bioresource Engineering; Mr. Doug Hassard in the Department of Plant Science; previous students Bei Wang and Shahram Emami; and everyone in the bioprocessing group of the Department of Agricultural and Bioresource Engineering. Without your help, I could not finish this thesis.

I acknowledge the financial support from Saskatchewan Flax Development Council, Saskatchewan Agriculture and Food Research Chair in Agricultural Material Utilization and Bioprocess Engineering, Agriculture Development Fund of Saskatchewan Agriculture, Saskatchewan Agri-Food Innovation Fund, Natural Sciences and Engineering Research Council of Canada and Agriculture and Agri-Food Canada. I

also would like to acknowledge the Departments of Mechanical Engineering, Civil Engineering, Electrical Engineering, Plant Science, and Biology at the University of Saskatchewan and the Northern Alberta Institute of Technology (NAIT) and the Centre for Agri-Industrial Technology (CAIT) in Edmonton, AB, Saskatchewan Research Council (SRC), and Norwesco Canada Ltd., Saskatoon for the use of their facilities and equipment.

This thesis could not have happened without the love and consistent encouragement from my beloved parents and my sister. Thanks to my colleagues and all my friends, both inside and outside of the Department of Agricultural and Bioresource Engineering.

TABLE OF CONTENTS

LIST OF TABLES

LIST OF FIGURES

NOMENCLATURE

A = acrylic acid treated

A = cross-sectional area (m^2)

A_0 = the cross sectional area of the sprue (m^2)

A_1 = the cross sectional area of the runner (m^2)

A_2 = the cross sectional area of the gate in the mold (m^2)

$A_3 = A_4$ = the cross sectional area of the mold cavity (m^2)

A_p = cross-sectional area of the plunger (m^2)

ADL = acid detergent Lignin (% dry matter)

ADF = acid detergent fiber (% dry matter)

B = the plate thickness (m)

b = width of specimen (m)

C = sodium chlorite treated

C = calibration coefficient

C_{ff} = coefficient of energy loss due to pipe fittings

C_{fc} = coefficient of energy loss due to sudden contraction

C_{fe} = coefficient of energy loss due to sudden expansion

C_p = specific heat (kJ/kg°C)

D = the pipe diameter/the diameter of the sprue and runner (m)

d = thickness of specimen (m)

d_c = capillary diameter (0.05 in)

d_b = barrel diameter (0.375 in or 0.9525cm)

E_H = modulus of elasticity in bending (Pa)

E_f = the energy lost due to friction (m^2/s^2)

E_c = the energy supplied by pump (m^2/s^2)

E_{major} = energy loss due to viscous liquid in the straight portions of a pipe (Pa)

E_{minor} = energy loss due to various components used in pipeline systems (Pa)

E_{ff} = energy losses due to pipe fittings (include elbows, tees, and values) (Pa)

E_{fc} = energy losses due to sudden contraction (Pa)

E_{fe} = energy losses due to sudden expansion (Pa)

F_{max} = the maximum peak load (N)

F = fiber content

F' = force acting on the plunger (kgf or lbf)

f = friction factor

g = the gravity (m/s^2)

g' = body force vector

H = the height of rectangular part of the mold (m)

HF_{sample} = heat flow rate measured from the sample test (J/s)

HF_{blank} = heat flow rate measured from the blank test (J/s)

h = half the thickness of mold cavity (m)

I = electric current (A)

K = consistency coefficient ($Pa \cdot s^n$)

k = thermal conductivity (W/m°C)

k' = thermal conductivity before calibration (W/m°C)

k_w = thermal conductivity of water from reference (W/m°C)

k_w' = thermal conductivity of measured agar-gelled water (W/m°C)

k_m = thermal conductivity of the matrix (W/m°C)

k_f = thermal conductivity of the fiber (W/m°C)

L = length (m)

L_0 = original measured length (m)

l_c = length of capillary tube (1.0063 in)

m = mass (g)

$\dot{m}$ = flow rate (kg/s or g/s)

M_f = mass fraction of flax fiber (g)

M_m = mass fraction of matrix (g)

$M\%$ = water absorption (%)

M_0 = initial weight (g)

M_1 = the weight of sample after water immersion (g)

N_{Re} = Reynolds number

NDF = neutral detergent fiber (% dry matter)

N = alkali treated

n = flow behavior index

P = potassium permanganate treated

P = pressure or injection pressure (Pa)

P' = load (N)

P_0 = the pressure in the sprue (MPa)

P_1 = the pressure at the end of the sprue (MPa)

P_2 = the pressure at the gate (MPa)

P_3 = the pressure at the beginning of mold cavity (MPa)

P_4 = the pressure at the end of mold cavity (MPa)

P_I = pressure reading after pressurizing the reference volume (psi)

P_{II} = pressure reading after including V_C (psi)

Q = material volume flow rate (m^3/s)

Q '= heat input per meter of line source (W/m)

q' = heat flux vector

R = the radius of cylinder (m)

R' = specific resistance of the heating wire (Ohms/m)

r = radius (m)

S = silane treated

S = flexural strength (Pa)

$\dot{S}$ = rate of heat generation due to chemical reaction (kw/m^3)

SD_α = standard deviation of thermal diffusivity

SD_k = standard deviation of thermal conductivity

SD_ρ = standard deviation of density

SD_{Cp} = standard deviation of specific heat

s = slope of the tangent to the initial straight-line portion in load-deflection curve (N/m)

T = temperature or injection temperature (°C)

T_w = mold wall temperature (°C)

T_m = melt temperature also known as injection temperature (°C)

T_e = ejection temperature (°C)

t_c = minimum cooling time during injection molding (s)

t_1 = time of material to fill the sprue and runner (s)

t_3 = time of material to fill the mod cavity (s)

t = time (s)

U = untreated/non-chemical treated (fiber)

u = velocity/flow speed (m/s)

u' = velocity vector

u_0 = the flow velocity in the sprue (m/s)

u_1 = the flow velocity at the end of the sprue (m/s)

u_2 = the flow velocity at the gate (m/s)

u_3 = the flow velocity at the beginning of mold cavity (m/s)

u_4 = the flow velocity at the end of mold cavity (m/s)

$\bar{u}$ = the average velocity (m/s)

υ = specific volume (m^3/kg)

V = volume of sample (cm^3)

V_C = volume of sample cell (cm^3)

V_R = reference volume (cm^3)

V_f = the volume fraction of the fiber

V_{xh} = crosshead speed (in/min)

W = the width of rectangular part of the mold (m)

X = the length of the mold cavity (m)

x = the distance of material in flow direction (m)

z = the height (m)

ρ = density (kg/m^3 or g/cm^3)

ρ_f = density of flax fiber (g/cm^3)

ρ_m = density of matrix (g/cm^3)

ρ_c = density of the composite (g/cm^3)

ρ_i = ideal density (g/cm^3)

$\rho_{measured}$ = measured density (g/cm^3)

$\rho_{deviation}$ = density deviation

α = thermal diffusivity of material (m^2/s)

γ = shear rate (s^{-1})

τ = shear stress (Pa)

τ_w = the shear stress at wall (Pa)

$\underline{\underline{\tau}}$ = second-order deviatoric stress tensor

σ_t = tensile strength (Pa)

μ = viscosity (Pa·s)

μ_a = apparent viscosity (Pa·s)

$\frac{du}{dy}$ = velocity gradient or shear rate in the direction perpendicular to the layers (m/s).

$\frac{dT}{dt}$ = heating rate (K/s)

1. INTRODUCTION AND OBJECTIVES

Fiber-reinforced composites have been used in aerospace, automotive, plastics, and other industries (Mallick 1988) because they could offer either comparable to or better strengths than traditional pure polymer materials. The traditional fibers in commercial use are various types of glass, carbon, aluminum oxide, boron fibers, etc. In recent years, research on the replacement of man-made fibers with natural fibers as reinforcement in plastic composites has increased dramatically. This is because natural fiber has the advantage of lower density, lower price, non-toxic, and environmentally friendly over man-made fiber (Mohanty et al. 2003; Van de Velde and Kiekens 2002). There are many works in the literature reporting the use of cellulosic fibers such as sisal, jute, flax, hemp, henequen, and others in composites as reinforcements (Fung 2003a; Keller 2003; Garkhail et al. 2000; Herrera-Franco et al. 1997; Karmaker and Youngquist 1996). Natural fiber-reinforced composites, also referred to as biocomposites, could be used in the plastics industry, automobile, and packaging industries to cut material costs (Bledzki and Gassan 1999). Some of their potential applications in this field are door and instrument panels, package trays, glove boxes, arm rests, and seat backs (Pervaiz and Sain 2003).

The most suitable reinforcements for biocomposite among natural fibers are the bast (bark) fibers, e.g. flax fiber and hemp fibers. Flax fibers have been used as the reinforcement in composites in Germany (Van de Velde and Kiekens 2002) and the United Kingdom (Sankari 2000). Canada is one the largest flaxseed producing countries

in the world. More than half of all Canadian seed flax is produced in Saskatchewan, with the remaining grown in Manitoba and Alberta (Warick 2001). But the utilization of flax fiber in biocomposites in Canada is not as developed as in Europe. The Flax Canada Steering Committee is developing and implementing a long-range strategy called 'Flax Canada 2015' to gain five million acres of flax crop by 2015 and provide a farm gate value of $1.5 billion (Fitzpatrick 2006). With the huge amount of seed flax production each year, more flax straw is left in the fields and burned by farmers because flax stalk requires a much longer time to degrade than many other agricultural residues (Anthony 2001). Therefore, studies on developing products from flax straw or flax fiber by-product will benefit both the plastic industries and Canadian flax growers.

Thermoset, thermoplastic starch, and polyolefines (polyethylene and polypropylene) are all matrix materials for natural-fiber reinforced composites. Polypropylene is the most common matrix studied in biocomposites because of its low cost, unproblematic ecological recycling, and good heat resistance (Rosato et al. 2000). Although polyethylene has suitable characteristics as a matrix in natural fiber-reinforced composites (Van de Velde and Kiekens 2001) compared with polypropylene, studies on polyethylene being used as a matrix still need to be developed. Polyethylene has a very low glass transition temperature (T_g= -110°C) associated with a good retention of mechanical properties, including flexibility and impact resistance at low temperatures (Charrier 1991), which makes it a competitive material as a matrix.

In the past, natural fiber composites were made by hand, making it highly labor-intensive work and difficult to be introduced to the industry. Nowadays, modern manufacturing techniques are used to make natural fiber-reinforced composite involving extrusion, rotational molding, compression molding, injection molding, and many others.

Injection molding is a widely used molding technique in polymer and plastic processing. Compared with other molding processes, it has the advantages of fast cycle times, molding accuracy, relatively low labor of large scale production runs, and a wide range of products (Rosato et al. 2000). There are many researchers who studied injection molding to process natural fiber-reinforced composites (Bakar et al. 2003, Mohanty et al. 2003a, Keller 2003). However, reports on how parameters and factors of injection molding influence the properties of biocomposites are very limited (Saint et al. 2003; Fung et al. 2003a), especially on flax fiber-polyethylene biocomposites. To understand the processing and optimize injected biocomposite properties, it is necessary to study the operation of injection molding for flax fiber-polymer composites.

The overall goal of this research is to develop an effective method of processing flax fiber-reinforced polyethylene biocomposites by using injection molding, and to study the factors that influence the processing of composite and its properties. Thus, this research mainly focuses on how to manufacture biocomposites by injection molding and how biocomposite properties are influenced by injection molding. The specific objectives are:

a) to process flax fiber-polyethylene biocomposite via injection molding and determine the basic procedure of processing;
b) to determine the appropriate chemical method for flax fiber pre-treatment to improve the bonding between fiber and matrix and increase the qualities of biocomposites;
c) to compare and choose appropriate flax fiber as reinforcement and polyethylene as matrix in the biocomposites;
d) to investigate how fiber content influences the biocomposite properties;

e) to investigate how factors including temperature and pressure affect the injection molding process and biocomposite properties;

f) to investigate the rheology and thermal properties of biocomposites and thereby understand the basic mechanisms of injection molding, and predict filling time and cooling time during injection molding.

To achieve these objectives, flax fibers from same field but with different purity, plus polyethylene were studied as materials and they were processed to biocomposites via injection molding. To optimize the processing, the experiments were designed in four parts. Firstly, chemical treatments were applied on flax fibers to modify fiber surface and improve the bonding between fiber and polyethylene. Secondly, different grades of flax fibers and polyethylene were compared to be chosen as materials. Thirdly, the factors that affect biocomposite properties including fiber content and injection temperature and pressure were studied to understand the basic factors of injection molding. Finally, due to the complexity of injection molding, the rheology and thermal properties of biocomposites were studied to predict the filling time and cooling time during injection molding under a simplified mold.

The literatures related with this research are reviewed in Chapter 2. Chapter 3 is the materials and methods, including the detailed description on how the experiments were conducted and how the properties were tested. The results are presented and discussed in Chapter 4. Chapters 5 and 6 give the summary, conclusions, and the suggestions for further research. Statistical analysis, some detailed experimental data, as well as theory background on predicting equation of filling time are given in the Appendixes.

2. LITERATURE REVIEW

This chapter reviews the material properties including reinforced material-flax fiber and plastic matrix-polyethylene as well as mechanical and thermal properties of natural fiber reinforced plastic composites. Manufacturing methods of biocomposites, especially injection molding technique are discussed. The basic background of flow behavior and mechanism related with injection molding are introduced.

2.1 Material properties

The major constituents of flax fiber-reinforced plastics composite are flax fiber as the reinforcement and plastic polymer as matrix.

2.1.1 Properties of natural fibers

Natural fibers, especially bast (bark) fibers, such as flax, hemp, jute, henequen, and many others were investigated by some researchers as fiber reinforcement for composites in recent years (Singleton et al. 2003; Keller 2003; Valadez-Gonzalez et al .2003; Oksman et al. 2003). Advantages of natural fibers over man-made fibers include low density, low cost, recyclability and biodegradablility. These advantages make natural fibers potential replacement for glass fibers in composite materials.

Flax (*Linum usitatissimum*) is an annual crop used both for fiber and its edible seed. Two general types of flax are grown – fiber flax and seed flax. Fiber flax is grown

for the use of its fiber and primarily grown in Europe and Asia (Berglund and Zollinge 2002). Seed flax is grown for the oil in its seed. Canada produces seed flax. The stalk from seed flax consists of fiber bundles located between the epidermis (bark surface) and an inner woody core (shive) (Anthony 2001).

The major natural fiber components are cellulose, hemicellulose, lignin, pectin, waxes, and water soluble substances. Lignin and pectin act mainly as bonding agents. The composition of flax fibers and other natural fibers is shown in Table 2.1. The chemical properties of fibers are influenced by plant growth time, botanical classification of fiber, and even stalk height. Thus, the composition may differ even for the same kind of fiber.

Table 2.1 Chemical composition of natural fiber (Baley 2002; Mohanty et al. 2001; Rowell et al. 1997).

Type of fiber	Cellulose (%)	Hemi-cellulose (%)	Pectin (%)	Lignin (%)	Wax (%)
Bast fiber					
Fiber flax	64.1-71.0	11.0-20.6	1.8-2.3	2.0-2.9	1.5
Seed flax	43.0-47.0	24.0-26.0		21.0-23.0	
Kenaf	31.0-57.0	15.0-19.0	21.5-23.0		2.0-5.0
Jute	45.0-71.5	12.0-26.0	13.6-21.0	0.2	0.5-2.0
Hemp	57.0-77.0	3.7-13.0	14.0-22.4	0.9	0.8
Ramie	68.6-91.0	0.6-0.6	5.0-16.7	1.9	
Core fiber					
Kenaf	37.0-49.0	15.0-21.0	18.0-24.0		2.0-4.0
Jute	41.0-48.0	21.0-24.0	18.0-22.0		0.8
Leaf fiber					
Sisal	47.0-78.0	7.0-11.0	10.0-24.0	10.0	0.6-1.0
henequén	77.6	13.1	4.0-8.0		

Cellulose is a hydrophilic glucan polymer of D-glucopyranose units, which are linked together by β-(1-4)-glycosidic bonds (Rowell et al. 1997). The large amount of hydroxyl group in cellulose gives natural fiber hydrophilic properties when used to

reinforce hydrophobic plastic matrices; the result is a poor interface and resistance to moisture absorption (Alvarez et al. 2003). The hemicellulosic and pectic materials play important roles in fiber bundle integration and fiber bundle strength and individual fiber strength. Hemicellulosic polymers are branched, fully amorphous, and have a significantly lower molecular weight than cellulose. Because of its open structure containing many hydroxyl and acetyl groups, hemicellulose is partly soluble in water and hygroscopic (Wallenberger and Weston 2004). "Lignins are amorphous, highly complex, mainly aromatic polymers of phenylpropane units" (Rowell et al. 1997). But lignins have the least water sorption among the natural fiber components (Wallenberger and Weston 2004). Flax fibers are low in lignin content, but flax shives approaches close to that of the wood species (Sain and Fortierb 2002).

Although natural fiber cannot achieve as high as mechanical properties of glass fibers, it was reported that flax fibers exhibited very good mechanical properties compared to other natural plant fibers (Table 2.2). This, together with good availability and competitive price, makes flax fiber promising for future use as fiber reinforcement in biocomposites. In natural fibers, strength usually increases with moisture content and decreases with temperature, whereas, the Young's modulus decreases as water is absorbed (Baley 2002). Defects ('nodes' or 'dislocations') in fibers are often the break points during a tensile test and may influence the mechanical properties (Davies and Bruce 1998).

Flax fiber has a true density of 1.53 to 1.54 g/cm^3 (Baley 2002; Batra 1998). "Elementary flax fibers are assembled into bundles of 10 to 40 fibers maintained together by pectin" and exhibit a polygonal shape with 5 to 7 sides (Baley 2002). One general feature of flax fibers is their non-uniform geometrical characteristics. The fibers

are thicker near the root and become thinner nearer the tip. On average, a flax fiber is 19 μm in width and 33 mm in length (Baley 2002). However, the transverse and the longitudinal dimensions of flax fiber could be in the range of 5–76 μm and 4–77 mm, respectively, showing a wide distribution of the geometrical dimensions (Baley 2002).

Table 2.2 Mechanical properties of natural fibers compared with conventional reinforcing fibers (Wallenberger and Weston 2004; Bledzki and Gassan 1999; Paul et al. 1997).

Fiber	Density (g/cm^3)	Elongation (%)	Tensile Strength (MPa)	Young's Modulus (GPa)
Cotton	1.50-1.60	3.0-10.0	287-597	5.5-12.6
Jute	1.3-1.46	1.5-1.8	393-800	10.0-30.0
Flax	1.40-1.50	1.2-3.2	345-1500	27.6-80.0
Hemp	1.48	1.6	550-990	70.0
Ramie	1.50	2.0-3.8	220-938	61.4-128.0
Sisal	1.33-1.50	2.0-14	400-700	9.0-38.0
Coir	1.20	15.0-30.0	175-220	4.0-6.0
E-glass	2.50	2.5-3.0	2000-3500	70.0
S-glass	2.50	2.8	4570	86.0
Aramide (normal)	1.40	3.3-3.7	3000-3150	63.0-67.0

Generally, natural fiber is processed below 200ºC. Compared with glass and carbon fiber, flax fiber has low thermal degradation temperature. The thermal degradation of natural fibers involves two main steps, one in the temperature range 200–290ºC and the other, in the range of 300ºC or higher (Saheb and Jog 1999; Manfredi et al. 2006). The first one is the thermal depolymerization of the hemicellulose and the cleavage of glycosidic linkages of cellulose. The second one is related to the decomposition of the α-cellulose (Manfredi et al. 2006). Lignin degrades at a temperature around 200ºC (Sharifah and Martin 2004), but the range is as broad as between 200 and 500°C (Manfredi et al. 2006). Sometimes lignin degradation cannot be observed from thermal analysis curves because it overlaps with that of hemicellulose

and α-cellulose decomposition (Manfredi et al. 2006).

2.1.2 Surface modification of natural fibers

Because the hydrophilic nature of natural fibers often causes low interfacial properties between fiber and hydrophobic plastic matrix, chemical modifications are considered to optimize the interface of fibers. Chemicals may activate hydroxyl groups or introduce new moieties that can effectively interlock with the matrix. The development of a definitive theory for the mechanism of bonding by chemicals in composites is a complex problem. Generally, chemical coupling agents are molecules possessing two functions. The first function is to react with hydroxyl groups of cellulose and the second is to react with functional groups of the matrix. Bledzki and Gassan (1999) outlined several mechanisms of coupling in materials, namely: a) elimination of weak boundary layers; b) production of a tough and flexible layer; c) development of a highly crosslinked interphase region with a modulus intermediate between that of substrate and of the polymer; d) improvement of the wetting between polymer and substrate; e) formation of covalent bonds with both materials; and f) alteration of acidity of substrate surface.

The different chemical modifications of natural fibers aimed at improving the adhesion with a polymer matrix were performed by a number of researchers. Some examples of chemical treatments are listed as follows:

Alkaline treatment

Alkaline treatment is also known as mercerization which is one of the most used chemical treatments for natural fibers when used to reinforce thermoplastics and

thermosets. The important modification done by alkaline treatment is the disruption of hydrogen bonding in the network structure, thereby increasing surface roughness. Addition of aqueous sodium hydroxide (NaOH) to natural fiber promotes the ionization of the hydroxyl group to the alkoxide (Agrawal et al. 2000):

$$\text{Fiber-OH} + \text{NaOH} \longrightarrow \text{Fiber-O-Na} + H_2O \quad (2.1)$$

Thus, alkaline processing directly influences the cellulosic fibril, the degree of polymerization and the extraction of lignin and hemicellulosic compounds (Jähn 2002).

In alkaline treatment, fibers are immersed in NaOH solution for a given period of time. A solution of 5% aqueous NaOH had been used to treat jute and sisal fibers for 2 h up to 72 h at room temperature (Ray et al. 2001; Mishra et al. 2001). Jacob and co-researchers (2004) examined the effect of NaOH concentration (0.5, 1, 2, 4 and 10%) in treating sisal fiber-reinforced composites and concluded that maximum tensile strength resulted from the 4% NaOH treatment at room temperature. Mishra and co-researchers (2002) reported that NaOH treated (5%) sisal fiber-reinforced polyester composite had better tensile strength than 10% NaOH treated composites. Alkaline treatment also significantly improved the mechanical, impact fatigue, and dynamic mechanical behaviors of fiber-reinforced composites (Sarkar and Ray 2004; Joseph and Thomas 1996).

Silane treatment

Silane is a chemical compound with chemical formula SiH_4. Silane coupling agents may reduce the number of cellulose hydroxyl groups in the fiber-matrix interface. In the presence of moisture, hydrolyzable alkoxy group leads to the formation of silanols. The silanol then reacts with the hydroxyl group of the fiber, forming stable

covalent bonds to the cell wall that are chemisorbed onto the fiber surface (Agrawal et al. 2000). The reaction schemes are given as follows (Agrawal et al. 2000):

$$CH_2CHSi(OC_2H_5)_3 \xrightarrow{H_2O} CH_2CHSi(OH)_3 + 3C_2H_5OH \quad (2.2)$$

$$CH_2CHSi(OH)_3 + \text{Fiber-OH} \longrightarrow CH_2CHSi(OH)_2O\text{-Fiber} + H_2O \quad (2.3)$$

Silane coupling agents were found to be effective in modifying natural fiber-polymer matrix interface and increasing the interfacial strength. Three-aminopropyl trimethoxy silane with concentration of 1% in a solution of acetone and water (50/50 by volume) was reported to be used to modify the flax surface at the interval of 2 h (Joseph and Thomas 1996). Rong and co-researchers (2001) soaked sisal fiber in a solution of 2% aminosilane in 95% alcohol for 5 min at a pH value of 4.5 to 5.5 followed by 30 min air drying for hydrolyzing the coupling agent. Silane solutions in a water and ethanol mixture with concentration of 0.033% and 1% were also carried by other researchers (Agrawal et al. 2000; Valadez-Gonzalez et al. 1999) to treat henequén fibers and oil palm fibers. It was verified that the interaction between the silane coupling agent modified fiber and the matrix was much stronger than that of alkaline treatment, which led to composites with higher tensile strength from silane-treated than alkaline-treated fiber (Valadez-Gonzalez et al. 1999). Thermal stability of the composites was also improved after silane treatment (Agrawal et al. 2000).

Acrylation treatment

Acrylic acid (CH_2=CHCOOH) is also used in graft polymerization to modify fiber surface (Xu et al. 2002; Karlsson and Gatenholm 1999). This reaction is initiated by free radicals of the cellulose molecule. The cellulose is treated with an aqueous

solution with selected ions and exposed to a high energy radiation. Then, the cellulose molecule cracks and radicals are formed (Bledzki 1999). Acrylation reaction is expected to occur at the hydroxyl groups of the fiber as shown below (Sreekala et al. 2000):

$$\text{Fiber-OH} + CH_2{=}CH\text{-COOH} \xrightarrow{NaOH} \text{Fiber-O-}CH_2\text{-}CH_2\text{-COOH} \qquad (2.4)$$

Sreekala and co-researchers (2002) reported that fibers were mixed with 10% NaOH for about 30 min and then treated with solution containing different concentrations of acrylic acid at 50ºC for 1h. The fibers were washed with water/alcohol mixture and dried.

Permanganate treatment

Permanganate is a compound that contains permanganate group, MnO_4^-. Permanganate treatment leads to the formation of cellulose radical through MnO_3^- ion formation. Then, highly reactive Mn^{3+} ions are responsible for initiating graft copolymerization as shown below (Wallenberger and Weston 2004):

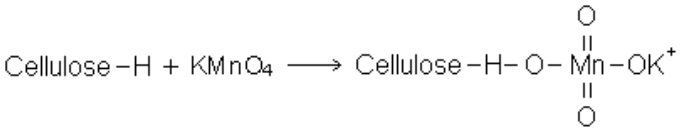

(2.5)

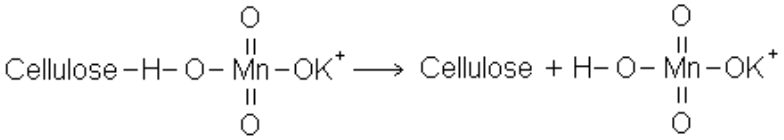

(2.6)

Most permanganate treatments are conducted by using potassium permanganate ($KMnO_4$) solution (in acetone) in different concentrations with soaking duration from 1 to 3 min after alkaline pre-treatment (Sreekala et al. 2002; Joseph et al. 1999; Paul et al.

1997; Joseph and Thomas 1996). Paul and co-workers (1997) dipped alkaline-treated sisal fibers in permanganate solution at concentrations of 0.033, 0.0625 and 0.125% in acetone for 1 min. As a result of permanganate treatment, the hydrophilic tendency of the fibers was reduced, and thus, the water absorption of fiber-reinforced composite decreased. The hydrophilic tendency of fiber decreased as the $KMnO_4$ concentrations increased. But at higher $KMnO_4$ concentrations of 1%, degradation of cellulosic fiber occurred which resulted in the formation of polar groups between fiber and matrix.

Other chemical treatments

Sodium chlorite ($NaClO_2$) is usually used in bleaching fibers; however, it can delignify lignocellulosics. Studies have been conducted wherein it was used in fiber surface treatment for composites. Mishra and co-researchers (2002) dipped untreated sisal fiber, for use in sisal-polystyrene biocomposites, in sodium chlorite solution with a liquor ratio of 25:1 at 75ºC for 2 h. It was reported that flexural strength was increased for bleached fiber composite because of lower stiffness and more flexible character of fibers after delignification. After delignification, the polymer replaces the role of lignin in fibers and makes composites more hydrophobic and tougher (Mishra et al. 2002).

Other coupling agents like benzoyl peroxide (Sreekala et al. 2000; Joseph and Thomas 1996), acetic anhydride (Sreekala and Thomas 2003; Nair et al. 2001; Hill et al. 1998), maleic acid anhydride (Joseph et al. 2003; Oever and Peijs 1998; Gassan and Bledzki 1997), isocyanates (George et al. 1996; Maldas et al. 1989), and stearic acid (Zafeiropoulos 2002; Paul et al. 1997) were also studied and used to modify the surface between fiber and matrix. Most researchers found these treatments were effective and showed better interfacial bonding.

2.1.3 Matrix materials - thermoplastics

Both thermoplastic and thermoset materials can be reinforced and made into composites. Thermoset was first introduced as matrix to be reinforced with natural fibers (Garkhail et al. 2000). Recently, developments shifted to thermoplastic matrix composites. This is because thermoplastics are more easily molded in manufacturing technologies (e.g. injection molding, extrusion, etc.) than reinforced thermosets (Murphy 1998). Another reason for thermoplastics being used as matrix is that they often need the additional strength or additional stiffness gained from reinforcement (Strong 2000).

Van de Velde and Kiekens (2001) compared 12 common type thermoplastics with different properties used as matrix in natural fiber-reinforced composites. They concluded that polypropylene (PP), low density polyethylene (LDPE), and high density polyethylene (HDPE) were suitable to be matrix in natural fiber-reinforced composites because they had lower characteristic temperatures and higher mold shrinkage although their mechanical properties were relatively low. PP and PE are all categorized as polyolefin. The basic repeating unit for PP and PE is alkyl and hydrogen group as given in Figure 2.1. PP has been studied as a matrix in fiber-reinforced composites by many researchers because of its low cost and good thermal stability (Arbelaiz et al. 2005; Aranberri-Askargorta et al. 2003; Wielage et al. 2003). Other thermoplastics including polyesteramide (PEA), poly(3-hydroxybutyrate-co-3hydroxyvalerate) (PHBV), polylactic acid (PLA), polyphenylene sulfide (PPS), polyether ether ketone (PEEK), polycarbonate (PC), polyamide 6 (PA-6), polybutylene terephthalate (PBT), etc. with better mechanical properties than PP and PE but also more costly, were also chosen as matrix in manufacturing composites reinforced with natural fibers (Campbell 2004; Keller 2003; Oksman et al. 2003; Wielage et al. 2003; Van de Velde and Kiekens 2001).

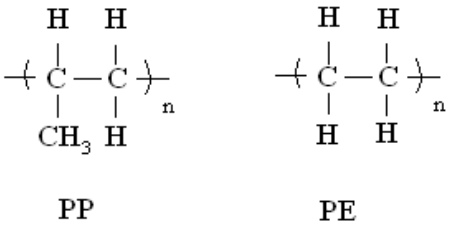

Figure 2.1 Polymer repeating unit for polypropylene (PP) and polyethylene (PE) (Strong 2000).

The three PE materials are distinguished on the basis of density. These are LDPE, HDPE, and linear low density polyethylene (LLDPE). LDPE is defined as polymerized ethylene having a nominal density of 0.910 to 0.925 g/cm^3 (Rosato et al. 2000). The density of HDPE is typically around 0.960 g/cm^3 because of more ordered crystallite and more tightly packed phase in HDPE than LDPE (Crawford and Throne 2000). LLDPE has a density like LDPE, around 0.918 to 0.940 g/cm^3 (Strong 2000) but a linear structure like HDPE. The main difference between these three general types of PE in the way the molecules interact are caused by the amount and type of branching (Strong 2000), as shown in Figure 2.2.

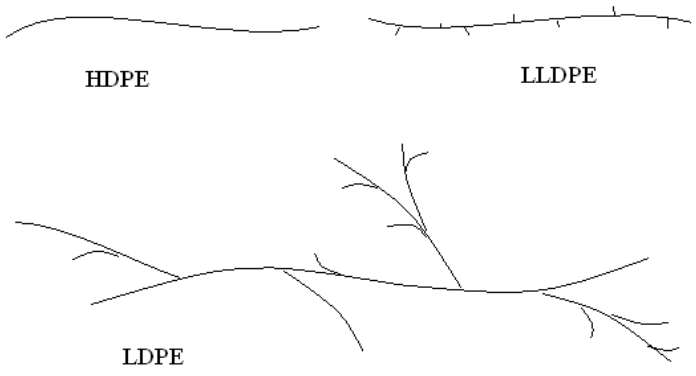

Figure 2.2 Molecular architecture of various polyethylenes (Rosen 1993).

Characteristic temperatures including glass transition temperature (T_g), melt point (T_m), and process temperature (T_p) and mechanical properties are important for distinguishing and processing of polymers. "Glass transition (T_g) is the center of temperature range in which an amorphous material changes from glass-brittle to being viscous" (Baijal 1982). Above T_g, the polymer becomes rubbery and capable of elastic or plastic deformation without fracture. Processing temperature (T_p) is the recommended temperature for polymer processing which should be higher than the melt point within a range of temperature. In flax fiber-reinforced plastic composite, the processing temperature should remain relatively low to avoid possible degradation of flax fiber when exposed to high temperatures. So PE is a good choice with its lower melting point and lower processing temperatures than other thermoplastics (Van de Velde and Kiekens 2001). Table 2.3 lists some of the physical, mechanical, and thermal properties of PE. The low energy consumption, low cost, good thermal insulator, and ease of manufacturing of PE are also extra advantages to be considered as matrix in composites (Strong 2000).

Most plastics are hydrophobic and have mold shrinkage which is the amount of shrinkage (%) when the polymer is cooled down (Van de Velde and Kiekens 2001). Mold shrinkage occurs in all thermoplastic parts due to thermal and other contractions (Strong 2000). Crystalline polymers (Nylon, HDPE, PP, etc.) give the worst problems (shrinkages 1-4%), while amorphous polymers (PC, polystyrene, etc.) have less mold shrinkage (Rosato et al. 2000). By adding fiber into plastic, mold shrinkages of composites are all reduced (ASM International 2003). HDPE and LLDPE have greater stiffness or strength than LDPE (Strong 2000). HDPE also has good chemical resistance and excellent stiffness from room temperature to the boiling point of water (Crawford

2000). The mechanical properties are influenced by the mechanical properties of both matrix and reinforcement. Only when the composites reinforced with low fiber content, the matrix mechanical properties become more important (Van de Velde and Kiekens 2001). So PE is well suited for use as matrix material in flax reinforced composite despite its relatively low mechanical properties.

Table 2.3 Properties of PE polymers (ASM International 2003; Van de Velde and Kiekens 2001; Strong 2000).

Thermal and Mechanical Properties	**PE**		
	LDPE	**HDPE**	**LLDPE**
Density (g/cm^3)	0.910-0.925	0.935-0.1	0.918-0.940
W_{24h}(%)*	<0.015	<0.01-0.20	
T_g (ºC)**	-20 - -125	-20 - -110	-120
T_m (ºC)***	105-116	120-140	
T_p (ºC)****	150-230	150-290	
Mold shrink (%)	1.5-5.0	1.5-5.0	
Specific heat (kJ/kgºC)	1.901-1.989	1.566-2.281	
Tensile strength (MPa)	10-12	14.5-38.0	15-32
Young's modulus (GPa)	0.055-0.380	0.413-1.490	
Flexural modulus (GPa)		0.41-1.07	
Ultimate tensile strain (%)	90-800	12-1000	

* W_{24h}: Water absorption
** T_g: Glass transition temperature
*** T_m: Melt point
**** T_p: Process temperature

2.2 Properties of natural fiber-reinforced plastic composites

Natural fiber-reinforced plastic composites have the advantage of higher mechanical properties than pure plastics. Their properties are influenced by both the plastic matrix and fiber reinforcements.

2.2.1 Mechanical properties of fiber-reinforced plastic composites

Most biocomposite mechanical properties are determined mainly by a tensile test. Others are determined by bending (flexural), impact, and creep tests. Tensile strength is the maximum ability of a material to withstand forces that tend to pull it apart (Shah 1984). Flexural strength describes the ability of the material to withstand bending forces applied perpendicular to its longitudinal axis (Shah 1984). Testing methods for biocomposite tensile, flexural, and other mechanical properties are usually based on the testing method for plastics.

Both the matrix and fiber properties influence the mechanical properties of biocomposites. Most researchers (Singleton et al. 2003; Voorn et al. 2001; Wollerdorfer and Bader 1998) found that adding flax fiber increased the tensile strength of the composites. The maximum reinforcement effect was found in a range of fiber content and the composite tensile strength was decreased exceeding certain fiber content (Thomason 2005). However, some researchers (Oksman et al. 2003; Santos and Pezzin 2003) found the opposite result, in that the addition of flax fiber in the composites did not significantly improve composite tensile strength because of the poor adhesion between flax fibers and polymer matrix. It was also found that the composite tensile strength was more sensitive to the matrix properties, whereas the tensile modulus was more dependent on the fiber properties (Saheb and Jog 1999).

The mechanical properties of thermoplastic composites can be improved by improving the bonding between the fiber and matrix, for example, surface treatment on fiber or polymer could increase the mechanical properties of biocomposites (Mohanty et al. 2001; Bledzki and Gassan 1999). The length of reinforced fiber in composites also influences the mechanical properties of biocomposites. The mechanical properties such

as strength, modulus and toughness increase generally with increasing fiber length (Fu et al. 2000).

2.2.2 Thermal properties of fiber-reinforced plastic composites

Generally, the melting point of fiber-reinforced biocomposites is in the range of the melting point of the matrix. For example, Tjong and co-workers (1999) prepared maleated polypropylene (MPP) composites reinforced with tetrabutyl orthotitanate-treated methyl cellulosic fiber (MC) by two extrusion steps followed by injection molding. The melting temperatures of all reinforced composites exhibited similar melting point (difference of -1.2°C to 0.1°C) as the melting temperature of MPP (167.9°C) determined by differential thermal analysis (DTA) measurements. The incorporation of MC to MPP had no effect on the melting temperature of MPP.

Thermal conductivity of biocomposites can be affected by both fiber and matrix thermal conductivities. Thermal conductivity of a composite is a function of the thermal conductivity of the plastic matrix and the fiber, and their volume fraction. Kalaprasad and co-researchers (2000) reported that the thermal conductivity values of LDPE and sisal-reinforced LDPE composite were almost similar. They also found that the difference between the values of the thermal conductivity shown by PE and glass fiber-PE composite was greater than that of the natural fiber-reinforced polyethylene composite.

2.3 Fiber-reinforced plastic composites – processing techniques

Fiber-reinforced plastic composite manufacturing is similar with thermoplastic processing. Most thermoplastic processing operations involve heating, forming into the

desired shape, and then cooling. Processing techniques used on thermoplastics could also be used on in the processing of short fiber-reinforced plastic composites. These include rotational molding, compression molding, extrusion, injection molding, etc. Sheet forming, pultrusion, and tape lay-up processes are used to manufacture long fiber-reinforced plastic composites (Advani and Sozer 2002).

2.3.1 Extrusion

The extrusion process basically consists of continuously shaping a polymer through the orifice of a suitable mold (die), and subsequently solidifying it into a product (Henson 1997). There are single-screw and twin screw extruders available. Compared with single-screw, co-rotating twin-screw extruders produces more shear and improve mixing capabilities (ASM International 2003). Extrusion is the most efficient and widely used process for melting plastic resin and mixing reinforcements into the molten plastic, leading to high production volumes. The temperature in the extruder should be high enough to ensure the polymer fully melted and low enough to avoid burning the fiber. For example, Oladipo and Wichman (1999) extruded wood fiber-HDPE composite at a working temperature of 150ºC and a screw speed of 100 rpm, while polymer melting point is between 120 and 135ºC.

Extrusion is needed for injection molded composite products before injection molding. This is because injection molding machines and screws are much shorter than extruders and therefore, the ratio of length to diameter for injection molding screws is lower than for extruders. The lower length to diameter ratio of the screw in injection machine makes it less efficient in mixing and non- homogenous melt comparison with

extruders. For this reason, if the composite is processed by injection molding, prior extrusion compounding is necessary for the materials.

2.3.2 Injection molding

Injection molding is an important plastic processing method with the characteristic of rapid production rates and high volume production. Injection molding can manufacture geometrically complex components with accurate dimensions and the process is automated. But there is limitation on fiber fraction and fiber length when using injection molding to process fiber-reinforced biocomposites (Advani and Sozer 2002) because higher natural fiber fraction and longer fiber length will make molding difficult. During injection molding, the following takes place: a) the material is fed through a hopper into the screw zone and melted; b) then the material is forced under pressure into the mold by axial motion of the screw; c) once the material is in the mold, it is shaped and cooled; d) the mold is opened and the product is ejected, and e) then the mold is closed and it is ready to start the next cycle.

The major components of injection molding machine are the plasticating unit (injection and hydraulic units), clamping unit, and the mold (Rosato et al. 2000). The cross-section of injection unit and the mold in a single screw injection molding machine is given as an example in Figure 2.3.

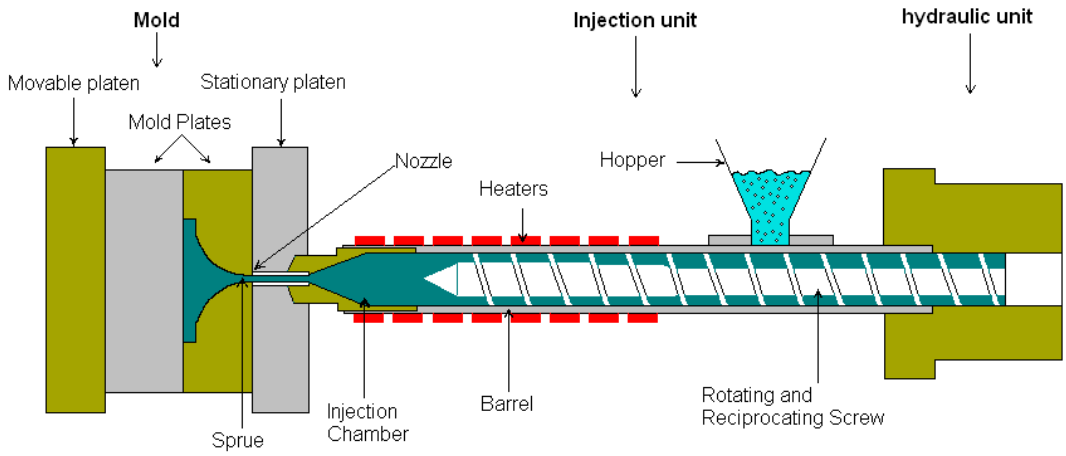

Figure 2.3 A single screw injection molding machine (The Santa Clara University Design Center 1998).

The injection unit melts the polymer and injects the polymer into the mold. The hydraulic system controls the axial reciprocation of the screw, allowing it to act like a plunger. The mold basically consists of a sprue, a runner, a cavity gate, and a cavity (Rosato et al. 2000). An example of molded product obtained from Northern Alberta Institute of Technology (Edmonton, AB) is given in Figure 2.4. During the injection, air in the cavity or cavities is released to prevent melt burning and the formation of voids in the product. The clamping system opens and closes the mold, and generates sufficient force to prevent the mold from opening. There is also a control system on the machine to monitor and control the processing parameters, including the temperature, pressure, injection speed, position, etc.

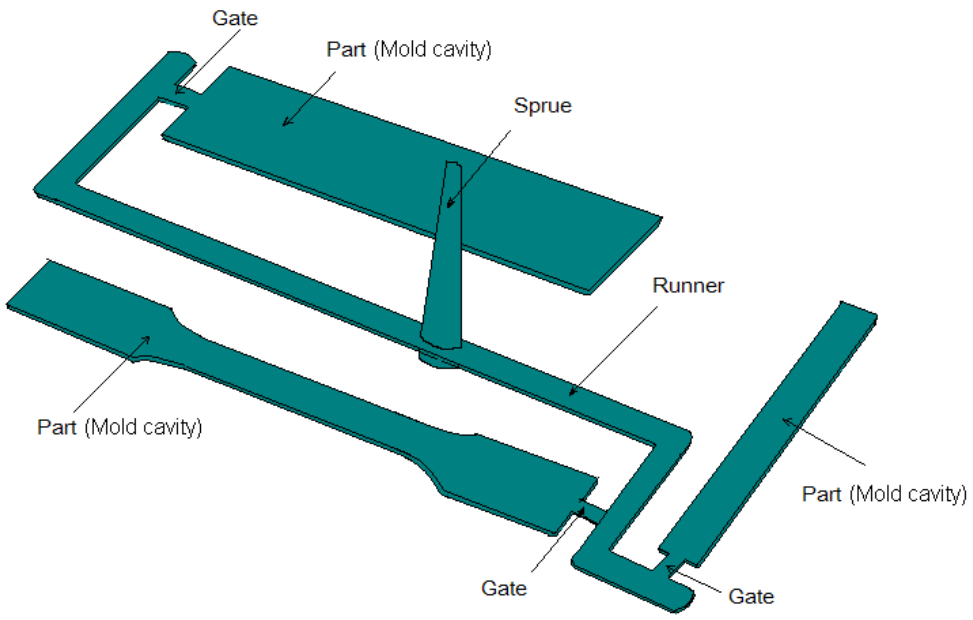

Figure 2.4 Injection mold used in experiments including the delivery system and molded parts.

Many factors including temperature, pressure, type of material, shape of molded parts, and many others, influence the quality of injection molded products. To achieve consistent quality, each of these parameters must be accurately controlled to ensure that the material fill the mold with exactly the same amount during each cycle (Dubois and Rederich 1974). Many parts of an injection mold will influence the final product's performance including the cavity shape, gating, parting line, vents, undercuts, ribs, hinges, etc. (Rosato et al. 2000). If a mold is determined to be used in injection molding, then the pressure, temperature, and time are mainly considered in injection process. During injection molding, high melt temperatures are used to permit plastic or composites to be injected quickly into the mold with minimum strain. High melt temperatures normally give maximum clarity, minimum sunburst, and minimum

warpage in the molded parts (Rosato et al. 2000). If the melt temperature is too low, molding will be difficult, requiring excessive injection pressures and longer plunger-forward times.

Many thermoplastic materials require thorough drying prior to molding, to avoid the formation of voids or degradation at molding temperatures. All thermoplastics are, in principle, suitable for injection molding, but since fast flow rates are needed, grades with good fluidity (high melt index) are normally preferable (Charrier 1991).

There are some of research publications (Weidenfeller et al. 2005; Martins and Paoli 2001; Fu et al. 2000) dealing with the processing and properties of polypropylene-glass fiber composites processed by injection molding. However, studies on how injection molding parameters influence the properties of natural fiber-polyethylene composites are very limited (Herrera-Franco et al. 1997). Most researchers studied the mechanical or physical properties of composites but not on injection molding process control. Saint-Martina and co-workers (2003) observed that the hydraulic holding pressure level had a significant effect on voids rate of glass fiber-reinforced PP composite during injection molding when compared with factors like mold temperature, melt temperature, and injection speed. Fung (2003b) studied the pre-impregnation technique in the injection molding of sisal fiber-reinforced PP composites. They found that reinforcement efficiency for low injection temperature (170-180°C) specimens was slightly higher than high injection temperature (190-210°C) samples.

2.3.3 Flow analysis in injection molding

The purpose of flow analysis is to gain a comprehensive understanding of the mold-filling process. However, flow analysis is quite a complex thermo-mechanical

problem to understand. Models range all the way from a simple Poiseullle's equation (Equations 2.7 and 2.8) (Rosato and Rosato 1995) for Newtonian fluid flow to much more complex mathematical models involving three fundamental laws of physics when melted polymer flow, i.e. the principles of conservation of mass, momentum, and energy (Equations 2.9 to 2.11) (Kim and Turng 2004).

$$Q = \frac{R^4 \pi \Delta P}{8 \mu L} \qquad \text{(cylindrical shapes)} \tag{2.7}$$

$$Q = \frac{W H^3 \Delta P}{12 \mu L} \qquad \text{(rectangular shapes)} \tag{2.8}$$

$$\text{Continuity: } \frac{\partial \rho}{\partial t} + \nabla \cdot (\rho u') = 0 \tag{2.9}$$

$$\text{Momentum: } \rho \frac{Du'}{Dt} = -\nabla p + \nabla \cdot \underline{\underline{\tau}} + \rho g' \tag{2.10}$$

$$\text{Energy: } \rho C_p \frac{DT}{Dt} = -\nabla \cdot q' - T \left[\frac{\partial p}{\partial T} \right]_\upsilon (\nabla \cdot u') + \underline{\underline{\tau}} : \nabla u' + \dot{S} \tag{2.11}$$

Equations 2.7 and 2.8 are applied to Newtonian fluids, where:

Q = material volume flow rate (m^3/s),

μ = viscosity (Pa·s),

P = pressure (Pa),

R = the radius of cylinder (m),

W = the width of rectangular part of the mold (m),

H = the height of rectangular part of the mold (m), and

L = the length of rectangular part of the mold (m).

In equations 2.9 to 2.11,

ρ = density (kg/m^3),

C_p = specific heat (kJ/kg°C),

T = temperature (°C),

υ = specific volume (m^3/kg),

$\dot{S}$ = rate of heat generation due to chemical reaction (kw/m^3),

u' = velocity vector,

g' = body force vector,

q' = heat flux vector, and

$\underline{\underline{\tau}}$ = second-order deviatoric stress tensor.

To equate this numbers of unknowns and equations, additional equations such as constitutive equation and thermal constitutive equation are also required.

Indeed, apart from some attempts to introduce a full 3D approach (Barriere et al. 2003; Chang and Yang 2001), the analysis is currently still often restricted to 2D or the Hele-Shaw (or thin film) approximation (Courbebaisse 2005; Su et al. 2004), which is warranted by the fact that most injection molded parts have the characteristic of being thin. Some simulation software were developed for analysis of injection molding and were used in solving equations, such as C-MOLD (Su et al. 2004), Liquid Injection Molding Simulation (LIMS) (Deléglise et al. 2005), Flow-3D and Telluride program package (Mcfarland and Colton 2004; Greene and Wilkes 1997), ANSYS 5.7 package-2D fluid modeling (Mcfarland and Colton 2004), and many others. Due to the complex nature of injection molding, simulation usually focus on one or two factors, usually including the prediction of pressure and temperature (Su et al. 2004; Pantani et al. 2001), filling time (Deléglise et al. 2005; Su et al. 2004), tracking of moving melt front (Wang

2005), characterization of crystallization kinetics (Kim et al. 2005), and modeling fiber orientation (Vincent et al. 2005).

Unlike other manufacturing processes, the quality and performance of injection-molded parts depend not only on the material and the shape of the part but also on how the material is processed during molding (Rosato and Rosato 1995). To analyze injection molding, the three main steps, namely filling, packing/holding, and cooling stages, have to be recognized (Pantani et al. 2005; Courbebaisse 2005). During the filling stage, a hot material melt rapidly fills a cold mold reproducing a cavity of the desired product shape. During the packing/holding stage, the pressure is raised and extra material is forced into the mold. Upon 'cooling', the solidified part shaped by the cavity within the mold is ejected out. Most simulation and modeling just address the filling stages (Trochu et al. 2006; Courbebaisse 2005; Deléglise et al. 2005) and no studies on natural fiber biocomposites were conducted.

Because most injection molded polymeric parts have complicated three-dimensional configurations and the melted polymer is generally non-Newtonian and non-isothermal, it is extremely difficult to analyze the filling process without simplifications. Some assumptions are usually made in the simulation of the filling stages, which also is known as underfill flow process (Wang 2005). Examples of assumptions during filling stages are: a) the fluid is incompressible and flow is laminar; b) the gravity is neglected; c) no slip between fluid and solid wall; and d) the fluid is Newtonian or non-Newtonian. In the packing stage, melt compressibility can no longer be neglected, making it a compressible fluid and thus, more complicated to analyze. While in the cooling stage, the velocity of melted polymer is almost zero. Thus, convection and dissipation terms in the energy equation can be neglected.

2.3.4 Power-law fluids and laminar flow

Because thermoplastic materials are subjected to temperatures above their melting point during injection molding, the resistance to deformation and flow in terms of viscosity is therefore important since materials must undergo deformation in order to flow into the mold of a certain geometry. Viscosity is expressed in different ways between Newtonian fluid and Non-Newtonian fluids.

For a Newtonian fluid, the viscosity (μ, Pa·s) is given by the equation (Singh and Heldman 2001):

$$\tau = \mu\left(\frac{du}{dy}\right) \tag{2.12}$$

where: τ = shear stress (Pa), and

$\frac{du}{dy}$ = velocity gradient or shear rate in the direction perpendicular to the layers (m/s).

In non-Newtonian fluids, τ versus $\frac{du}{dy}$ is not linear. Models relating τ and $\frac{du}{dy}$ are different for various non-Newtonian fluids. Non-Newtonian fluids could be divided into three broad groups: time-independent fluids (including shear thinning, shear thickening, Hershel Bulkley and Bingham fluids), time-dependent fluids (including phsopectic and thixotropic fluid), and viscoelastic fluids (Singh and Heldman 2001; Skelland 1967).

Most melted polymers exhibit shear thinning behavior (0<n<1), which means that viscosity decreases at higher shear rate. Shear thinning liquids are also called

pseudoplastic or power-law liquid (Singh and Heldman 2001). The shear stress and shear rate for a power-law liquid is given as (Singh and Heldman 2001):

$$\tau = K\left(\frac{du}{dy}\right)^n \tag{2.13}$$

where: K = consistency coefficient (Pa·s^n), and

n = flow behavior index.

The viscosity measured for power-law liquid at a specific shear rate is called apparent viscosity μ_a (Skelland 1967) given as:

$$\mu_a = K\left|\frac{du}{dy}\right|^{n-1} = \frac{\tau}{du/dy} \tag{2.14}$$

Incompressible laminar flow of power-law fluid in the pipes (cylindrical cross section) has been developed by some researchers (Wilkes 1999; Rosen 1993; Wilkinson 1960). The velocity $u(r)$ at radius r is given as (Rosen 1993):

$$u(r) = \frac{\left[\left(\frac{\Delta P}{\Delta x}\right)\left(\frac{1}{2K}\right)\right]^{\frac{1}{n}}}{1/n+1}\left[R^{\left(\frac{1}{n}\right)+1} - r^{\left(\frac{1}{n}\right)+1}\right] \tag{2.15}$$

And the volumetric flow rate Q in tube is (Rosen 1993; Wilkinson 1960):

$$Q = \left[\left(\frac{\Delta P}{\Delta x}\right)\left(\frac{1}{2K}\right)\right]^{\frac{1}{n}}\left[\frac{\pi}{(1/n)+3}\right]R^{\left(\frac{1}{n}\right)+3} \tag{2.16}$$

where: P = pressure (Pa),

x = the distance of material in flow direction (m), and

R = the radius of cylinder (m).

In the case of laminar flow in fixed parallel plates, the velocity $u(y)$ of power-law fluid at longitude distance y is given as (Wang 2005):

$$u(y) = \left[\left(\frac{dP}{dx}\right)\left(\frac{1}{K}\right)\right]^{\frac{1}{n}}\left(\frac{n}{n+1}\right)\left(y^{\frac{1}{n}+1} - h^{\frac{1}{n}+1}\right). \tag{2.17}$$

The relationship between volumetric flow rate Q and pressure ΔP is given as (Skelland 1967):

$$Q = 2W(2h)^2\left(\frac{n}{2n+1}\right)\left[\left(\frac{\tau_w}{K}\right)\right]^{\frac{1}{n}} \tag{2.18}$$

where: W = the width of plate (m),

$2h$ = the height between two parallel plates (m),

x = the distance of material in latitude flow direction (m), and

$\tau_w = \frac{2h\Delta P}{\Delta x}$ is the shear stress (Pa) at wall.

2.3.5 Pressure drop in laminar flow

During injection molding, injection pressure drops when material flows inside the mold, which includs the pressure loss within the heating cylinder, thorough the nozzle, sprue and runners, through the gate, and then through the cavity (Rosato and Rosato 1995).

Since energy is neither created nor destroyed within the fluid system, the total energy of the fluid at one point in the system must equal the total energy at any other point plus any transfers of energy either into or out of the system. The Bernoulli Equation (energy equation) is a statement of the conservation of energy in a form useful for solving problems involving fluids. For a non-viscous, steady flow fluid, the sum of

pressure ($\frac{P}{\rho}$), potential (gz), and kinetic ($\frac{u^2}{2}$) energies per unit volume is constant at any point. It could be written in the following form (Singh and Heldman 2001; Johnson 1999):

$$\frac{\partial}{\partial s}\left(\frac{u^2}{2}+\frac{P}{\rho}+gz\right)=0 \tag{2.19}$$

or $$z_1 g+\frac{u_1^2}{2}+\frac{P_1}{\rho_1}=z_2 g+\frac{u_2^2}{2}+\frac{P_2}{\rho_2}+E_f-E_c \tag{2.20}$$

where: u = flow speed (m/s),

g = the gravity (m/s^2) ,

z = the height (m),

E_f = the energy lost due to friction (m^2/s^2), and

E_c = the energy supplied by pump (m^2/s^2).

To calculate the pumping requirements for non-Newtonian liquids, the energy equation is modified to incorporate the non-Newtonian properties, which becomes (Singh and Heldman 2001):

$$z_1 g+\frac{u_1^2}{2\alpha}+\frac{P_1}{\rho_1}=z_2 g+\frac{u_2^2}{2\alpha}+\frac{P_2}{\rho_2}+E_f-E_c \tag{2.21}$$

For laminar flow and shear-thinning liquid,

$$\alpha=\frac{(2n+1)(5n+3)}{3(3n+1)^2}, \tag{2.22}$$

For turbulent flow, α =1.

The energy lost due to friction E_f could be written in two terms:

$$E_f=E_{major}+E_{minor} \tag{2.23}$$

where E_{major} equals $\sum \frac{2fL\left(\bar{u}\right)^2}{D}$, is the energy loss due to the flow of viscous liquid in the straight portions of a pipe (Singh and Heldman 2001). The friction factor f is only a function of Reynold number (N_{Re}), $f = \frac{16}{N_{\mathrm{Re}}}$, or f could be taken from Singh and Heldman (2001). For power-law fluid, the Reynolds number is defined as (Kreith 1999):

$$N_{\mathrm{Re}} = \left(\frac{D^n \left(\bar{u}\right)^{2-n} \rho}{8^{n-1} K} \right) \left(\frac{4n}{3n+1} \right)^n \tag{2.24}$$

where: D = the pipe diameter (m).

$E_{\min or}$ is the energy loss due to various components used in pipeline systems, such as valves, tees, and elbows, and contraction and expansion of the pipeline. It could be written in three terms:

$$E_{\min or} = E_{ff} + E_{fc} + E_{fe} \tag{2.25}$$

E_{ff}, E_{fc}, E_{fe} are energy losses due to pipe fittings (include elbows, tees, and values), sudden contraction, and sudden expansion, respectively. For Newtonian fluid, they are expressed (Singh and Heldman 2001):

$$E_{ff} = C_{ff} \frac{\left(\bar{u}\right)^2}{2}; E_{fc} = C_{fc} \frac{\left(\bar{u}_2\right)^2}{2}; E_{fe} = C_{fe} \frac{\left(\bar{u}_2\right)^2}{2} \tag{2.26}$$

where: u_2 = upstream velocity (m/s);

C_{ff}, C_{fc}, C_{fe} = coefficient of energy loss due to pipe fittings, sudden contraction, and sudden expansion, respectively.

Typical values of loss coefficient (C_{ff}) for various fittings could be taken from Singh and Heldman (2001). Coefficients of energy loss due to sudden contraction for Newtonian fluid were evaluated as (Singh and Heldman 2001):

$$C_{fc} = 0.4\left[1.25 - \left(\frac{A_2}{A_1}\right)\right] \quad \text{when } \frac{A_2}{A_1} < 0.715 \tag{2.27}$$

$$C_{fc} = 0.75\left[1 - \left(\frac{A_2}{A_1}\right)\right] \quad \text{when } \frac{A_2}{A_1} > 0.715 \tag{2.28}$$

$$C_{fe} = \left(1 - \frac{A_1}{A_2}\right)^2 \tag{2.29}$$

Singh and Heldman (2001) concluded that in laminar flow of non-Newtonian fluid, C_{ff}, C_{fc}, and C_{fe} can be calculated using the following expressions:

$$C'_{ff} = \frac{500 \times C_{ff}}{N_{\mathrm{Re}}} \; ; \; C'_{fc} = \frac{500 \times C_{fc}}{N_{\mathrm{Re}}} ; \; C'_{fe} = \frac{500 \times C_{fe}}{N_{\mathrm{Re}}} ; \tag{2.30}$$

The expansion loss in laminar flow for a power-law fluid was also calculated directly as (Wilkinson 1960; Skelland 1967):

$$E_{fe} = \left(\frac{Q}{A_1}\right)^2 \left(\frac{3n+1}{2n+1}\right)\left[\frac{n+3}{2(5n+3)}\left(\frac{A_1}{A_2}\right)^2 - \left(\frac{A_1}{A_2}\right) + \frac{3(3n+1)}{2(5n+3)}\right] \tag{2.31}$$

where: A_1, A_2 = the flow cross sectional area before contraction (or expansion) and after contraction (or expansion), respectively.

The contraction could not be analytically solved like expansion. But experiments performed by scientists indicated that there was no appreciable difference between non-Newtonian and Newtonian fluid pressure losses in either laminar or turbulent flow (Wilkinson 1960; Skelland 1967).

2.3.6 Minimum cooling time

During injection molding, the material may be released from the mold as soon as its outer layer is sufficiently rigid. Cost savings could be realized if the minimum cooling time is controlled and the total molding cycle time is shortened. Minimum cooling time is related with the thickness of the molding part, temperature difference between the mold and polymer, and mold release temperature which is known as ejection temperature. Higher mold temperature will cause a longer cooling time (Rosato and Rosato 1995).

Minimum cooling time (t_c) in injection molding could be predicted from the following equation (Rosato and Rosato 1995):

$$t_c = \frac{B^2}{\alpha\pi^2} \ln\left[\frac{4}{\pi}\left(\frac{T_m - T_w}{T_e - T_w}\right)\right] \tag{2.32}$$

where α = thermal diffusivity of material (m^2/s),

T_w = mold wall temperature (°C),

T_m = melted material temperature (°C),

T_e = ejection temperature (°C), and

B = the plate thickness (m).

Thermal diffusivity (α, m^2/s) is the ratio of thermal conductivity (k, W/m°C) to volumetric heat capacity (ρC_p):

$$\alpha = \frac{k}{\rho C_p} \tag{2.33}$$

where C_p = specific heat (kJ/kg°C), and

ρ = density (kg/m^3).

Generally, the thermal conductivity of a polymer is low and varies with polymer structures (ASM International 2003). Sombatsompop and Wood (1997) obtained the thermal conductivity of LDPE whose value ranged from 0.209 to 0.269 W/m°C. Woo and co-workers (1995) measured the thermal conductivity of HDPE and found that above temperature 135°C the thermal conductivity of HDPE was 0.435 W/m°C. Thermal conductivity of melted polymer could be measured by line-source method also known as hot-wire method (Carvalho et al. 1996; Lobo and Cohen 1990), Lee's disc method (Sombatsompop and Wood 1997), or transient plane sources method (Kalaprasad et al. 2000). But there is no report on thermal conductivity of oilseed flax fiber as well as natural fiber-plastic composite at temperature higher than its melting point. Specific heat (or specific heat capacity) of polymer is often measured by differential scanning calorimetry (Weidenfeller et al. 2004; Woo et al. 1995). Transient plane source method was also used to measure specific heat (Almanza et al. 2004).

2.4 Summary

The literature showed that studies on natural fiber-reinforced composites, or biocomposites had increased dramatically in recent years due to the advantages of natural fibers, such as low density, low cost, and recyclability over synthetic fibers.

Flaxseed fiber grown in Canada is a choice fiber for reinforcement and polyethylene is appropriate as a matrix in biocomposites. The research on oilseed flax fiber and polyethylene biocomposites has the potential benefit for the Canadian environment and agricultural industry. This chapter reviewed the chemical, physical,

mechanical and thermal properties of flax fiber and polyethylene, as well as biocomposites.

Among the manufacturing methods, injection molding is a widely used technique to process biocomposites with the advantages of rapid producing rate and high product quality. However, there were no comprehensive studies performed on flax fiber-polyethylene biocomposites, especially the material behaviour during injection molding. There were also no research results showing how processing variables and injection molding factors influence the properties of flax fiber-HDPE biocomposites. This chapter reviewed the processing principles of injection molding including the mechanism of molding, operation variables, minimum cooling time, and some other possible factors that influence processing of biocomposites. The material flow inside the mold is a complex behavior involving fluid dynamics and heat transfer, and simulation. Flax fiber-PE biocomposite flowing inside the mold can be considered as Non-Newtonian fluid laminar flow. The reviews were conducted from the aspects of flow analysis methods, rheological properties, and laminar flow of power-law fluid to facilitate the understanding of biocomposite injection molding.

3. MATERIALS AND METHODS

To achieve the objectives, the materials were processed to biocomposites and the properties of material and biocomposites were measured. The influence of various materials, chemical treatments, and molding conditions on the properties of biocomposites and processing were also investigated. This chapter discusses the materials, equipment, and methods of conducting experiments and the analysis of results.

3.1 Materials

Flaxseed fibers and polyethylene (LLDPE and HDPE) were considered as basic materials to process biocomposites. Other chemicals were used in fiber chemical treatments or increasing processability of the formulation.

3.1.1 Flax fibers

Flaxseed fiber grown in Saskatchewan was used as raw material. Flax fiber could be separated from flax straw using a decortication machine with further cleaning, hackling, sorting, and other processes. There were three grades of flax fibers obtained from Biofiber Industries (formerly Durafibre Inc., Canora, SK) as shown in Figure 3.1. The difference between grades is due to the purity of fiber, wherein some grades still had shives (woody part of the straw) remaining in the fiber.

Figure 3.1 Three flax fiber materials used in experiments.

The shive content in the fiber materials were determined by picking up the shive from 100 g flax fiber, and, then weighing the fiber and shive separately using a weighing scale (OHAUS Corporation, Florham Park, NJ). The pure fiber and shive contents in each fiber material were then calculated and the three grades of flax fibers were assigned as shown in Table 3.1.

Table 3.1 Flax fiber materials.

Flax Fiber	Fiber Content (% wt.)	Shive Content (% wt.)
I	98-99	1-2
II	85	15
III	42	58

3.1.2 Polyethylene

Linear low density polyethylene (LLDPE) was procured from ExxonMobil Chemical Canada, Toronto, ON. High density polyethylene (HDPE) was from Nova Chemicals, Mooretown, ON. LLDPE and HDPE have similar linear structure, but LLDPE has lower density (0.938 g/cm^3) than HDPE (0.963 g/cm^3). LLDPE and

HDPE have lower melting point among plastics which make them processable at temperature below the degradation temperature of natural fibers.

3.1.3 Other materials

Technical grade chemicals including sodium hydroxide (EM Industries, Inc., Gibbstown, NJ), triethoxyvinylsilane (Sigma-Aldrich, Inc., St. Louis, MO), alcohol (Commercial Alcohols, Inc., Brampton, ON), potassium permanganate (EM Industries, Inc., Gibbstown, NJ), acetone (BDH, Inc., Toronto, ON), sodium chlorite (A Johnson Matthey Company, Inc., WardHill, MA), and acrylic acid (Lancaster Synthesis, Inc., Pelham, NH) were acquired and used for fiber surface modifications. Pure refined wax-parowax (Conros Corp., North York, ON) was also used.

3.2 Experimental equipment and basic procedures

The overall process followed for flax fiber-polyethylene biocomposites is given in Figure 3.2.

There are several critical steps in processing biocomposites, namely, chemical and physical treatments of fiber, mixing of fiber and plastic, extrusion, and injection molding.

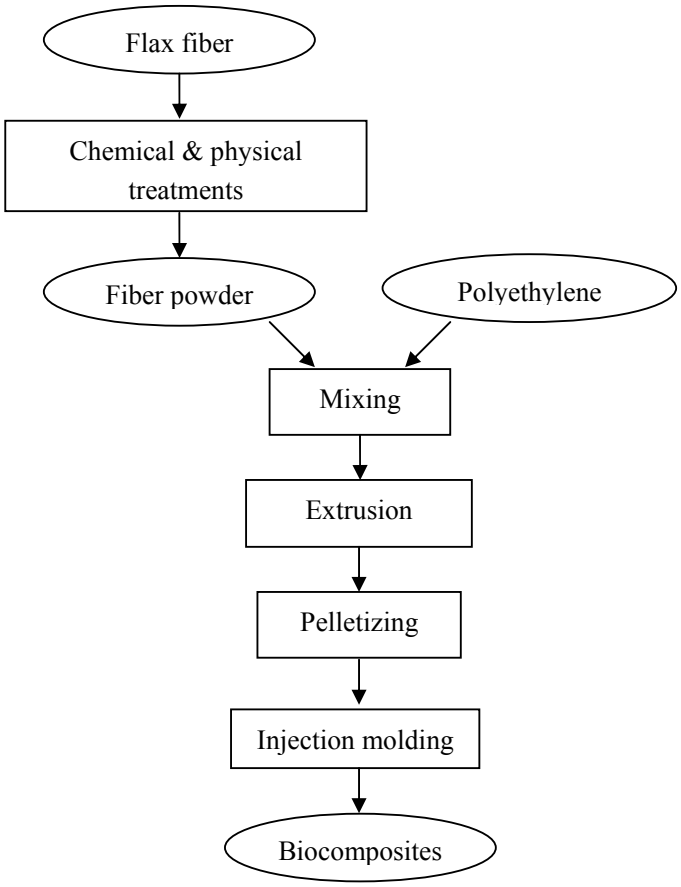

Figure 3.2 Processing scheme of flax fiber-reinforced plastic composites**.**

3.2.1 Pretreatment of flax fibers and mixing of fiber and plastic

The flax fibers were first washed or chemically treated. Then the fiber was dried at 70°C in air oven for 24 h. The dried fiber was then ground by the grinding mill (Falling Number, Huddinge, Sweden) with 2 mm screen to fiber powder, making it ready for mixing with polyethylene.

The mixing of flax fiber powders and polyethylene matrix was carried in a blender (Waring Products Corporation, New York, NY) as shown in Figure 3.3. Because it is a rotating mixer without heat given on the materials, extrusion process is needed for further mixing.

Figure 3.3 Rotating blender for mixing fiber with polymer.

3.2.2 Extrusion compounding equipment and process

The mixture of fiber and plastic was then fed into the twin-screw extruder (Werner & Pfleiderer, Ramsey, NJ) located at the Centre for Agri-Industrial Technology (CAIT) of Alberta Agriculture, Food and Rural Development in Edmonton, AB. as shown in Figure 3.4. Extrusion was conducted in order to avoid the separation of fiber from the polymer during the later molding process.

The extruder parameters controlled were screw speed and temperature. There are five temperature zones on the screw barrel to heat the material as shown in Figure 3.5. The twin-screws were rotated to convey, melt, mix, and pump the material out of the die. The die is a six-hole die with a diameter of 3 mm for each hole. The extrusion barrel zone temperatures from 1 to 5 were kept constant at 90, 110, 120, 130, and 140ºC for fiber-LLDPE mixture, and 90, 120, 130, 140, 160ºC for fiber-

HDPE mixture, respectively. The screw speed was set at 150 rpm. These parameter controls were adapted from Wang's (2004) thesis and previous experimental experience and these were kept consistent for all biocomposite processing.

Figure 3.4 Twin-screw extruder (Werner & Pfleiderer, Ramsey, NJ) used for compounding at Centre for Agri-Industrial Technology (Edmonton, AB).

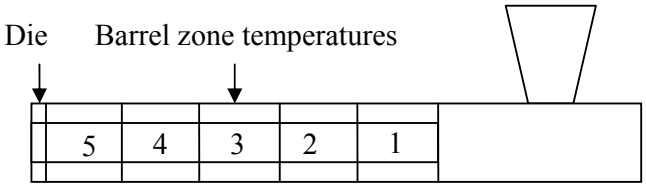

Figure 3.5 Cross-sectional view of the extruder with five separate heating zones.

The extrudates were then pelletized using a grinding mill (Retsch GmbH 5657 HAAN, West Germany) at Parkland Plastics in Saskatoon, SK.

3.2.3 Injection molding equipment and process

The pelletes after extrusion were then injection molded to special shape of biocomposite products. At the beginning of study, injection molding was conducted at the Saskatchewan Research Council (SRC, Saskatoon, SK). Because of the limitation of the mold in SRC and their injection machine was manufactured in 1971 without automatic molded-part release, further investiagtion on injection molding was moved to Northern Alberta Institute Technology (NAIT), in Edmonton, AB.

Injection molding at Saskatchewan Research Council (SRC)

The injection molding machine (Battenfeld Maschinen, Austria) in SRC is shown in Figure 3.6. The dimensions of the specimen in the mold (Figure 3.7) were designed according to test standard ASTM D638-97 (ASTM 1997a) (Table 3.2) to make it easy for further tensile testing on biocomposites.

Figure 3.6 Injection molding machine (Battenfeld Maschinen, Austria) at Saskatchewan Research Council (SRC).

Figure 3.7 Injection mold for making tensile test specimen (left) and specimens after molding (right).

Three temperatures namely, nozzle, back, and ahead temperature were monitored in the injection control system. Nozzle temperature was the temperature at which heating of the material started, and ahead temperature was the temperature of the material finally being injected into the mold. Back temperature was the temperature in the middle of screw.

Table 3.2 Design dimensions for specimen mold (ASTM D638-97).

Dimensions	**mm (in)**
Width of narrow section	13 (0.50)
Length of narrow section	57 (2.25)
Width overall	19 (0.75)
Length overall	165 (6.5)
Gage length	50 (2.00)
Distance between grips	115 (4.5)
Radius of fillet	76 (3.00)
Thickness	3.2 ± 0.4 (0.13 ± 0.02)

Injection molding at Northern Alberta Institute Technology (NAIT)

Except for the biocomposites prepared for studying the effect of chemical treatments which were injection molded at SRC, the rest of injection molding

experiments were conducted using the injection molding machine (Battenfeld Maschinen, Germany) of NAIT as shown in Figure 3.8.

Figure 3.8 Injection molding machine (Battenfeld Maschinen, Germany) at Northern Alberta Institute Technology (NAIT).

There were four controlled temperature zones in the heater barrels of this injection molding machine shown in Figure 3.9. Temperature was increased from zone D to A. Temperature zone A was close to the injection chamber where the material was injected into the mold. The operating temperature must lie in the range between the melting point temperature and the degradation temperature of the material. The recommended processing temperature for HDPE is 150-290°C (Strong 2000), but usually natural fibers start to degrade above 200°C. Thus, for biocomposites, the characteristic temperatures both of the fiber and the polymer should be considered. The total injection cycle time includes the time of mold closing, filling, packing and holding, cooling, mold opening, and ejection. Shown in

the injection molding control panel are injection, hold, back, and open time (Figure 3.10).

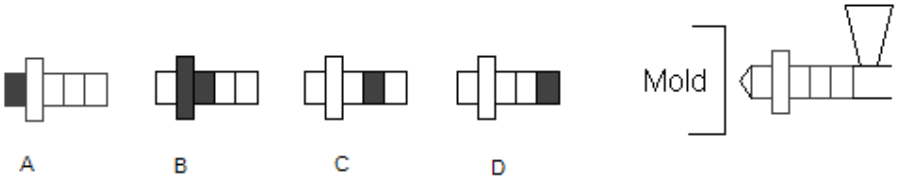

Figure 3.9 Temperature zones in the injection molding machine.

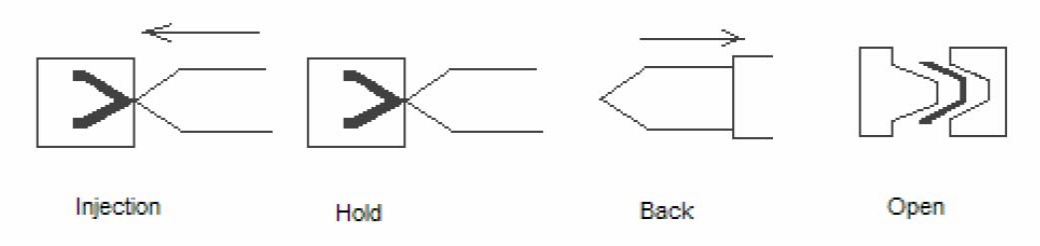

Figure 3.10 Injection cycle time setting at injection molding machine.

The mold was designed for polymer mechanical properties testing. The molded product was of three parts, namely, tensile specimen with dimensions according to ASTM D638-97 (ASTM 1997a), flexural specimen with dimensions following ASTM D790-97 (ASTM 1997b), and a rectangular specimen (Figure 3.11).

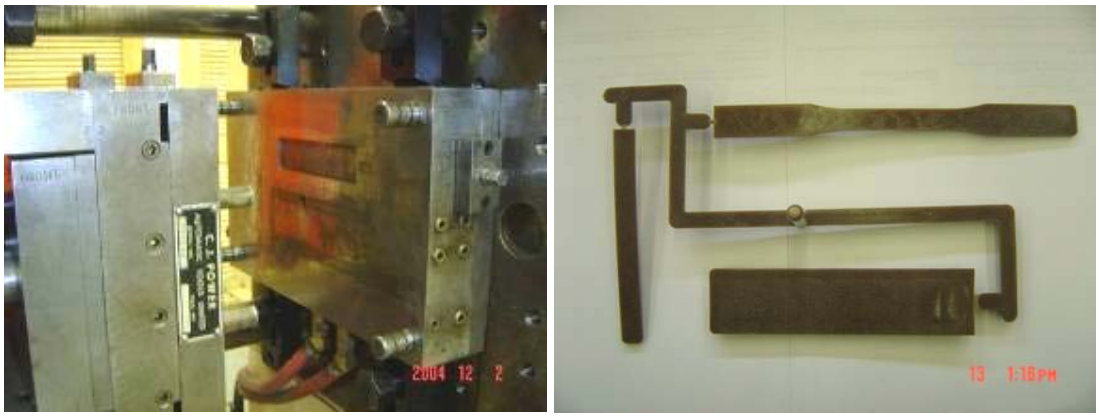

Figure 3.11 The mold and molded specimens of the injection molding machine at NAIT.

3.3 Experimental design and processing of biocomposites

To attain the objectives outlined in chapter 1, the materials were processed to biocomposites under different conditions, and the properties of material and biocomposites were measured. Experiments on the effects of chemical treatments, choosing of fiber and PE materials, and influence of fiber content and injection parameters on injection molding were conducted.

3.3.1 Experiments for choosing chemical treatments and polyethylene for further studies

To compare the effects of chemical treatments on fiber and fiber-polyethylene composites, referring to literatures and pervious research (Wang 2004; Mishra et al. 2002; Sreekala et al. 2000), six pretreatments including non-chemical treatment (U) and five chemical treatments (N, S, P, A, C) were conducted on flax fiber III as shown in the following:

***Untreated* (U):** The flax fiber was washed with 2% detergent solution and distilled water, then dried in an air oven at 70°C for 24 h. The dried fiber was designated as untreated fiber (U).

***Alkali treatment* (N):** Fiber was washed with 2% detergent solutions first. It was then immersed in 5% sodium hydroxide (NaOH) solution for 3 h. The fiber was then washed thoroughly with distilled water and dried in an air oven at 70°C for 24 h. The fiber was designated as alkali treated (N).

***Silane treatment* (S):** Fiber was washed with 2% detergent solutions and soaked in 5% NaOH solution for 0.5 h and washed with distilled water. Then it was soaked in 2.5% triethoxysilane coupling agent solution (alcohol water mixture at 60:40) for 0.5h, and the pH was adjusted between 3.5 and 4.0. Finally, it was washed with distilled water and dried in the oven at 70°C for 24 h. The fiber was designated as silane treated (S).

***Potassium permanganate treatment* (P):** Fiber was washed with 2% detergent solutions and soaked in 2% NaOH solution for 1 h, and then soaked in 0.2% potassium permanganate ($KMnO_4$) solution (in 2% acetone) for 10 min. Finally, it was put into thermostatic water bath at 50ºC for 2 h to catalyze the reaction, washed with distilled water and dried at 70°C for 24 h. The fiber was designated as potassium permanganate treated (P).

***Acrylic acid treatment* (A):** Fibers was washed with 2% detergent solutions and immersed in 10% NaOH solution for 0.5 h, and then soaked in 5% acrylic acid

solution at 50ºC for 1 h, washed with distilled water and dried at 70°C for 24 h. The fiber was designated as acrylic acid treated (A).

Sodium chlorite treatment **(C):** Fibers was washed with 2% detergent solutions and soaked in 5% NaOH solution for 1 h, and then soaked in sodium chlorite solution (sodium chlorite: water = 1:25) at 70ºC for 2 h, washed with distilled water and dried at 70°C for 24 h. The fiber was designated as sodium chlorite treated (C).

The fibers after treatment were ground to 2 mm powder and mixed with the matrix (LLDPE or HDPE) at fiber mass content of 10%. The mixture was extrusion compounded, pelleted, ground, and injection molded to fiber III-PE biocomposites. Tables 3.3 and 3.4 list the biocomposite processed in this part of the experimental program. No replication of treatment combinations listed in these tables was done. Pure LLDPE and HDPE were also extruded and injection molded for comparison purposes.

The effects of chemical treatments were compared after measuring tensile strength, water absorption, and morphology of biocomposites. At the same time, the effect of LLDPE and HDPE as matrix were also observed from the testing results and one matrix would be chosen as the matrix to be used for further studies.

Table 3.3 LLDPE and Fiber III-LLDPE biocomposite samples.

Sample ID		Fiber Treatment
Fiber III-LLDPE Biocomposites	U-L	U
	N-L	N
	S-L	S
	P-L	P
	A-L	A
	C-L	C
LLDPE	LLDPE	--

Table 3.4 HDPE and Fiber III-HDPE biocomposite samples.

Sample ID		Fiber Treatment
Fiber III-HDPE Biocomposites	U-H	U
	N-H	N
	S-H	S
	P-H	P
	A-H	A
	C-H	C
HDPE	HDPE	--

For extrusion compounding, please refer to section 3.2.2. The injection molding was conducted at SRC. All biocomposites were processed at the same injection molding conditions. The temperature setting was: nozzle temperature at 70°C, back temperature at 160°C, and ahead temperature at 180°C. The cooling time was 30 s and injection pressure was set at 4.8 MPa.

3.3.2 Experiments for choosing flax fiber for further studies

Among three flax fiber materials (I, II, and III), one fiber material was to be chosen as the reinforcement to be used in future studies. The experiments in comparing these fiber materials were carried as explained in the following paragraphs.

Untreated (U) flax fibers (I, II, III) or acrylic acid treated (A) fibers were ground using the grinding mill equipped with 2 mm screen and mixed with HDPE. The mixes were then extrusion compounded and injection molded to biocomposites. The experimental trials are listed in Table 3.5.

Table 3.5 Biocomposites prepared for choosing fiber materials.

Trial	Fiber material in biocomposites*	Fiber treatment
1	I	U
2	I	A
3	II	U
4	II	A
5	III	U
6	III	A

*Composition of biocomposites is 10% fiber, 89% HDPE, 1% wax by mass.

The fiber mass content was set at 10% for all biocomposites. Details of extrusion compounding can be found in section 3.2.2. The injection molding was conducted at NAIT using the following injection temperatures (Figure 3.9): A-188°C (370°F), B-188°C (370°F), C-182°C (360°F), D- 165°C (330°F). The processing time settings (Figure 3.10) were: injection – 10 s, hold – 20 s, back – 20 s, open – 15 s. Injection pressure was 5.5 MPa (800 psi). Then the tensile, flexural, water absorption and morphology properties of these three flax fiber-HDPE biocomposites were tested. Chemical composition and melting point of final fiber to be chosen were also determined.

3.3.3 Experiments for determine the factors affecting injection molding of biocomposites

Fiber content in biocomposite will change its properties and may require different injection molding conditions. When considering how injection molding factors such as temperature and pressure influence the properties of biocomposite, the influence of fiber content was also considered as one of the factors. The materials were flax fiber I and HDPE. To process the biocomposites, flax fiber was first

acrylic acid treated, ground through 2 mm screen using the grinding mill, mixed with HDPE, then extrusion compounded (refer to section 3.2.2) and injection molded to biocomposite specimens. Injection molding was conducted in NAIT, and time was set as: injection - 10 s, hold - 15 s, back - 20 s, open - 15 s.

Three factors, namely, fiber content (% mass), injection temperature, and injection pressure were investigated as to their influence on mechanical properties and water absorption of biocomposites. The experimental design including factors and levels are shown in Table 3.6.

Table 3.6 Three-factor experimental design used in injection molding experiment.

Trial	Fiber content (% mass)	Injection Temperature (ºC)	Injection Pressure (MPa)
1	10	166-188 *	4.8
2	10	166-188	6.9
3	10	177-200 **	4.8
4	10	177-200	6.9
5	20	166-188	4.8
6	20	166-188	6.9
7	20	177-200	4.8
8	20	177-200	6.9
9	30	166-188	4.8
10	30	166-188	6.9
11	30	177-200	4.8
12	30	177-200	6.9

* Injection temperatures are D=166ºC, C=182ºC, B=188ºC and A=188ºC
** Injection temperatures are D=177ºC, C=190ºC, B=200ºC and A=200ºC

The three levels of fiber content were 10%, 20%, and 30% by mass. The two levels of injection temperatures were: 1) D=166ºC (330ºF), C=182ºC (360ºF), B=188ºC (370ºF), A=188ºC (370ºF); and 2) D=177ºC (350ºF), C=190ºC (375ºF), B=200ºC (390ºF), A=200ºC (390ºF). During plotting and discussion of results,

injection temperature was designated by temperature at zone A, the temperature at which the biocomposites finally heated. The two levels of the injection pressure were 4.8 MPa (700 psi) and 6.9 MPa (1000 psi).

Tensile and flexural properties, water absorption, and density of biocomposite samples were measured to compare the effects of the three factors on biocomposite properties. SPSS (SPSS Inc., Chicago, IL) and SAS (SAS Institute, Cary, NC) were used to analyze whether the three factors have significant influence on the properties.

3.3.4 Filling time prediction

The filling time in injection molding means the duration of material flow inside the mold. It starts from the time that the hot material is injected into the mold and ends when the mold is filled with the material. But during filling, the flowing material inside the mold is considered an incompressible fluid. After filling stage, packing/holding stage starts, the pressure is raised and extra material is forced into the mold. Because the material in packing stage is compressible fluid, it is very complicated to analyze. Only filling time is considered in this research. Filling time may be affected by material rheological properties, thermal properties, and mold shape. The rheological properties of biocomposites were measured using a rheometer and filling time was predicted using a one-dimensional approach. To predict the filling time, a simplified mold was assumed as shown in Figure 3.12. The dimensions of the sprue, runner, and mold cavity are shown in Figure 3.13. In this

mold, the sprue and the runner were cylindrical (circular cross section) and the mold cavity is a rectangular slab (rectangular cross section).

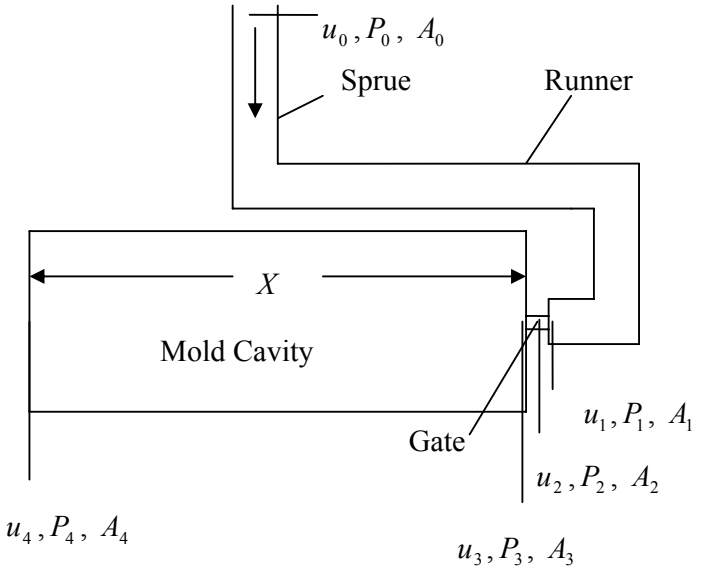

Figure 3.12 Mold used to predict injection filling and cooling times.

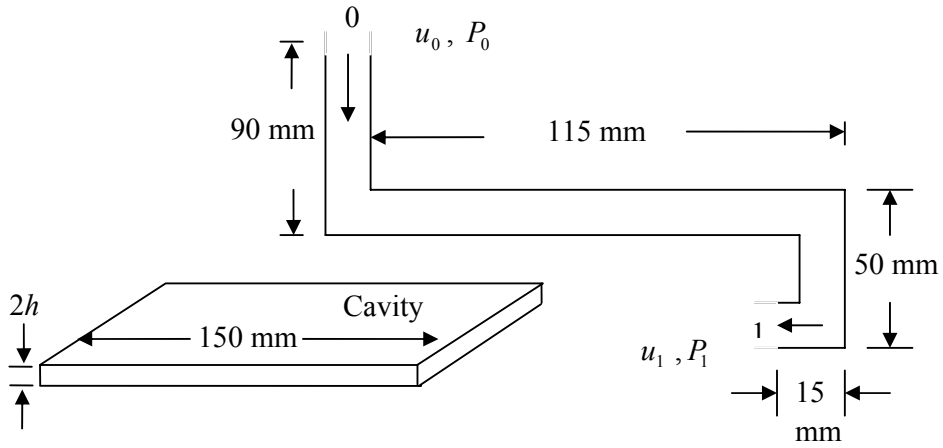

Figure 3.13 Dimensions of sprue, runner, and mold cavity in the mold used to predict injection filling and cooling times.

The total length of flow in sprue and runner is assumed as: L = 90 + 115 + 50 + 15 mm = 0.27 m.

The length of flow in the mold cavity is X = 150 mm = 0.15 m.

The diameter of the sprue and runner is D = 9 mm = 0.009 m; radius R= 4.5 mm = 0.0045 m.

The thickness ($2h$) of mold cavity is $2h$ = 4 mm; h = 2 mm = 0.002 m.

The cross sectional area of the sprue and runner is: $A_0 = A_1 = \pi \times (0.0045)^2 = 64 \times 10^{-6}$ m^2.

The area of A_2 is $A_2 = 9 \times 0.5$ $mm^2 = 4.5 \times 10^{-6}$ m^2.

$A_3 = A_4 = 37 \times 4$ $mm^2 = 148 \times 10^{-6}$ m^2.

Assumptions

Some simplification and assumptions were made when the material (fluid) is flowing inside the mold during the filling stage of injection molding. The following are the assumptions:

(1) the material has the characteristics of a power-law fluid when it flows inside the mold, therefore $\tau = K\left(\frac{du}{dy}\right)^n$;

(2) fluid flow is steady one-directional, one dimensional laminar flow;

(3) the fluid is incompressible during the filling stage;

(4) the gravitational effect is neglected, so the density is constant;

(5) there is no slip between the fluid and the solid wall;

(6) the influence of differential temperature between flow and mold is ignored;

(7) the sprue and runner are assumed as cylindrical;

(8) the flow in the cavity is assumed as flow between two parallel plates;

(9) the friction during the fluid flow in the mold is neglected;

(10) the pressure of the front flow at the end of filling stage is assumed as zero when flow reached the end edge of cavity.

Mass balance

In the filling stage, the fluid is assumed to be incompressible. For any two points during fluid flow, the fluid density is constant, $\rho_1 = \rho_2$. The continuity of mass flow across the control volume is expressed as:

$$\dot{m}_1 = \dot{m}_2 \tag{3.1}$$

That is $$\rho_1 A_1 u_1 = \rho_2 A_2 u_2 \tag{3.2}$$

Thus, $$A_1 u_1 = A_2 u_2 \tag{3.3}$$

where: $\dot{m}$ = flow rate (kg/s or g/s),

ρ = fluid density (kg/m^3 or g/cm^3),

A = cross sectional area (m^2), and

u = local velocity (m/s).

During the filling stage, the continuity equation (Equation 3.2) is applied to one-dimensional incompressible steady flow which gives:

$$u_0 A_0 = u_1 A_1 = u_2 A_2 = u_3 A_3 = u_4 A_4 \tag{3.4}$$

where $$u_0 = u_1 \tag{3.5}$$

$$u_2 = \frac{A_1}{A_2} u_1 \tag{3.6}$$

$$u_3 = \frac{A_1}{A_3} u_1 \tag{3.7}$$

$$u_3 = u_4 \tag{3.8}$$

Velocity of melt flow

The materials (HDPE and biocomposites) flow inside the sprue and runner are assumed to be laminar flow in a cylinder. The average velocity $\bar{u}$ for one dimensional laminar flow of non-Newtonian fluid is (refer to Appendix A):

$$\bar{u} = \frac{Q}{\pi R^2} = \left[\left(\frac{\Delta P}{\Delta x}\right)\frac{1}{2K}\right]^{\frac{1}{n}}\left(\frac{n}{1+3n}\right)R^{\frac{1}{n}+1} \tag{3.9}$$

From above equation and ignoring the influence of friction, the average velocity u_1 is given as:

$$u_1 = \left[\left(\frac{P_0 - P_1}{L}\right)\frac{1}{2K}\right]^{\frac{1}{n}}\left(\frac{n}{1+3n}\right)R^{\frac{1}{n}+1} \tag{3.10}$$

The material flow inside the mold cavity is supposed to be a fully developed laminar flow in fixed parallel plates because the thickness of the mold cavity is quite small compared with the width and length. The average velocity $\bar{u}$ for laminar flow in parallel plates is (refer to Appendix B):

$$\bar{u} = \frac{Q}{2hW} = \frac{n}{(2n+1)}\left[\left(\frac{\Delta P}{dx}\right)\left(\frac{1}{K}\right)\right]^{\frac{1}{n}} h^{\frac{1}{n}+1} \tag{3.11}$$

The velocity u_3 and u_4 become:

$$u_3 = u_4 = \frac{n}{(2n+1)}\left[\left(\frac{P_3 - P_4}{X}\right)\left(\frac{1}{K}\right)\right]^{\frac{1}{n}} h^{\frac{1}{n}+1} \tag{3.12}$$

If it is assumed that $P_4 = 0$ at the end of incompressible filling stage while just before the material touches the mold edge, then u_3 becomes:

$$u_3 = \frac{n}{(2n+1)}\left[\left(\frac{P_3}{X}\right)\left(\frac{1}{K}\right)\right]^{\frac{1}{n}} h^{\frac{1}{n}+1} \tag{3.13}$$

At the cavity gate, the cross section area of flow is suddenly decreased (from runner to gate) and then suddenly increased (from gate to mold cavity), so there is pressure loss due to sudden contraction (E_{fc}) and expansion (E_{fe}). If we suppose that P_1 and P_3 are the pressures at the two edges of the cavity gate as shown in Figure 3.14, then by Bernoulli equation 2.21, the pressure drop is:

$$\frac{P_1 - P_3}{\rho} = E_{fc} + E_{fe} \tag{3.14}$$

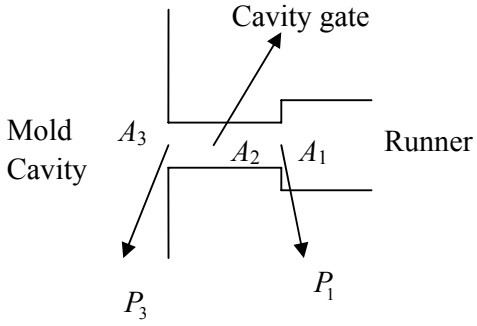

Figure 3.14 Pressure P_1 and P_3 assumed as close as to the edge of cavity gate.

Skelland (1967) and Wilkinson (1960) reported that experiments indicated there was no appreciable difference between non-Newtonian and Newtonian fluid pressure losses due to contraction in either laminar or turbulent flow. Thus, the fluid was assumed as Newtonian when calculating pressure loss due to contraction in Non-Newtonian fluid. Since $\frac{A_2}{A_1} < 0.715$, by equations 2.26, 2.27 and 3.10, we get:

$$E_{fc} = 0.4\left[1.25 - \left(\frac{A_2}{A_1}\right)\right]\frac{\left(\overline{u_2}\right)^2}{2}$$

$$= 0.2\left[1.25 - \left(\frac{A_2}{A_1}\right)\right]\left(\frac{A_1}{A_2}\right)^2\left[\left(\frac{P_0 - P_1}{L}\right)\frac{1}{2K}\right]^{\frac{2}{n}}\left(\frac{n}{1+3n}\right)^2 R^{\frac{2}{n}+2} \tag{3.15}$$

By equation 2.31, the expansion loss in laminar flow for a power-law fluid is given as (Wilkinson 1960; Skelland 1967):

$$E_{fe} = \left(\frac{Q}{A_2}\right)^2\left(\frac{3n+1}{2n+1}\right)\left[\frac{n+3}{2(5n+3)}\left(\frac{A_2}{A_3}\right)^2 - \left(\frac{A_2}{A_3}\right) + \frac{3(3n+1)}{2(5n+3)}\right] \tag{3.16}$$

where $Q = u_2 A_2 = u_1 A_1$ (3.17)

Substituting equations 3.10 and 3.17 into equation 3.16:

$$E_{fe} = \left(\frac{A_1}{A_2}\right)^2\left(\frac{3n+1}{2n+1}\right)\left[\frac{n+3}{2(5n+3)}\left(\frac{A_2}{A_3}\right)^2 - \left(\frac{A_2}{A_3}\right) + \frac{3(3n+1)}{2(5n+3)}\right]\left[\left(\frac{P_0 - P_1}{L}\right)\frac{1}{2K}\right]^{\frac{2}{n}}\left(\frac{n}{1+3n}\right)^2 R^{\frac{2}{n}+2} \tag{3.18}$$

Combining equations 3.15 and 3.18 into 3.14, the relationship between P_1 and P_3 is given as:

$$P_1 - P_3 = 0.2\rho\left[1.25 - \left(\frac{A_2}{A_1}\right)\right]\left(\frac{A_1}{A_2}\right)^2\left[\left(\frac{P_0 - P_1}{L}\right)\frac{1}{2K}\right]^{\frac{2}{n}}\left(\frac{n}{1+3n}\right)^2 R^{\frac{2}{n}+2} +$$

$$\left(\frac{A_1}{A_2}\right)^2 \rho\left(\frac{3n+1}{2n+1}\right)\left[\frac{n+3}{2(5n+3)}\left(\frac{A_2}{A_3}\right)^2 - \left(\frac{A_2}{A_3}\right) + \frac{3(3n+1)}{2(5n+3)}\right]\left[\left(\frac{P_0 - P_1}{L}\right)\frac{1}{2K}\right]^{\frac{2}{n}}\left(\frac{n}{1+3n}\right)^2 R^{\frac{2}{n}+2} \tag{3.19}$$

By substituting u_1(Equation 3.10), u_3(Equation 3.13) into $u_3 = \frac{A_1}{A_3}u_1$ (Equation 3.7), then:

$$P_3 = (P_0 - P_1)\left(\frac{X}{2L}\right)\left(\frac{A_1}{A_3}\right)^n\left(\frac{R}{h}\right)^{1+n}\left(\frac{2n+1}{1+3n}\right)^n \tag{3.20}$$

Combining Equations 3.19 and 3.20, we get:

$$P_1 - 0.2\rho\left[1.25 - \left(\frac{A_2}{A_1}\right)\right]\left(\frac{A_1}{A_2}\right)^2\left[\left(\frac{P_0 - P_1}{L}\right)\frac{1}{2K}\right]^{\frac{2}{n}}\left(\frac{n}{1+3n}\right)^2 R^{\frac{2}{n}+2} -$$

$$\left(\frac{A_1}{A_2}\right)^2 \rho\left(\frac{3n+1}{2n+1}\right)\left[\frac{n+3}{2(5n+3)}\left(\frac{A_2}{A_3}\right)^2 - \left(\frac{A_2}{A_3}\right) + \frac{3(3n+1)}{2(5n+3)}\right]\left[\left(\frac{P_0 - P_1}{L}\right)\frac{1}{2K}\right]^{\frac{2}{n}}\left(\frac{n}{1+3n}\right)^2 R^{\frac{2}{n}+2} =$$

$$(P_0 - P_1)\left(\frac{X}{2L}\right)\left(\frac{A_1}{A_3}\right)^n\left(\frac{R}{h}\right)^{1+n}\left(\frac{2n+1}{1+3n}\right)^n \tag{3.21}$$

where K, n will be determined from experiment on viscosity measurement, X, L, R, and h are related with the mold dimensions.

Equation 3.21 gives the relationship between P_0 and P_1. At a given pressure P_0 and a given mold cavity size, P_1 could be solved from equation 3.21. After P_1 is solved, P_3 could be calculated using equation 3.20. Then u_1 and u_3 could be calculated from equations 3.10 and 3.7, respectively.

Filling time

The time to fill the sprue and runner (t_1) is estimated as:

$$t_1 = \frac{L}{u_1} \tag{3.22}$$

The time to fill the cavity (t_3) is:

$$t_3 = \frac{X}{u_3} \tag{3.23}$$

The gate is very short, so the time to fill through the gate (t_2) is neglected. Thus, the total time to fill the mold (t) is:

$$t = t_1 + t_3 \tag{3.24}$$

Thus, t is the filling time of the mold shown in Figure 3.12. Shorter than this time, the flow cannot fill the whole mold; longer than this time, the flow becomes compressible fluid.

Biocomposite sample preparation for measuring rheological properties

As shown in equation 3.21 and to predict the filling time, the values of consistency coefficient (K) and flow behavior index (n) for biocomposite materials need to be determined first by viscosity measurement. Flax fiber I-HDPE biocomposites and pure HDPE were prepared as samples whose viscosities are measured. Flax fiber I was acrylic acid treated, ground and mixed with HDPE, and extrusion compounded at temperature and screw rotational speed referred to in section 3.2.2. Then the extruded biocomposites were pelletized and ground using a grinding mill with a 2 mm screen. Three biocomposites were prepared with fiber content of 10%, 20%, and 30% by mass, respectively, and they were designated as A1, A2, and A3 biocomposite, respectively. The biocomposite powders were the samples whose rheological properties were to be measured.

3.3.5 Minimum cooling time prediction

Equation 2.32 was used to estimate the minimum cooling time (t_c) in injection molding. Combining the mold in Figures 3.12 and 3.13, the minimum cooling time for such a rectangular molded product becomes:

$$t_c = \frac{(2h)^2}{\alpha \pi^2} \ln\left[\frac{4}{\pi}\left(\frac{T_m - T_w}{T_e - T_w}\right)\right] \tag{3.25}$$

where α = material thermal diffusivity (m^2/s), $\alpha = \frac{k}{\rho C_p}$

k = material thermal conductivity (W/m°C),

C_p = material specific heat (kJ/kg°C),

h = half of the thickness of material inside the mold (m),

T_w = mold wall temperature (°C),

T_m = melted material temperature (°C), and

T_e = ejection temperature (°C).

It is assumed that the material's original temperature (T_m) is the injection temperature set on the injection machine. The thickness ($2h$) of the material being molded is 0.004 m and mold wall temperature (T_w) is 40°C; then the minimum cooling time at a certain ejection temperature (mold open temperature) can be predicted.

Biocomposite sample preparation for measuring thermal diffusivity

Biocomposite preparation was the same as what was described in section 3.3.4. The density (ρ), thermal conductivity (k), and specific heat (C_p) of biocomposites were measured as described in section 3.4.3, 3.4.9, and 3.4.10, respectively. After that, the thermal diffusivity (α, m^2/s) of material is calculated from the following equation:

$$\alpha = \frac{k}{\rho C_p} \tag{3.26}$$

Since thermal diffusivity was calculated as a secondary quantity, the standard deviation of thermal diffusivity (SD_α) was calculated from equation (Emami at al. 2007):

$$SD_\alpha = \sqrt{\left(\frac{\partial \alpha}{\partial k} SD_k\right)^2 + \left(\frac{\partial \alpha}{\partial \rho} SD_\rho\right)^2 + \left(\frac{\partial \alpha}{\partial C_p} SD_{C_p}\right)^2} \quad (3.27)$$

where SD_k = standard deviation of measured thermal conductivity,

SD_ρ = standard deviation of measured density, and

$SD_{C\rho}$= standard deviation of measured specific heat.

3.4 Testing of material and biocomposite properties

Material and biocomposite properties are important in determining the effect of processing on the product and analyze the mechanism during processing. These properties include the chemical and physical, morphological, mechanical, rheological, and thermal properties.

3.4.1 Determination of fiber chemical composition using fiber analyzer

Determination of flax fiber chemical composition was carried using the ANKOM 200/220 Fiber Analyzer (ANKOM Technology, Fairport, NY) shown in Figure 3.15. Acid detergent lignin (ADL), acid detergent fiber (ADF), neutral detergent fiber (NDF) and ash were determined as percent of dry matter following the procedure documents of the Fiber Analyzer (ANKOM Technology Method 2005).

Figure 3.15 ANKOM 200/220 Fiber Analyzer (ANKOM Technology, Fairport, NY).

Crude fat in the fiber was not considered since there were no reports on fat composition of flax fibers. Thus, percentages of cellulose, hemicellulose, and lignin were determined from the following equations:

Lignin (% dry matter) = ADL (3.28)

Cellulose (% dry matter) = ADF – ADL (3.29)

Hemicellulose (% dry matter) = NDF – ADF (3.30)

3.4.2 Morphological analysis by Scanning Electron Microscopy (SEM)

SEM was used to analyze the morphological structure of fibers and fiber-plastic composites. The materials were first coated with gold using an Edwards S150B sputter coater (BOC Edwards, Wilmington, MA) to make the sample conductive. The coated sample was then taken microscope images using SEM505 (Philips Electron Optics，Eindhoven, Netherlands) at 300KV. By observing the surface of flax fiber and biocomposite, the microstructures of materials were compared.

Figure 3.16 Scanning electron microscope (Philips Electron Optics， Eindhoven, Netherlands).

3.4.3 Density measurement

The density of a material is the mass per unit volume. Three replicates of density analysis were performed for each sample. Material mass (m, g) was measured by a Galaxy 160D weighing scale (OHAUS Scale Corporation, Florham Park, NJ). The volume of a sample (V, cm^3) was measured using a gas-operated (nitrogen gas) multi-pycnometer (Quantachrome Corporation, Boynton Beach, FL) shown in Figure 3.17.

Figure 3.17 Gas-operated multi-pycnometer (Quantachrome Corporation, Boynton Beach, FL).

The multi-pycnometer is an instrument specifically designed to measure the true volume of various quantities of solid materials. The technique employs the Archimedes principle of fluid displacement by measuring the pressure difference when a known quantity of gas penetrates the finest pores of materials. The volume of the material was determined from the following equation:

$$V = V_C - V_R[(P_I / P_{II}) - 1] \tag{3.31}$$

where V = Volume of sample (cm^3),

V_C = volume of sample cell (cm^3),

V_R = reference volume (cm^3),

P_I = pressure reading after pressurizing the reference volume (psi), and

P_{II} = pressure reading after including V_C (psi).

Then the experimental density (ρ, g/cm^3) is calculated as:

$$\rho = m/V \tag{3.32}$$

For composites, another density of importance is the ideal density, which is the predicted density of composites knowing the density of each component. The density of flax fiber and polymer matrix was measured; then the ideal density (ρ_i) of the biocomposite was calculated using the following equation (Stroshine 2000):

$$\rho_i = \frac{1}{\frac{M_f}{\rho_f} + \frac{M_m}{\rho_m}} \tag{3.33}$$

where M_f = mass fraction of flax fiber (g),

M_m = mass fraction of matrix (g), e.g. HDPE,

ρ_f = density of flax fiber (g/cm^3), and

ρ_m = density of matrix, e.g. HDPE (g/cm^3).

3.4.4 Tensile test

Tensile test of biocomposite specimens followed ASTM Standard test method D638 (ASTM 1997a). The test specimens were conditioned at temperature of 23 ± 2°C and relative humidity of 50 ± 5% for more than 40 h prior to the test. The Instron Universal testing machine (SATEC Systems Inc., Grove City, PA – Figure 3.18) or Instron Model 1122 testing machine (Instron Corp., Canton, MA – Figure 3.19) were used to perform the tensile strength test at a crosshead speed of 5 mm/min. Each test was performed until tensile failure occurred. The test was conducted on 5 specimens per biocomposite sample. The maximum (peak) load (F_{max}, N) was read from the instrument. The tensile strength (σ_t, Pa) was then calculated according to the following equation:

$$\sigma_t = \frac{F_{\max}}{A} \tag{3.34}$$

where A = cross-sectional area (m^2).

The percent elongation of biocomposite is the percentage increase in length of the specimen at its breaking point and is calculated from the following equation:

$$\%Elongation = \frac{L - L_0}{L_0} \times 100 \tag{3.35}$$

where L_0 = original measured length (m), and

L = length of the specimen at its breaking point (m).

Figure 3.18 Instron Universal testing machine (SATEC Systems Inc., Grove City, PA).

Figure 3.19 Instron Model 1122 testing machine (Instron Corp., Canton, MA).

3.4.5 Flexure test

The three-point testing method was used to determine the flexural strength and modulus according to ASTM D790 (ASTM 1997b). The test specimens for composite sample had nominal dimensions of 3.2 mm × 12.7 mm × 64 mm. Before

testing, the specimens were conditioned at a temperature of 23 ± 2°C and relative humidity of 50 ± 5% for more than 40 h.

The flexural strength (S) was determined using the maximum fiber stress (ASTM 1997b) as equation:

$$S = \frac{3P'L}{2bd^2} \tag{3.36}$$

where S = flexural strength (Pa),

P' = load (N),

L = length of span (m),

b = width of specimen (m), and

d = thickness of specimen (m).

The flexural modulus is the modulus of elasticity and "is the ratio, within the elastic limit, of stress to corresponding strain" (ASTM 1997b). It is determined from equation 3.37:

$$E_H = \frac{L^3 s}{4bd^3} \tag{3.37}$$

where E_H = modulus of elasticity in bending (Pa), and

s = slope of the tangent to the initial straight-line portion of the load deflection curve (N/m).

The testing was conducted using the Instron model 1011 testing machine (Instron Corp., Canton, MA) as shown in Figure 3.20. Each biocomposite sample had 5 specimens to test. Flexural strength and modulus were recorded from the computer connected to the testing unit.

Figure 3.20 Flexural testing using the Instron model 1011 testing machine (Instron Corp., Canton, MA).

3.4.6 Water absorption

Water absorption is used to determine the amount of water absorbed by a biocomposite. The water absorption test followed ASTM standard test method D570 (ASTM 1998). The test specimen was in the form of a bar 76.2 mm long, 25.4 mm wide and 3.2 mm thick. Before the measurement, the sample was dried in an air oven at 50°C for 24 h, cooled in a desiccator, and immediately weighed to the nearest 0.001 g which is then taken as the dry initial weight of the sample, M_0. Then the specimen was placed in a container of distilled water maintained at a temperature of 23 ± 1°C for 24 h as shown in Figure 3.21. After 24 h, the specimen was removed from water; water was wiped off the surface of the sample with a dry cloth; and the sample was immediately weighed to the nearest 0.001 g, which is designated as M_1.

For each biocomposite sample, 3 specimens were meausred. The water absorption of the sample was calculated as percent weight change (*M%*) determined as follows:

$$M\% = \frac{M_1 - M_0}{\mathrm{M}_0} \times 100 \tag{3.38}$$

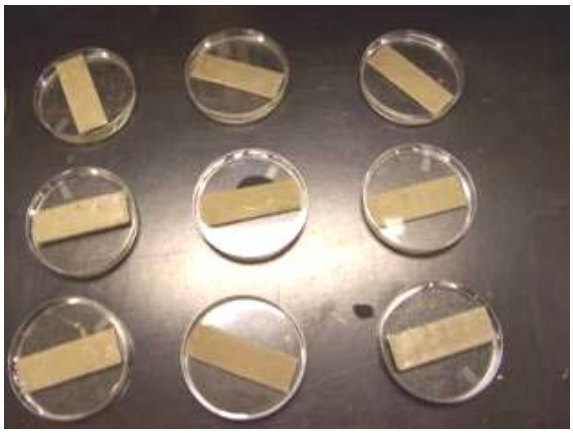

Figure 3.21 Water absorption measurement.

One exception in the specimen dimension mentioned previously, was when comparing biocomposite samples from experiments on fiber chemical treatment effects (section 3.3.1). The dimensions of these particular specimens were 36 mm × 19 mm × 3.2 mm due to the limitation of the previous injection mold.

3.4.7 Viscosity measurement

Viscosity is the resistance to flow when polymers or biocomposites are melted. This property helps in the understanding of the rheology of materials. If a biocomposite has high viscosity, it is difficult to deform the material to the required shape. To study the rheological property of a material, the Model 3211 capillary rheometer (Instron Corp., Canton, MA) was used (Figure 3.22).

Figure 3.22 Capillary rheometer (model 3211, Instron Corp., Canton, MA).

The viscosities of melted HDPE and biocomposites were measured at temperatures of 170, 180, 190, and 200°C in two replicates per sample. Five drive (crosshead) speeds on the rheometer were used, namely, 0.06, 0.2, 0.6, 2.0, 6.0, and 20.0 cm/min (0.03, 0.1, 0.3, 1.0, 3.0, and 10.0 inch/min) which could be converted to shear rate using equation 3.40. The melted sample was extruded through the die of defined dimensions and the force required to extrude the melt was read from the meter when the reading stabilized. The shear stress (**τ,** Pa) was calculated from equation 3.39 (Instron 1993).

$$\tau = \frac{F'}{4A_p\left(l_c / d_c\right)} \tag{3.39}$$

where τ = shear stress (Pa),

A_p = cross-sectional area of the plunger (0.9525 cm diameter),

F' = force acting on the plunger (kgf or lbf),

l_c = length of capillary tube (1.0063 in), and

d_c = capillary diameter (0.05 in).

The wall shear rate (γ, s^{-1}) for a non-Newtonian fluid (Instron 1993) is calculated from:

$$\gamma = \frac{2}{15}\frac{3n+1}{4n} V_{xh} \frac{d_b^2}{d_c^3} \tag{3.40}$$

where n = the slope of the graph of $\ln \tau$ versus $\ln\left(\frac{8V}{d_c}\right)$,

$$n = \frac{d \ln \tau}{d \ln\left(\frac{8V}{d_c}\right)},$$

$$V = \frac{V_{xh}}{60}\left(\frac{d_b}{d_c}\right)^2,$$

V_{xh} = crosshead speed (in/min), and

d_b = barrel diameter (0.375 in or 0.9525cm).

From equation 3.41, consistency coefficient K ($Pa \cdot s^n$) and flow behavior index n could be estimated from the curve of shear stress vs. shear rate.

$$\tau = K(\gamma)^n \tag{3.41}$$

Apparent viscosity (μ_a , Pa·s) was calculated as:

$$\mu_a = \tau / \gamma = K(\gamma)^{n-1} \tag{3.42}$$

3.4.8 DSC measurement of thermal characteristic temperatures measured by DSC

Differential scanning calorimetry (DSC) is a technique that measures the amount of energy required to establish a nearly zero temperature difference between

the sample and a reference material (Walshaw et al. 1998). DSC measurements provide quantitative and qualitative information about endothermic and exothermic reactions, as well as changes in heat capacity of a material, therefore it can be used to measure a number of characteristic properties of a sample. A schematic DSC curve demonstrating the appearance of several common features, e.g. glass transition, crystallization, and melting point of a plastic is given in Figure 3.23. Polymer absorbs heat when being melted and releases heat during degradation. Therefore, the melting point and degradation temperatures of polymers or composites could be observed from the DSC curve.

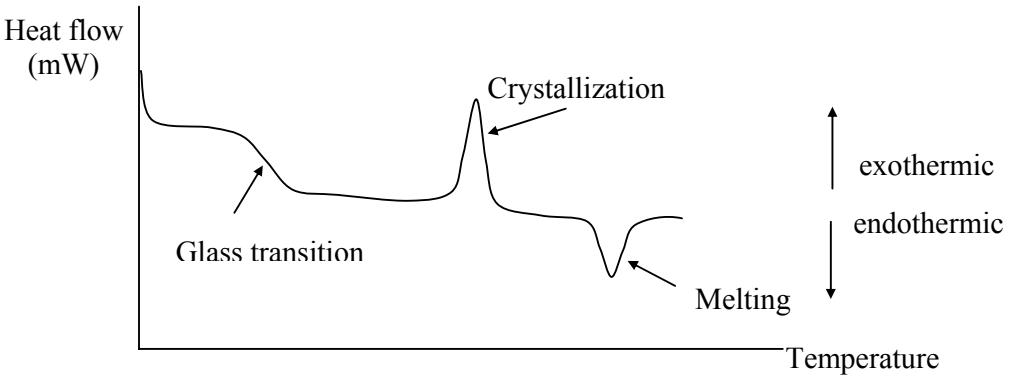

Figure 3.23 Schematic DSC curve demonstrating the appearance of several common features (Wang 2004).

DSC analyses of flax fiber I was performed using the DSC 2910 (TA Instruments, New Castle, DE). Analyses of HDPE and biocomposites were performed using TG-DSC 111 (Setaram Scientific & Industrial Equipment, Caluire, France). DSC 2910 was calibrated using a reference sample of sapphire and TG-

DSC 111 used a blank reference sample. A heating rate of 5ºC/min was used in both DSC equipments.

Figure 3.24 Differential scanning calorimetry - DSC 2910 (on the left) and TG-DSC 111 (on the right) used in measuring thermal characteristics of sample.

3.4.9 Thermal conductivity measurement at high temperature

Thermal conductivity of biocomposite at temperatures above melting point was measured based on the line source method (Lobo and Cohen 1990). This method considers the heat transfer from probe to the material as the case of heat transfer in an infinite length cylinder. A constant finite quantity of heat Q' was produced per unit of length at certain time. The change in temperature ($T_2 - T_1$) at time interval ($t_2 - t_1$) is given by (Lobo and Cohen 1990):

$$T_2 - T_1 = \frac{Q'}{4\pi k'} \ln\left(\frac{t_2}{t_1}\right) \tag{3.43}$$

where k' = thermal conductivity of the sample before calibration (W/m°C),

Q' = heat input per meter of line source (W/m),

T = temperature (°C), and

t = time (s).

To account for the deviations of the experimental result from the ideal result, a coefficient (C) for the probe is usually established by calibrating the system (Lobo and Cohen 1990).

$$k = Ck' = C\frac{Q'}{4\pi(T_2 - T_1)}\ln\left(\frac{t_2}{t_1}\right) \tag{3.44}$$

The actual experiment may differ in many respects from an ideal situation, such as limited sample size, and length-to-diameter ratio of probe. It was reported that length-to-diameter ratio of a probe greater than 20 could decrease the experimental error due to heat flow by axial conduction (Blackwell and Misener 1951). The sample diameter should be large enough so that the transient heat wave from the probe does not reach the wall of the container. And it should also be minimized so that it could achieve steady state in the shortest time. Lobo and Cohen (1990) reported that a diameter of 8 to 10 mm for a sample was suitable. Based on the above theory, a probe with J-type thermocouples and constantan wire as heater element was designed and assembled to measure thermal conductivity of melted HDPE and biocomposites. The barrel of the Model 3211 capillary rheometer was used as material container and heating source for material.

Probe construction

The probe was constructed from a hollow brass tube. The outer diameter of the brass tube was 1.6 mm and its length was 96 mm. Figure 3.25 shows the schematic diagram of the probe. The end of the tube was sealed with a silver solder

which can resistant temperatures as higher as 210°C. An insulated constantan heating wire (0.254 mm diameter) was extended into the end of the tube and back to the top to make a bifilar constantan wire heating element. A J-type thermocouple (iron-constantan, 0.127 mm diameter) was inserted into the brass tube up to the middle. The wires were all coated with a high thermal conductivity paste (Wakefield Engineering Inc., Wakefield, MA) before inserting them into the hollow brass tube (Opoku et al. 2006). Heat-shrink wrappers, a PTFE (Polytetrafluoroethylene) thread seal tape, and a ceramic fiber rope were used to connect the tube to the extended wires and cover the tube to the extended wires.

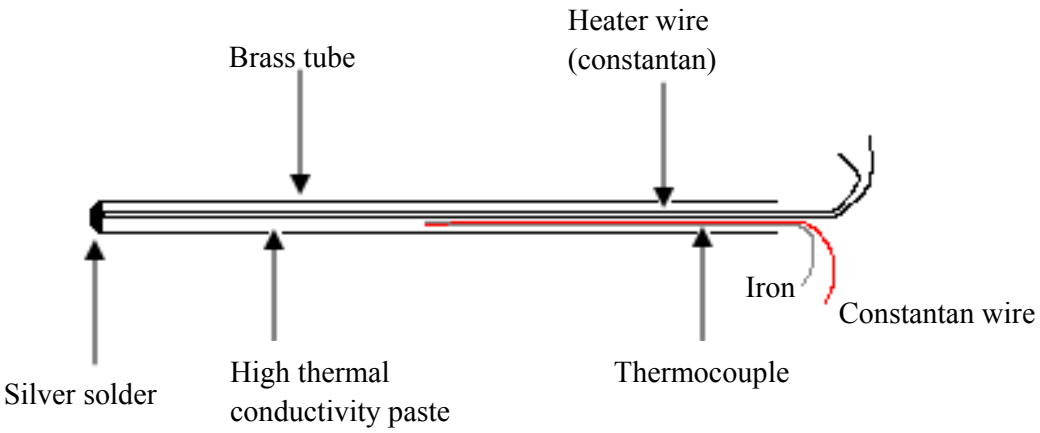

Figure 3.25 Schematic diagram of the probe to measure thermal conductivity.

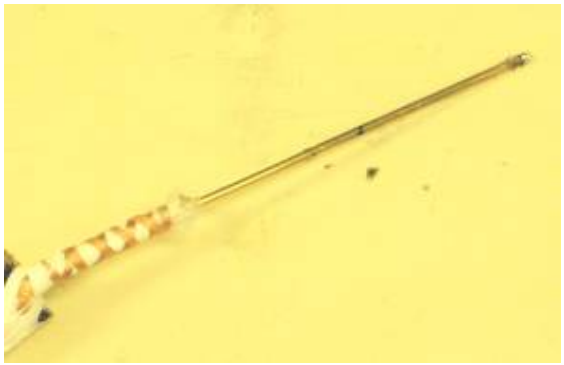

Figure 3.26 The assembled probe used for thermal conductivity measurement.

Measurement instruments setup

The heater wire was connected with a common electric wire (0.8128 mm diameter) outside the probe. It was connected to a 3000 series Switchmode laboratory power supply (Anatek Electronics Ltd. Vancouver, BC), which supplied a constant current to heat the probe. The current through the heating wire was read from a DM-9900 digital multimeter (ABRA Electronics Corp., Champlain, NY) connected to the power supply. An extended J-type thermocouple wire (ASB/Glass 0.8128 mm diameter) was connected to a digital thermometer (OMEGA HH509R, Omega Engineering, Inc. Stamford, CT), which was used to collect time-temperature data. The time-temperature data were observed and recorded by a computer.

The heat produced by the probe's heater is insufficient to melt the test materials and maintain the desired temperatures. Therefore, an external heat source to maintain the temperature of the molten material was necessary. The heater barrel of the capillary rheometer 3211 (Instron Corp., Canton, MA) was used as the heating source and the container for plastic and biocomposite materials. The diameter of the heater barrel was 9 mm, making it suitable as material container according to Lobo

and Cohen (1990). Figures 3.27 and 3.28 show the instrumental setup in measuring the thermal conductivity of melted polymer and biocomposites.

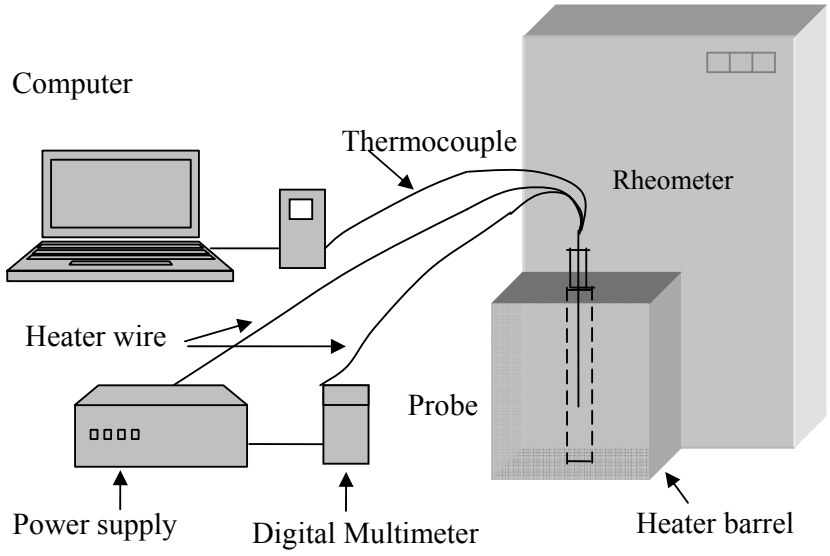

Figure 3.27 Schematic diagram of instrument set up for the thermal conductivity measurement of polymer and biocomposite.

Figure 3.28 Instrumentation setup to measure thermal conductivity of melted HDPE and biocomposites.

When measuring the thermal conductivity of the flax fiber, a controlled environmental chamber (B-M-A Inc., Ayer, MA. - Figure 3.29) was used as the external heat source. The probe was put in the center of a metal container (cross sectional area = 22.5 mm^2; length = 150 mm). Fifty grams of chopped fiber was pressed into the container to ensure that the air inside the fiber was expelled for air has lower thermal conductivity.

Figure 3.29 Environmental chamber for heat fiber during thermal conductivity measurement.

Measurement procedure

Each sample (HDPE or biocomposite) was loaded into the heater barrel and heated to the desired temperature. The probe was then inserted vertically down into the center of the sample. For fiber material, the powdered fiber with inserted probe was put into the environmental chamber to be heated. The sample and the probe were then allowed several minutes to attain thermal equilibrium with the surrounding environment. After this, a small constant voltage was applied to the probe heater for 50 s (Poloski et al. 2002). The change in the probe temperature was recorded via the

data-acquisition system during this period. The time-temperature data obtained were analyzed using a spreadsheet program. Then, the thermal conductivity of the sample was calculated from equation 3.45 as:

$$k = C\frac{Q'}{4\pi(T_2 - T_1)}\ln\left(\frac{t_2}{t_1}\right) \tag{3.45}$$

where $Q' = I^2R'$ = heat input per meter of line source (W/m),

I = electric current (A),

R' = specific resistance of the heating wire (20 Ohms/m),

C = coefficient of probe calibration,

k = thermal conductivity of the sample (W/m°C),

T = temperature (°C), and

t = time (s).

The raw data of temperature change and time obtained from the system were imported into Microsoft Excel. By plotting (T_2-T_1) vs. $ln(t)$, the slope of the straight line, s, was determined by linear regression. Then, the thermal conductivity of the sample from equation 3.45 was converted to:

$$k = C\frac{I^2R'}{4\pi s} \tag{3.46}$$

It was reported by Woo and co-researchers (1995) that the thermal conductivity of HDPE increased with temperature up to 135°C, after which it remained constant. Thus, the thermal conductivity of HDPE was considered to be constant in the temperature range of 170 to 200°C. The thermal conductivity of each

sample was measured within this temperature range. The value of thermal conductivity reported for all samples are the average of three measurements.

Due to lack of literature data, the thermal conductivity of surface-treated flax fiber was also measured from room temperature to 200°C. The container containing the fiber and the probe was placed in the environmental chamber and allowed to attain thermal equilibrium with the surrounding. The same measurement procedure used for the composites was then followed to measure the thermal conductivity of fiber.

System calibration

The calibration of the probe was performed using distilled water as a reference fluid. The thermal conductivity of water at 24ºC is 0.6042 W/m°C (Singh and Heldman 1993). Agar-gelled water (1% agar) was prepared and its thermal conductivity was measured at room temperature in 3 replicates using the probe. The ratio of the thermal conductivity of the reference fluid, k_w (0.6042 W/m°C), to that of agar-gelled water, k_w', gave the calibration coefficient (C) of the probe. The relationship between k_w and k_w' is given by

$$k_w = Ck_w' \tag{3.47}$$

3.4.10 Measurement of specific heat capacity of biocomposites

Specific heat is the amount of heat required per unit mass of substance to raise its temperature by one degree. Specific heat capacity (C_p) of the sample was

measured using the TG-DSC111 (Setaram Scientific & Industrial Equipment, Caluire, France). Measurements were carried out in the temperature range of 30 to 250ºC at a heating rate of 5ºC/min. Precision determination of C_p requires two tests under the same experimental conditions. The first test (blank test) was carried out with two empty vessels without the sample; the second test (sample test) was carried out with the vessels and the sample. Specific heat C_p (kJ/kg°C) was calibrated and automatic calculated by computer systems connected to the DSC according to equation 3.48. Two DSC scans were carried out for each sample to ensure reproducibility.

$$C_p = \frac{HF_{sample} - HF_{blank}}{Sensitivity(T) Mass_{sample} \frac{dT}{dt}} \tag{3.48}$$

where HF_{sample} = heat flow rate measured from the sample test (kJ/s),

HF_{blank} = heat flow rate measured from the blank test (kJ/s),

Sensitivity = system calibration value,

$Mass_{sample}$ = mass of sample (kg), and

$\frac{dT}{dt}$ = heating rate (K/s).

3.5 Statistical analysis of data

The SAS (SAS Institute, Cary, NC) and SPSS (SPSS Inc., Chicago, IL) statistical softwares were used on some experimental data analysis. Linear or non-linear regression models could be developed from SPSS or SAS softwares based on experimental values. Analysis of variance (ANOVA) was used to test the differences

and significance among the independent factors. Tests of between-subjects effects gave the interaction information between factors. Multiple comparisons by Tukey's method in SPSS were applied to compare the means and difference of two and more than two factors. The level of significance used in the aforementioned statistical analyses was 5%.

4. RESULTS AND DISCUSSION

In chapter 3, experiments were designed to achieve the objectives listed in chapter 1, including the comparison of chemical treatments, choosing materials (fiber and matrix), the effect of fiber content on properties, and the influence of injection molding factors. The results of these experiments are presented and discussed in this chapter.

4.1 Selection of chemical treatment and polymers

Six treatments including untreated (U), alkaline (N), silane (S), potassium permanganate (P), acrylic acid (A), and sodium chlorite (C) treatments were conducted on flax fiber material III. These fibers were then mixed with PE (LLDPE and HDPE, respectively) at 10% fiber mass content and processed to biocomposites as discussed in section 3.3.1. Fiber mass content was maintained at 10% in biocomposites and the remaining 90% was plastic matrix. At the same time, pure LLDPE and HDPE were also injection molded for comparison. To compare the effect of fiber chemical treatments on biocomposites, fiber surface morphological properties, biocomposite tensile strength, and water absorption were determined.

4.1.1 Morphological properties of the chemical-treated flax fibers

Six treatments (U, N, S, P, A, C) were carried on flax fiber. After the fibers were dried, SEM images were taken on the treated fiber surfaces. SEM is a frequently used technique to investigate the morphological characteristics of fibers and fiber-plastic composites (Mohanty et al. 2004; Colom et al. 2003; Baley 2002). Figure 4.1 shows the surfaces of untreated (U) and treated (N, S, P, A, C) flax fibers taken by SEM.

The SEM micrograph of the untreated fiber (Figure 4.1-a) shows the presence of natural waxy substances on the fiber surface. Such waxy substances contributed to the ineffective fiber-matrix bonding and poor surface wet-out (Mohanty et al. 2003). The micrographs on Figures 4.1-b to 4.1-f reveal that all chemical modifications smooth the fiber surface. This is probably due to the removal of the fiber's outer surface layer through dissolution in chemical solutions during treatments. The smooth surface is observed among silane- and acrylic acid-treated fibers (Figure 4.1-c and e), showing the best effect on the removal of the waxy layer. Sodium chlorite (Figure 4.1-f) treatment not only smoothed the fiber surface, but also bleached the fiber. Compared with other treatments, potassium permanganate-treated fiber has the roughest surface. As the waxy layer was being removed, oxidation took place between permanganate and the fiber, which was similarly observed by Li and co-researchers (2000).

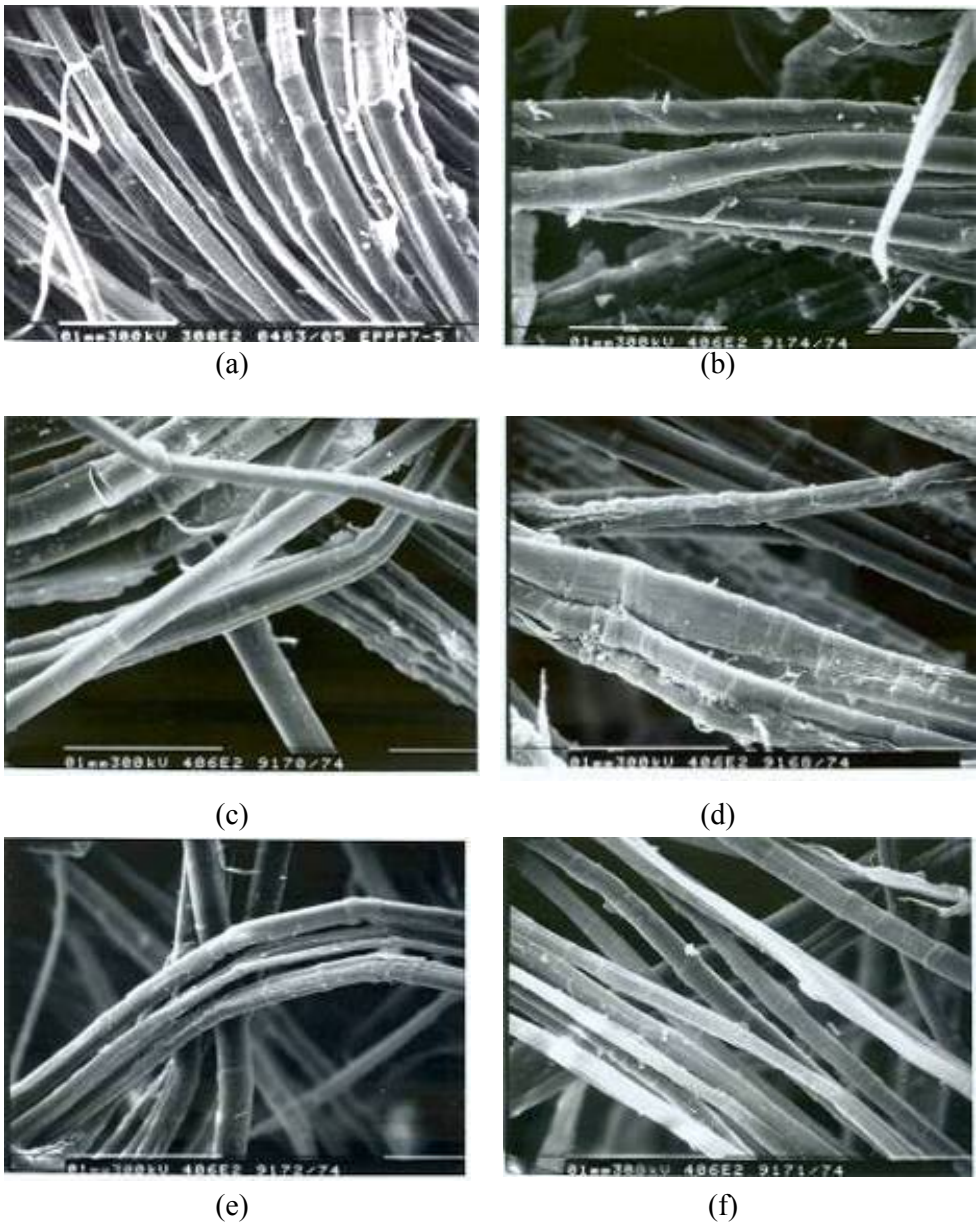

Figure 4.1 Scanning electronic micrographs of flax fiber III surface after different surface modifications: (a) untreated (U); (b) alkali-treated (N); (c) silane-treated (S); (d) potassium permanganate-treated (P); (e) acrylic acid-treated (A); (f) sodium chlorite-treatment (C).

4.1.2 Tensile strength of flax fiber-PE biocomposites

The tensile strength of unreinforced molded LLDPE and HDPE and their treated fiber reinforced-biocomposites are presented in Figures 4.2 and 4.3. Results showed that HDPE as well as fiber-HDPE biocomposites had higher tensile strength than LLDPE and fiber-LLDPE biocomposites.

The tensile strength of injection molded pure LLDPE was the lowest at 13.43 MPa. Addition of flax fiber into LLDPE or HDPE, which formed biocomposites, all resulted in higher tensile strength. Statistical analysis (Tables C.1 and C.2 in Appendix C) proved that there was significant difference between the tensile strength of unreinforced matrix (LLDPE or HDPE) and all that of the fiber reinforced-biocomposites. This indicated that adding flax fiber into LLDPE or HDPE significantly improved the tensile strength of the biocomposite.

As discussed previously, since flax fiber has a higher tensile strength than polyethylene and polypropylene, it can be used to reinforce PE and PP. Some studies were carried on henequén fiber-HDPE composites (Herrera-Franco et al. 1997), sisal fiber-polypropylene composites (Fung et al. 2003a), flax fiber-polypropylene composites, and flax fiber-polylactic acid composites (Oksman et al. 2003); they all found that the incorporation of natural fiber into plastic increased the tensile strength in comparison with the unreinforced plastic matrix.

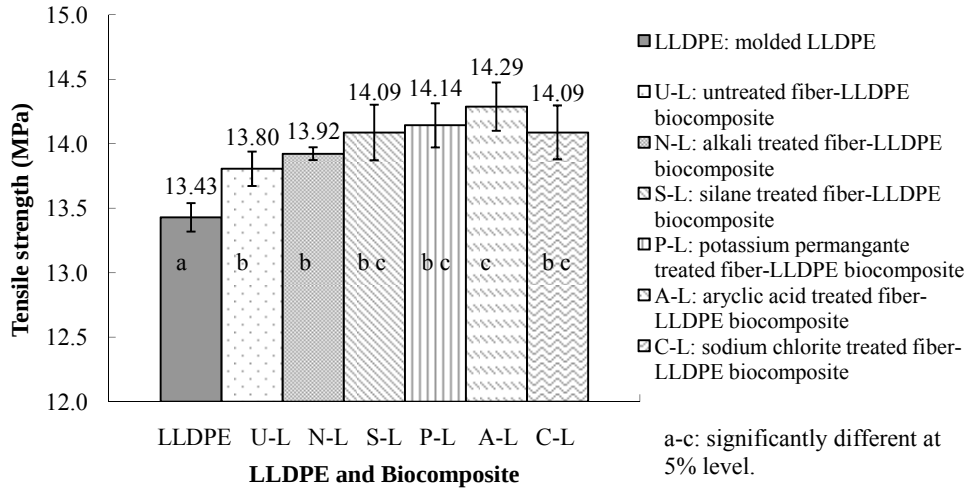

Figure 4.2 Tensile strength of LLDPE and flax fiber-LLDPE biocomposites.

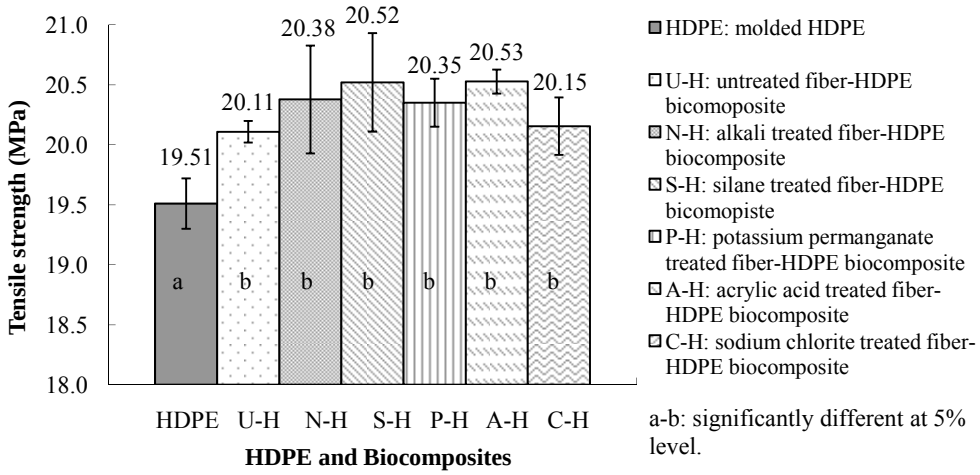

Figure 4.3 Tensile strength of HDPE and flax fiber-HDPE biocomposites.

Among biocomposites, the one without chemical modification (U-L and U-H) had the lowest tensile strength in both LLDPE- and HDPE-based biocomposites (Figures 4.2 and 4.3). All chemical treatments improved the tensile strength of the biocomposites compared with untreated fiber biocomposites.

In both LLDPE- and HDPE-based biocomposites, acrylic acid treated fiber-reinforced biocomposites had higher tensile strengths than other chemical treated fiber-reinforced biocomposites. For LLDPE-based biocomposites, statistical analysis (refer to Table C.1 in Appendix C) showed that acrylic acid-treatment (A) of fiber significantly improved the biocomposite tensile strength compared with those reinforced with untreated (U) and alkali-treated (N) fibers. But for HDPE-based biocomposites, there was no significant statistical difference (refer to Table C.2 in Appendix C) observed among chemical treatments (U, N, S, P, A, C).

Chemical treatments of natural fibers have been widely studied by many researchers (Li et al. 2007), but there is no agreement on which one is the best. Most chemical treatments improved the tensile properties of natural fiber-reinforced composites. For example, Valadez-Gonzalez and co-workers (1999) made short henequén fiber-HDPE composites consisting of 20% fiber by volume; the alkaline and silane treatments were applied on the fiber. No noticeable increase in the tensile strength was observed for biocomposites reinforced with alkaline treated fiber. But there was an increase in the tensile strength (27 MPa) from composites reinforced with silane treated fiber, compared to composites with untreated fiber (21 MPa). However, not every treatment showed improvement on tensile properties. Cantero and co-workers (2003) did not find any significant influence of maleic anhydride or vinyl trimethoxy silane treatment on the tensile and flexural strength of flax fiber-PP composites when compared with untreated fiber-PP composites.

4.1.3 Water absorption of flax fiber-PE biocomposites

Water absorption is generally considered to be a disadvantage in composites. Yet natural fiber-thermoplastic biocomposites always have higher water absorption than the plastic polymer itself. Therefore, fiber surface modification, which can reduce the hydroxyl groups in the cell wall of cellulose molecules, is undertaken to reduce the water absorption of biocomposites.

The water absorption of molded LLDPE, HDPE and their fiber III-reinforced biocomposites are shown in Figures 4.4 and 4.5. The percentage of fiber by mass in the biocomposites was 10%.

LLDPE and HDPE are hydrophobic and non-polar; their water absorption values were all less than 0.01%. Adding flax fiber into them invariably increased the water absorption of the biocomposites.

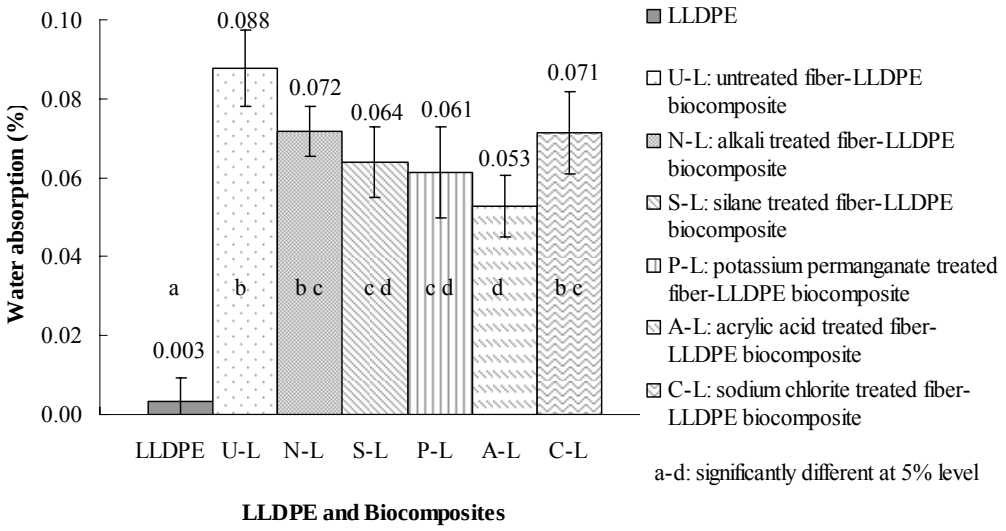

Figure 4.4 Water absorption of molded LLDPE and fiber-LLDPE biocomposites.

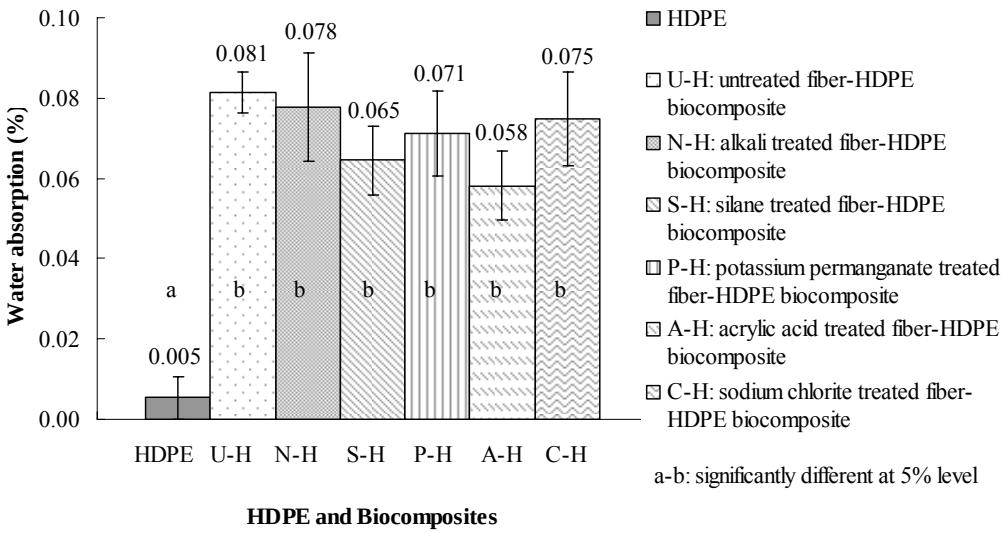

Figure 4.5 Water absorption of molded HDPE and fiber-HDPE biocomposites.

The LLDPE and HDPE biocomposites reinforced with untreated flax fiber had water absorption values of 0.088 and 0.081%, respectively. As expected, fiber chemical treatment reduced the water absorption of biocomposites. For both LLDPE and HDPE based biocomposites, acrylic acid and silane treatments were relatively effective for decreasing water absorption; while sodium chlorite and alkali treated fiber-LLDPE composites had a lower effect. Acrylic acid treatment decreased the water absorption by 40 and 28% of the respective LLDPE and HDPE biocomposites in comparison with untreated fiber-LLDPE or -HDPE biocomposites.

Statistical analysis showed significant difference on water absorption between the pure LLDPE and all fiber-LLDPE biocomposites (Table C.3 in Appendix C). The same result was observed for HDPE and fiber-HDPE biocomposites (Table C.4 in Appendix C), indicating an obvious influence of flax fiber on biocomposite water absorption. For fiber-LLDPE composites, treatments A,

P, and S significantly decreased the biocomposite water absorption compared with untreated fiber-LLDPE biocomposite. For fiber-HDPE composites (Table C.4 in Appendix C), there was no significant statistical difference on water absorption between the biocomposite reinforced with untreated fiber and biocomposites reinforced with chemically treated fibers.

Chemical treatments have been used to decrease the water absorption of natural fiber-reinforced composites as reported by many researchers (Mohanty et al. 2001; Bledzki and Gassan 1999). Paul and co-workers (1997) reported that permanganate treatment reduced the hydrophilic tendency of sisal fibers, and thus, the water absorption of sisal fiber-reinforced composite decreased. Wang and co-workers (2003) also found that silane and other chemical treatments decreased the water absorption of flax fiber-PE composites in comparison with untreated fiber composites.

4.1.4 Acrylic acid treatment

Based on the results in sections 4.1.1 to 4.1.3, acrylic acid treatment of fiber showed a relatively better effect on biocomposite properties namely, high tensile strength and low water absorption compared to other selected chemical treatments. Thus, it was chosen to be used in further studies.

Acrylic acid can reduce the hydrophilic nature of the NaOH treated fiber and react with the cellulosic hydroxyl (OH^-) group of the fiber. Therefore, it can reduce the water absorption of fiber and further influence the biocomposite's water

absorption. Two possible chemical reactions during acrylic acid (CH_2=CHCOOH) treatment of flax fiber may be anticipated and are shown in the following (Sreekala et al. 2000; Agrawal et al. 2000):

(1) Fiber-OH + CH_2=CH-COOH $\xrightarrow{NaOH}$ Fiber-O-CH_2-CH_2-COOH

(2) Fiber-OH + NaOH $\longrightarrow$ Fiber – O-Na^+ + H_2O

Fiber-O-Na^+ + CH_2=CHCOOH $\longrightarrow$ CH_2=CHCOO-Fiber + NaOH

It was also indicated that the bonding between fiber and matrix was improved after chemical treatment of the fiber from the tensile test results. This could be observed and explained from the SEM micrographs on the biocomposite surface. The surfaces of untreated fiber-HDPE biocomposite and A treated fiber-HDPE biocmposites are shown in Figure 4. 6.

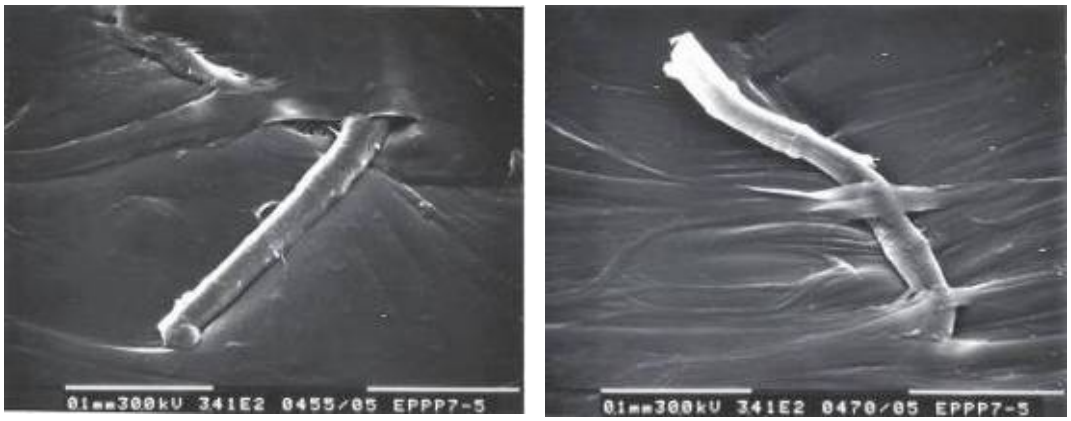

(a) (b)

Figure 4.6 Scanning electronic micrographs on the surface of flax fiber and fiber-HDPE biocomposites: (a) untreated fiber-HDPE biocomposites; (b) acrylic acid treated flax fiber–HDPE biocomposites.

There is small pore observed between the untreated fiber and HDPE surface (Figure 4.6-a), indicating poor bonding. While in acrylic acid treated flax fiber-HDPE surface (Figure 4.6-b), it is observed that there is direct contact between fiber and HDPE matrix. Although there is still fiber pull out on the fiber-HDPE biocomposite, some of them were coated with the HDPE matrix.

The acrylic acid treated fiber-HDPE biocomposite showed the highest tensile strength in section 4.1.2. It means that there was improved bonding between fiber and matrix in the biocomposite, and therefore, during tension, it required more pulling force to break the sample. This can be explained from the SEM images taken on the tensile fracture surfaces of fiber-HDPE biocomposites (Figure 4.7).

Figures 4.7-a and 4.7-b are the fracture surfaces of fiber-HDPE composite using the untreated fiber. There is a tear between the fiber and HDPE, showing that the bonding between the fiber and the HDPE is not strong enough. In the case of breaking surfaces of acrylic acid-treated fiber-HDPE composite (Figures 4.7-c and d), there is no such tearing found, indicating a stronger interaction between the fiber and matrix. Colom and co-workers (2003) took SEM micrographs on the tensile failure surface of aspen wood fiber-HDPE composite and found that untreated fibers appeared to be free of adhesion to the matrix, but some fibers were coated with the matrix after silane treatment although there was fiber pullout.

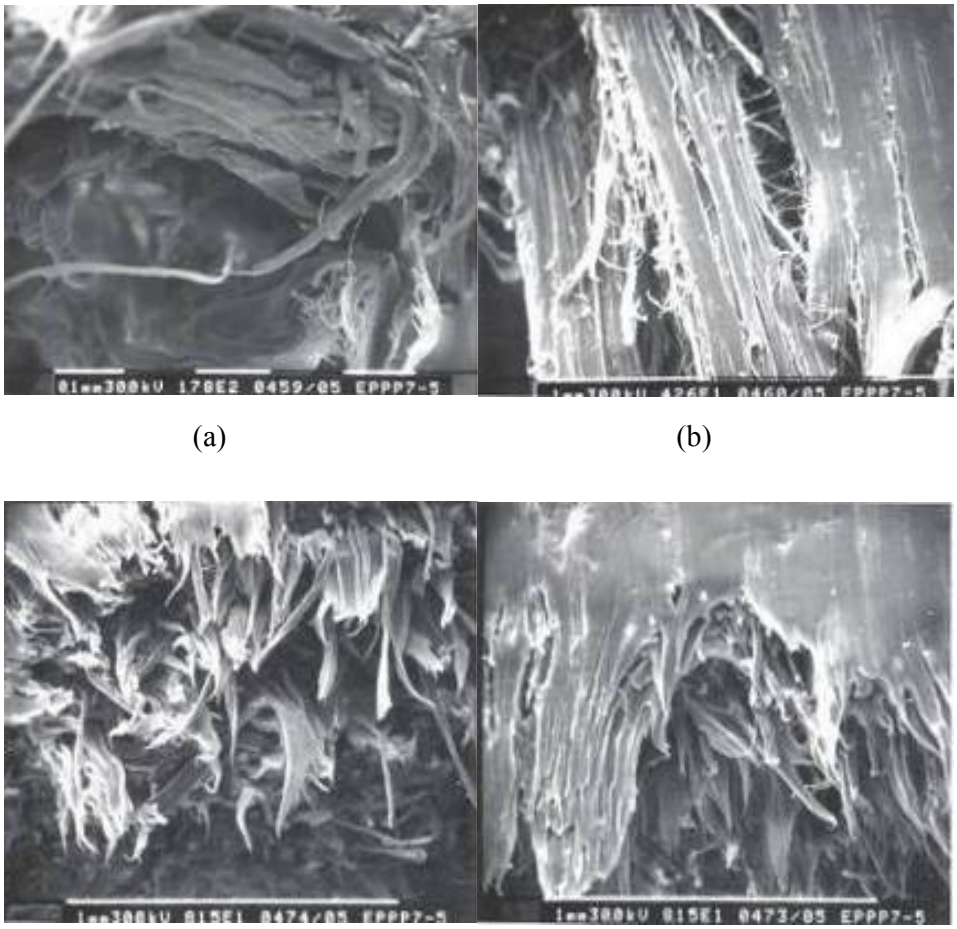

(a) (b)

(c) (d)

Figure 4.7 Scanning electronic micrographs on the tensile fracture surfaces of untreated fiber-HDPE (a and b) and acrylic acid-treated fiber-HDPE (c and d) biocomposites.

Joffe and co-workers (2003) did acrylic acid treatment on flax fiber and reported that surface treatment significantly improved the adhesion between the fiber and the matrix (vinylester resin) and therefore, the mechanical properties of the composite improved as well.

4.1.5 Characteristic temperature of HDPE

Comparing in terms of tensile properties, the results in 4.1.2 and 4.1.3 showed that HDPE-based biocomposites had higher tensile strength than LLDPE-based biocomposites. HDPE and LLDPE composites had similar water absorption. Thus, HDPE was used as matrix in subsequent studies.

It was reported that polyethylene had lower characteristic temperature suitable to be used as matrix in natural fibers biocomposites (Van de Velde and Kiekens 2001). To understand the characteristic temperature of material HDPE19007, the DSC was used to generate a thermogram as shown in Figure 4.8.

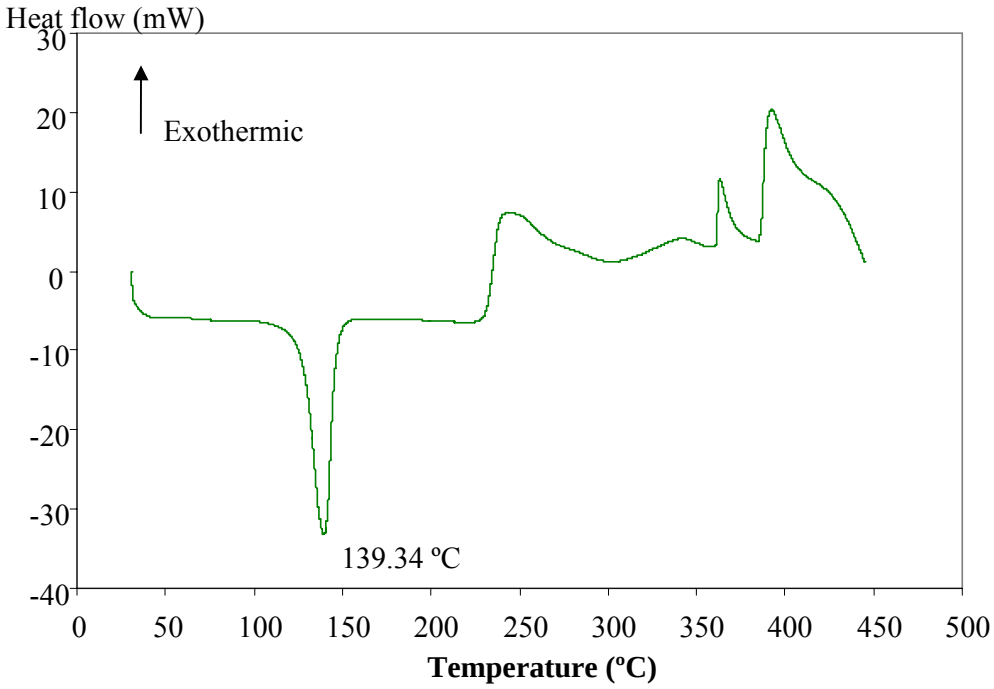

Figure 4.8 Thermogram of high density polyethylene generated by the differential scanning calorimeter (DSC 2910-TA Instruments, New Castle, DE).

Melting is an endothermic progress. As shown on Figure 4.8, the heat flow decreases (became negative) when temperature is above 120ºC because additional energy is absorbed to melt the material The peak in the thermogram shows that the melting temperature of HDPE is 139.34ºC.

There are no exothermic or endothermic reactions in the region between 160 to 240ºC, which suggest that HDPE is stable between this temperature range. So, the recommended processing temperature for HDPE is 160 to 240ºC. Compared with polypropylene, polyamide and other thermoplastics (Van de Velde and Kiekens 2001), the processing temperature of HDPE is relative lower. This makes HDPE suitable for use as matrix when combined with natural fiber to process into biocomposite, because natural fiber also requires lower processing temperature. It is also observed that the first exothermic peak for HDPE is approximately at 250ºC, indicating that HDPE start to degrade at around 250ºC, and then at approximately 360 to 400ºC.

Liu and co-workers (2002) studied characteristic temperature of HDPE by DSC from room temperature to 180ºC and observed that the melting temperature of HDPE was 133.8ºC and the crystallization temperature was 117ºC.

4.2 Selection of flax fibers

The 3 purities of flax fibers listed in section 3.1.1 were processed to fiber-HDPE biocomposites following the procedure outlined in section 3.3.2. Each fiber material was either untreated (U) or acrylic acid (A) treated. After measuring the

properties of biocomposites, one material was to be chosen as the subsequent fiber material.

4.2.1 Chemical composition and morphological properties of flax fibers

The analysis on chemical composition of flax fiber was carried by using ANKOM 200/220 Fiber Analyzer (ANKOM Technology, Fairport, NY) and the results are shown in Table 4.1. Flax fiber I (98-99% pure flax fiber) had the highest cellulose and the lowest lignin content. As the shive content increased, lignin content also increased. Fiber III (42% fiber + 58% shive) had the lowest cellulose content, and the highest hemicellulose and lignin content. Flax shive contained more lignin and hemicellulose, and less cellulose than pure flax fiber.

Table 4.1 Chemical composition of flax fibers.

Materials (purity of fiber)	**Cellulose (%)**	**Hemicellulose (%)**	**Lignin (%)**
Fiber I (98-99%)	83.77	5.79	1.16
Fiber II (85%)	79.99	6.76	2.38
Fiber III (42%)	66.36	10.40	9.21
Flax shive	47.22	11.52	20.89

It was reported that flax shives was composed of 53% cellulose, 13% hemicellulose, 24% lignin; while flax fiber was composed of 78% cellulose, 6% hemicellulose, 5% lignin (Sain and Fortierb 2002). The difference in the composition of fibers can be attributed to growing and processing conditions as well as test methods.

The morphological properties of three fiber surfaces (focus on the surface of pure fiber inside the material) were investigated by SEM and the results are shown in Figure 4.9.

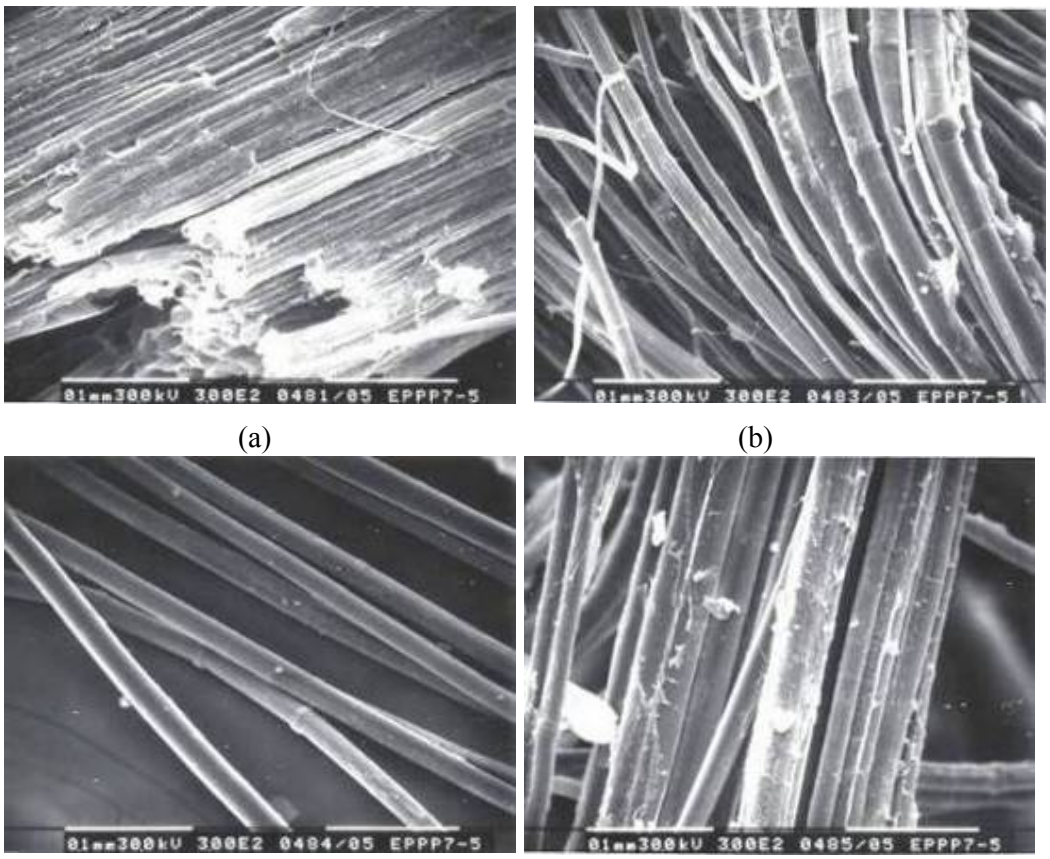

Figure 4.9 Morphology on material surfaces by SEM: (a) flax shive surface; (b) fiber I surface; (c) fiber II surface; (d) fiber III surface.

Fiber I, II, and III originated from the same field. The extraneous material in these three fibers was the shive. It can be observed that the flax shive surface (Figure 4.9-a) had obviously different characteristics than that of flax fiber I, II and III (Figure 4.9-b, c, d). Flax shive is the woody part of flax stem and is brittle at low

moisture. But it was hard to identify the surface difference of fibers I and III; they differed only in terms of fiber purity. It was found that fiber II obtained from the company was the cleanest and had the smoothest fiber surface.

4.2.2 Tensile strength of biocomposites

The three flax fibers were processed to fiber-HDPE biocomposites and their tensile strengths are presented in Figure 4.10.

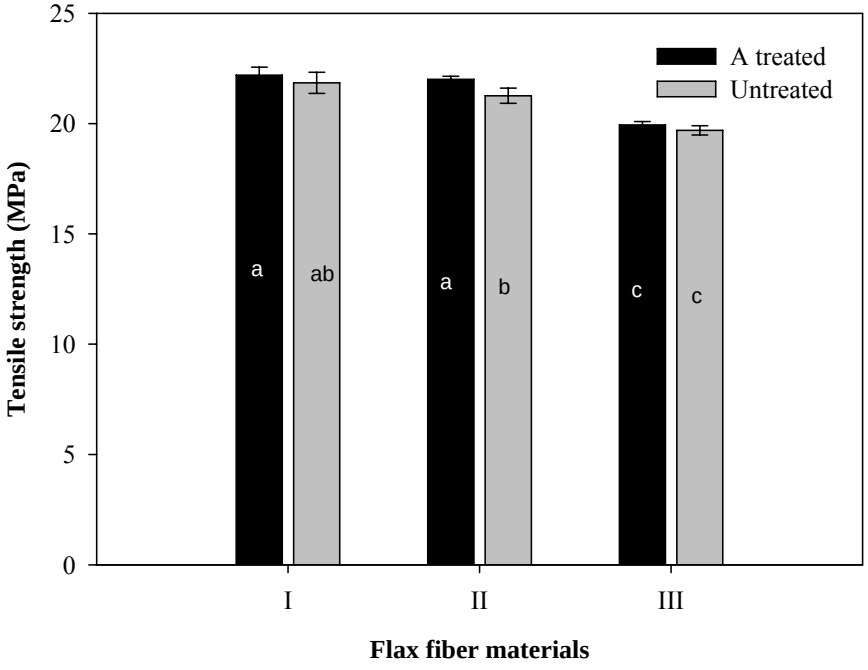

Figure 4.10 Tensile strengths of flax fiber-HDPE biocomposites after untreated (U) or acrylic acid (A) fiber treatments (fiber in composite = 10% wt.; a-c: significantly different at 5% level).

Among the three flax fiber materials, fiber I (98-99% pure fiber) reinforced biocomposite resulted in the highest tensile strength, while the fiber material III-reinforced biocomposite had the lowest tensile strength. Statistical analysis (Table

D.1 in appendix D) revealed that the tensile strength of fiber III-reinforced biocomposite significantly differed from fiber I and II-reinforced biocomposite. More shives were included in Fiber III, indicating that the reinforcement effect of shives was less than that of fiber. It was concluded by Bledzki and Gassan (1999) that lignin had lower mechanical properties than those of cellulose. Flax shives included more lignin; therefore, it reduced tensile strength in biocomposite.

Figure 4.10 also reveals that acrylic acid treatment of fiber increased the tensile strength of biocomposites at all three fiber-reinforced biocomposites. The highest tensile strength was observed in acrylic acid treated fiber I-HDPE biocomposites. Except using fiber II as reinforcement, no statistical difference (Table D.1 in appendix D) was observed before and after treatment.

Statistical analysis (Table D.2 in appendix D) compared the effect of fiber materials and treatments on the tensile strength; it showed that both fiber materials and fiber treatments had significant influence on the biocomposite tensile strength. Fiber material had higher F value, indicating that its effect was more evident than that of fiber treatment on the tensile strength of biocomposites. There was no interaction between the fiber materials and fiber treatment on the tensile strength of biocomposites. This shows that the effect of treatments did not depend on the type of fiber materials. Therefore, the result in section 4.1.2 that acrylic acid treatment resulted in the best effect among five chemical treatments can be applied to all three fiber materials.

4.2.3 Flexural properties of biocomposites

Figures 4.11 and 4.12 show the flexural strength and modulus of biocomposites reinforced with three fiber types. Again, it was found that acrylic acid treated fiber-HDPE biocomposites achieved higher flexural strength and modulus than untreated fiber-HDPE biocomposites.

To consider the effect of both fiber materials and fiber treatment on the flexural properties, statistical analysis was conducted (refer to Tables D.3 - D.6 in Appendix D). The results showed that both fiber material and fiber treatment had significant influence on biocomposite flexural strength and modulus. No interaction effect between fiber materials and fiber treatment was observed.

It can be seen that fiber I-HDPE biocomposite has higher flexural strength than fiber II and fiber III biocomposites (Figure 4.11). In the case of fiber after acrylic acid treatment, the flexural strength of fiber I-HDPE biocomposite was 29.54 MPa, about 18% higher than that of fiber III-HDPE biocomposite and 5% higher than that of fiber II-HDPE biocomposite.

The same trend was observed for flexural modulus of biocomposites (Figure 4.12). The tensile modulus of acrylic acid treated fiber I-HDPE biocomposite was 22% higher than that of acrylic acid treated fiber III biocomposite and 6.8% higher than that of acrylic acid treated fiber II biocomposite.

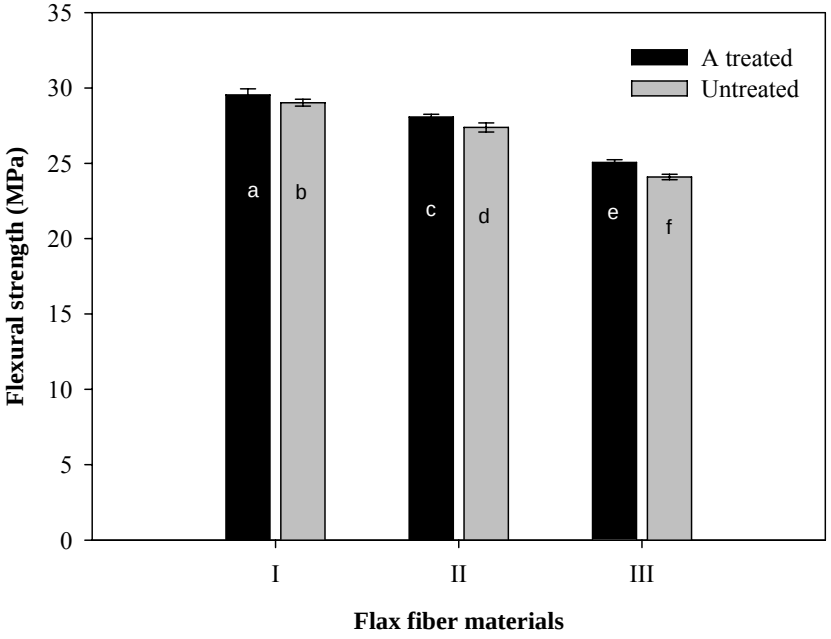

Figure 4.11 Flexural strengths of different flax fiber-HDPE biocomposites after untreated (U) or acrylic acid (A) fiber treatments (fiber in composite = 10% wt.; a-f: significantly different at 5% level).

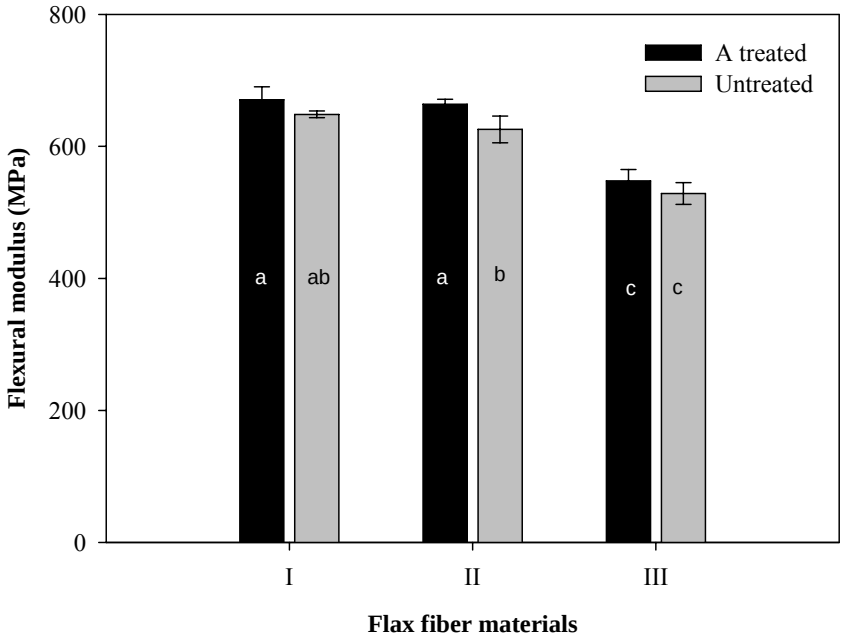

Figure 4.12 Flexural modulus of different flax fiber-HDPE biocomposites after untreated (U) or acrylic acid (A) fiber treatments (fiber in composite = 10% wt.; a-c: significantly different at 5% level).

Statistical analysis (Table D.4 in Appendix D) showed significant differences in flexural strengths of all flax fiber-HDPE biocomposites. In terms of flexural modulus (Table D.5 in Appendix D), no significant difference was observed between fiber I- and fiber II-HDPE biocomposite after the same fiber treatment, but fiber III-HDPE biocomposite had significant difference with fiber I- and fiber II-HDPE biocomposites.

Overall, fiber I-HDPE biocomposites showed the best performance in terms of flexural properties. Fiber II was comparable to fiber I in terms of flexural modulus of biocomposites.

4.2.4 Water absorption of biocomposites

Biocomposite water absorption is presented in Figure 4.13. It can be observed that acrylic acid treatment of fiber decreased the water absorption of all three fiber-HDPE biocomposites compared to the untreated fiber-HDPE biocomposites. The lowest water absorption was observed in acrylic acid treated fiber I-HDPE biocomposites. Statistical analysis (refer to Table D.7 in Appendix D) revealed that there was no interaction effect between fiber materials and fiber treatments on the water absorption of biocomposites, proving that acrylic acid treatment, which resulted in the best effect on minimizing the water absorption of fiber-III-HDPE biocomposites among the six treatments used (result of section 4.1.3), can be applied to all three fiber material-reinforced biocomposites.

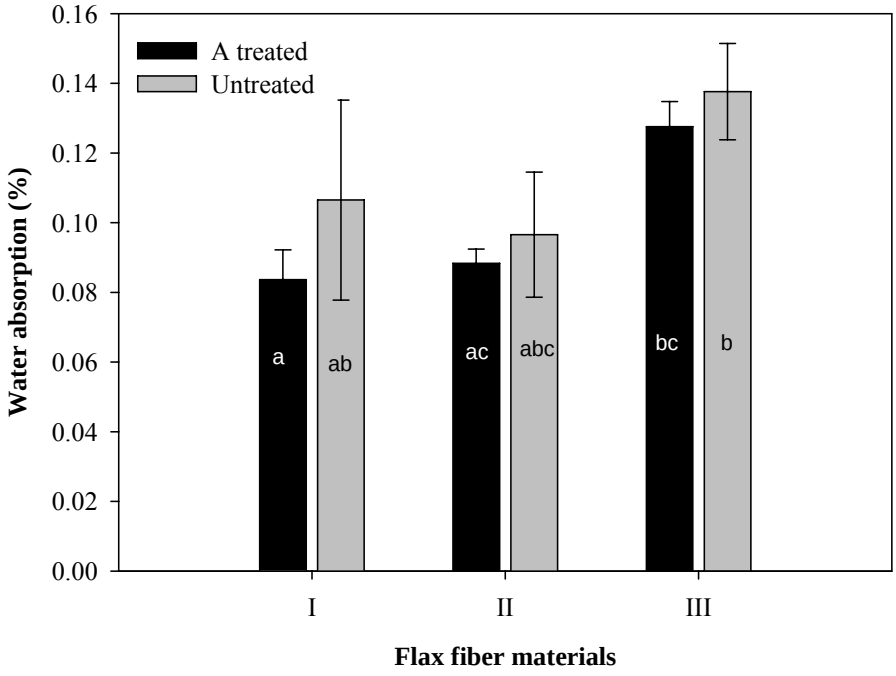

Figure 4.13 Water absorption of different flax fiber-HDPE biocomposites after untreated (U) or acrylic acid (A) fiber treatments (fiber in composite = 10% wt.; a-c: significantly different at 5% level).

Of the two factors, statistical analysis (Table D.7 in Appendix D) also showed that in comparison with fiber treatment, the fiber material had significant influence on the biocomposite water absorption. Thus, it is necessary to choose a type of fiber to achieve the lowest water absorption of biocomposite.

Figure 4.13 shows that fiber III-HDPE biocomposites resulted in the highest water absorption on both biocomposite types reinforced with untreated and acrylic acid treated fibers. As seen in Table 4.1, fiber III included 58% flax shive, which was much higher than in fiber I and II. There are chemical and physical differences between shive and fiber of flax. One is that flax shive contains more hemicellulose and lignin. It was reported that lignin had the least water sorption among

components of bast fibers (Wallenberger and Weston 2004), while hemicellulose was easiest to absorb water (Wallenberger and Weston 2004). From this point, it seemed that more hemicellulose inside fiber shive and fiber III resulted in higher water absorption. Another difference can be observed from the surface characteristics of flax shive and fiber (Figure 4.9). The flax shive is woody and rough on the surface; it gives more paths for water to be adsorbed. So the bond between flax shive and matrix may be weaker than that of the fiber and matrix, thus making flax shive more susceptible to water absorption.

In the case of untreated flax fiber I- and II-HDPE biocomposites, the biocomposite reinforced with fiber II had lower water absorption than fiber I. This may be explained from SEM micrographs of fiber surfaces (Figure 4.9-b, c). Fiber II surface is observed to be smoother and cleaner than fiber I, resulting in better adhesion between fiber and the HDPE matrix interface, and consequently lower water absorption. But after acrylic acid treatment of the fiber, the biocomposite reinforced with fiber I had lower water absorption than fiber II, indicating that chemical modification made fiber I less water absorbent than fiber II. This may be because chemical treatment works better on flax fiber with high fiber content.

Statistical comparison of means (Table D.8 in Appendix D) shows that fiber I- and fiber II-HDPE biocomposites have no significant difference in terms of water absorption, but A-treated fiber I-HDPE biocomposite significantly differ from fiber III-HDPE biocomposite. Sain and Fortier (2002) also pointed out that flax shive absorbed moisture easily because flax shive has higher hemicellulose content.

4.2.5 Chemical and thermal properties of untreated and treated flax fiber I

Combining the results from mechanical properties testing and water absorption measurement, acrylic acid treated flax fiber I showed the best performance in tensile and flexural properties and water resistance of its biocomposites. The chemical and thermal properties of fiber I, as well as the thermal properties of fiber I-HDPE biocomposites were then analyzed and the results are given as follows:

Chemical composition of untreated and acrylic acid treated flax fiber I

The chemical composition of flax fiber I before and after acrylic acid treatment is listed on Table 4.2. Acrylic acid treatment could increase the cellulose content and decrease the hemicellulose and lignin contents of the fiber.

Table 4.2 Chemical composition of treated and untreated flax fibers.

Flax Fiber	Cellulose (%)	Hemicellulose (%)	Lignin (%)
Untreated flax fiber I	83.77	5.79	1.16
Acrylic acid treated flax fiber I	86.88	5.23	0.68

Rong and co-workers (2001) also found that chemical treatment (alkali treatment) removed hemicellulose and lignin in sisal fiber. Cox and co-workers (1999) emphasized that hemicelluloses are readily hydrolyzed by acids and even soluble in water at high temperature. Thus, removal of hemicellulose can decrease the water absorption in the final product. Cellulose with high crystallinity and

cohesive density is insoluble in water and is more resistant to dilute acids; however, they can swell and dissolve in strong acid, strong alkali, or concentrated salt solution (Cox et al. 1999).

Characteristic temperatures of untreated and acrylic acid treated flax fiber I

The thermal characteristics of flax fiber I and acrylic acid-treated flax fiber I were determined using the DSC. The resulting DSC thermograms are shown in Figures 4.14 and 4.15.

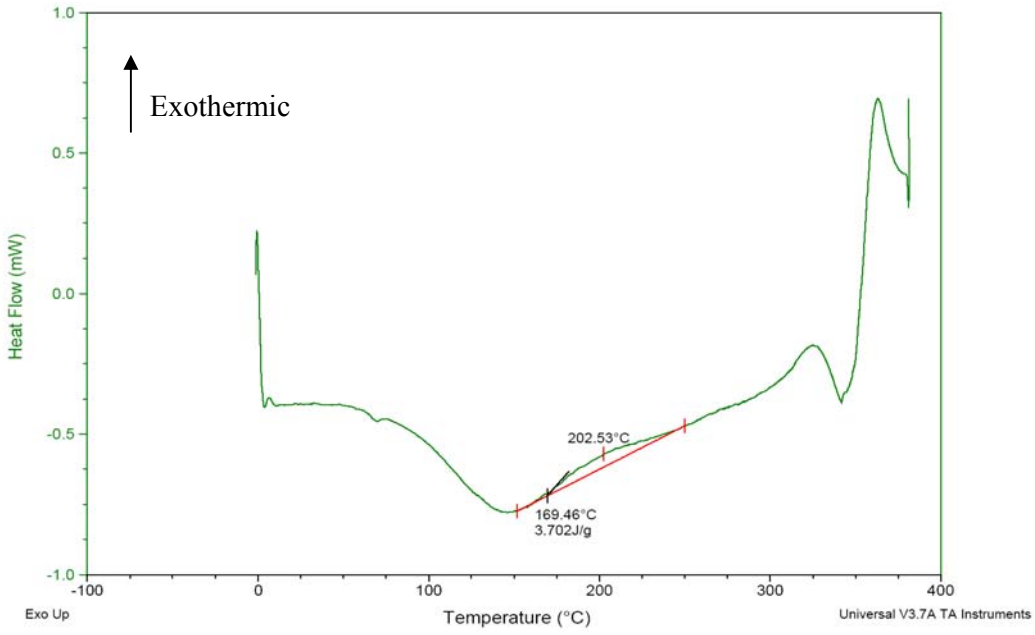

Figure 4.14 DSC thermogram of untreated flax fiber I (fiber purity: 98-99%).

In the DSC thermogram of untreated and treated flax fibers (Figure 4.14), a broad endothermic curve after temperature of 100°C was observed, indicating the

presence of water (Aziz and Ansell 2004). Aziz and Ansell (2004) observed an endotherm in the temperature range of 50-175°C on hemp fiber.

Figure 4.14 shows that above 169ºC, there is a first slight exothermic peak at 202.53ºC, indicating the first decomposition temperature of untreated flax fiber, and this may be due to the degradation of lignin. The decomposition temperature of lignin was normally around 200ºC (Aziz and Ansell 2004). But it was also reported that the degradation of lignin took place in a broad range of temperature from 200 to 500ºC (Manfredi et al. 2006). The first decomposition temperature of acrylic acid treated flax fiber I was observed at 209.39ºC as given in Figure 4.15. This result shows that chemical treatment improved the heat stability of flax fiber.

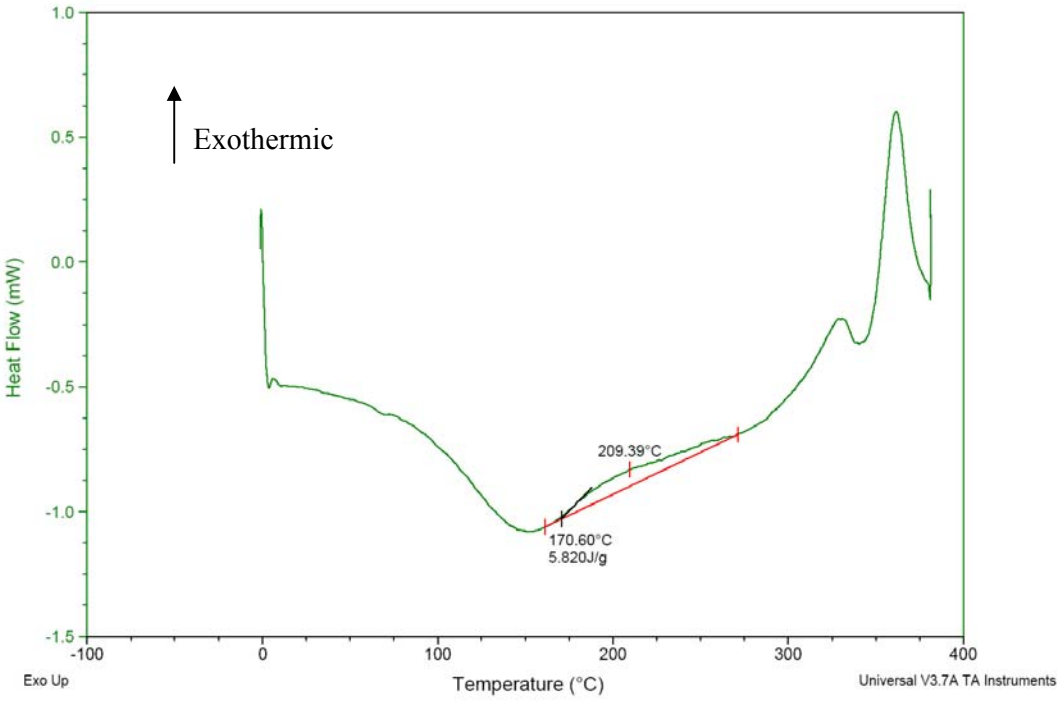

Figure 4.15 DSC thermogram of acrylic acid-treated flax fiber I (fiber purity: 98-99%).

The other polysaccharides such as cellulose and hemicellulose degrade at higher temperature. Manfredi and co-workers (2006) concluded that the degradation of natural fibers may involve two main steps: the first one is the thermal depolymerization of the hemicellulose and the cleavage of glycosidic linkages of cellulose; the second one is related to the decomposition of the α-cellulose. There are two peaks observed in both curves at temperature above 300ºC, indicating the decomposition temperatures of hemicellulose and cellulose. Manfredi and co-researchers (2006) reported that the sisal fiber started to degrade at 215ºC; hemicellulose and α-cellulose decomposition temperatures of sisal fiber were 290ºC and 340ºC, respectively. They also investigated the thermal degradation of flax fiber and found that the decomposition temperatures of hemicellulose and α-cellulose in flax fiber were 285ºC and 345ºC, respectively.

The complete degradation temperatures of flax fibers are not low, but the gradual exothermic reaction in the DSC thermograms indicate that the fiber start to decompose above approximately 200ºC. Therefore, the processing temperature of fiber should be controlled below certain temperature (e.g. 200ºC) to avoid weight loss and discoloration of biocomposites due to excessive heating.

Characteristic temperatures of flax fiber I-HDPE biocomposites

Figure 4.16 shows the DSC thermogram of untreated flax fiber I-HDPE and acrylic acid treated flax fiber I-HDPE biocomposites. The decrease of heat flow in DSC thermograms indicates the melting point of biocomposite.

It was found that the melting temperature of biocomposite (with 10% fiber content) decreased if the fiber were chemically treated. The melting point of untreated flax fiber I-HDPE biocomposite was 138.8°C, while that of acrylic acid treated fiber I-HDPE biocomposite was 137.4°C. No exothermic or endothermic peaks were observed in the DSC thermogram in the range of 160 to 220°C, indicating the steady state of biocomposites. This range of temperatures could be used as processing temperatures of flax fiber-HDPE biocomposites.

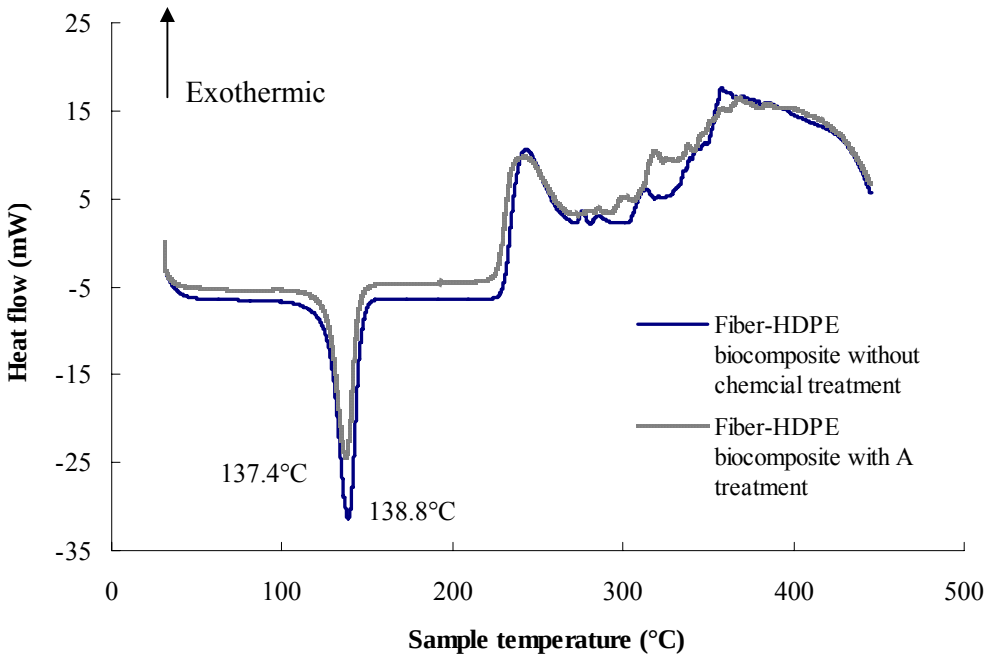

Figure 4.16 DSC thermogram of untreated flax fiber I-HDPE biocomposite and acrylic acid-treated flax fiber I-HDPE biocoposite.

Compared with the HDPE melting temerpature of 139.34°C (Figure 4.8), it was found that the addition of flax fiber into HDPE decreased the melting temperature. Acrylic acid treatment also decreased the melting temperature of the biocomposite in comparison with untreated fiber biocomposite. But all these

changes were in a very small range. Manfredi and co-workers (2006) reported the presence of moisture on their sisal or flax fiber-polyester composites, but this was not observed in our studies.

4.3 Factors affecting injection molding of biocomposites

After the fiber and matrix materials have been selected and the most appropriate chemical treatment of fiber has been determined, the next experiments were conducted to determine how injection molding affects processing and biocomposite properties.

Injection temperature and injection pressure are the important parameters to be controlled during injection molding. However, if the fiber content is changed in the biocomposite, it may change the physical and rheological properties of composite, and might require different injection conditions. In this section, three factors: a) injection temperature; b) injection pressure; and c) fiber content (mass content) were investigated as to their influence on the properties of acrylic-acid treated flax fiber I-HDPE biocomposites.

The experiments conducted were described in section 3.3.3. Injection temperatures were set at two levels: 1): D=166ºC, C=182ºC, B=188ºC, A=188ºC; and 2): D=177ºC, C=190ºC, B=200ºC, A=200ºC. The two levels of injection pressure were 4.8 MPa and 6.9 MPa. The three fiber contents were: 10, 20, and 30% by mass of the biocomposite. A total 12 biocomposite types corresponding to the above treatment combinations were molded, and their properties were tested and analyzed.

4.3.1 Factors affecting tensile properties of biocomposites

The experimental results for biocomposite tensile strength and tensile elongation at different fiber contents, temperatures, and injection pressures are presented in Table 4.3.

Table 4.3 Tensile strength and elongation of biocomposites under different injection molding conditions.

Trial	Fiber Content (% wt.)	Injection Temperature (ºC)	Injection Pressure (MPa)	Tensile Strength*** (MPa)		Tensile Elongation*** (%)	
				Mean	St.dev.	Mean	St.dev.
1	10	166-188 *	4.8	20.87 bc	0.83	7.33 cd	3.86
2	10	166-188	6.9	21.63 cd	0.23	15.16 e	5.07
3	10	177-200 **	4.8	19.77 a	0.17	7.96 d	3.59
4	10	177-200	6.9	20.23 ab	0.19	6.86 bcd	1.57
5	20	166-188	4.8	21.97 d	0.39	4.34 abcd	0.36
6	20	166-188	6.9	22.01 d	0.42	4.30 abcd	0.52
7	20	177-200	4.8	20.94 bc	0.44	2.88 abc	1.12
8	20	177-200	6.9	20.45 ab	0.29	2.43 abc	0.98
9	30	166-188	4.8	23.98 e	0.41	3.42 abcd	1.33
10	30	166-188	6.9	23.77 e	0.41	2.13 ab	1.01
11	30	177-200	4.8	22.02 d	0.62	1.85 a	0.53
12	30	177-200	6.9	22.41 d	0.60	2.07 ab	1.22

* Injection temperatures are D=166ºC, C=182ºC, B=188ºC and A=188ºC.
** Injection temperatures are D=177ºC, C=190ºC, B=200ºC and A=200ºC.
***Average of 5 specimens.
a-e: values in the same group are not significantly different at 5% level (Tables E.1 and E.2 in Appendix E).

The highest tensile strength was found in biocomposite with 30% fiber and processed at low injection temperature (D=166ºC, C=182ºC, B=188ºC and A=188ºC) and low injection pressure (4.8 MPa). But it has the same significant level as high injection pressure (6.9 MPa). The lowest tensile elongation was found in biocomposite containing 30% fiber with processing conditions of high injection temperature (D=177ºC, C=190ºC, B=200ºC and A=200ºC) and low injection

pressure (4.8MPa). But there was no significant difference on the tensile elongation of all 30% fiber biocomposites.

Statistical analysis (Tables E.3 and E.4 in Appendix E) showed that the tensile strength and elongation were significantly dependent on fiber content and injection temperature. But injection pressure had no significant influence on biocomposite tensile strength and elongation at break. According to the measured tensile strength and elongation at break values, the surface plot of tensile strength and elongation as affected by fiber content, injection temperature, and injection pressure can be drawn (Figures E.1 - E.8 in Appendix E) using Tecplot software (Amtec Engineering, Inc., Bellevue, WA). The effects of these three factors on tensile properties are discussed in the following sub-sections.

Fiber content

Statistical analysis (Tables E.3 and E.4 in Appendix E) showed that fiber content was the most significant impact factor on the biocomposite tensile strength and elongation.

It can be seen that the tensile strength increased with increasing fiber content. The average tensile strength of the biocomposites with 30% fiber increased by 11.7% compared with the biocomposites with 10% fiber. It is well known that the use of reinforcement, e. g. fiber in a thermoplastic matrix, increases the biocomposite tensile and flexural strength and modulus (Karmaker and Youngquist 1996; Herrera-Franco et al. 1997; Ota et al. 2005). For example, Joseph and co-workers (1999b) observed that the tensile strength of sisal fiber-PP composites with 10% fiber

increased only by 1.7%, 20% fiber increased by 4.2%, 30% fiber increased by 5.7%, 40% fiber increased by 10.6% compared with pure PP.

It was found that the tensile elongation of biocomposites dramatically decreased with increased fiber content, indicating that more stress was required to produce a given amount of strain when the biocomposite had higher fiber content. The average elongation was around 10% for the biocomposites containing 10% fiber, but when fiber content in composite increased to 15% and above, the tensile elongation of the composite became much lower.

The tensile elongation of a pure HDPE can be as high as 1000%, but the tensile elongation of a fiber-reinforced composite is usually less than 5% (Matweb 2007). In the case of biocomposites, adding 20% fiber into HDPE can reduce the tensile elongation to less than 5%. Thomason (2005) found that the tensile elongation of glass fiber- reinforced polypropylene decreased almost linearly with fiber content.

Injection temperature

It was found that biocomposites achieved higher tensile strength at lower injection temperature regardless of fiber content (10 to 30%). Low injection temperature (D=166ºC, C=182ºC, B=188ºC and A=188ºC) resulted in higher tensile strength than high injection temperature (D=177ºC, C=190ºC, B=200ºC and A=200ºC).

Ota and co-workers (2005) investigated the effect of four groups of injection temperature (170, 180, 190, 200 ºC) on the tensile properties of PP and glass fiber-PP

composites. They reported a tendency of slightly decreasing tensile strength and modulus with the injection temperature.

The reason why injection temperature of 168-188ºC resulted in better tensile strength than temperature of 177-200ºC could be explained by the heat properties of HDPE and flax fiber. HDPE can be processed at temperature of 160 to 240ºC (refer to section 4.1.5), but the flax fiber started to decompose at temperature above 200 ºC (refer to section 4.2.5). It was also emphasized by Fung and co-researchers (2003a) that high injection molding temperature (210ºC) caused the thermal depolymerization of hemicellulose and the glycosidic linkages of cellulose. Therefore, the high temperature will cause the fiber loss and reduce the reinforcement effect.

In the case of tensile elongation (Figures E.6 - E.8 in Appendix E), it showed that lower injection temperature resulted in higher tensile elongation in all biocomposites with fiber content increasing from 10% to 30%. But when the fiber content increased to 30%, the influence of injection temperature and pressure on the tensile elongation of biocomposite is not as obvious as that in 10% and 20% fiber content. It was said that the material was of high toughness if it had high ultimate tensile strength and high elongation (Matweb 2007). As shown in this study, lower injection temperature resulted in a biocomposite with high toughness.

Injection pressure

It is also observed (Figures E.3 - E.8 in Appendix E) that the influence of injection pressure on tensile strength and elongation is not significant. The influence of injection pressure to tensile strength was not as obvious as temperature. But it can be seen that the higher injection pressure (6.9 MPa) resulted in higher tensile strength, especially at lower injection temperature (D=166ºC, C=182ºC, B=188ºC and A=188ºC). This may be because at low temperature, the biocomposite has a higher viscosity which requires more pressure to push material into the mold.

Injection pressure from 4.8 to 6.9 MPa did not significantly influence tensile elongation, which can be seen from Figures E.6 – E.8 (Appendix E) as well. For the biocomposites with fiber content higher than 20%, the injection pressure did not change the tensile elongation. But at low fiber content of 10% (Figure E6), higher tensile elongation was observed at higher injection pressure.

Statistical model

Based on the experimental data, the equations for tensile strength and tensile elongation as a function of fiber content, injection temperature, and injection pressure were developed.

The effects of the fiber content, injection temperature, and injection pressure (independent variables) on tensile strength and tensile elongation (dependent variables) were modeled first (refer to Tables E.5 to E.8 in Appendix E). In the model, the injection temperature referred to Zone A temperature, which was: 188ºC = injection temperatures of D=166ºC, C=182ºC, B=188ºC and A=188ºC; 200ºC =

injection temperatures of D=177ºC, C=190ºC, B=200ºC and A=200ºC. The equations were determined using multiple-linear-regression by SAS software (SAS Institute, Cary, NC) as given in the following:

Tensile strength:

$$\sigma_t = 2.4111F + 0.1106\ T + 5.4376\ P + 0.0036\ F^2 + 0.0944\ P^2 - 0.0122\ FT - 0.3597FP - 0.0318\ TP + 0.0018\ FTP \quad (4.1)$$

R^2=0.9996

where σ_t = Tensile strength (MPa),

F = Fiber content (0 to 30%),

T = Injection temperature (188 to 200ºC), and

P = Injection pressure (4.8 to 6.9 MPa).

Tensile elongation:

$$\%\ Elongation = 26.9880\ F + 3.6362\ T - 63.4573\ P + 0.05162\ F^2 + 21.0045\ P^2 - 7.0941\ FT - 0.1475\ FP + 0.9157\ TP + 0.0356\ FTP \quad (4.2)$$

R^2=0.8733

where *% Elongation* = Tensile elongation (%).

The above equations show the relationship between tensile properties and the three variables (fiber content, injection temperature, and injection pressure). It showed a very good fit of the model of tensile strength (R^2=0.9996) with experimental data. But injection pressure is a variable affected by product shape and size. Statistical analysis (Tables E.3 and E.4 in Appendix E) also showed that injection pressure had no significant influence on biocomposite tensile strength and

elongation. So regression models (Tables E.9 - E.12 in Appendix E) excluding injection pressure were developed. With fiber content (F, %) and injection temperature (T, ºC) as independent variables, tensile strength (σ_t, MPa) and tensile elongation (*% Elongation*, %) as dependent variables, the linear equations are given by:

Tensile strength:

$$\sigma_t = 28.9516 + 0.2531\ F + 0.0049\ F^2 - 0.0002\ T^2 - 0.0017\ FT \quad (4.3)$$

R^2=0.8748

Tensile elongation:

$$\%\ Elongation = 61.5657 - 3.6912\ F + 0.0226\ F^2 - 0.0011 T^2 + 0.0126\ FT \quad (4.4)$$

R^2=0.6090

Figures 4.17 and 4.18 present the variations of tensile strength and elongation with fiber content and injection temperature by Matlab (The MathWorks, Inc. Natick, MA) using polynomial linear models of equations of 4.3 and 4.4. The surface responses revealed the same trend as discussed previously. The above developed equations were only applied for the biocomposite containing 10 to 30% treated flax fiber. Because in the study, the biocomposite extrusion became difficult when fiber content was higher than 30%, no investigations were conducted at fiber content higher than 30%. Thomason (2005) studied the injection molding of long glass fiber-PP composites; they found the maximum reinforcement effect was obtained at 40-50 % wt. fiber, above this level, the strength of the material decreased.

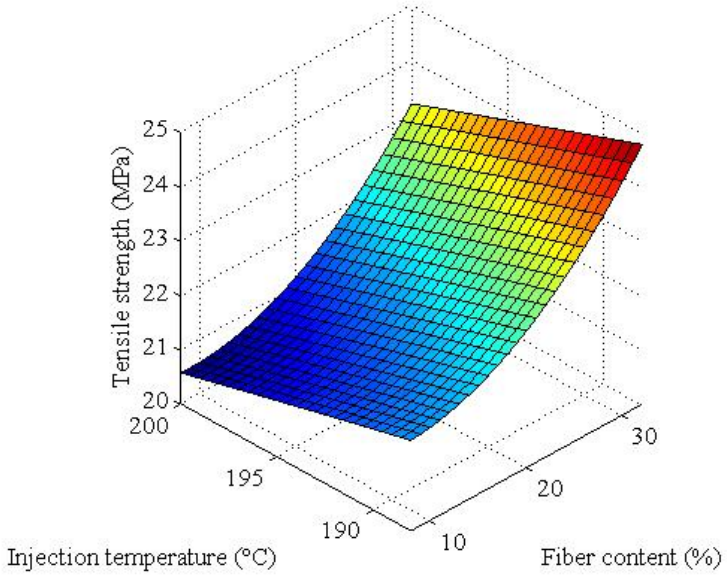

Figure 4.17 Estimated tensile strength of flax fiber-HDPE biocomposites as affected by fiber mass content and injection temperature.

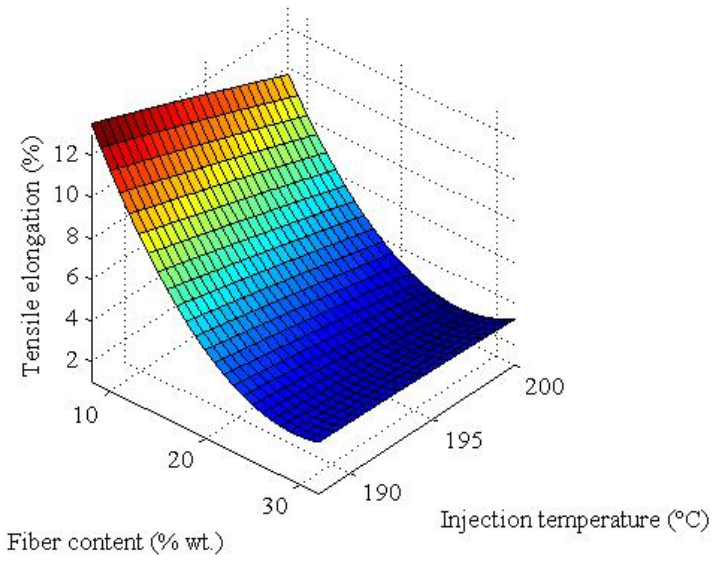

Figure 4.18 Estimated tensile elongation of flax fiber-HDPE biocomposites as affected by fiber mass content and injection temperature.

In terms of tensile elongation, Thomason (2002) also found that the addition of even a small fraction of reinforcement (short glass fiber) dramatically lowered the tensile elongation of its PP composite, which agreed with our results. They also found that the tensile elongation decreased almost linearly with the fiber content in the range of 10 to 50%.

4.3.2 Factors affecting flexural properties of biocomposites

Table 4.4 shows the flexural strength and modulus of biocomposites at different fiber content, injection temperature, and injection pressure. The highest flexural strengthes were found in the biocomposite which contained 30% fiber and was processed at low injection temperature (D=166ºC, C=182ºC, B=188ºC, A=188ºC). Injection pressure (4.8 MPa and 6.9 MPa) did not cause significant difference on flexural strength at this temperature and fiber content. The highest flexural modulus was found in the biocomposite which included 30% fiber and processed at low injection temperature, but high injection pressure (6.9 MPa).

Statistical analysis (Tables E.15 and E.16 in Appendix E) shows that all three factors significantly influenced the flexural strength and modulus. This indicated that flexural properties are easier to be influenced by processing conditions than tensile properties. Among the three factors, the factor with the most impact was fiber content, followed by injection temperature; the factor with the least impact was injection pressure.

Table 4.4 Flexural strength and modulus of biocomposites under different injection molding conditions.

Trial	Fiber Content (% wt.)	Injection Temperature (ºC)	Injection Pressure (MPa)	Flexural Strength*** (MPa)		Flexural Modulus*** (%)	
				Mean	St.dev.	Mean	St.dev.
1	10	166-188 *	4.8	28.92 b	0.53	613.51 bc	40.89
2	10	166-188	6.9	29.04 bc	0.42	641.20 bcd	0.14
3	10	177-200 **	4.8	26.78 a	0.47	542.14 a	18.55
4	10	177-200	6.9	28.15 b	0.82	581.62 ab	7.63
5	20	166-188	4.8	30.15 c	0.17	695.48 d	13.55
6	20	166-188	6.9	32.07 d	0.43	772.28 e	20.81
7	20	177-200	4.8	29.22 bc	0.83	696.64 d	53.48
8	20	177-200	6.9	28.65 b	0.37	661.58 cd	10.90
9	30	166-188	4.8	38.36 f	0.58	1215.94 g	31.28
10	30	166-188	6.9	38.20 f	0.89	1284.96 h	29.88
11	30	177-200	4.8	35.83 e	0.26	1128.50 f	5.34
12	30	177-200	6.9	36.71 e	0.40	1259.80 gh	48.69

* Injection temperatures are D=166ºC, C=182ºC, B=188ºC and A=188ºC.
** Injection temperatures are D=177ºC, C=190ºC, B=200ºC and A=200ºC.
***Average of 5 specimens.
a-h: values in the same group are not significantly different at 5% level (Tables E.13 and E.14 in Appendix E).

As shown in Table 4.4, the highest flexural strength and modulus were from biocomposite containing 30% fiber and processed at low injection temperature. The average flexural strength of biocomposites with 30% fiber was 37.28 MPa, 32% higher than that of biocomposites with 10% fiber. The flexural modulus of biocomposites with 30% fiber was 105% higher than biocomposites with 10% fiber. Comparing with the results of tensile properties, the addition of flax fiber in biocomposite improved the flexural properties in a more significant manner than tensile properties.

It was found that the low injection temperature (D=166ºC, C=182ºC, B=188ºC and A=188ºC) led to higher flexural strength and modulus for the biocomposites with fiber content of 10 to 30%. It also (Figures E.9 and E.10 in

Appendix E) indicated that a high pressure led to a higher flexural strength and modulus. But when fiber content was lower (10%), the influence of pressure on flexural strength was not as obvious as in higher fiber content.

Statistical model

Using the SAS software, multiple regression analysis (Tables E.17 - E.20 in Appendix E) was run to determine the relationship between the biocomposite flexural properties and fiber content, injection temperature, and injection pressure.

Flexural strength:

$$S = 0.64296\,F - 0.23732\,T + 22.93215\,P + 0.02729\,F^2 - 2.25425\,P^2 + 0.00030\,FT + 0.06950\,FP + 0.02062\,TP - 0.00041\,FTP \quad (4.5)$$

$R^2 = 0.9996$

where S = Flexural strength (MPa),

F = Fiber content (0 to 30%),

T = Injection temperature (188 to 200ºC), and

P = Injection pressure (4.8 to 6.9MPa).

Flexural modulus:

$$E_H = 47.6249\,F + 3.5528\,T + 377.2449\,P + 2.0196\,F^2 - 6.2423\,P^2 - 0.5479\,FT - 17.8535\,FP - 1.5763\,TP + 0.1002\,FTP \quad (4.6)$$

$R^2 = 0.9978$

where E_H = Flexural modulus (MPa).

The models had high R^2, showing a good fit to the experimental data. Again,

the relationship between flexural properties and fiber content (F) and injection temperature (T) were developed (Tables E.21 - E.24 in Appendix E) as equations 4.7 and 4.8.

Flexural strength:

$$S = 43.2127 - 0.2364\,F + 0.0273\,F^2 - 0.0003\,T^2 - 0.0021\,FT \quad (4.7)$$

$R^2 = 0.9677$

Flexural modulus:

$$E_H = 1437.0460 - 56.8179\,F + 2.0196\,F^2 - 0.0146\,T^2 + 0.0382\,FT \quad (4.8)$$

$R^2 = 0.9745$

Figures 4.19 and 4.20 plot the response surface of flexural strength and flexural modulus according to equations 4.7 and 4.8. The changes of flexural strength and modulus with variations in fiber content and injection temperature can be observed from the surface plot. The flexural strength and modulus increased with increasing the fiber content. This was in agreement with studies conducted by Thomason (2002) and Mishra and co-researchers (2003). They all found an increase in flexural strength of composites with the addition of more glass fiber in polyester hybrid or polypropylene matrix. A lower injection temperature was preferred to obtain a composite with higher flexural strength and modulus. But in the case of flexural modulus, the changing of injection temperature did not influence the flexural modulus too much.

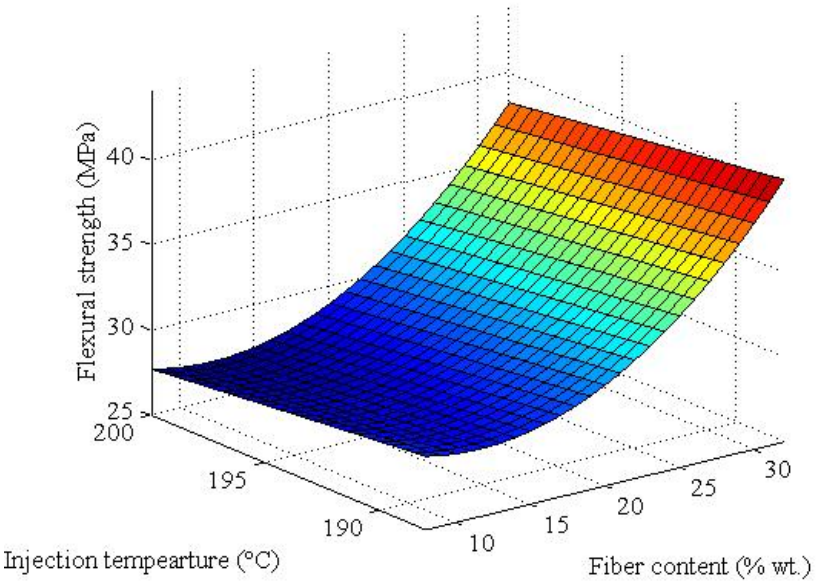

Figure 4.19 Estimated flexural modulus of flax fiber-HDPE biocomposites as affected by fiber mass content and injection temperature.

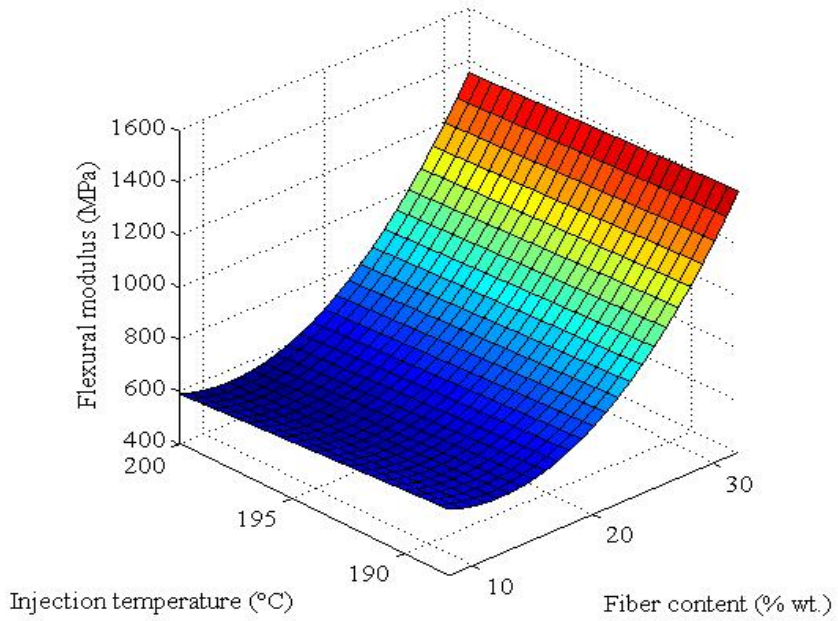

Figure 4.20 Estimated flexural modulus of flax fiber-HDPE biocomposites as affected by fiber mass content and injection temperature.

4.3.3 Factors affecting water absorption of biocomposites

Since water inside the composite may affect its physical and mechanical properties, low water absorption is desired in the final biocomposites by adjusting operating parameters. Table 4.5 presents the water absorption values of flax fiber-HDPE biocomposite at various processing conditions.

Table 4.5 Water absorption of biocomposites under different injection molding conditions.

Trial	Fiber Content (% mass)	Injection Temperature (ºC)	Injection Pressure (MPa)	Water Absorption*** (%)	
				Mean	St. dev.
1	10	166-188 *	4.8	0.0432 a	0.0202
2	10	166-188	6.9	0.0481 a	0.0099
3	10	177-200 **	4.8	0.0599 a	0.0140
4	10	177-200	6.9	0.0902 ab	0.0146
5	20	166-188	4.8	0.1550 bc	0.0055
6	20	166-188	6.9	0.1926 cd	0.0170
7	20	177-200	4.8	0.2977 e	0.0136
8	20	177-200	6.9	0.2526 de	0.0428
9	30	166-188	4.8	0.2011 cd	0.0150
10	30	166-188	6.9	0.2368 de	0.0055
11	30	177-200	4.8	0.5590 f	0.0382
12	30	177-200	6.9	0.5128 f	0.0363

* Injection temperatures are D=166ºC, C=182ºC, B=188ºC and A=188ºC.
** Injection temperatures are D=177ºC, C=190ºC, B=200ºC and A=200ºC.
***Average of 3 specimens.
a-f: values in the same group are not significantly different at 5% level (Table E.25 in Appendix E)

Natural fibers are highly hydrophilic in nature, they easily absorb water. Therefore, incorporation of natural fibers into polymeric matrices will generally increase the water sorption ability of the product (Sreekala et al. 2002). The same result was observed in this study; increased fiber content increased the water absorption of the bicomposites.

Table 4.5 shows that the highest water absorption of biocomposites was obtained at 30% fiber content and higher injection temperature. When the fiber content in biocomposite was 30% and the injection temperature was lower (D=166ºC, C=182ºC, B=188ºC and A=188ºC), the average water absorption of biocomposite was 0.22%; but at the same fiber content, when injection temperature increased (D=177ºC, C=190ºC, B=200ºC and A=200ºC), the average biocomposite water absorption increased to 0.54%. This indicates that it is very important to control the injection temperature to decrease the biocomposite water absorption when the fiber content is higher.

Statistical analysis (Table E.26 in Appendix E) showed that fiber content and injection temperature significantly influenced the biocomposite water absorption, while injection pressure did not. Fiber content was the most important factor to influence the biocomposite water absorption.

The response surface curves of water absorption as affected by processing conditions are in Figures E.17 to E.20 (Appendix E) based upon the experimental data. When injection temperature was below 195°C, the biocomposite water absorption did not change with injection pressure. But when injection temperature was higher than 195°C, increasing injection pressure led to higher water absorption.

Statistical model

A linear regression equation was developed (Tables E.27 and E.28 in Appendix E) to study of relationship between water absorption and processing

variables (fiber content, injection temperature, and injection pressure) using SAS software. The equation is shown as the following:

$$M\% = -0.51798\,F - 0.02843\,T + 1.75460\,P + 0.00048\,F^2 - 0.16691\,P^2 + 0.00267\,FT + 0.02457\,FP + 0.00103\,TP - 0.00013\,FTP \quad (4.9)$$

$R^2 = 0.9813$

where $M\%$ = Water absorption (%),

F = Fiber content (0 to 30%),

T = Injection temperature (188 to 200ºC), and

P = Injection pressure (4.8 to 6.9 MPa).

Since the influence of pressure on water absorption was not significant (Table E.26 in Appendix E), the relationship between dependent variable (water absorption, $M\%$) and independent variables (fiber content, F and injection temperature, T) is developed (Tables E.29 and E.30 in Appendix E) in equation 4.10 with a high R^2. Then the surface curve according to equation 4.10 is plotted in Figure 4.21 by using Matlab (The MathWorks, Inc. Natick, MA).

$$M\% = 1.0034 - 0.2143\,F - 5.5975\times10^{-5}\,F^2 - 2.9689\times10^{-5}\,T^2 + 0.0012\,FT \quad (4.10)$$

$R^2 = 0.9641$

Figure 4.21 showed that as the biocomposite included less than 20% flax fiber, changing the injection temperature did not result in a big difference on the biocomposite water absorption. But when the fiber content increased to 20-30%, the biocomposite water absorption was obviously influenced by injection temperature. There was an increase of water absorption when injection temperature was higher

than 195°C. This was because at higher temperature, fiber degradation occurred, thus more pores were formed between the fiber and matrix interface, which gave paths for water to enter the biocomposites.

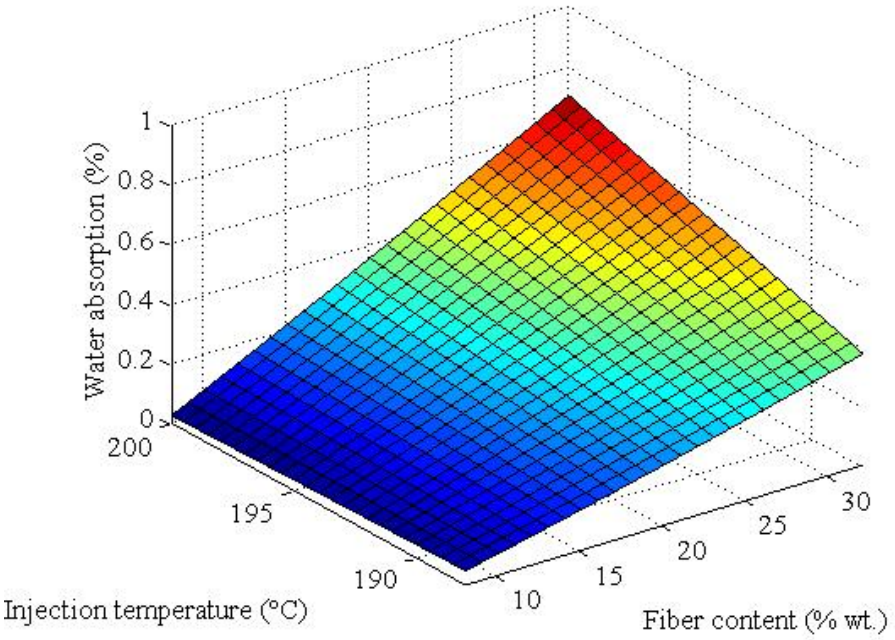

Figure 4.21 Estimated water absorption of flax fiber-HDPE biocomposites as affected by fiber mass content and injection temperature.

The water absorption of chemically treated sisal fiber-polyester composites (76.2 mm × 25.4 mm; sisal =30% wt.; 24h) was 10.6% (Mishra et al. 2003). It was said that standard glass fiber sheet moulding compound was allowed to contain maximum 0.5% wt. water (Voorn et al. 2001). The water absorption of flax fiber-HDPE biocomposites in our experiment was much lower (injection-molded) than that of the sisal-polyester composites (unheated compression-molded product). Furthermore, the water absorption of injection molded flax fiber-HDPE biocomposites can be minimized if the injection temperature were kept below 195°C.

4.4 Rheological properties and prediction of filling time

Injection filling time is a function of material properties and mold size. This section deals with injection filling time using a given mold shown in section 3.3.4 (Pages 53 and 54). When the shape of a biocomposite product is maintained the same, then the rheological properties of the material are the main factor affecting the filling time.

Flax fiber-HDPE biocomposites with fiber content of 10, 20, and 30% were prepared following the procedure in section 3.3.4 (Page 60). The biocomposites were labeled A1, A2, and A3. Pure HDPE was also measured for comparison. The measurement of apparent viscosity of HDPE and biocomposites was conducted at temperature 170, 180, 190, and 200°C to determine the value of consistency coefficient (K) and flow behavior index (n). Filling time was predicted according to section 3.3.4.

4.4.1 Rheological properties of biocomposites

It was reported that the viscosity of HDPE followed a power law behavior when shear rate was in the range of 1 to 10^4 or 10 to 10^3 s^{-1} (Dealy and Larson 2006; Nichetti and Manas-Zloczower 1998). Therefore, the power law model ($\tau = K(\gamma)^n$) was used to analyze the rheological properties of HDPE and HDPE-based composites. The shear stress and shear rate of HDPE and biocomposites A1, A2, and A3 were measured by Instron capillary rheometer (Model 3211, Instron Corp., Canton, MA). The shear stress (τ) vs. shear rate (γ) were plotted (Figures F.1 - F.4

in Appendix F) and power law model was used to analyze the flow behavior of materials.

Consistency coefficient and flow behavior index

According to the equation of $\tau = K(\gamma)^n$, consistency coefficient K (also known as consistency index) and flow behavior index n (also known as power law index) were determined and their values are shown in Table 4.6.

Table 4.6 Consistency coefficient (K) and flow behavior index (n) value for HDPE and flax fiber-HDPE biocomposites.

Sample	**Rheological Parameters**	**Temperature (°C)**			
		170	**180**	**190**	**200**
HDPE	n	0.67	0.72	0.69	0.68
	K (Pa·s^n)	2201.30	1496.80	1545.20	1468.90
Biocomposite A1*	n	0.61	0.63	0.65	0.66
	K (Pa·s^n)	3663.10	2881.20	2408.50	2081.90
Biocomposite A2**	n	0.53	0.52	0.54	0.57
	K (Pa·s^n)	6686.00	6032.00	5126.50	3924.80
Biocomposite A3***	n	0.49	0.49	0.49	0.52
	K (Pa·s^n)	11352.00	10115.00	9562.20	7011.40

* A1 = Flax fiber-HDPE biocomposite includes 10% fiber by mass content.
** A2 = Flax fiber-HDPE biocomposite includes 20% fiber by mass content.
*** A3 = Flax fiber-HDPE biocomposite includes 30% fiber by mass content.

Linear regression models describing the relationship between K, n and the temperature and fiber content were developed. Linear regression equations obtained for K and n after SPSS analysis (Tables G.1 - G.4 in Appendix G) were:

$$K = 14854.8775 - 75.3220\,T + 261.7995F \quad (4.11)$$

$$n = 0.4884 + 0.0011T - 0.0067F \quad (4.12)$$

where T = Temperature between 170 to 200°C,

F = Fiber content between 0 to 30% wt., and

R^2 = 0.9157 for equation 4.11 and R^2 = 0.9500 for equation 4.12.

From these equations, K and n values for acrylic acid treated flax fiber-HDPE biocomposites could be estimated at a given fiber content and processing temperature.

It can be seen that the consistency coefficient (K) of biocomposite increased with fiber content (F), and decreased with temperature (T). Higher K value indicated more shear stress by the melt at certain shear rate and more resistance occurred during the flow.

The n value decreased with increasing fiber content and slightly increased with temperature. Flow behavior index (n) indicates the sensitivity of viscosity with shear rate and it was reported that the lower value of n, the more sensitive was viscosity with shear rate (El-Mashad et al. 2005).

Consistency coefficient (K) and flow behavior index (n) were used in some equations instead of viscosity in analyzing the flow of non-Newtonian fluids (Reynolds 1971). Therefore, information on K and n is necessary for studying the dynamic flow behavior of power law fluids. The various application grades of HDPE will cause various melt flow, therefore K and n values may be different. It was reported that HDPE has a K value of 20000 $Pa \cdot s^n$ and n value of 0.41 at 180°C by Osswald and Menges (2003). While Nichetti and Manas-Zloczower (1998) reported two HDPE samples with n value of 0.298 and 0.305 at 190°C.

Apparent viscosity

Viscosity is the most widely used parameter when determining the behavior of polymers during processing (Osswald and Menges 2003). For non-Newtonian fluids, the ratio of shear stress to shear rate is called of apparent viscosity instead of viscosity. Apparent viscosities (μ_a , Pa·s) of HDPE and biocomposites were calculated from the equation 3.42.

Figures 4.22 to 4.25 show the apparent viscosity of HDPE and biocomposites as a function of shear rate. It was observed that apparent viscosity increased with increasing fiber content. It was also found that as temperature increased from 170 to 200°C, the apparent viscosity values of HDPE and biocomposites decreased. This was the same trend as that reported on how viscosity of HDPE and other polymers change with temperature (Osswald and Menges 2003). Osswald and Menges (2003) reported that HDPE have a viscosity of ca. 10^3 Pa·s at temperature of 180°C when shear rate was 100 s^{-1}. They also showed that HDPE has a lower viscosity when temperature increased to 320°C.

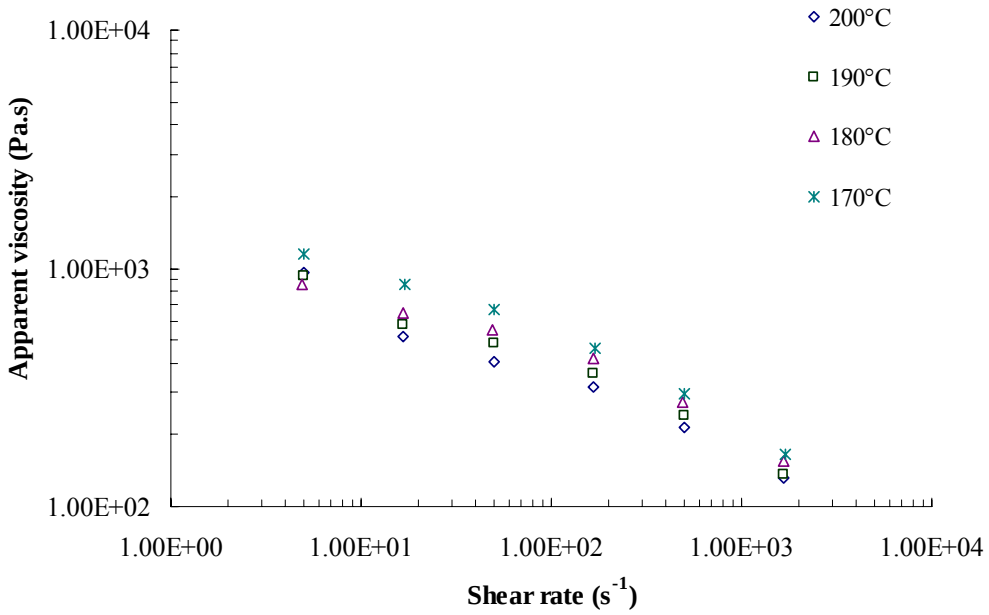

Figure 4.22 Apparent viscosity of pure HDPE as function of shear rate.

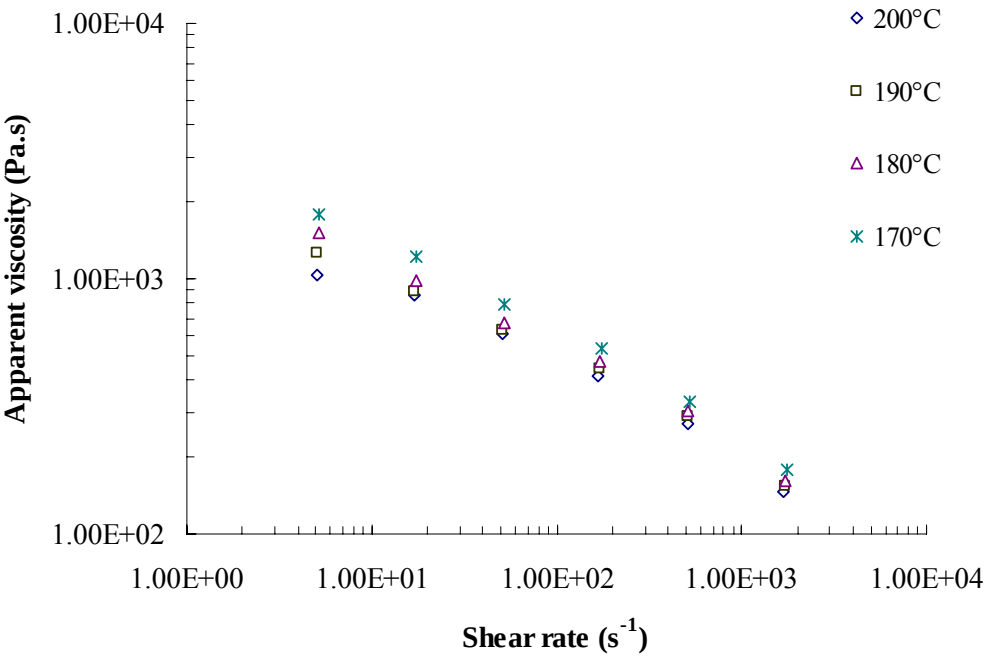

Figure 4.23 Apparent viscosity of biocomposite A1 (fiber = 10% wt.) as function of shear rate.

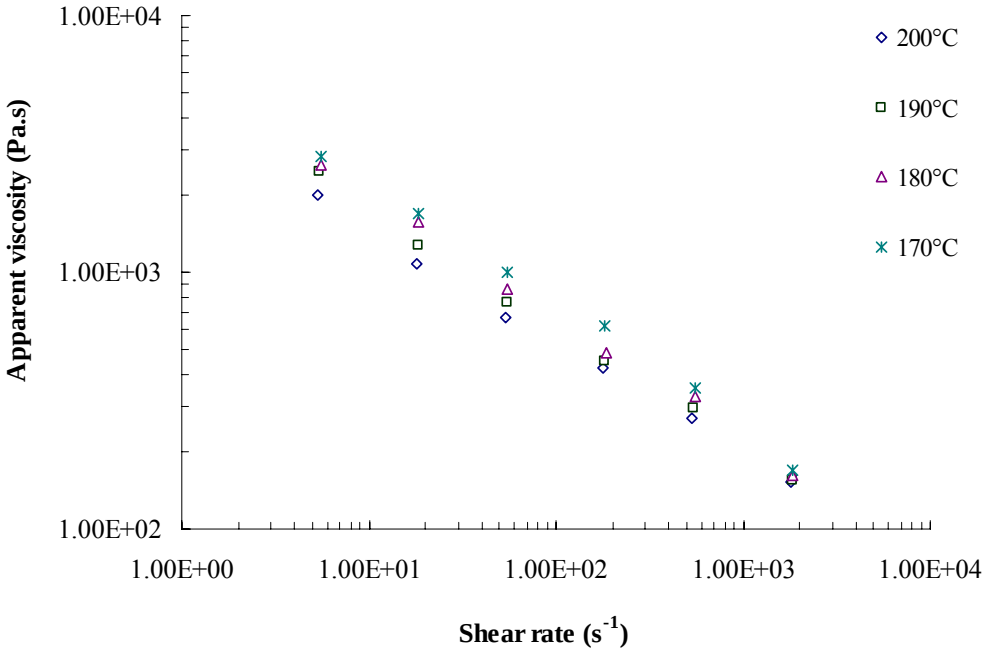

Figure 4.24 Apparent viscosity of biocomposite A2 (fiber = 20% wt.) as function of shear rate.

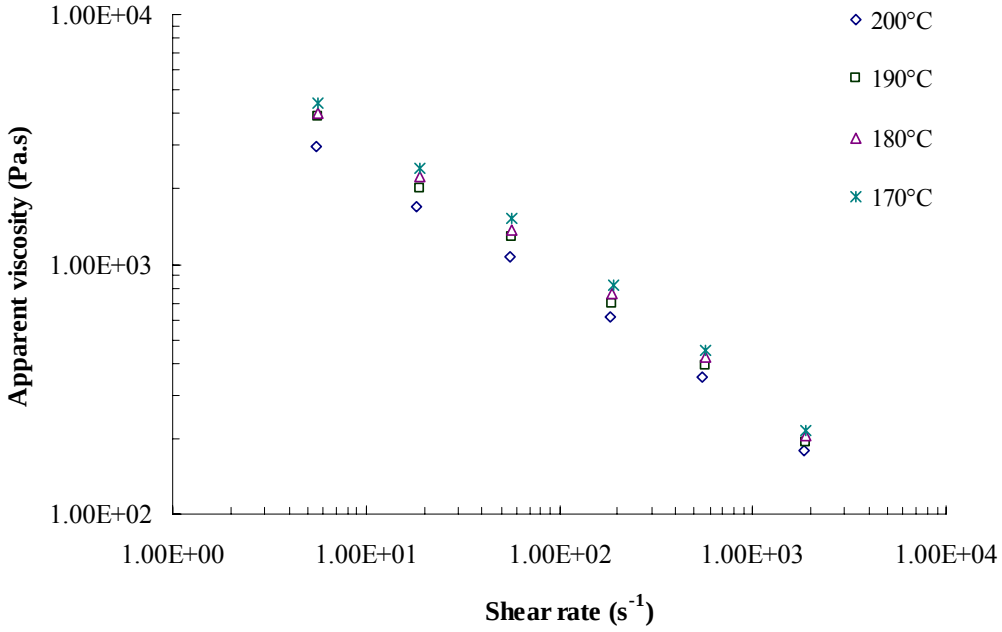

Figure 4.25 Apparent viscosity of biocomposite A3 (fiber = 30% wt.) as function of shear rate.

Statistical analysis (refer to Tables G.5 and G.6 in Appendix G) was conducted to determine how apparent viscosity was affected by temperature, fiber content, and shear rate. Nonlinear regression model was considered because apparent viscosity has a power relationship with shear rate. The nonlinear regression equation of apparent viscosity (μ_a) obtained for biocomposites is:

$$\mu_a = -11.1515T + 51.5857F + 4231.2\,(\gamma)^{-0.1754} \quad (4.13)$$

where T = temperature between 170 to 200°C,

F = A treated flax fiber content between 0 to 30% wt.,

γ = shear rate, s^{-1}, and

$R^2 = 0.89$.

From Equation 4.13, apparent viscosity of biocomposite could be predicted at a given temperature (between 170 to 200°C), fiber content (0 to 30% wt) and shear rate.

It was widely observed that the viscosity of polymers significantly decreased with shear rate especially when it was higher than a critical value (Osswald and Menges 2003; Nichetti and Manas-Zloczower 1998). To further compare the significance of these three variables (temperature, fiber content, and shear rate) on the apparent viscosity, the above model was converted to linear models by converting $(\gamma)^{-0.1754}$ to one variable. Stepwise regression method in SPSS (refer to Tables G.7 and G.8 in Appendix G) was used to estimate the best set of predictor variables for the regression model. It showed that all the variables had significant effect on the apparent viscosity. Among three independent variables, the most

significant to influence apparent viscosity was shear rate, followed by fiber content. Temperature (170 to 200°C) showed the weakest influence on biocomposite apparent viscosity.

4.4.2 Prediction of filling time during injection molding

As shown in Section 3.3.4, filling time is a function of average velocity of melt flow, and velocity is a function of pressure. Equation 3.21 in Chapter 3 described the relationship between pressure (P_1, P_0) with K, n, and mold dimension (A_1, A_2, A_3, R, h, X, L) is:

$$P_1 - 0.2\rho\left[1.25 - \left(\frac{A_2}{A_1}\right)\right]\left(\frac{A_1}{A_2}\right)^2\left[\left(\frac{P_0 - P_1}{L}\right)\frac{1}{2K}\right]^{\frac{2}{n}}\left(\frac{n}{1+3n}\right)^2 R^{\frac{2}{n}+2} -$$

$$\left(\frac{A_1}{A_2}\right)^2 \rho\left(\frac{3n+1}{2n+1}\right)\left[\frac{n+3}{2(5n+3)}\left(\frac{A_2}{A_3}\right)^2 - \left(\frac{A_2}{A_3}\right) + \frac{3(3n+1)}{2(5n+3)}\right]\left[\left(\frac{P_0 - P_1}{L}\right)\frac{1}{2K}\right]^{\frac{2}{n}}\left(\frac{n}{1+3n}\right)^2 R^{\frac{2}{n}+2} =$$

$$(P_0 - P_1)\left(\frac{X}{2L}\right)\left(\frac{A_1}{A_3}\right)^n\left(\frac{R}{h}\right)^{1+n}\left(\frac{2n+1}{1+3n}\right)^n$$

The above equation can be written as:

$$P_1 - a(P_0 - P_1)^{\frac{2}{n}} - b(P_0 - P_1) = 0 \tag{4.14}$$

where:

$$a = \left\{\begin{array}{l} 0.2\left[1.25 - \left(\frac{A_2}{A_1}\right)\right] + \\ \left(\frac{3n+1}{2n+1}\right)\left[\frac{n+3}{2(5n+3)}\left(\frac{A_2}{A_3}\right)^2 - \left(\frac{A_2}{A_3}\right) + \frac{3(3n+1)}{2(5n+3)}\right] \end{array}\right\}\rho\left(\frac{A_1}{A_2}\right)^2\left(\frac{n}{1+3n}\right)^2 R^{\frac{2}{n}+2}\left(\frac{1}{2KL}\right)^{\frac{2}{n}},$$

and

$$b = \left(\frac{X}{2L}\right)\left(\frac{A_1}{A_3}\right)^n\left(\frac{R}{h}\right)^{1+n}\left(\frac{2n+1}{1+3n}\right)^n$$

If P_0 is assumed as the injection pressure, then P_1 in equation 4.14 could be solved by Newton's method (also known as the Newton–Raphson method) (Ypma 1995) by Matcad (MathSoft, Inc. Needham, MA). The Matcad program of using Newton's method and the values of a and b for HDPE and biocomposites are in Appendix H. Equation 4.14 can be reduced to:

$$P_1 - b(P_0 - P_1) = 0 \tag{4.15}$$

therefore:

$$P_1 = \frac{b}{1+b} P_0 \tag{4.16}$$

Combining equation 3.20 and equation 4.16, P_3 becomes:

$$P_3 = P_0 \left(\frac{1}{1+b} \right) \left(\frac{X}{2L} \right) \left(\frac{A_1}{A_3} \right)^n \left(\frac{R}{h} \right)^{1+n} \left(\frac{2n+1}{1+3n} \right)^n \tag{4.17}$$

Substituting equation 4.16 into equation 3.10, u_1 becomes:

$$u_1 = \left[\left(\frac{P_0 - P_1}{L} \right) \frac{1}{2K} \right]^{\frac{1}{n}} \left(\frac{n}{1+3n} \right) R^{\frac{1}{n}+1} = \left[\left(\frac{P_0 - \frac{b}{1+b} P_0}{L} \right) \frac{1}{2K} \right]^{\frac{1}{n}} \left(\frac{n}{1+3n} \right) R^{\frac{1}{n}+1}$$

$$= \left[\left(\frac{1}{1+b} \right) \frac{1}{2KL} \right]^{\frac{1}{n}} \left(\frac{n}{1+3n} \right) R^{\frac{1}{n}+1} P_0^{\frac{1}{n}} \tag{4.18}$$

From equation 3.7 and equation 4.18, u_3 can be written as:

$$u_3 = 0.432 \left[\left(\frac{1}{1+b} \right) \frac{1}{2KL} \right]^{\frac{1}{n}} \left(\frac{n}{1+3n} \right) R^{\frac{1}{n}+1} P_0^{\frac{1}{n}} \tag{4.19}$$

The filling time (t) in equation 3.24 included the time to fill the cylindrical sprue and runner (t_1) and the time to fill the rectangular mold part (t_2), thus it becomes:

$$t = t_1 + t_3 = \frac{L}{u_1} + \frac{X}{u_3} = cP_0^{-\frac{1}{n}} + dP_0^{-\frac{1}{n}} = (c+d)P_0^{-\frac{1}{n}} \tag{4.20}$$

where $c = L^{\frac{1}{n}+1}\left[\left(\frac{1}{1+b}\right)\frac{1}{2K}\right]^{-\frac{1}{n}}\left(\frac{n}{1+3n}\right)^{-1} R^{-(1+\frac{1}{n})}$, and

$$d = \frac{1}{0.432} X\left[\left(\frac{1}{1+b}\right)\frac{1}{2KL}\right]^{-\frac{1}{n}}\left(\frac{n}{1+3n}\right)^{-1} R^{-(1+\frac{1}{n})}.$$

Equation 4.20 can be used to predict the time to fill the mold as described in Figure 3.12 for HDPE and biocomposite materials after knowing their rheological properties.

Based on the mold shown in Figure 3.12, the filling time for HDPE and biocomposites A1, A2, and A3 are estimated and the results are shown in Figures 4.26 to 4.29.

The required filling time dramatically decreased when injection pressure increased. It also shows that increasing the injection temperature can significantly decrease the filling time especially at lower injection pressure. This is because the material viscosity decreases with temperature, where the flow resistance at high temperature is smaller than that at low temperature.

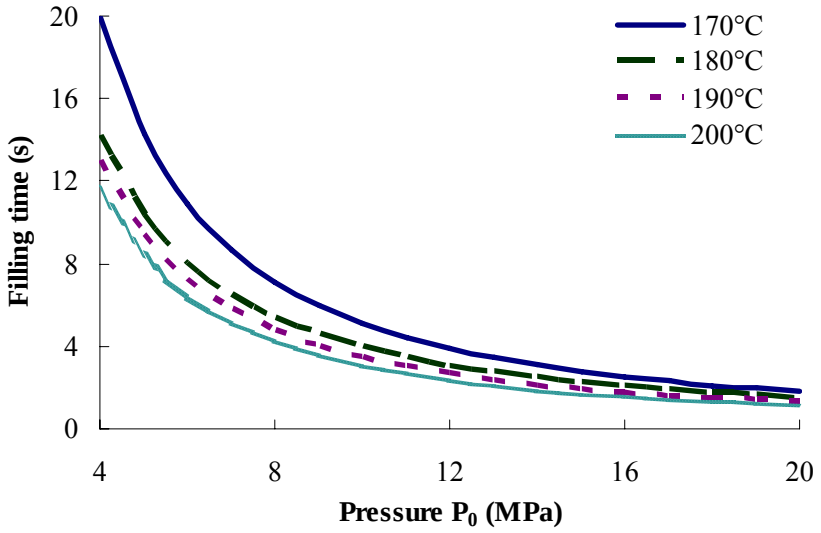

Figure 4.26 Filling time for HDPE at different injection temperatures.

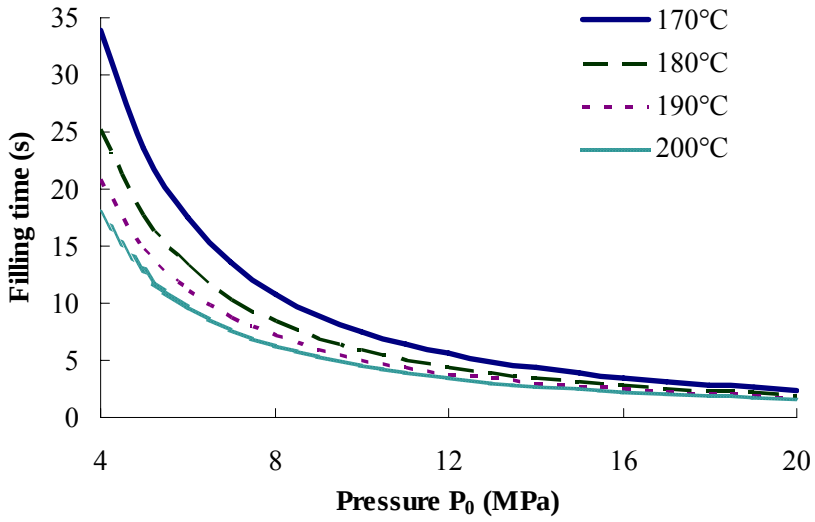

Figure 4.27 Filling time for biocomposite A1 (fiber = 10% wt.) at different injection temperatures.

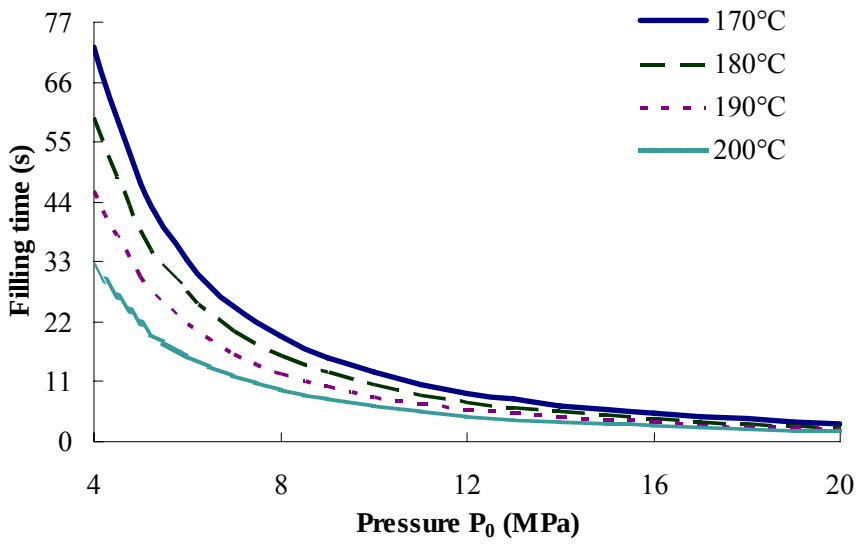

Figure 4.28 Filling time for biocomposite A2 (fiber = 20% wt.) at different injection temperatures.

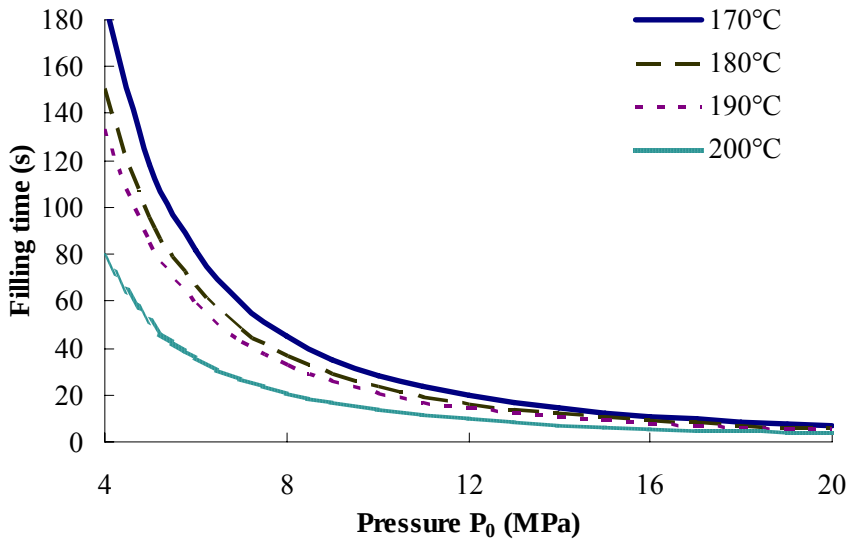

Figure 4.29 Filling time for biocomposite A3 (fiber = 30% wt.) at different injection temperatures.

Comparing with pure HDPE, the biocomposites required longer time to fill the injection mold. This can also be observed clearly from Figure 4.30, which is the filling time needed for biocomposites and HDPE when injection temperature is at 190°C. Filling time dramatically increased with increasing the fiber content. The reason for this can be explained from the rheological testing results in section 4.4.1. Adding fiber into HDPE increased the material's resistance to the flow causing a longer filling time.

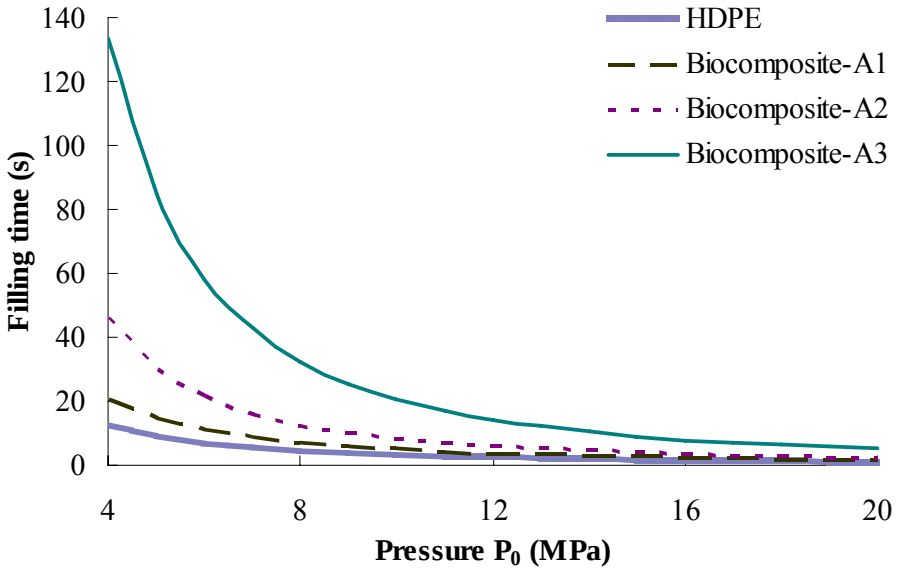

Figure 4.30 Filling time of HDPE and biocomposites at 190°C.

The reduction of filling time plays an important role on the overall cycle time and process cost, but it is mostly studied in Resin Transfer Molding process (Trochu et al. 2006; Deléglise et al. 2005). Trochu and co-workers (2006) considered a liquid phase resin as Newtonian-fluid and studied the relationship of pressure drop with time during injection. Most flow analyses on injection molding are very complex,

needing experimental and numerical modeling, or computer-aided engineering simulation tools. Barriere and co-workers (2003) determined the optimal process parameters in metal injection molding which combined the use of experiments, modeling and numerical simulations. Studies on natural fiber-reinforced composite have not been reported yet.

The filling time studied in this work used many assumptions listed in section 3.3.4, so it may differ with the actual filling time. If the effect of heat transfer during the filling process were to be included, the actual filling time may be longer than the predicted filling time. However, if the pressure loss due to the friction during the fluid flow in the mold were to be considered, the actual P_1 will be less than the calculated value (from equation 4.16), and velocity in equation 3.10 will be larger than the calculated value, so the filling time will be shorter than the predicted time. Although the flow analysis in this study was not on a 2-D or 3-D approach and had limitations of application, it could give insight or brief information during the injection molding of flax fiber-HDPE biocomposites or power-law fluid materials.

4.5 Thermal properties of biocomposites and prediction of cooling time

During injection molding of biocomposites, a typical cycle time can be divided into several stages: (1) the material is injected into the mold; (2) the mold is held under the pressure; (3) the mold is cooled; and (4) the mold is opened and the product is ejected out from the mold. Then the mold is closed and clamped for the next cycle. The cooling time for stage (3) is one factor that increases the cost of

injection molding process (ASM International 2003). A short cooling time is desirable.

As shown in equation 3.25, the minimum cooling time (t_c) during injection molding can be predicted (Rosato and Rosato 1995), where cooling time t_c is related with material thermal diffusivity (α, m^2/s), injected material temperature (T_m,°C), mold wall temperature (T_w,°C), ejection temperature (T_e,°C), and material thickness ($2h$, m). This equation uses a one-dimensional finite difference scheme to calculate temperature as a function of time through the thickness of a plate shape of material. When the center of the plate reaches the specified ejection temperature, the analysis is stopped and the minimum cooling time is determined (ASM International 2003). To estimate the minimum cooling time, the thermal diffusivity of the material needs to be determined first.

The thermal diffusivity (α, m^2/s) of biocomposite was calculated using its definition, $\alpha = \frac{k}{\rho C_p}$, where thermal diffusivity is the ratio of thermal conductivity (k, W/m°C) to specific heat (C_p, kJ/kg°C) and density (ρ, kg/m^3). The material thermal conductivity, specific heat and density were measured. The test temperature was chosen to represent the processing temperature range of biocomposites, which was from 170 to 200°C.

4.5.1 Thermal conductivity of biocomposites

In the temperature range of 170 to 200°C, thermal conductivities of HDPE and biocomposites were measured followed the procedure of section 3.4.9.

Probe calibration

The probe was calibrated to minimize the error from the experimental result to the idealized result. The agar-gelled water (1% agar) was used as reference to calibrate the system coefficient. The measured thermal conductivity of the agar-gelled water using the self-constructed probe is listed in Table 4.7.

Table 4.7 Measured thermal conductivity of agar-gelled water (1% agar).

Temperature (°C)	Thermal conductivity (W/m°C)	Average (W/m°C)	St. dev.
23.7	0.6044		
24.7	0.6812	0.6363	0.0400
23.9	0.6233		

Comparing the measured value with 0.6042 W/m°C obtained for water in reference (Singh and Heldman 1995), the calibration coefficient C (from equation 3.45) is:

$$C = \frac{k}{k'} = \frac{0.6042}{0.6363} = 0.9495 \tag{4.21}$$

Thermal conductivity of HDPE and flax fiber

It was reported that the thermal conductivity of HDPE increased with temperature up to 135°C, after which, it remained constant (Woo et al. 1995). Thus, the thermal conductivity of HDPE was considered to be constant in the temperature range of 170 to 200°C. The value of thermal conductivity reported for HDPE are the average of three measurements as shown in Table 4.8.

Table 4.8 Thermal conductivity of molten HDPE.

Temperature (°C)	Thermal conductivity (W/m°C)	Average (W/m°C)	St. dev.
170	0.4365		
187	0.4237	0.4281	0.0073
188	0.4241		

Woo and co-workers (1995) reported that the thermal conductivity of melted HDPE varied from 0.25 to 0.435 W/m°C within different grades. Osswald and Menges (2003) reported that the thermal conductivity of HDPE was 0.63 W/m/°C. The value obtained for the thermal conductivity of HDPE in this work was within the reported range and was therefore acceptable.

Due to lack of literature data, the thermal conductivity measurement of flax fiber was conducted from room temperature to 200°C. The variation of the thermal conductivity of acrylic acid-treated flax fiber with temperature is shown in Figure 4.31.

It can be observed that the thermal conductivity of flax fiber increased with temperature first, then it remained practically constant at temperature higher than 80°C. The average thermal conductivity of treated flax fiber at temperatures above 80°C was 0.1187 W/m°C with a standard deviation of 0.0011 W/m°C.

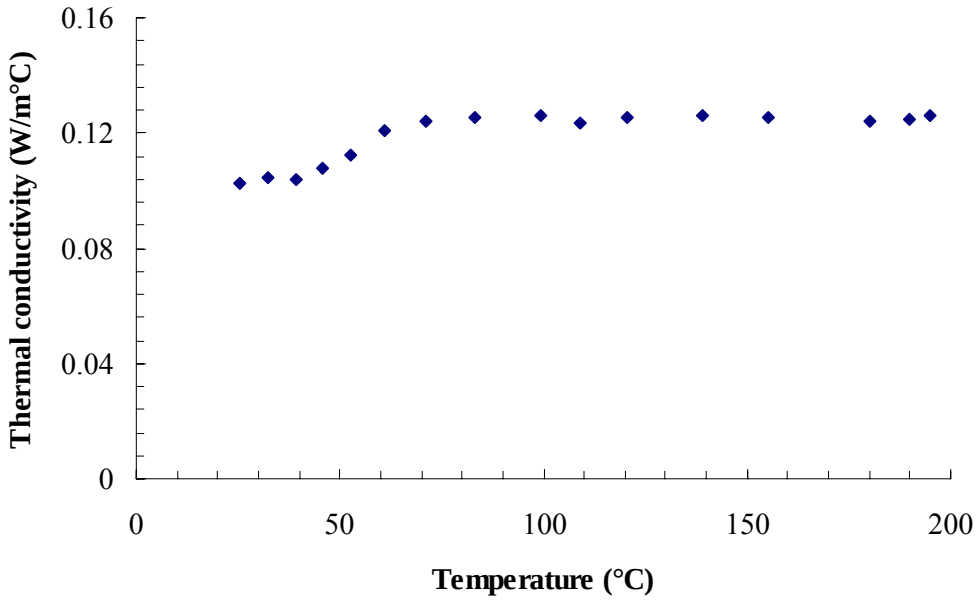

Figure 4.31 Thermal conductivity of acrylic acid treated flax fiber as a function of temperature.

Thermal conductivity of biocomposites

Since the thermal conductivity of treated fiber and HDPE all remained constant at temperature of 170 to 200°C, the thermal conductivity of the biocomposites was assumed to be constant. The measured thermal conductivity of the flax fiber-HDPE biocomposites as a function of fiber content is shown in Figure 4.32.

It was found that the thermal conductivity of biocomposites was mainly affected by fiber content. It decreased with increasing flax fiber content, indicating that flax fiber had lower thermal conductivity than the HDPE matrix. The flax fiber-HDPE biocomposite with 10% fiber had a thermal conductivity of 0.4018 W/m°C, less than the thermal conductivity of HDPE (0.4281 W/m°C), and higher than that of

biocomposite containing 20% fiber (0.3684 W/m°C) and 30% fiber (0.3367 W/m°C). Because there was no information on the thermal conductivity of natural fiber composites, the theoretical thermal conductivity models were used to verify the experimental results.

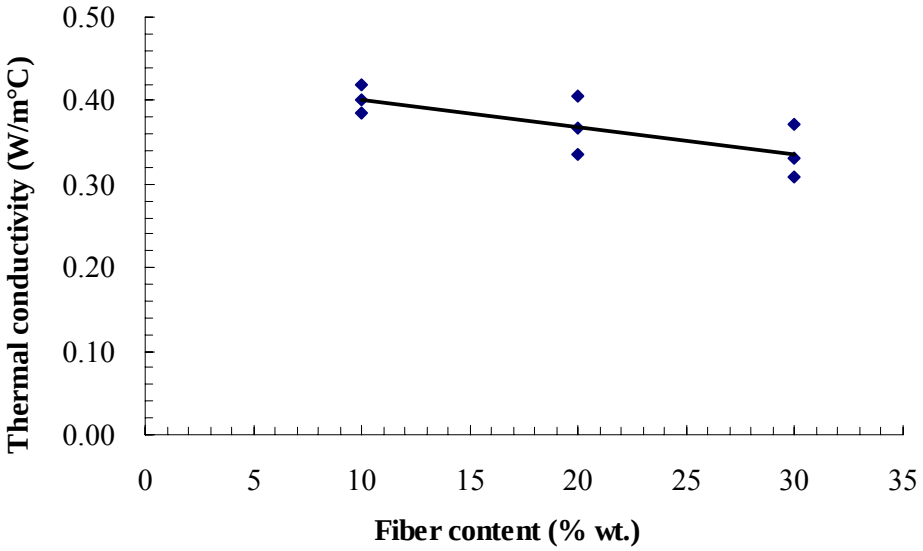

Figure 4.32 Measured thermal conductivity of the biocomposites as a function of fiber content.

Estimating thermal conductivity of biocomposites by using thermal conductivity prediction models

Thermal conductivity of composites can be estimated by knowing the thermal conductivity of each component of composites. Some theoretical and empirical models have been proposed to predict the thermal conductivity of composites, including parallel (Kalaprasad et al. 2000), series (Kalaprasad et al. 2000), Maxwell

(Tavman 1998), and Russell (Tavman 1998). These models are expressed as follows:

Parallel model: $k = V_f k_f + (1 - V_f) k_m$ (4.22)

Series model: $\frac{1}{k} = \frac{V_f}{k_f} + \frac{(1 - V_f)}{k_m}$ (4.23)

Maxwell model: $k = k_m \frac{k_f + 2k_m + 2V_f (k_f - k_m)}{k_f + 2k_m - V_f (k_f - k_m)}$ (4.24)

Russell model: $k = k_m \left[\frac{V_f^{2/3} + \frac{k_m}{k_f} \left(1 - V_f^{2/3}\right)}{V_f^{2/3} - V_f + \frac{k_m}{k_f} \left(1 + V_f - V_f^{2/3}\right)} \right]$ (4.25)

where k = the thermal conductivity of the composite (W/m°C),

k_m = the thermal conductivity of the matrix (W/m°C),

k_f = the thermal conductivity of the fiber (W/m°C),

V_f = the volume fraction of the fiber, and

$V_f = W_f \frac{\rho_c}{\rho_f}$ (Whittenberger et al. 1982), where W_f = the mass fraction of the fiber, and $\frac{\rho_c}{\rho_f}$ = the ratio of the density of the biocomposite (ρ_c) to that of treated flax fiber (ρ_f).

According to above models, the calculated and measured thermal conductivities of biocomposites are shown in Figure 4.33.

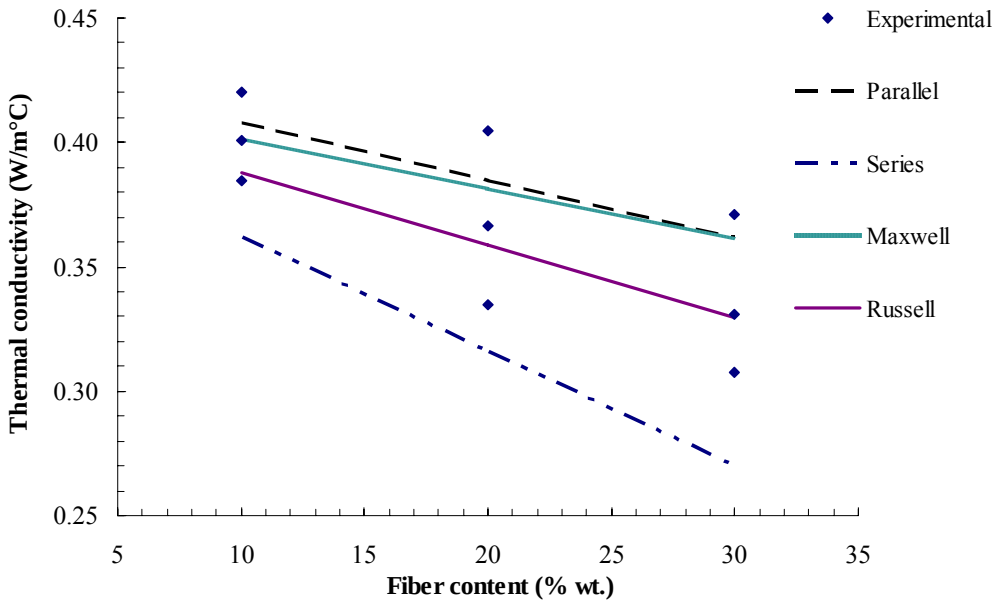

Figure 4.33 Measured and calculated thermal conductivity of the biocomposites.

The mean of measured thermal conductivity of the biocomposite was less than the value predicted from the parallel model, and higher than the value determined using the series model. The parallel and series models (Figure 4.34) were named according to the alignment of components in composites to heat flux direction (Kalaprasad et al. 2000). Figure 4.33 indicates that the fiber alignment in biocomposites was random, including both parallel and series alignments. But the measured value was closer to parallel model, indicating fiber alignment was closer to parallel alignment than series alignment.

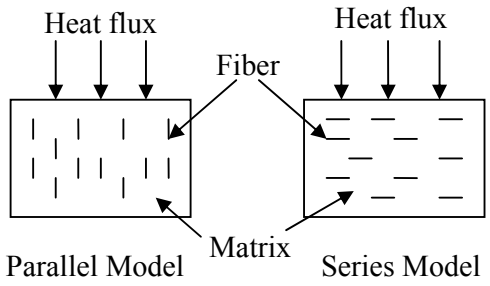

Figure 4.34 Conduction parallel and series models used to predict the thermal conductivity of composites (Kalaprasad et al. 2000).

The Maxwell model was reported to predict the effective thermal conductivity of composites at lower filler concentrations very well (Wong and Bollampally 1999). It can be seen that the thermal conductivity of biocomposites was best predicted by the Maxwell model when the fiber content was 10%. But when the fiber content increased to 30%, the Russell model which assumes that the fibers are isolated cubes of the same size dispersed in the matrix (Tavman 1998) gave the best predicted result. The measured thermal conductivity in this study was between the values predicted by the theoretical models, so the result of the measurement was acceptable.

4.5.2 Specific heat of biocomposites

Table 4.9 shows the specific heat capacity of HDPE and biocomposites measured between 170 to 200°C using DSC. As can be seen, the specific heat of the test materials increased gradually with temperature within this temperature range. Weidenfeller et al. (2004) found the same trend on magnetite and barite filled polypropylene. It was reported that the specific heats of polymers generally ranged

from 1.25 to 2.51 kJ/kg°C at ambient temperatures; the value of HDPE at room temperature was 1.85 kJ/kg°C (ASM International 2003). Osswald and Menges (2003) reported that the specific heat of HDPE was 2.3 kJ/kg°C, while Rosato and co-workers (2000) reported it as 3.77 kJ/kg°C, but the testing temperature was not specified.

Table 4.9 Specific heat of HDPE and flax fiber-HDPE biocomposites.

Materials	Temperature (°C)	Specific heat (kJ/kg°C)	
		Mean	St. dev.
Biocomposite A1*	170	2.44	0.01
	180	2.47	0.02
	190	2.50	0.04
	200	2.52	0.04
Biocomposite A2**	170	2.28	0.02
	180	2.29	0.01
	190	2.32	0.01
	200	2.34	0.01
Biocomposite A3***	170	2.25	0.02
	180	2.27	0.02
	190	2.29	0.03
	200	2.30	0.03
HDPE	170	2.48	0.04
	180	2.50	0.04
	190	2.52	0.04
	200	2.54	0.06

* A1 = Flax fiber-HDPE biocomposite includes 10% fiber by mass content.
** A2 = Flax fiber-HDPE biocomposite includes 20% fiber by mass content.
*** A3 = Flax fiber-HDPE biocomposite includes 30% fiber by mass content.

It is also observed from Table 4.9 that the specific heat capacity of the biocomposites was influenced by the fiber content. It decreased with increasing fiber content, showing that flax fiber required less energy to be heated up in comparison with HDPE.

A linear regression relationship between independent variables (temperature and fiber content) and dependent variable (specific heat, C_p) was created by SPSS (Tables I.1 - I.3 in Appendix I). It is:

$$C_p = 2.117 - 0.009F + 0.002T \tag{4.26}$$

where F = fiber content (0 to 30% wt.),

T = temperature (170 to 200°C), and

$R^2 = 0.8686$.

SPSS stepwise method showed that fiber content had more significant influence on C_p than temperature, at the temperature range of 170 to 200°C.

4.5.3 Density of materials and biocomposites

Density measurement followed the procedured described in section 3.4.3. The particle densities of treated flax fiber, HDPE, and biocomposites are presented in Figure 4.35. It can be observed that the density of the biocomposites increased as more fiber was added.

The ideal density (ρ_i) of the biocomposite was also calculated according to equation 3.33. Table 4.10 lists the ideal densities of biocomposites and their variation from measured values. Density deviation ($\rho_{deviation}$) was calculated from equation:

$$\rho_{deviation} = \frac{\rho_{measured} - \rho_i}{\rho_i} \times 100 \tag{4.27}$$

where $\rho_{measured}$ = measured density (g/cm^3).

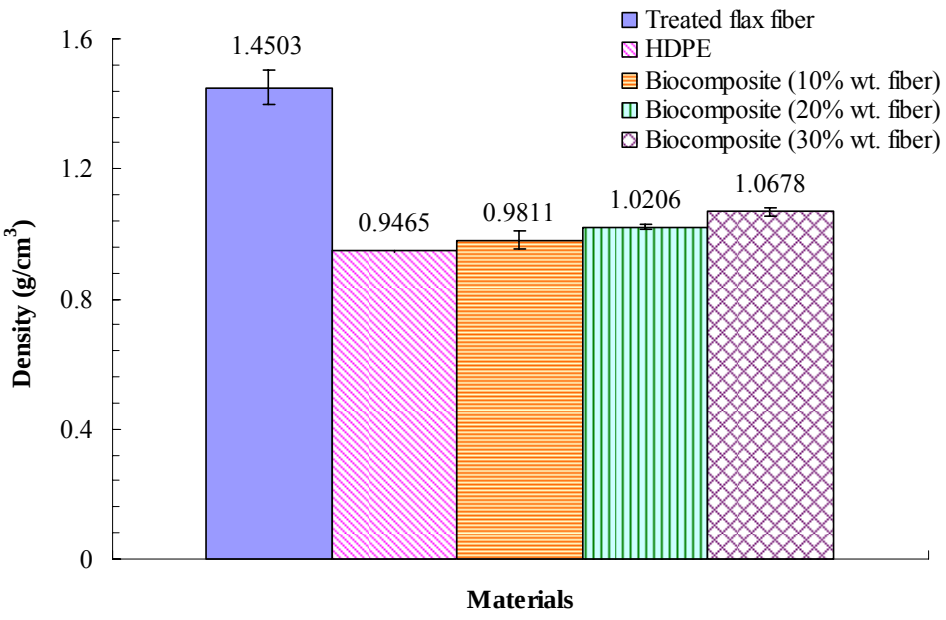

Figure 4.35 Measured density of test materials at room temperature.

Table 4.10 Deviation between ideal densities and measured densities of biocomposites.

Fiber Content (%) in biocomposites	Ideal Density (g/cm^3)	Density Deviation (%)
10	0.9869	-0.59
20	1.0233	-0.56
30	1.0624	0.51

The density deviation was less than 1%, showing a good match of the measured density and the ideal density. The above densities were measured and calculated at room temperature. Woo and co-researchers (1995) reported that the density of HDPE decreased with temperature when the temperature was above 135°C. Therefore, the density of HDPE and biocomposites should be lower than the measured value in the temperature range of 170 to 200ºC. But Ota and co-workers (2005) observed that injection temperature of 170 to 250ºC did not show any

significant change in density and crystallinity of glass fiber-polypropylene composites. In this study, the influence of the temperature on the density was ignored.

4.5.4 Thermal diffusivity of biocomposites

The thermal diffusivity values of the biocomposites calculated from equation $\alpha = \frac{k}{\rho C_p}$ were presented in Table 4.11.

Table 4.11 Thermal diffusivity of HDPE and flax fiber-HDPE biocomposites.

Materials	Temperature (°C)	Thermal diffusivity (m^2/s)	
		Mean	St. dev.
Biocomposite A1*	170	1.68×10^{-7}	7.45×10^{-9}
	180	1.66×10^{-7}	7.49×10^{-9}
	190	1.64×10^{-7}	7.62×10^{-9}
	200	1.63×10^{-7}	7.69×10^{-9}
Biocomposite A2**	170	1.59×10^{-7}	1.51×10^{-8}
	180	1.58×10^{-7}	1.50×10^{-8}
	190	1.56×10^{-7}	1.48×10^{-8}
	200	1.55×10^{-7}	1.47×10^{-8}
Biocomposite A3**	170	1.40×10^{-7}	1.34×10^{-8}
	180	1.39×10^{-7}	1.32×10^{-8}
	190	1.38×10^{-7}	1.32×10^{-8}
	200	1.37×10^{-7}	1.31×10^{-8}
HDPE	170	1.82×10^{-7}	4.40×10^{-9}
	180	1.81×10^{-7}	4.30×10^{-9}
	190	1.79×10^{-7}	4.30×10^{-9}
	200	1.78×10^{-7}	5.00×10^{-9}

* A1 = Flax fiber-HDPE biocomposite includes 10% fiber by mass content.
** A2 = Flax fiber-HDPE biocomposite includes 20% fiber by mass content.
*** A3 = Flax fiber-HDPE biocomposite includes 30% fiber by mass content.

The linear regression equation fitted to the measured thermal diffusivity (α, m^2/s) of biocomposite was developed by SPSS stepwise method (Tables J.1 to J.3 in Appendix I):

$$\alpha = 2.06 \times 10^{-7} - 1.32 \times 10^{-7} F - 1.38 \times 10^{-7} T \quad (4.28)$$

where F = fiber content (0 to 30% wt.),

T = temperature (170 to 200°C), and

$R^2 = 0.9799$.

It was found that fiber content had a significant influence on the thermal diffusivity of biocomposites. The thermal diffusivity of the biocomposites decreased with fiber content. This means that biocomposites containing flax fiber required longer time to be heated or cooled than the un-reinforced HDPE polymer. The influence of temperature on the thermal diffusivity within the temperature range used in this work was less than the influence of fiber content. Thermal diffusivity slightly decreased with the temperature. Because the density as a function of temperature was ignored in this study, the real thermal diffusivity of HDPE and biocomposites would be higher than reported in Table 4.11.

Rosato and co-workers (2000) reported that HDPE has a thermal diffusivity of 1.39×10^{-7} m^2/s. Woo and co-researchers (1995) observed that the thermal diffusivity of HDPE was around 2.5×10^{-7} m^2/s at a temperature range of 160 to 200°C. They found that the thermal diffusivity of HDPE increased with temperature at temperatures higher than 150°C, but the increase was not significant. There were no available data of biocomposite thermal diffusivity as reference. The thermal diffusivity of HDPE measured in this work was in the range of the reported values; therefore, the thermal diffusivity of biocomposites can be adopted.

4.5.5 Minimum cooling time during injection molding

In injection molding, cooling time is the time to cool the molded material to ejection temperature, which typically occupies more than one third of the whole molding cycle (Xu and Kazmer 1999). Therefore, estimating and optimizing cooling time play an important role in injection operations to reduce the cycle time and increase production rates.

The minimum cooling time (t_c) during injection molding was estimated from equation 3.20. This equation was mostly used to study the relationship between minimum cooling time and plate thickness (ASM International 2003; Beiter et al. 1995), or mold temperature (Rosato et al. 2000). The thermal diffusivity of HDPE and biocomposites used the measured value in the section 4.5.4. Then molded material thickness (also known as wall thickness, $2h$), mold temperature (T_w), material injection temperature (T_m), and ejection temperature (T_e) were chosen to perform the analysis.

Cooling time vs. mold temperature

The relationship between minimum cooling time (t_c) and mold temperature is presented in Figure 4.36 according to the assumptions:

$2h$ (molded material thickness) = 4mm,

T_m (injection temperature of material) =190°C, and

T_e (ejection temperature) = 100°C.

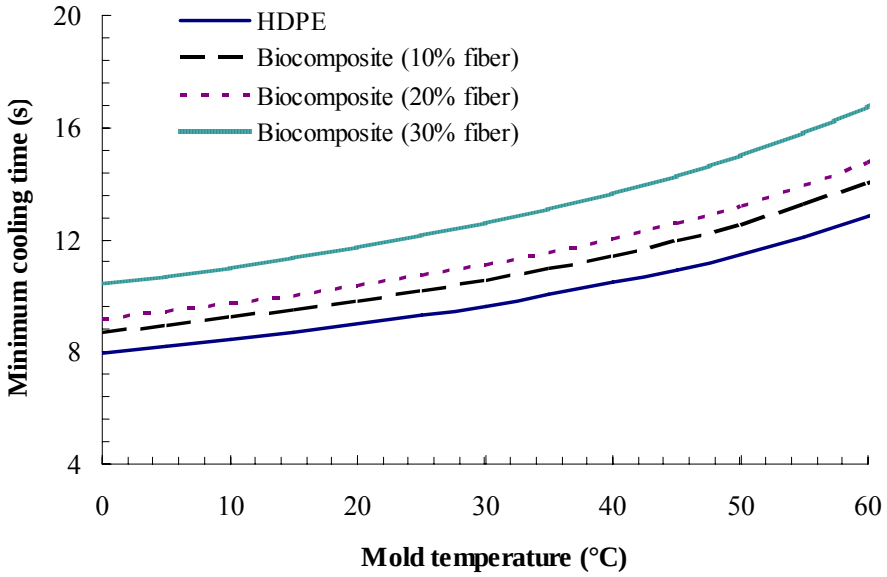

Figure 4.36 Minimum cooling time versus mold temperature when injection temperature was 190°C.

It was found that cooling time increased with mold temperature. The same result was found by Rosato and co-workers (2000). The mold temperature for HDPE ranged from 4 to 38°C (Rosato et al. 2000) or 40°C (Prystay and Garcia-Rejon 1999). Lower mold temperature is usually set to remove the heat quickly from the material and thus achieve short cycles (Rosato et al. 2000). But low mold temperature may also cause problems such as short shots, surface wrinkles or too large dimensions (Creese 1999). So the mold temperature of biocomposites cannot be set too low in order to achieve good product quality. Figure 4.36 shows that the cooling time of biocomposites increased about 2-3 s when mold temperature increased from 10 to 40°C. Therefore, mold temperature of 40°C is set up for the subsequently analysis.

Cooling time vs. molded material thickness

Cooling time curves as a function of molded material thickness (*2h*) are shown in Figure 4.37, and the following assumptions were used:

T_w (mold wall temperature) = 40°C,

T_m (injection temperature of material) = 190°C, and

T_e (ejection temperature) = 100°C.

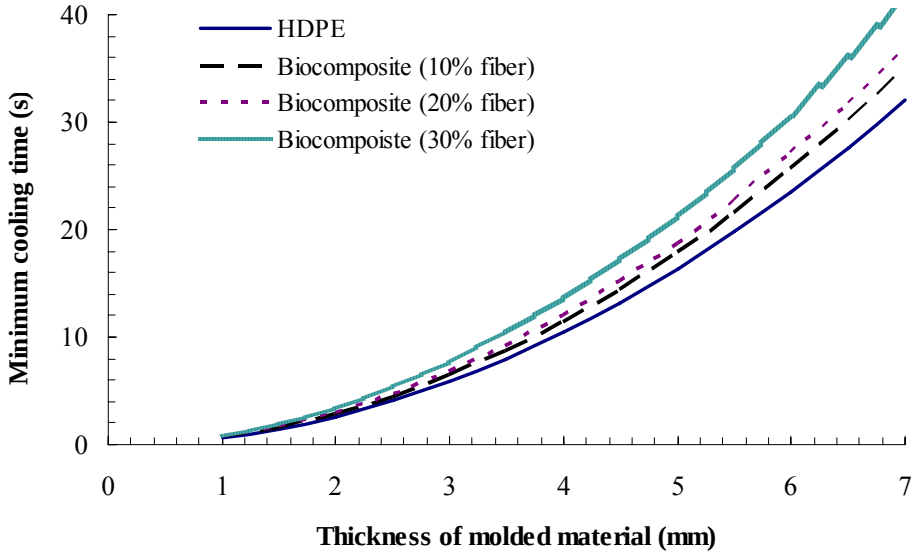

Figure 4.37 Minimum cooling time versus molded material thickness when injection temperature was 190°C.

It was found that the biocomposite with more fiber content required longer cooling time. Because biocomposites had lower thermal diffusivity than HDPE, they need longer time to conduct heat and cool down.

The minimum cooling time increased with the thickness of molded material. Beiter and co-workers (1995) studied the cooling time of polycarbonate (PC), polybutylene terephthalate (PBT), and acrylonitrile butadiene styrene (ABS) plastic

as a function of thickness from 0.5 mm to 7 mm. They found that the wall thickness had a significant influence on cooling time. The cooling time versus wall thickness was also predicted on unfilled PC plastic (ASM International 2003). It was found that when wall thickness changed from 1.5 mm to 4.0 mm, the cooling time increased from 4 s to 22 s, indicating the thickness of material largely influent the cooling time.

Cooling time vs. injection and ejection temperatures

The minimum cooling time is the duration at which the molded material is being cooled from injection temperature to ejection temperature; thus, higher injection temperature causes longer cooling time and higher ejection temperature leads to shorter cooling time. The same results are found as shown in Figures 4.38 and 4.39. To predict the cooling time as affected by injection or ejection temperature, the thickness of molded material ($2h$) was assumed to be 4 mm and mold wall temperature was assumed to be 40°C.

It was found that cooling time increased approximately by 2 s when injection temperature increased from 170 to 200°C, indicating that the influence of injection temperature on cooling time was not very obvious. Zook and co-workers (1998) also found that the effect of melt temperature (injection temperature) on cooling time was not significant.

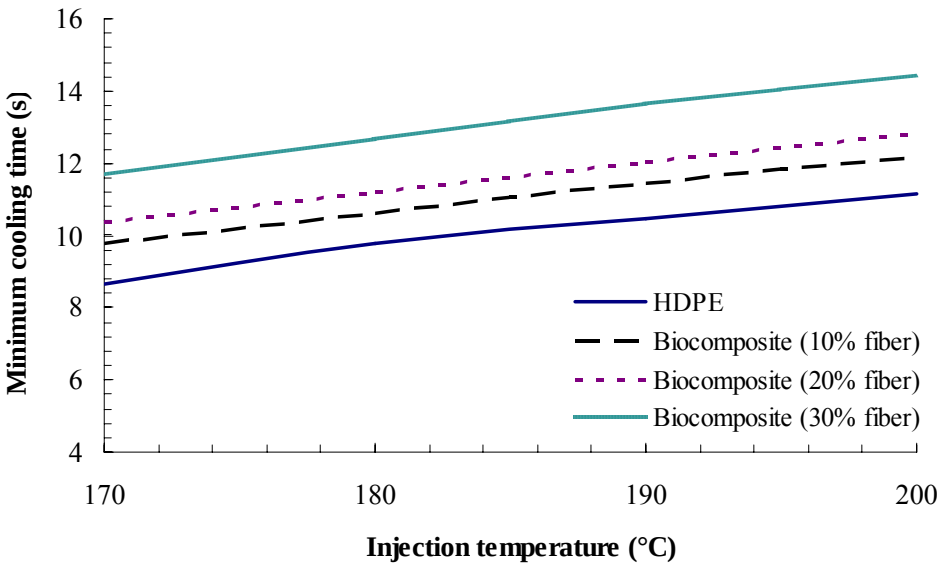

Figure 4.38 Minimum cooling time versus injection temperature when ejection temperature was set at 100°C.

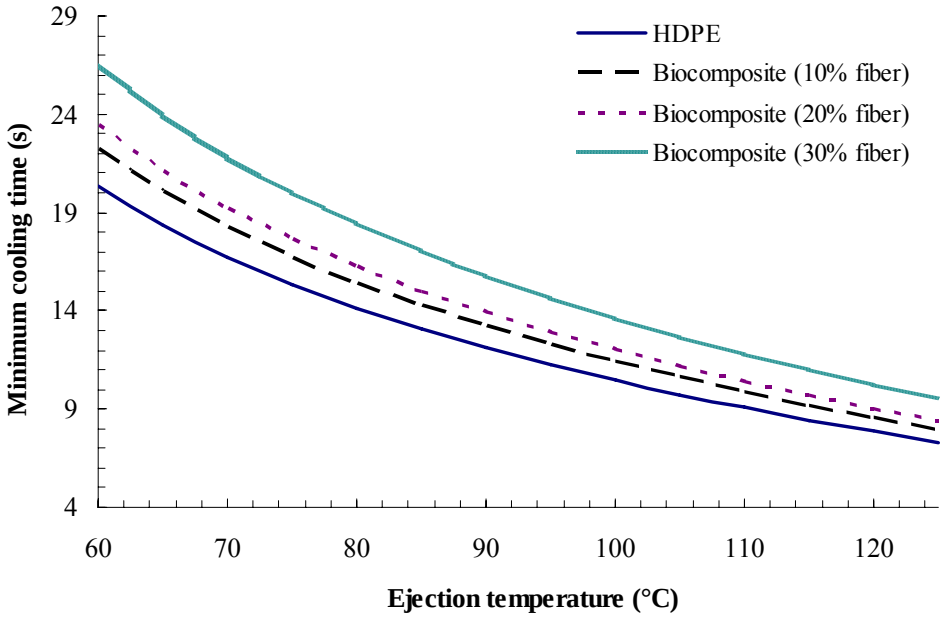

Figure 4.39 Minimum cooling time versus ejection temperature when injection temperature was set at 190°C.

The ejection temperature is the temperature when the material is cool enough for the mold to open (Isayev 1987). The ejection temperature point should be in a state that the material inside the mold cannot flow, but it is still soft enough to be ejected. There are many ways to determine the ejection temperature. Spring and Williams (1999) investigated three of the most popular methods to determine the ejection temperature of thermoplastic material. They found these methods resulted in very different ejection temperature. One method used the vicat softening temperature test according to ASTM D1525 (ASTM 1997c). One method used the heat deflection temperature as ejection temperature. With this method, Rosato and co-workers (2000) reported that HDPE usually has an ejection temperature of 60 to 90°C. The third method determined ejection temperature by DSC cooling trace: for a semi-crystallization material, it is the temperature after crystallization peak (Spring and Williams 1999). Ejection temperature was around 120°C for HDPE (Rana et al. 1999) since the crystallization temperature of HDPE was near 130°C (Wen et al. 1999).

Figure 4.39 shows that the cooling time decreases by about 10 s when ejection temperature increases from 60 to 100°C. Such a deviation will play an important role in determining the ejection temperature in industrial applications since a 10 s error in cycle time represents a 20% loss in productivity and significantly greater loss in profitability (Xu and Kazmer 1999). Overall, higher ejection temperature caused shorter cooling time (Morales et al. 2001). Thus, the relatively higher ejection temperature is preferred in injection molding.

5. SUMMARY AND CONCLUSIONS

In this study, oilseed flax fiber-reinforced polyethylene biocomposites had been developed using injection molding for the first time in Western Canada. The factors that influence the processing and the biocomposite properties were also investigated.

5.1 Summary

Natural fiber such as flax fiber is a renewable resource with the advantage of lower density, reduced energy consumption, and low cost compared with man-made fiber. Therefore, studies of natural fiber-reinforced plastic composites have increased. However in Canada, the studies in this area are still tentative. Canada is the largest oilseed flax producer in the world; most oilseed flax straw is disposed in the field without sustainable utilization. Thus, a utilization scheme of combining flax fiber and plastic to produce biocomposite can benefit not only the farmers and industries, but also the environment.

In this study, oilseed flax fiber grown in Canada was added into polyethylene to make fiber-reinforced polyethylene biocomposites via injection molding. Three materials with different fiber purity (designated fiber I, fiber II, and fiber III) were compared in their effect on reinforcement. Polyethylene, namely LLDPE and HDPE, were the main matrix investigated in this research, especially HDPE. This is

because polyethylene with low tensile strength and low processing temperatures were suitable to be reinforced by natural fibers. Compared to polypropylene, researches on polyethylene-based biocomposites are not well developed.

Different chemical pretreatments were conducted on flax fiber surface to decrease the fiber water absorption and increase the adhesion between the fiber and matrix. Six pretreatments were conducted on flax fiber-III material, including a non-chemical treatment (untreated (U)) and chemical treatments, namely, alkali (N), silane (S), potassium permanganate (P), acrylic acid (A), and sodium chlorite (C). At the same time, the morphological properties, characteristic temperatures of treated fiber, HDPE, and biocomposites were examined. One chemical treatment was chosen finally for studies on operational parameters during injection molding of flax fiber-HDPE biocomposite.

To investigate how injection molding parameters, including injection temperature, injection pressure, as well as fiber content, affect processing and biocomposite properties, the tensile, flexural properties, and water absorption of biocomposites were studied. Polynomial linear models were fitted to experimental data for tensile, flexural properties, and water absorption of biocomposite as affected by these parameters.

The rheological property and thermal diffusivity of biocomposites at the processing temperature range of 170 to 200 ºC were determined for the first time. The consistency coefficient (K) and flow behavior index (n), apparent viscosity of biocomposites and HDPE were determined by measuring the shear stress and shear

rate using a capillary rheometer. The injection filling time was predicted based on a simple mold. The thermal diffusivity of biocomposites and HDPE was determined by performing the measurement of thermal conductivity, specific heat, and density. The minimum cooling time, which was a function of material thickness, mold temperature, injection and ejection temperatures, was predicted during injection molding.

5.2 Conclusions

The basic procedure to process flax fiber-polyethylene biocomposite via injection molding has been determined in this study. Based on the results of experiments and the analysis of data, the following conclusions are made:

5.2.1 Chemical treatments

1. All fiber chemical treatments were effective in increasing the tensile strength and decreasing the water absorption of biocomposites compared with non-chemical treatment of flax fiber. SEM micrographs also revealed that all chemical modifications smoothed the fiber surface.
2. PE biocomposites reinforced with acrylic acid treated fiber exhibited the highest tensile strength and the lowest water absorption. The second highest was that of PE-silane treated fiber.

4. SEM micrographs on the biocomposite surface and tensile fracture surfaces showed that acrylic acid treatment reduced the hydrophilic nature of the fiber and improved the bonding between fiber and matrix.
5. Acrylic acid treatment decreased the hemicellulose and lignin content of the fiber. This treatment slightly increased the degradation temperature of flax fiber, but did not obviously change the melting and processing temperature of biocomposite. It was chosen to be the chemical treatment method of fiber for further investigations.

5.2.2 Selection of matrix and reinforcement

1. Adding flax fiber into polyethylene significantly influenced the tensile strength and water absorption of biocomposites.
2. The biocomposite with HDPE as matrix had higher tensile strength than biocomposites with LLDPE as matrix. The water absorption of HDPE and LLDPE biocomposites were close. HDPE was chosen as the matrix used in biocomposites for all the following experiments.
3. DSC analysis showed the melting point of HDPE was approximately 139ºC, and the recommended processing temperature for HDPE was 160 to 240ºC.
4. Among three oilseed flax fiber materials (fiber I, fiber II and fiber III), fiber I has the highest fiber content of 98-99%; fiber III has the lowest fiber content of 42% (the remaining was flax shive). The flax fiber contained more cellulose while the flax shive contained more hemicellulose and lignin.

5. Fiber I-HDPE biocomposite exhibited the highest tensile and flexural properties, showing that higher purity of flax fiber results in better mechanical properties of biocomposites. Flax fiber III biocomposite exhibited the lowest tensile and flexural strength, indicating flax shive had lower reinforcement effect than flax fiber.
6. Fiber I biocomposites showed the lowest water absorption, while flax fiber III biocomposites had the highest water absorption, showing that flax shive absorb more water than flax fiber. Thus, fiber I was chosen as fiber material to make biocomposites for all the following experiments.

5.2.3 Influence of fiber content, injection temperature and pressure on the processing and properties of biocomposites

1. Compared with injection temperature and pressure, fiber content was the most significant impact factor of influencing the mechanical properties of biocomposites.
2. Increased fiber content (from 10 to 30% wt.), dramatically increased the tensile and flexural properties, as well as the water absorption of biocomposites.
3. Low injection temperature (D=166ºC, C=182ºC, B=188ºC and A=188ºC) resulted in a higher tensile and flexural strength, and lower water absorption of biocomposites than high injection temperature (D=177ºC, C=190ºC, B=200ºC and A=200ºC). When the fiber content increased especially from 20 to 30%, the

biocomposite water absorption was significantly influenced by injection temperature.

4. Injection pressure changing from 4.8 MPa to 6.9 MPa did not significantly affect the biocomposite tensile properties and water absorption. But it significantly affected the flexural properties. The higher injection pressure was preferred to achieve higher tensile strength and flexural properties.
5. When injection temperature was below 195°C, the biocomposite water absorption did not change with injection pressure. But when injection temperature was higher than 195°C, higher pressure led to higher water absorption.
6. The statistical models of biocomposite tensile, flexural, and water absorption properties as a function of fiber content, injection temperature, and injection pressure were developed.

5.2.4 Rhelogical properties of biocomposites and injection filling time

1. Melts of biocomposites and HDPE were non-Newtonian fluids and the power law model fitted well to the experimental data.
2. Linear regression models describing the relationship between consistency coefficient (K), flow behavior index (n) and the temperature, fiber content were developed, respectively.
3. Apparent viscosity of biocomposites increased with fiber content and decreased with temperature, showing that lower fiber content and higher injection temperature caused less resistance to material flow.

4. The nonlinear regression equation of the apparent viscosity (μ_a) of biocomposites as function of fiber content, temperature, and shear rate was obtained. Among the three independent variables, the most significant variable to influence the apparent viscosity was shear rate, followed by fiber content and temperature (170 to 200°C).
5. Equations to predict injection time filling a rectangular mold were developed under the one-dimensional approach based on the assumptions of laminar flow. The filling time was related with the material consistency coefficient (*K*) and flow behavior index (*n*), mold dimensions, pressure, and injection temperature.
6. Compared with pure HDPE, the biocomposites required longer time to fill the injection mold. Increased the fiber content in biocomposites significantly increased the mold filling time.
7. As injection pressure increased, the injection filling time dramatically decreased. Increasing the injection temperature also decreased the filling time, especially when injection pressure was lower.

5.2.5 Thermal diffusivity of biocomposites and minimum cooling time during injection molding

1. The thermal conductivity of HDPE, flax fiber, and biocomposites did not change with temperature in the temperature range of 170 to 200ºC. But increased fiber content, the thermal conductivity of the biocomposite decreased. The measured thermal conductivities of the biocomposites ranged from 0.4018 W/m°C to 0.3367 W/m°C when fiber content increased from 10 to 30% wt. The experimental values

were acceptable by comparing measured values with theoretical and empirical models.

2. A linear regression relationship between specific heat of biocomposites and the injection temperature and fiber content was developed.

3. It was found that the thermal diffusivity of biocomposites decreased with increasing fiber content, and varied from 1.37×10^{-7} to 1.68×10^{-7} m^2/s. The influence of temperature (170 to 200 ºC) on diffusivity was not obvious.

4. The minimum cooling time during injection molding was related with biocomposite thermal diffusivity, molded product dimensions, mold temperature, and injection and ejection temperatures.

5. The biocomposite containing more fiber content required longer cooling time. The minimum cooling time increased with the thickness of molded material, mold temperature, and injection temperature. The cooling time decreased with the ejection temperature. The material thickness and ejection temperature largely influenced the cooling time.

6. RECOMMENDATIONS FOR FUTURE RESEARCH

This research developed flax fiber-HDPE biocomposites via injection molding. The following are suggestions for future studies and research:

1. The basic mechanical, morphological, rheological, and thermal properties for such biocomposites were studied in theory. These are valuable information to apply such biocomposites in industries and carry out the future research. But the relationship between the quality of biocomposites and the application was not established. Such biocomposites have great potential applications in plastic, automative, and construction industries. There is a need to develop biocomposites tailored to certain applications and promote them in the future.
2. Studies can be extended to the different properties of raw materials and biocomposites, such as impact properties, thermal stability, and ultraviolet resistance. This will help in finding applications of biocomposites in various areas.
3. Additives for fiber-reinforced biocomposites could be studied to improve special properties, such as: heat stability, flowability, resistance from microbial attack and color.
4. The rheological properties and flow behavior of biocomposites during injection molding have been investigated in this study based on a one-dimensional approach. Further investigation is suggested on two dimensional heat flow

analysis using the principles of conservation of mass, momentum, and energy. There is a need to develop a computer model to closely simulate injection molding of biocomposites.

5. The thermal diffusivity of biocomposites in temperatures lower than 170°C was not determined in this study. Further work in this range should be done to help understand the thermal properties of biocomposites in a broader temperature range.
6. The change of density of biocomposites with temperature was ignored in this research. The investigation and development of this measurement are suggested for future studies.

REFERENCES

Advani, S. G. and E. M. Sozer. 2002. *Process Modeling in Composites Manufacturing*. New York, NY: Marcel Dekker, Inc.

Almanza, O., MA. Rodríguez-Pérez and JA. de Saja. 2004. Measurement of the thermal diffusivity and specific heat capacity of polyethylene foams using the transient plane source technique. *Polymer International* 53: 2038-2044.

Agrawal, R., N. S. Saxena, K. B. Sharma, S. Thomas and M. S. Sreekala. 2000. Activation energy and crystallization kinetics of untreated and treated oil palm fibre reinforced phenol formaldehyde composites. *Materials Science and Engineering A* 277: 77-82.

Alvarez, V. A., R. A. Ruscekaite and A. Vazquez, 2003. Mechanical properties and water absorption behavior of composites made from a biodegradable matrix and alkaline-treated sisal fibers. *Journal of Composite Materials* 37(17): 1575-1588.

ANKOM Technology. 2005. ANKOM Technology Method. http://www.ankom.com/09_procedures/procedures.shtml (2007/01/06).

Arbelaiz, A., B. Fernández, J. A. Ramos, A. Retegi, R. Llano-Ponte and I. Mondragon. 2005. Mechanical properties of short flax fibre bundle/polypropylene composites: Influence of matrix/fibre modification, fibre content, water uptake and recycling. *Composites Science and Technology* 65: 1582-1592.

Anthony, W. S. 2001. Decortication of straw from seed flax. ASABE Paper No. 016079. St. Joseph, MI: American Society of Agricultural Engineers.

Aranberri-Askargorta, I., T. Lampke and A. Bismarck. 2003. Wetting behavior of flax fibers as reinforcement for polypropylene. *Journal of Colloid and Interface Science* 263: 580-589.

ASM International. 2003. *Characterization and Failure Analysis of Plastics*. Materials Park, OH: The Materials Information Society - International.

ASTM. 1997a. ASTM D638-97: Standard test method for tensile properties of plastics. ASTM Standard 1997. New York, NY: American Society for Testing and Materials.

ASTM. 1997b. ASTM D790-97: Standard test methods for flexural properties of unreinforced and reinforced plastics and electrical insulating materials. ASTM Standard 1997. New York, NY: American Society for Testing and Materials.

ASTM. 1997c. ASTM D1525-97: Standard test method for vicat softening temperature of plastics. ASTM Standard 1997. New York, NY: American Society for Testing and Materials.

ASTM. 1998. ASTM D570-98: Standard test method for water absorption of plastics. ASTM Standard 1998. New York, NY: American Society for Testing and Materials.

Aziz, S. H. and M. P. Ansell. 2004. The effect of alkalization and fibre alignment on the mechanical and thermal properties of kenaf and hemp bast fibre composites: Part I – polyester resin matrix. *Composites Science and Technology* 64: 1219-1230.

Baley, C. 2002. Analysis of the flax fibers tensile behaviour and analysis of the tensile stiffness increase. *Composites Part A: Applied Science and Manufacturing* 33: 939-948.

Baijal, M. D. 1982. *Plastics Polymer Science and Technology*. New York, NY: John Wiley & Sons, Inc.

Bakar, M. S. A., P. Cheang and K. A. Khor. 2003. Mechanical properties of injection molded hydroxyapatite-polyetheretherketone biocomposites. *Composites Science and Technology* 63: 421-425.

Barriere, Th., B. Liu and J. C. Gelin. 2003. Determination of the optimal process parameters in metal injection molding from experiments and numerical modeling. *Journal of Materials Processing Technology* 143-144: 636-644.

Batra, SK. 1998. *Handbook of Fiber Science and Technology*. New York, NY: Marcel Dekker.

Beiter, K., J. Cardinal and K. Ishii. 1995. Design for injection molding: balancing mechanical requirements, manufacturing costs, and material selection. http://www-mml.stanford.edu/publications/1995/1995.ASME.CICD.Beiter.pdf (2007/08/24).

Berglund, D. R. and R. K. Zollinger. 2002. Flax Production in North Dakota. http://www.ag.ndsu.edu/pubs/plantsci/crops/a1038w.htm.(2006/12/04).

Blackwell, J. H. and A. D. Misener. 1951. Approximate solution of a transient heat flow problem. *Proceedings of the Physical Society (London)* 64: 1132-1133.

Bledzki, A. K. and J. Gassan. 1999. Composites reinforced with cellulose based fibers. *Progress in Polymer Science* 24: 221-274.

Cantero, G., A. Arbelaiz, R. Llano-Ponte and I. Mondragon. 2003. Effects of fiber treatment on wettability and mechanical behaviour of flax/polypropylene composites. *Composites Science and Technology* 63:1247-1254.

Campbell, F. C. 2004. *Manufacturing Processes for Advanced Composites*. Oxford, UK: Elsevier Advanced Technology.

Carvalho, G. D., E. Frollini and N. D. Santos. 1996. Thermal conductivity of polymers by hot-wire method. *Journal of Applied Polymer Science* 62: 2281-2285.

Chang, R. and W. Yang. 2001. Numerical simulation of mold filling in injection molding using a three-dimensional finite volume approach. *International Journal for Numerical Methods in Fluids* 37: 125-148.

Colom, X., F. Carrasco, P. Pagès and J. Cañavate. 2003. Effects of different treatments on the interface of HDPE/lignocellulosic fiber composites. *Composites Science and Technology* 63: 161-169.

Courbebaisse, G. 2005. Numerical simulation of injection moulding process and the pre-modelling concept. *Computational Materials Science* 34: 397-405.

Cox, M., E. EI-Shafey, A. Pichugin and Q. Appleton. 1999. Preparation and characterization of a carbon adsorbent from flax shive by dehydration with sulfuric acid. *Journal of Chemical Technology and Biotechnology* 74: 1019-1029.

Crawford, R. J. and J. L.Throne. 2000. *Rotational Molding Technology*. Norwich. UK: William Andrew Publishing.

Creese, R. C. 1999. *Introduction to Manufacturing Processes and Materials*. Boca Raton, FL: CRC Press.

Deléglise, M., C. Binétruy and P. Krawczak. 2005. Solution to filling time prediction issues for constant pressure driven injection in RTM. *Composites Part A: Applied Science and Manufacturing* 36: 339-344.

Davies, G. C. and D. M. Bruce. 1998. Effect of environmental relative humidity and damage on the tensile properties of flax and nettle fibers. *Textile Research Journal* 68: 623–629.

Dealy, J. M. and R. G. Larson. 2006. *Structure and Rheology of Molten Polymers*. Munich, Germany: Carl Hanser Verlag.

Dubois, J. H. and W. J. Rederich. 1974. *Plastics*. New York, NY: van Nostrand Reinhold Company.

El-Mashad, H. M., W. K. P. van Loon, G. Zeeman and G. P. A. Bot. 2005. Rheological properties of dairy cattle manure. *Bioresource Technology* 96(5): 531-535.

Emami, S., L. G. Tabil and R. T. Tyler. 2007. Thermal properties of chickpea flour, isolated chickpea starch, and isolated chickpea protein. *Transactions of the ASABE* 50(2): 597-604.

Fitzpatrick, K. 2006. Flax Canada 2015-Enhancing the value of flax through innovation and collaboration. http://www.cropweek.com/pdf/2006/flaxcanada2015_09jan2006.pdf (2006/12/05).

Fu, S. Y., B. Lauke, E. Mäder, C. Y. Yue and X. Hu. 2000. Tensile properties of short-glass fiber- and short-carbon-fiber-reinforced polypropylene composites. *Composites Part A: Applied Science and Manufacturing* 31: 1117-1125.

Fung, K. L., X. S. Xing, R. K. Y. Li, S. C. Tjong and Y. W. Mai. 2003a. An investigation on the processing of sisal fibre reinforced polypropylene composites. *Composites Science and Technology* 63(9): 1255-1258.

Fung, Ch-P. 2003b. Manufacturing process optimization for wear property of fiber-reinforced polybutylene terephthalate composites with grey relational analysis. *Wear* 254: 298-306.

Gassan, J. and A. K. Bledzki. 1997. The influence of fiber-surface treatment on the mechanical properties of jute-polypropylene composites. *Composites Part A: Applied Science and Manufacturing* 28: 1001–1005.

Garkhail, S. K., R. W. H. Heijenrath and T. Peijs. 2000. Mechanical properties of natural-fiber-mat-reinforced thermoplastics based on flax fibers and polypropylene. *Applied Composite Materials* 7: 351-372.

George, J., R. Janardhan, J. S. Anand, S. S. Bhagawan and S. Thomas. 1996. Melt rheological behaviour of short pineapple fibre reinforced low density polyethylene composites. *Polymer* 37(24): 5421-5431.

Greene, J. P. and J. O. Wilkes. 1997. Numerical analysis of injection molding of glass fiber reinforced thermoplastics, part 1: injection pressures and flow. *Polymer Engineering and Science* 37(3): 590-602.

Henson, F. 1997. *Plastic Extrusion Technology*, 2nd ed. New York. NY: Hanser Publishers.

Herrera-Franco, P., A. Valade-Gonzalez and M. Cervantes-Uc. 1997. Development and characterization of a HDPE-sand-natural fiber composite. *Composites Part B* 28B: 331-343.

Hill, A. S. C., H. P. S. Abdul Khalil and M. D. Hale. 1998. A study of the potential of acetylation to improve the properties of plant fibres. *Industrial Crops and Products* 8(1): 53-63.

Isayev, A. I. 1987. *Injection and Compression Molding Fundamentals*. New York, NY: CRC Press LLC.

Instron 1993. Basic theory of Capillary Rheology. Manual No. 10-364-1(B). Canton, MA: Instron.

Jacob, M., S. Thomas and K. T. Varughese. 2004. Mechanical properties of sisal/oil palm hybrid fiber reinforced natural rubber composites. *Composites Science and Technology* 64: 955-965.

Jähn, A. 2002. Characterization of alkali treated flax fibers by means of FT Raman spectroscopy and environmental scanning electron microscopy. *Spectrochimica Acta Part A: Molecular and Biomolecular Spectroscopy* 58: 2271-2279.

Joffe, R., J. Andersons and L. Wallström. 2003. Strength and adhesion characteristics of elementary flax fibres with different surface treatments. *Composites Part A: Applied Science and Manufacturing* 34:603-612.

Johnson, A. T. 1999. *Biological Process Engineering*. New York, NY: John Wiley & Sons, Inc

Joseph, K. and S. Thomas. 1996. Effect of chemical treatment on the tensile properties of short sisal fiber-reinforced polyethylene composites. *Polymer* 37: 5139-5149

Joseph, K., R. D. T. Filho, B. James, S. Thomas and L. H. de. Carvalho. 1999a. A review on sisal fiber reinforced polymer composites. *Revista Brasileira de Engenharia Agricola e Ambienta* 3: 367-379.

Joseph, P. V., K. Joseph and S. Thomas. 1999b. Effect of processing variables on the mechanical properties of sisal-fiber-reinforced polypropylene composites. *Composites Science and Technology* 59(11): 1625-1640.

Joseph, P. V., K. Joseph, S. Thomas, C. K. S. Pillai, V. S. Prasad, G. Groeninckx and M. Sarkissova. 2003. The thermal and crystallisation studies of short sisal fibre reinforced polypropylene composites. *Composites Part A: Applied Science and Manufacturing* 34(3): 253-266.

Kalaprasad, G., P. Pradeep, G. Mathew, C. Pavithran and S. Thomas. 2000. Thermal conductivity and thermal diffusivity analyses of low-density polyethylene composites reinforced with sisal, glass and intimately mixed sisal/glass fibres. *Composites Science and Technology* 60(16): 2967-2977.

Karlsson, J. O. and P. Gatenholm. 1999. Cellulose fibre-supported pH-sensitive hydrogels. *Polymer* 40(2): 379-387.

Karmaker, A. C. and J. A. Youngquist. 1996. Injection molding of polypropylene reinforced with short jute fibers. *Journal of Applied Polymer Science* 62: 1147-1151.

Keller, A. 2003. Compounding and mechanical properties of biodegradable hemp fiber composites. *Composites Science and Technology* 63: 1307-1316.

Kim, K. H., A. I. Isayev, K. Kwon and C. van Sweden. 2005. Modeling and experimental study of birefringence in injection molding of semicrystalline polymers. *Polymer* 46: 4183-4203.

Kim, S-W. and L-S. Turng. 2004. Developments of three-dimensional computer-aided engineering simulation for injection moulding. *Modeling and Simulation in Materials Science and Engineering* 12: S151–S173.

Kreith, F. 1999. *Fluid Mechanics.* New York, NY: CRC Press LLC.

Lobo, H. and C. Cohen. 1995. Measurement of thermal conductivity of polymer melts by the line-source method. *Polymer Engineering and Science* 30(2):65-70.

Li, X., L. G. Tabil and S. Panigrahi. 2007. Chemical treatments of natural fiber for use in natural fiber-reinforced composites: A review. *Journal of Polymers and the Environment* 15:25-33.

Li, Y., Y-W. Mai and L. Ye. 2000. Sisal fibre and its composites: A review of recent developments. *Composite Science and Technology* 60:2037-2055.

Liu, C., J. Wang and J. He. 2002. Rheological and thermal properties of m-LLDPE blends with m-HDPE and LDPE. *Polymer* 43(13): 3811-3818.

Maldas, D., B. V. Kokat, and C. Daneault. 1989. Influence of coupling agents and treatments on the mechanical properties of cellulose fiber-polystyrene composites. *Journal of Applied Polymer Science* 37: 751-775.

Mallick, P. K. 1988. *Fiber-Reinforced Composites-Materials, Manufacturing, and Design.* New York, NY: Marcel Dekker, Inc.

Manfredi, B. L., E. S. Rodríguez, M. Wladyka-Przybylak and A. Vázquez. 2006. Thermal degradation and fire resistance of unsaturated polyester, modified acrylic resins and their composites with natural fibres. *Polymer Degradation and Stability* 91(2): 255-261.

Martins, M. H. and M-A De Paoli. 2001. Polypropylene compoounding with recycled material I. Statistical response surface analysis. *Polymer Degradation and Stablility*. 7: 293-298.

Mathcad. 2000. Matcad 2000 Professional. Needham, MA: MathSoft, Inc.

Matlab. 2006. Version 7.2.0.232 (R2006a). Natick, MA: The MathWorks, Inc.

MatWeb. 2007. Tensile property testing of plastics. http://www.matweb.com/reference/tensilestrength.asp. (2007/02/08).

Mcfarland, A. W. and J. S. Colton. 2004. Production and analysis of injection molded micro-optic components. *Polymer Engineering and Science* 44(3): 564-580.

Mishra, S., M. Misra, S. S. Tripathy, S. K. Nayak and A. K. Mohanty. 2001. Graft copolymerization of acrylonitrile on chemically modified sisal fibers. *Macromolecular Materials and Engineering* 286: 107-113.

Mishra, S., M. Misra, S. S. Tripathy, S. K. Nayak and A. K. Mohanty. 2002. The influence of chemical surface modification on the performance of sisal-polyester biocomposites. *Polymer Composites* 23(2): 164-170.

Mishra, S., A. K. Mohanty, L. T. Drzal, M. Misra, S. Parija, S.K.Nayak and S. S. Tripathy. 2003. Studies on mechanical performance of biofibre/glass reinforced polyester hybrid composites. *Composites Science and Technology* 63:1377-1385

Mohanty, A. K., M. Misra and L. T. Drzal. 2001. Surface modifications of natural fibers and performance of the resulting biocomposites: An overview. *Composite Interfaces* 8: 313-343.

Mohanty, A. K., A. Wibowo, M. Misra and L. T. Drzal. 2003. Effect of process engineering on the performance of natural fiber reinforced cellulose acetate biocomposites. *Composites Part A: Applied Science and Manufacturing* 35: 363-370.

Morales, R., S. Villarroel, H. Andrade, H. Rojas and A. Sanchez. 2001. Experimental validation of a mold filling/cooling software. In *Antec 2001 Conference Proceedings*. Volume 1. 3656. Brookfield, CT: Society of Plastic Engineers, Inc.

Murphy, J. 1998. *Reinforced Plastics Handbook*. Oxford, UK: Elsevier Advanced Technology.

Nair, K. C. M., S. Thomas and G. Groeninckx. 2001. Thermal and dynamic mechanical analysis of polystyrene composites reinforced with short sisal fibres. *Composites Science and Technology* 61(16): 2519-2529.

Nichetti, D. and I. Manas-Zloczower. 1998. Viscosity model for polydisperse polymer melts. *Journal of Rheology* 42(4): 951-969.

Oever, M. and T. Peijs. 1998. Continuous-glass-fibre-reinforced polypropylene composites II. Influence of maleic-anhydride modified polypropylene on fatigue behaviour. *Composites Part A: Applied Science and Manufacturing* 29(3): 227-239.

Oksman K., M. Skrifvars and J.-F. Selin. 2003. Natural fibers as reinforcement in polylactic acid (PLA) composites. *Composites Science and Technology* 63: 1317-1324.

Oladipo, A. B. and I. S. Wichman. 1999. Experimental study of opposed flow flame spread over wood fiber/thermoplastic composite materials. *Combustion and Flame* 118: 317-326.

Opoku, A., L. G. Tabil, B. Crerar and M. D. Shaw. 2006. Thermal conductivity and thermal diffusivity of timothy hay. *Canadian Biosystems Engineering* 48: 3.1-3.7.

Osswald, T. A. and G. Menges. 2003. *Materials Science of Polymers for Engineers,* 2nd ed. Munich, Germany: Hanser Publishers.

Ota, W.N., S.C. Amico and K.G. Satyanarayana. 2005. Studies on the combined effect of injection temperature and fiber content on the properties of polypropylene-glass fiber composites. *Composites Science and Technology* 65(6):873-881.

Pantani, R., I. Coccorullo, V. Speranza and G. Titomanlio. 2005. Modeling of mrphology evolution in the injection molding process of thermoplastic polymers. *Progress in Polymer Science* 30(12): 1185-1222.

Paul, A., K. Joseph and S. Thomas. 1997. Effect of surface treatments on the electrical properties of low-density polyethylene composites reinforced with short sisal fibers. *Composites Science and Technology* 57(1):67-79.

Pervaiz, M. and M. M. Sain. 2003. Carbon storage potential in natural fiber composites. *Resources, Conservation and Recycling* 39: 325-340.

Poloski, A. P., P. R. Bredt, A. Schmidt, R. G. Swoboda, J. W. Chenault and S. R. Gano. 2002. Thermal Conductivity and Shear Strength of K Basin Sludge. http://www.pnl.gov/main/publications/external/technical_reports/PNNL-13911.pdf (2006/10/10).

Rana, D., K. Cho, B. H. Lee and S. Choe. 1999. Is metallocene polyethylene blend with HDPE more compatible than with PP? In *Metallocene Technology in Commercial Applications*, ed. G. M. Benedikt, 19. Norwich, NY: William Andrew Inc.

Ray, D., B. K. Sarkar, A. K. Rana and N. R. Bose. 2001. Effect of alkali treated jute fibers on composite properties. *Bulletin of Material Sciences* 24: 129-135.

Reynolds, A. J. 1971. *Thermofluid Dynamics*. New York, NY: Wiley-Interscience.

Rong, M. Zh., M. Q. Zhang, Y. Liu, G. Ch. Yang and H. M. Zeng. 2001. The effect of fiber treatment on the mechanical properties of unidirectional sisal-

reinforced epoxy composites. *Composites Science and Technology* 61: 1437-1447.

Rosato, D. V. and V. D. Rosato. 1995. *Injection Molding Handbook,* 2nd ed. New York, NY: Chapman & Hall.

Rosato, D. V., V. D. Rosato and G. M. Rosato. 2000. *Injection Molding Handbook, 3rd ed*. Norwell, MA: Kluwer Academic Publishers.

Rosen, S. L. 1993. *Fundamental Principles of Polymeric Materials,* 2nd ed. New York, NY: John Wiley & Sons, Inc.

Rowell, R. M., R. A. Young and J. K. Rowell. 1997. *Paper and Composites from Agro-based Resources*. Boca Raton, FL: CRC Lewis Publishers.

Prystay, M. and A. Garcia-Rejon. 1999. Application of thermography for the optimization of the blow molding process. In *Imaging and Image Analysis Applications for Plastics,* ed. Rourdeyhimi, B., 226. Norwich, NY: William Andrew Inc.

Saheb, D. N. and J. P. Jog. 1999. Natural fiber polymer composites: A review. *Advances in Polymer Technology* 18(4): 351-363.

Sain, M. and D. Fortierb. 2002. Flax shives refining, chemical modification and hydrophobisation for paper production. *Industrial Crops and Products* 15: 1-13.

Saint-Martina, G., F. Schmidt, P. Devos and C. Levaillant. 2003. Voids in short fiber-reinforced injection-moulded parts: Density control vs. mass control. *Polymer Testing* 22: 947-953.

Sankari, H. 2000. Comparison of bast fiber yield and mechanical fiber properties of hemp. *Industrial Crops and Products* 11: 73-84.

The Santa Clara University Design Center. 1998. Injection system. http://www.scudc.scu.edu/cmdoc/dg_doc/develop/process/control/b1000002.htm#210955 (2004/02/20).

Santos, P. and S. H. Pezzin. 2003. Mechanical properties of polypropylene reinforced with recycled-pet fibres. *Journal of Materials Processing Technology* 143-144: 517-520.

Sarkar, B. K. and D. Ray. 2004. Effect of the defect concentration on the impact fatigue endurance of untreated and alkali treated jute–vinylester composites

under normal and liquid nitrogen atmosphere. *Composites Science and Technology* 64: 2213-2219.

SAS. 1999-2001. The SAS System for Windows. Ver. 8.02. Cary, N.C.: SAS Institute, Inc.

Shah, V. 1984. *Handbook of Plastics Testing Technology*. New York, NY: John Wiley and Sons Inc.

Sharifah, H. A. and P. A. Martin. 2004. The effect of alkalization and fibre alignment on the mechanical and thermal properties of kenaf and hemp bast fibre composites: Part 1 – polyester resin matrix. *Composites Science and Technology* 64(9): 1219-1230.

Singh, R. P. and D. R. Heldman. 1993. *Introduction to Food Engineering,* 2nd ed. San Diego, CA: Academic Press.

Singh, R. P. and D. R. Heldman. 2001. *Introduction to Food Engineering,* 3rd ed. San Diego, CA: Academic Press.

Singleton, A. C. N., C. A. Baillie, P. W. R. Beaumont and T. Peijs. 2003. On the mechanical properties, deformation and fracture of a natural fiber/recycled polymer composite. C*omposites Part B: Engineering* 34: 519-526.

Skelland, A. H. P. 1967. *Non-Newtonian Flow and Heat Transfer*. New York, NY: John Wiley & Sons, Inc.

Sombatsompop, N. and A. K. Wood. 1997. Measurement of thermal conductivity of polymers using an improved Lee's Disc Apparatus. *Polymer Testing* 16: 203-223.

Spring, M. and C. Williams. 1999. Investigation of methods used to determine ejection temperature for injection molding. In *Antec 1999 Conference Proceedings*. 3660. Brookfield, CT: Society of Plastic Engineers, Inc.

SPSS. 2005. SPSS 14.0 for WIndows. Ver. 1.0. Chicago, IL: SPSS, Inc.

Sreekala, M. S., M. G. Kumaran, S. Joseph, M. Jacob and S. Thomas. 2000. Oil palm fiber reinforced phenol formaldehyde composites: Influence of fiber surface modifications on the mechanical performance. *Applied Composite Materials* 7: 295-229.

Sreekala, M. S., M. G. Kumaran and S. Thomas. 2002. Water sorption in oil palm fiber reinforced phenol formaldehyde composites. *Composites Part A: Applied Science and Manufacturing* 33: 763-777.

Sreekala, M. S. and S. Thomas. 2003. Effect of fibre surface modification on water-sorption characteristics of oil palm fibres. *Composites Science and Technology* 63(6): 861-869.

Strong, A. B. 2000. *Plastics: Materials and Processing,* 2nd ed. Upper Saddle River, NJ: Prentice-Hall, Inc.

Su, Y-C., J. Shah and L. Lin. 2004. Implementation and analysis of polymeric microstructure replication by microinjection molding. *Journal of Micromechanics and Microengineering* 14: 415-422.

Tavman, I. H. 1998. Effective thermal conductivity of isotropic polymer composites. *International Communications in Heat and Mass Transfer* 25(5):723-732.

Tecplot. 2002. Tecplot for MS-Windows Ver.9.2-0-3. Bellevue, WA: Amtec Engineering, Inc.

Thomason, J. L. 2002. The influence of fibre length and concentration on the properties of glass fibre reinforced polypropylene: 5. Injection moulded long and short fibre PP. *Composites Part A: Applied Science and Manufacturing* 33: 1641-1652.

Thomason, J. L. 2005. The influence of fibre length and concentration on the properties of glass fibre reinforced polypropylene. 6. The properties of injection moulded long fibre PP at high fibre content. *Composites Part A: Applied Science and Manufacturing* 36(7): 995-1003.

Tjong, S. C., Y. Xu and Y. Z. Meng. 1999. Composites based on maleated polypropylene and methyl cellulosic fiber: mechanical and thermal properties. *Journal of Applied Polymer Science* 72: 1647–1653.

Trochu, F., E. Ruiz, V. Achim and S. Soukane. 2006. Advanced numerical simulation of liquid composite molding for process analysis and optimization. *Composites Part A: Applied Science and Manufacturing* 37(6): 890-902.

Valadez-Gonzalez, A., J. M. Cervantes-Uc, R. Olayo and P. J. Herrera-Franco. 1999. Chemical modification of henequén fibers with an organosilane coupling agent. *Composites Part B: Engineering* 30: 321-331.

Van de Velde, K. and P. Kiekens. 2001. Influence of fiber surface characteristics on the flax/polypropylene interface. *Journal of Thermoplastic Composite Materials* 14: 244-260.

Van de Velde, K. and P. Kiekens. 2002. Thermal degradation of flax: the determination of kinetic parameters with thermogravimetric analysis. *Journal of Applied Polymer Science* 83: 2634-2643.

Van de Weyenberg, I., J. Ivens, A. De Coster, B. Kino, E. Baetens and I. Verpoest. 2003. Influence of processing and chemical treatment of flax fibres on their composites. *Composites Science and Technology* 63:1241-1246.

Vincent, M., T. Giroud, A. Clarke and C. Eberhardt. 2005. Description and modeling of fiber orientation in injection molding of fiber reinforced thermoplastics. *Polymer* 46: 6719-6725.

Voorn, B. V., H. H. G. Smit, R. J. Sinke and B. de Klerk. 2001. Natural fiber reinforced sheet moulding compound. *Composites Part A: Applied Science and Manufacturing* 32: 1271-1279.

Wallenberger, F. T. and N. Weston. 2004. *Natural Fibers, Plastics and Composites.* New York, NY: Kluwer Academic Publishers.

Walshaw, J., G. W. Mathison, T. F. Fenton, G. Sedgwick, H. Hsu, G. Recinos-Diaz and A. Suleiman. 1998. Characterization of forages by differential scanning calorimetry and prediction of their chemical composition and nutritive value. *Animal Feed Science and Technology* 71: 309-323.

Wang, B., S. Panigrahi, L. Tabil, W. Crerar, T. Powell, M. Kolybaba and S. Sokhansanj. 2003. Flax fiber-reinforced thermoplastic composites. 2003 CSAE/ASAE Annual Intersectional Meeting. Paper number RRV03-0003. St. Joseph, MI: CSAE/ASAE.

Wang, B. 2004. Pre-treatment of flax fibers for use in rotationally molded biocomposites. MSc. Thesis. Saskatoon, SK: Department of Agricultural and Bioresource Engineering, University of Saskatchewan.

Wang, J. 2005. Analysis and modeling of underfill flow driven by capillary action in flip-chip packaging. Ph.D. Thesis. Saskatoon, SK: Department of Mechanical Engineering, University of Saskatchewan.

Warick, J. 2001. GM flax seed yanked off Canadian market - rounded up, crushed. The Saskatoon StarPhoenix. http://www.thestarphoenix.com (2004/06/30).

Weidenfeller, B., M. Höfer and F. R. Schilling. 2004. Thermal conductivity, thermal diffusivity, and specific heat capacity of particle filled polypropylene. *Composites Part A: Applied Science and Manufacturing* 35: 423-429.

Weidenfeller, B., M. Höfer and F. R. Schilling. 2005. Cooling behaviour of particle filled polypropylene during injection moulding process. *Composites Part A: Applied Science and Manufacturing* 36: 345-351.

Wen, S-S. L., C-K. Jen, K. T. Nguyen, A. Derdouri and Y. Simard. 1999. Recent advances in ultrasonic monitoring of the injection molding process. In *Antec 1999 Conference Proceedings*. 637. Brookfield, CT: Society of Plastic Engineers, Inc.

Whittenberger, J. D., F. I. Hurwitz, J. J. Ricca and R. M. Jurta. 1982. On determination of fibre fraction in continuous fibre composite materials. *Journal of Materials Science Letters* 1:249-252.

Wielage, B., T. Lampke, H. Utschick and F. Soergel. 2003. Processing of natural-fiber reinforced polymers and the resulting dynamic–mechanical properties. *Journal of Materials Processing Technology* 139: 140-146.

Wilkes, J. O. 1999. *Fluid Mechanics for Chemical Engineering.* Upper Saddle River, NJ: Prentice Hall PTR.

Wilkinson, W. L. 1960. *Non-Newtonian Fluids: Fluid Mechanics, Mixing and Heat Transfer*. New York, NY: Pergamon Press.

Wollerdorfer, M. and H. Bader. 1998. Influence of natural fibres on the mechanical properties of biodegradable polymers. *Industrial Crops and Products* 8(2): 105-112.

Wong, C. P. and R. S. Bollampally. 1999. Thermal conductivity, elastic modulus, and coefficient of thermal expansion of polymer composites filled with ceramic particles for electronic packaging. *Journal of Applied Polymer Science* 74: 3396-3403.

Woo, M. W., P. Wong, Y. Tang, V. Triacca, P. E. Gloor, A. N. Hrymak and A. E. Hamielec. 1995. Melting behavior and thermal properties of high density polyethylene. *Polymer Engineering and Science* 35(2): 151-156.

Xu, H. and D. Kazmer. 1999. A stiffness criterion for cooling time estimation. *International Polymer Processing (Germany)* 14(1):103-108.

Xu, Z. K., Q. W. Dai, Z. M. Liu, R. Q. Kou and Y. Y. Xu. 2002. Microporous polypropylene hollow fiber membrane Part I. Surface modification by the graft polymerization of acrylic acid. *Journal of Membrane Science* 196(2): 221-229.

Zafeiropoulos, N. E. 2002. Engineering and characterisation of the interface in flax fiber/polypropylene composite materials. Part I. Development and investigation of surface treatments. *Composites Part A: Applied Science and Manufacturing* 33: 1083-1093.

Zook, C., Y. Zhang and A. I. Isayev. 1998. Effect of moving boundary on channel flow of polymeric melts. In *Antec 1998 Conference Proceedings*. Volume 1. 790. Brookfield, CT: Society of Plastic Engineers, Inc.

APPENDIXES

APPENDIX A

Laminar flow in cylindrical tube

Since polymer melts and solutions are often transported and processed as Poisueille (laminar) flow (Rosen 1993), the material flow in the sprue and runner are simplified as laminar flow in cylindrical tube as shown in Figure A.1.

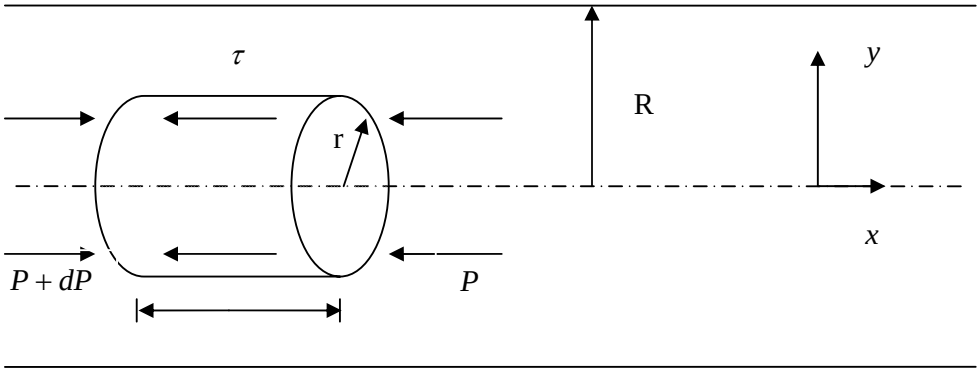

Figure A.1 Laminar flow in a tube of cylindrical cross section.

Assuming that the pressure in the fluid is a function of the distance along the tube only, then:

$$\pi r^2 dP = \tau 2\pi r dx \tag{A.1}$$

where τ is shear stress, P is pressure, $\pi r^2 dP$ is net pressure force, $\tau 2\pi r dx$ is the surface shear force.

$$\tau = \frac{r}{2}\left(\frac{dP}{dx}\right) \tag{A.2}$$

Since the axial fluid velocity u is a function of radial position,

$$du(r) = \frac{du}{dr} dr \tag{A.3}$$

Integrating with the boundary condition: $u(R) = 0$ (i.e., the fluid sticks to the wall) and u at radius $r = u(r)$ gives:

$$u(r) = \int_0^{u(r)} du(r) = \int_R^r \frac{du}{dr} dr \tag{A.4}$$

For power-law non-Newtonian fluid, the relationship between shear rate and shear stress from equation (1.13) is:

$$\frac{du}{dr} = \left(\frac{\tau}{K}\right)^{\frac{1}{n}} \tag{A.5}$$

Substituting the gradient (du/dr) in to equation (A.4) gives $u(r)$:

$$u(r) = \int_R^r \frac{du}{dr} dr = \int_R^r \left(\frac{\tau}{K}\right)^{\frac{1}{n}} dr \tag{A.6}$$

Substituting equation (A.2) to equation (A.4), the velocity profile becomes:

$$u(r) = \int_R^r \left(\frac{r}{2K}\frac{dP}{dx}\right)^{\frac{1}{n}} dr = \frac{\left[\left(\frac{dP}{dx}\right)\left(\frac{1}{2K}\right)\right]^{\frac{1}{n}}}{\frac{1}{n}+1}\left[R^{\left(\frac{1}{n}\right)+1} - r^{\left(\frac{1}{n}\right)+1}\right] \tag{A.7}$$

The differential volumetric flow rate is:

$$dQ = u(r)2\pi r dr \tag{A.8}$$

where $u(r)$ is the local velocity and $2\pi r dr$ is the area of the differential ring. Integrating over the tube cross section gives:

$$Q = 2\pi\int_0^R u(r) r dr = 2\pi\int_0^R \frac{\left[\left(\frac{dP}{dx}\right)\left(\frac{1}{2K}\right)\right]^{\frac{1}{n}}}{\frac{1}{n}+1}\left[R^{\left(\frac{1}{n}\right)+1} - r^{\left(\frac{1}{n}\right)+1}\right] r dr$$

$$= \left[\left(\frac{dP}{dx}\right)\left(\frac{1}{2K}\right)\right]^{\frac{1}{n}} \pi\left(\frac{n}{1+3n}\right) R^{\left(\frac{1}{n}\right)+3} \tag{A.9}$$

Then, average velocity $\bar{u}$ is calculated as:

$$\bar{u} = \frac{Q}{\pi R^2} = \left[\left(\frac{dP}{dx}\right)\frac{1}{2K}\right]^{\frac{1}{n}}\left(\frac{n}{1+3n}\right) R^{\frac{1}{n}+1} \tag{A.10}$$

From above equation, ignoring the influence of friction, take the average velocity $\bar{u}$ as u_1:

$$u_1 = \left[\left(\frac{P_0 - P_1}{L}\right)\frac{1}{2K}\right]^{\frac{1}{n}}\left(\frac{n}{1+3n}\right)R^{\frac{1}{n}+1} \tag{A.11}$$

APPENDIX B

Laminar flow between flat parallel plates

Plane Poiseuille flow is the fluid flows between fixed parallel plates, driven by pressure forces or by its own weight (Reynolds 1971). The forces act in the direction of motion on a cubical element which has unit depth perpendicular to the plane as shown in Figure B.1. In steady flow along a uniform channel, the fluid element will move at constant velocity. Then the net shear force $d\tau\ dx$ and net pressure force $dp\ dy$ will balance (Reynolds 1971). That is:

$$\left(\left(P + dP\right) - P\right)2y - 2\tau dx = 0 \tag{B.1}$$

$$\frac{d\tau}{dy} = \frac{dp}{dx} \tag{B.2}$$

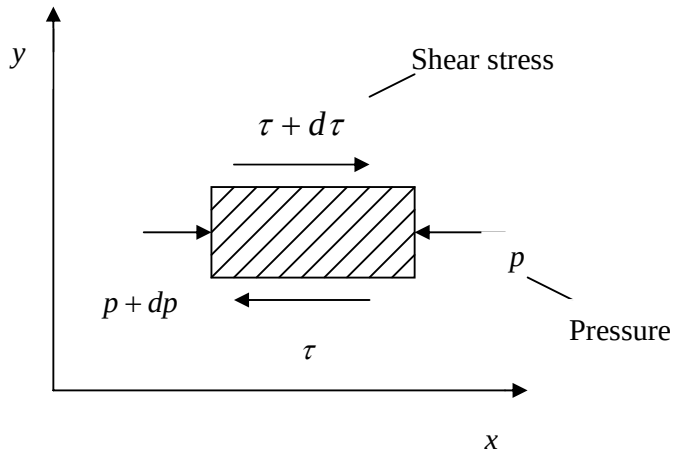

Figure B.1 Forces on the element of fluid in parallel laminar flow between fixed plates.

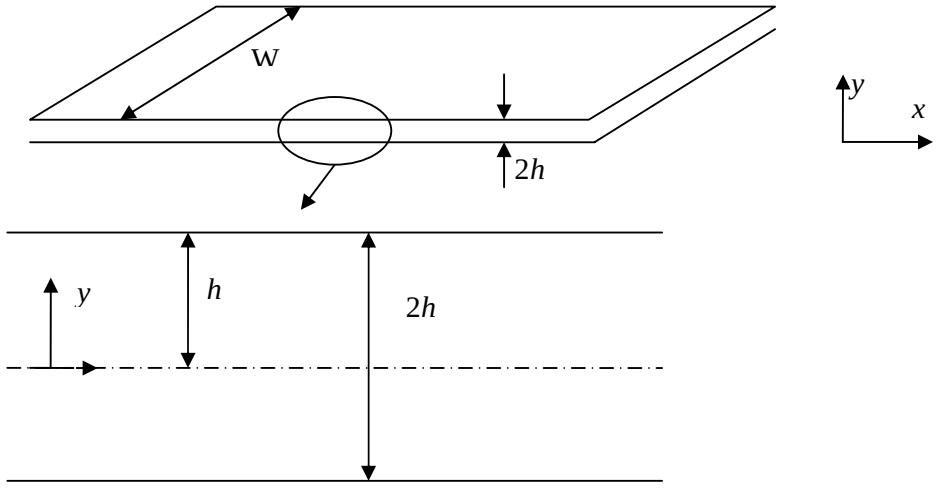

Figure B.2 Laminar flow between two parallel plates (mold cavity).

Laminar flow situation is shown in Figure B.2. Boundary condition:

$u(h) = 0$ at the wall. The velocity $u(y)$ is:

$$u(y) = \int_0^{u(y)} du(y) = \int_b^y \frac{du}{dy} dy \tag{B.3}$$

For power-law fluid, from equation (2.13),

$$\frac{du}{dy} = \left(\frac{\tau}{K}\right)^{\frac{1}{n}} \tag{B.4}$$

From equation (B.2), $\tau = \frac{dP}{dx} y$ (B.5)

Substituting equation (B.4) and (B.5) into equation (B.3) and integrating, velocity $u(y)$ becomes:

$$u(y) = \int_h^y \left(\frac{\tau}{K}\right)^{\frac{1}{n}} dy = \int_h^y \left(\frac{dP}{dx}\frac{y}{K}\right)^{\frac{1}{n}} dy$$

$$= \left[\left(\frac{dP}{dx}\right)\left(\frac{1}{K}\right)\right]^{\frac{1}{n}} \left(\frac{n}{n+1}\right)\left(y^{\frac{1}{n}+1} - h^{\frac{1}{n}+1}\right) \tag{B.6}$$

The volumetric flow rate Q is:

$$dQ = 2u(y)Wdy \tag{B.7}$$

where W is the width of the plate where fluid flow occurs.

$$Q = 2\int_0^h Wu(y)dy \tag{B.8}$$

Substituting equation (B.6) into equation (B.8) and integrating it, then:

$$Q = 2\int_0^h W\left[\left(\frac{dP}{dx}\right)\left(\frac{1}{K}\right)\right]^{\frac{1}{n}}\left(\frac{n}{n+1}\right)\left(y^{\frac{1}{n}+1} - h^{\frac{1}{n}+1}\right)dy$$

$$= 2W\left(\frac{n}{2n+1}\right)\left[\left(\frac{-dP}{dx}\right)\left(\frac{1}{K}\right)\right]^{\frac{1}{n}} h^{\frac{1}{n}+2} \tag{B.9}$$

Thus, the average velocity $\bar{u}$ is:

$$\bar{u} = \frac{Q}{2hW} = \frac{n}{(2n+1)}\left[\left(\frac{-dP}{dx}\right)\left(\frac{1}{K}\right)\right]^{\frac{1}{n}} h^{\frac{1}{n}+1} \tag{B.10}$$

APPENDIX C

SPSS analysis on fiber chemical treatments

Table C.1 SPSS Tukey test output on tensile strength of fiber-LLDPE biocomposites after surface modifications.

Composites (I)**	Composites (J)**	Mean Difference (I-J)	Sig. (P)	Composites (I)**	Composites (J)**	Mean Difference (I-J)	Sig. (P)
A-L	C-L	0.20	0.47	P-L	A-L	-0.14	0.80
	LLDPE	0.86(*)	<0.01		C-L	0.06	1.00
	N-L	0.37(*)	0.02		LLDPE	0.71(*)	<0.01
	P-L	0.14	0.80		N-L	0.22	0.36
	S-L	0.20	0.47		S-L	0.06	1.00
	U-L	0.48 (*)	<0.01		U-L	0.34(*)	0.04
C-L	A-L	-0.20	0.47	S-L	A-L	-0.20	0.47
	LLDPE	0.66(*)	<0.01		C-L	<-0.01	1.00
	N-L	0.16	0.69		LLDPE	0.66(*)	<0.01
	P-L	-0.06	1.00		N-L	0.16	0.70
	S-L	<0.01	1.00		P-L	-0.06	1.00
	U-L	0.28	0.13		U-L	0.28	0.13
LLDPE	A-L	-0.86(*)	<0.01	U-L	A-L	-0.48 (*)	<0.01
	C-L	-0.66 (*)	<0.01		C-L	-0.28	0.13
	N-L	-0.49 (*)	<0.01		LLDPE	0.38(*)	0.02
	P-L	-0.71(*)	<0.01		N-L	-0.12	0.91
	S-L	-0.66(*)	<0.01		P-L	-0.34(*)	0.04
	U-L	-0.38(*)	0.02		S-L	-0.28	0.13
N-L	A-L	-0.37 (*)	0.02				
	C-L	-0.16	0.69				
	LLDPE	0.49 (*)	<0.01				
	P-L	-0.22	0.36				
	S-L	-0.16	0.70				
	U-L	0.12	0.91				

Dependent Variable: Tensile strength (MPa).

Std. Error = 0.10.

Based on observed means.

* The mean difference is significant at the 5% level.

** For details of composition of composites and symbols used refer to Tables 3.3 and 3.4.

Table C.2 SPSS Tukey test output on tensile strength of fiber-HDPE biocomposites after surface modifications.

Composties (I)**	Composties (J)**	Mean Difference (I-J)	Sig. (P)	Composties (I)**	Composties (J)**	Mean Difference (I-J)	Sig. (P)
A-H	C-H	0.37	0.36	P-H	A-H	-0.18	0.95
	U-H	0.42	0.24		C-H	0.19	0.92
	N-H	0.15	0.98		U-H	0.24	0.81
	P-H	0.18	0.95		N-H	-0.03	1.00
	S-H	0.01	1.00		S-H	-0.17	0.95
	HDPE	1.02(*)	<0.01		HDPE	0.84(*)	<0.01
C-H	A-H	-0.37	0.36	S-H	A-H	-0.01	1.00
	U-H	0.05	1.00		C-H	0.37	0.38
	N-H	-0.22	0.86		U-H	0.41	0.25
	P-H	-0.19	0.92		N-H	0.14	0.98
	S-H	-0.37	0.38		P-H	0.17	0.95
	HDPE	.65(*)	0.01		HDPE	1.01 (*)	<0.01
U-H	A-H	-0.42	0.24	HDPE	A-H	-1.02(*)	<0.01
	C-H	-0.05	1.00		C-H	-0.65(*)	0.01
	N-H	-0.27	0.72		U-H	-0.60(*)	0.03
	P-H	-0.24	0.81		N-H	-0.87(*)	<0.01
	S-H	-0.41	0.25		P-H	-0.84(*)	<0.01
	HDPE	0.60(*)	0.03		S-H	-1.01 (*)	<0.01
N-H	A-H	-0.15	0.98				
	C-H	0.22	0.86				
	U-H	0.27	0.72				
	P-H	0.03	1.00				
	S-H	-0.14	0.98				
	HDPE	0.87(*)	<0.01				

Dependent Variable: Tensile strength (MPa).

Std. Error = 0.17.

Based on observed means.

*The mean difference is significant at the 5% level.

** For details of composition of composites and symbols used refer to Tables 3.3 and 3.4.

Table C.3 SPSS Tukey test output on water absorption of fiber-LLDPE biocomposites after surface modifications.

Composties (I)**	Composties (J)**	Mean Difference (I-J)	Sig. (P)	Composties (I)**	Composties (J)**	Mean Difference (I-J)	Sig. (P)
A-L	C-L	-0.02 (*)	0.03	P-L	A-L	0.01	0.72
	LLDPE	0.05 (*)	<0.01		C-L	-0.01	0.46
	N-L	-0.02(*)	0.04		LLDPE	0.06(*)	<0.01
	P-L	-0.01	0.72		N-L	-0.01	0.53
	S-L	-0.01	0.63		S-L	<-0.01	1.00
	U-L	-0.04(*)	<0.01		U-L	-0.03(*)	<0.01
C-L	A-L	0.02 (*)	0.03	S-L	A-L	0.01	0.63
	LLDPE	0.07(*)	<0.01		C-L	-0.01	0.55
	N-L	<0.01	1.00		LLDPE	0.06(*)	<0.01
	P-L	0.01	0.46		N-L	-0.01	0.62
	S-L	0.01	0.55		P-L	<0.01	1.00
	U-L	-0.02	0.06		U-L	-0.03(*)	<0.01
LLDPE	A-L	-0.05(*)	<0.01	U-L	A-L	0.04(*)	<0.01
	C-L	-0.07(*)	<0.01		C-L	0.02	0.06
	N-L	-0.07(*)	<0.01		LLDPE	0.08 (*)	<0.01
	P-L	-0.06(*)	<0.01		N-L	0.02	0.05
	S-L	-0.06(*)	<0.01		P-L	0.03(*)	<0.01
	U-L	-0.08 (*)	<0.01		S-L	0.03(*)	<0.01
N-L	A-L	0.02 (*)	0.04				
	C-L	<-0.01	1.00				
	LLDPE	0.07(*)	<0.01				
	P-L	0.01	0.53				
	S-L	0.01	0.62				
	U-L	-0.02	0.05				

Dependent Variable: Water absorption (%).

Based on observed means.

* The mean difference is significant at the 5% level.

** For details of composition of composites and symbols used refer to Tables 3.3 and 3.4.

Table C.4 SPSS Tukey test output on water absorption of fiber-HDPE biocomposites after surface modifications.

Composties (I)**	Composties (J)**	Mean Difference (I-J)	Sig. (P)	Composties (I)**	Composties (J)**	Mean Difference (I-J)	Sig. (P)
A-L	C-L	-0.02	0.38	P-L	A-L	0.01	0.65
	HDPE	0.05 (*)	<0.01		C-L	<-0.01	1.00
	N-L	-0.02	0.22		HDPE	0.07 (*)	<0.01
	P-L	-0.01	0.65		N-L	-0.01	0.97
	S-L	-0.01	0.98		S-L	0.01	0.97
	U-L	-0.02	0.11		U-L	-0.01	0.84
C-L	A-L	0.02	0.38	S-L	A-L	0.01	0.98
	HDPE	0.07(*)	<0.01		C-L	-0.01	0.82
	N-L	<-0.01	1.00		HDPE	0.06(*)	<0.01
	P-L	<0.01	1.00		N-L	-0.01	0.62
	S-L	0.01	0.82		P-L	-0.01	0.97
	U-L	-0.01	0.98		U-L	-0.02	0.38
HDPE	A-L	-0.05 (*)	<0.01	U-L	A-L	0.02	0.11
	C-L	-0.07(*)	<0.01		C-L	0.01	0.98
	N-L	-0.07(*)	<0.01		HDPE	0.08(*)	<0.01
	P-L	-0.07(*)	<0.01		N-L	<0.01	1.00
	S-L	-0.06(*)	<0.01		P-L	0.01	0.84
	U-L	-0.08(*)	<0.01		S-L	0.02	0.38
N-L	A-L	0.02	0.22				
	C-L	<0.01	1.00				
	HDPE	0.07 (*)	0.00				
	P-L	0.01	0.97				
	S-L	0.01	0.62				
	U-L	<-0.01	1.00				

Dependent Variable: Water absorption (%).

Based on observed means.

* The mean difference is significant at the 5% level.

** For details of composition of composites and symbols used refer to Tables 3.3 and 3.4.

APPENDIX D

SPSS analysis comparison of fiber materials

Table D.1 SPSS Tukey test output on tensile strength of three flax fiber-HDPE biocomposites by SPSS.

Composites (I)**	Composites (J)**	Mean Difference (I-J)	Std. Error	Sig. (P)
I-A	I-U	0.352	0.193	0.472
	II-A	0.192	0.193	0.916
	II-U	0.935(*)	0.193	0.001
	III-A	2.259 (*)	0.193	<0.001
	III-U	2.505(*)	0.193	<0.001
I-U	I-A	-0.352	0.193	0.472
	II-A	-0.160	0.193	0.959
	II-U	0.583	0.193	0.059
	III-A	1.907 (*)	0.193	<0.001
	III-U	2.153 (*)	0.193	<0.001
II-A	I-A	-0.192	0.193	0.916
	I-U	0.160	0.193	0.959
	II-U	0.744(*)	0.193	0.009
	III-A	2.068(*)	0.193	<0.001
	III-U	2.314(*)	0.193	<0.001
II-U	I-A	-.935 (*)	0.193	0.001
	I-U	-0.583	0.193	0.059
	II-A	-0.744(*)	0.193	0.009
	III-A	1.324(*)	0.193	<0.001
	III-U	1.570 (*)	0.193	<0.001
III-A	I-A	-2.259 (*)	0.193	<0.001
	I-U	-1.907 (*)	0.193	<0.001
	II-A	-2.068(*)	0.193	<0.001
	II-U	-1.324(*)	0.193	<0.001
	III-U	0.246	0.193	0.796
III-U	I-A	-2.505 (*)	0.193	<0.001
	I-U	-2.153 (*)	0.193	<0.001
	II-A	-2.314(*)	0.193	<0.001
	II-U	-1.570 (*)	0.193	<0.001
	III-A	-0.246	0.193	0.796

Dependent Variable: Tensile strength (MPa).

Based on observed means.

* The mean difference is significant at the 5% level.

** For details of composition of composites and symbols used refer to Table 3.5.

Table D.2 SPSS analysis of variance of the effect of fiber material and fiber treatment on the tensile strength of biocomposites.

Source	Type III Sum of Squares	df	Mean Square	F	Sig.(P)
Corrected Model	29.60(a)	5	5.92	63.37	<0.01
Intercept	13429.89	1	13429.89	143773.20	<0.01
Fiber material	27.75	2	13.88	148.55	<0.01
Fiber treatment	1.50	1	1.50	16.07	<0.01
Fiber material * Fiber treatment	0.34	2	0.17	1.84	0.18
Error	2.24	24	0.09		
Total	13461.72	30			
Corrected Total	31.84	29			

Dependent Variable: Tensile strength (MPa).
(a) R Square = 0.93.

Table D.3 SPSS analysis of variance of the effect of fiber material and fiber treatment on the flexural strength of different fiber-HDPE biocomposites.

Source	Type III Sum of Squares	df	Mean Square	F	Sig.(P)
Corrected Model	119.20(a)	5	23.84	362.61	<0.01
Intercept	22183.32	1	22183.32	337421.78	<0.01
Fiber material	114.99	2	57.50	874.53	<0.01
Fiber Treatment	3.96	1	3.96	60.22	<0.01
Fiber material * Fiber Treatment	0.25	2	0.12	1.89	0.17
Error	1.58	24	0.07		
Total	22304.09	30			
Corrected Total	120.78	29			

Dependent Variable: Flexural Strength (MPa).
(a) R Square = 0.99.

Table D.4 SPSS Tukey test output on flexural strength of three flax fiber-HDPE biocomposites.

Composites (I)**	Composites (J)**	Mean Difference (I-J)	Std. Error	Sig.(P)
I-A	I-U	0.522(*)	0.162	0.038
	II-A	1.472(*)	0.162	<0.001
	II-U	2.166(*)	0.162	<0.001
	III-A	4.486(*)	0.162	<0.001
	III-U	5.450(*)	0.162	<0.001
I-U	I-A	-0.522(*)	0.162	0.038
	II-A	0.950(*)	0.162	<0.001
	II-U	1.644(*)	0.162	<0.001
	III-A	3.964(*)	0.162	<0.001
	III-U	4.928(*)	0.162	<0.001
II-A	I-A	-1.472(*)	0.162	<0.001
	I-U	-0.950(*)	0.162	<0.001
	II-U	0.694(*)	0.162	0.003
	III-A	3.014(*)	0.162	<0.001
	III-U	3.978(*)	0.162	<0.001
II-U	I-A	-2.166(*)	0.162	<0.001
	I-U	-1.644(*)	0.162	<0.001
	II-A	-0.694(*)	0.162	0.003
	III-A	2.320(*)	0.162	<0.001
	III-U	3.284(*)	0.162	<0.001
III-A	I-A	-4.486(*)	0.162	<0.001
	I-U	-3.964(*)	0.162	<0.001
	II-A	-3.014(*)	0.162	<0.001
	II-U	-2.320(*)	0.162	<0.001
	III-U	0.964(*)	0.162	<0.001
III-U	I-A	-5.450(*)	0.162	<0.001
	I-U	-4.928(*)	0.162	<0.001
	II-A	-3.978(*)	0.162	<0.001
	II-U	-3.284(*)	0.162	<0.001
	III-A	-0.964(*)	0.162	<0.001

Dependent Variable: Flexural Strength (MPa).

Based on observed means.

* The mean difference is significant at the 5% level.

** For details of composition of composites and symbols used refer to Table 3.5.

Table D.5 SPSS Tukey test output on flexural modulus of three flax fiber-HDPE biocomposites.

Composites (I)**	Composites (J)**	Mean Difference (I-J)	Std. Error	Sig.(P)
I-A	I-U	22.160	9.798	0.248
	II-A	6.800	9.798	0.981
	II-U	44.860(*)	9.798	0.002
	III-A	122.920(*)	9.798	<0.001
	III-U	141.950(*)	9.798	<0.001
I-U	I-A	-22.160	9.798	0.248
	II-A	-15.360	9.798	0.626
	II-U	22.700	9.798	0.226
	III-A	100.760(*)	9.798	<0.001
	III-U	119.790(*)	9.798	<0.001
II-A	I-A	-6.800	9.798	0.981
	I-U	15.360	9.798	0.626
	II-U	38.060(*)	9.798	0.008
	III-A	116.120(*)	9.798	<0.001
	III-U	135.150(*)	9.798	<0.001
II-U	I-A	-44.860(*)	9.798	0.002
	I-U	-22.700	9.798	0.226
	II-A	-38.060(*)	9.798	0.008
	III-A	78.060(*)	9.798	<0.001
	III-U	97.090(*)	9.798	<0.001
III-A	I-A	-122.920(*)	9.798	<0.001
	I-U	-100.760(*)	9.798	<0.001
	II-A	-116.120(*)	9.798	<0.001
	II-U	-78.060(*)	9.798	<0.001
	III-U	19.030	9.798	0.402
III-U	I-A	-141.950(*)	9.798	<0.001
	I-U	-119.790(*)	9.798	<0.001
	II-A	-135.150(*)	9.798	<0.001
	II-U	-97.090(*)	9.798	<0.001
	III-A	-19.030	9.798	0.402

Dependent Variable: Flexural Modulus (MPa).

Based on observed means.

* The mean difference is significant at the 5% level.

** For details of composition of composites and symbols used refer to Table 3.5.

Table D.6 SPSS analysis of variance of the effect of fiber material and fiber treatment on the flexural modulus of different fiber-HDPE biocomposites.

Source	Type III Sum of Squares	df	Mean Square	F	Sig.(P)
Corrected Model	93451.81(a)	5	18690.36	77.88	<0.01
Intercept	11313994.41	1	11313994.41	47145.81	<0.01
Fiber material	87697.39	2	43848.69	182.72	<0.01
Fiber Treatment	5233.80	1	5233.80	21.81	<0.01
Fiber material * Fiber Treatment	520.63	2	260.31	1.09	0.35
Error	5759.49	24	239.98		
Total	11413205.71	30			
Corrected Total	99211.30	29			

Dependent Variable: Flexural Modulus (MPa).

(a) R Square = 0.94.

Table D.7 SPSS analysis of variance of the effect of fiber material and fiber treatment on the water absorption of different fiber-HDPE biocomposites.

Source	Type III Sum of Squares	df	Mean Square	F	Sig.
Corrected Model	0.01(a)	5	0.00	5.75	0.01
Intercept	0.21	1	0.21	832.19	<0.01
Fiber_material	0.07	2	<0.01	12.28	<0.01
Fiber_treatment	<0.01	1	<0.01	3.43	0.09
Fiber_material * Fiber_treatment	<0.01	2	<0.01	0.39	0.69
Error	<0.01	12	<0.01		
Total	0.22	18			
Corrected Total	0.01	17			

Dependent Variable: Water absorption (%).

(a) R Square = 0.71.

Table D.8 SPSS Tukey test output on water absorption of three flax fiber-HDPE biocomposites.

Composites (I)**	Composites (J)**	Mean Difference (I-J)	Std. Error	Sig.(P)
I-A	I-U	-0.023	0.013	0.510
	II-A	-0.005	0.013	0.999
	II-U	-0.013	0.013	0.907
	III-A	-0.044(*)	0.013	0.045
	III-U	-0.054(*)	0.013	0.012
I-U	I-A	0.0228	0.013	0.510
	II-A	0.018	0.013	0.719
	II-U	0.010	0.013	0.967
	III-A	-0.021	0.013	0.588
	III-U	-0.031	0.013	0.220
II-A	I-A	0.005	0.013	0.999
	I-U	-0.018	0.013	0.719
	II-U	-0.008	0.013	0.985
	III-A	-0.039	0.013	0.082
	III-U	-0.049 (*)	0.013	0.022
II-U	I-A	0.013	0.013	0.907
	I-U	-0.010	0.013	0.967
	II-A	0.008	0.013	0.985
	III-A	-0.031	0.013	0.223
	III-U	-0.041	0.013	0.065
III-A	I-A	0.044(*)	0.013	0.045
	I-U	0.021	0.013	0.588
	II-A	0.039	0.013	0.082
	II-U	0.031	0.013	0.223
	III-U	-0.010	0.013	0.965
III-U	I-A	0.054(*)	0.013	0.012
	I-U	0.031	0.013	0.220
	II-A	0.049 (*)	0.013	0.022
	II-U	0.041	0.013	0.065
	III-A	0.010	0.013	0.965

Dependent Variable: Water absorption (%).

Based on observed means.

* The mean difference is significant at the 5% level.

** For details of composition of composites and symbols used refer to Table 3.5.

APPENDIX E

Statistical analysis and surface plots related to experiments on factors affecting injection molding of biocomposites

Table E.1 Homogeneous subsets of tensile strength of biocomposite under SPSS Tukey HSD method.

Trial[#]	N	Subset				
		a	b	c	d	e
3	5	19.769				
4	5	20.231	20.231			
8	5	20.4509	20.450			
1	5		20.870	20.870		
7	5		20.936	20.936		
2	5			21.634	21.634	
5	5				21.968	
6	5				22.014	
12	5				22.023	
11	5				22.411	
10	5					23.771
9	5					23.983
Sig.		0.451	0.398	0.282	0.261	1.000

Based on Type III Sum of Squares.
The error term is Mean Square (Error) = 0.208.
Uses Harmonic Mean Sample Size = 5.
[#] The setting of trial refers to Table 3.6.
Means for groups in homogeneous subsets are displayed. The values in same subset mean no significant difference at 5% level.

Table E.2 Homogeneous subsets of tensile elongation of biocomposite under SPSS Tukey HSD method.

Trial[#]	N	Subset				
		a	b	c	d	e
11	5	1.852				
12	5	2.068	2.068			
10	5	2.132	2.132			
8	5	2.432	2.432	2.432		
7	5	2.876	2.876	2.876		
9	5	3.420	3.420	3.420	3.420	
6	5	4.500	4.500	4.500	4.500	
5	5	4.536	4.536	4.536	4.536	
4	5		6.864	6.864	6.864	
1	5			7.328	7.328	
3	5				7.964	
2	5					15.164
Sig.		0.783	0.069	0.058	0.105	1.000

Based on Type III Sum of Squares.
The error term is Mean Square (Error) = 5.270.
Uses Harmonic Mean Sample Size = 5.
[#]The setting of trial refers to Table 3.6.
Means for groups in homogeneous subsets are displayed. The values in same subset mean no significant difference at 5% level.

Table E.3 SPSS univariate analysis of variance of the effect of fiber content, injection temperature, and injection pressure on the biocomposite tensile strength.

Source	Type III Sum of Squares	df	Mean Square	F	Sig.(P)
Corrected Model	95.000(a)	11	8.636	41.529	<0.001
Intercept	28179.661	1	28179.661	135506.115	<0.001
Fiber_content (*F*)	61.886	2	30.943	148.793	<0.001
Injection_temperature (*T*)	29.539	1	29.539	142.044	<0.001
Injection_pressure (*P*)	0.014	1	0.014	0.070	0.793
F × *T*	0.500	2	0.250	1.201	0.310
F × *P*	2.556	2	1.278	6.144	0.004
T × *P*	0.425	1	0.425	2.042	0.159
F× *T* × *P*	0.081	2	0.041	0.196	0.823
Error	9.982	48	0.208		
Total	28284.643	60			
Corrected Total	104.982	59			

Dependent Variable: Tensile strength (MPa).
(a) R Square = 0.905.

Table E.4 SPSS univariate analysis of variance of the effect of fiber content, injection temperature, and injection pressure on the biocomposite tensile elongation.

Source	Type III Sum of Squares	df	Mean Square	F	Sig.(P)
Corrected Model	808.392(a)	11	73.490	13.945	<0.001
Intercept	1557.338	1	1557.338	295.500	<0.001
Fiber_content (*F*)	552.977	2	276.488	52.463	<0.001
Injection_temperature (*T*)	70.677	1	70.677	13.411	0.001
Injection_pressure (*P*)	11.197	1	11.197	2.125	0.151
F × *T*	23.446	2	11.723	2.224	0.119
F × *P*	47.244	2	23.622	4.482	0.016
T × *P*	25.611	1	25.611	4.860	0.032
F× *T* × *P*	77.240	2	38.620	7.328	0.002
Error	252.969	48	5.270		
Total	2618.698	60			
Corrected Total	1061.361	59			

Dependent Variable: Tensile elongation.

(a) R Square = 0.762.

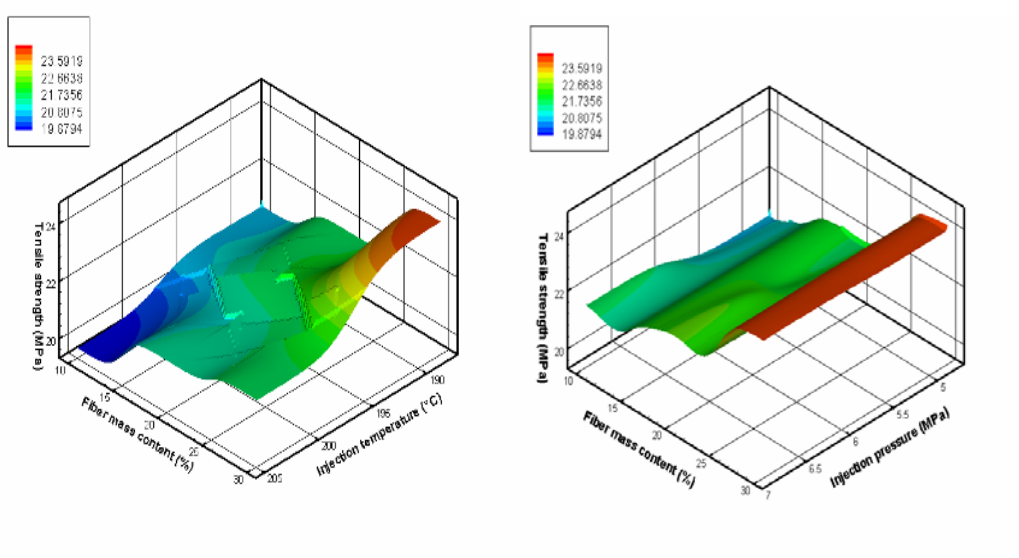

Figure E.1 Tensile strength of flax fiber-HDPE biocomposites as affected by fiber mass content, injection temperature*, and injection pressure plotted using Tecplot (Amtec Engineering, Inc., Bellevue, WA) by inverse-distance interpolation.

* Injection temperature refers to zone A temperature during injection molding which are: a) injection temperatures of 188ºC (D=166ºC, C=182ºC, B=188ºC, A=188ºC); and b) injection temperatures of 200ºC (D=177ºC, C=190ºC, B=200ºC, A=200ºC). This is applied for all the following 3-D surface plots.

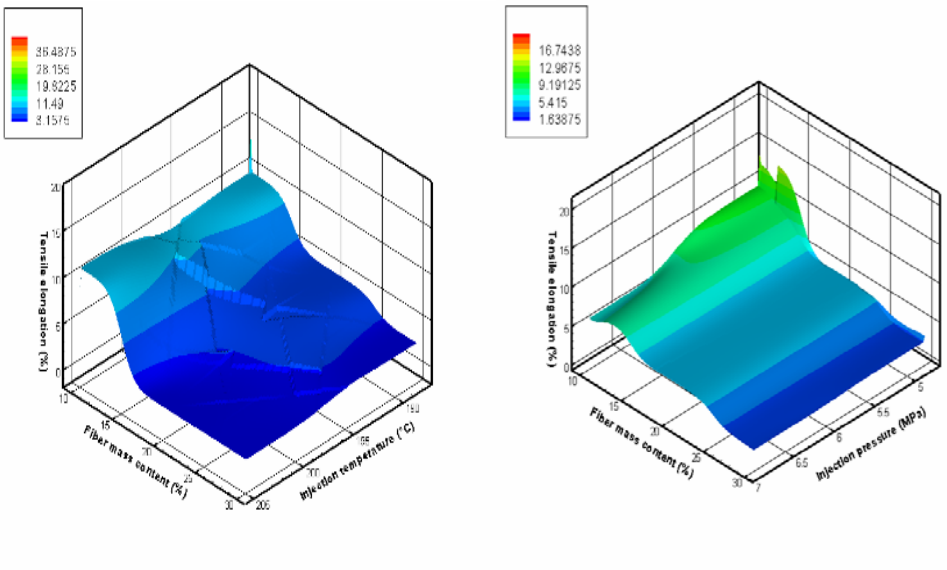

Figure E.2 Tensile elongation of flax fiber-HDPE biocomposites as affected by fiber mass content, injection temperature, and injection pressure plotted using Tecplot.

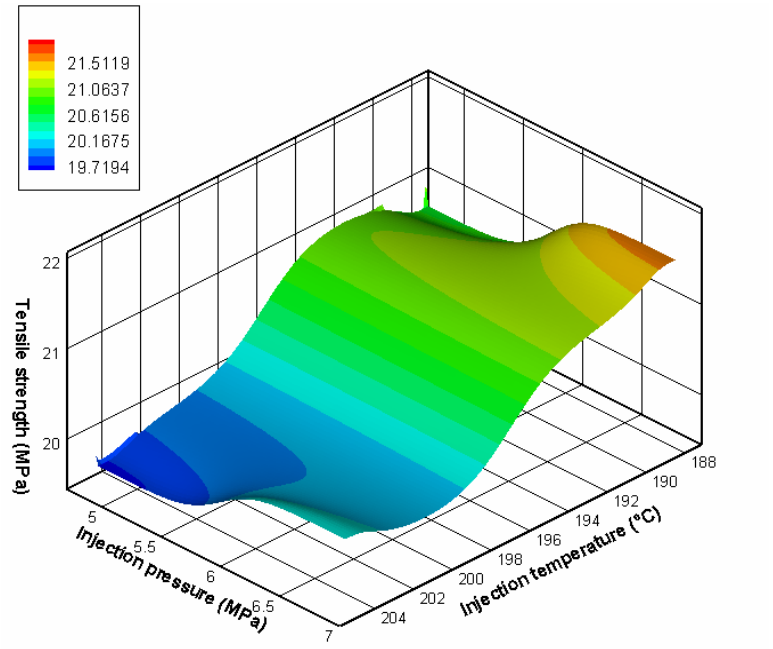

Figure E.3 Tensile strength of flax fiber-HDPE biocomposites (10% fiber content) as affected by injection temperature and injection pressure plotted using Tecplot.

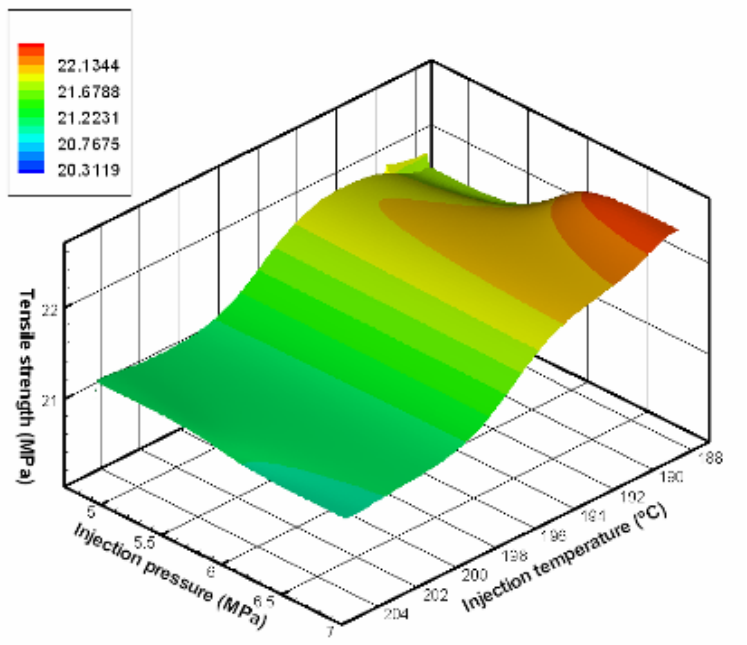

Figure E.4 Tensile strength of flax fiber-HDPE biocomposites (20% fiber content) as affected by injection temperature and injection pressure plotted using Tecplot.

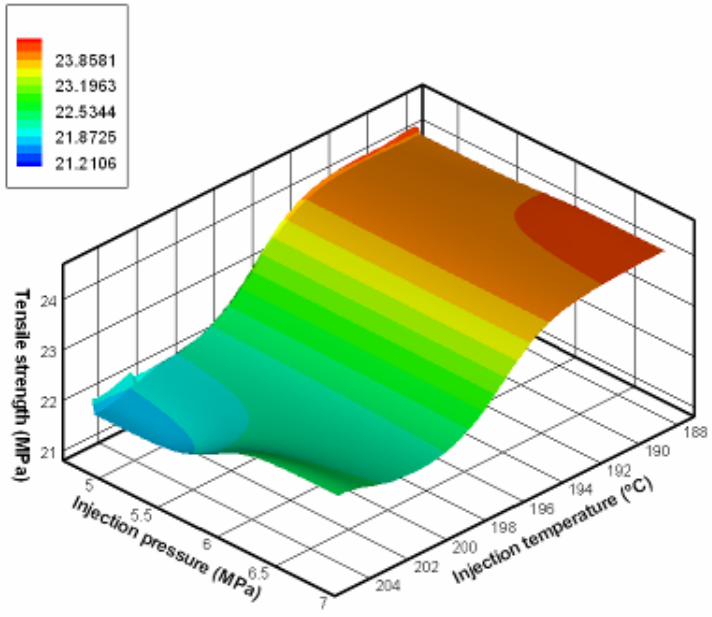

Figure E.5 Tensile strength of flax fiber-HDPE biocomposites (30% fiber content) as affected by injection temperature and injection pressure plotted using Tecplot.

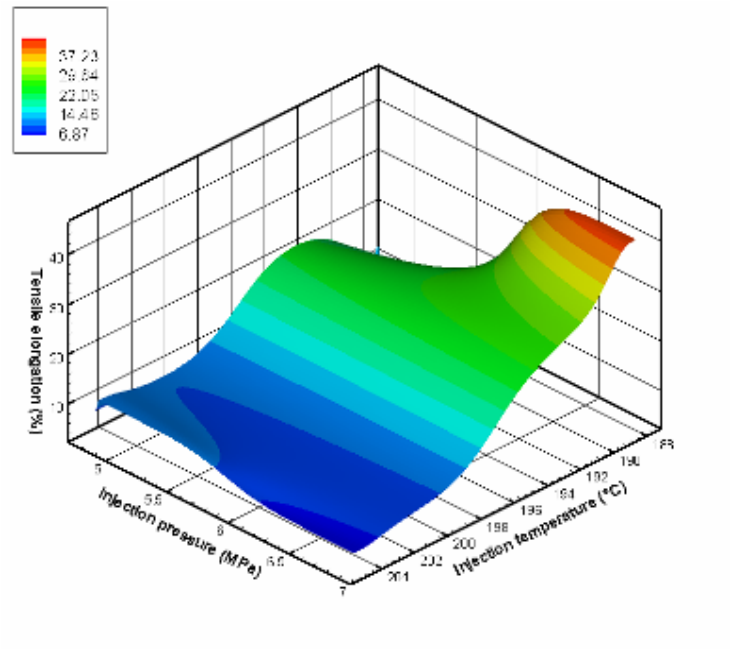

Figure E.6 Tensile elongation of flax fiber-HDPE biocomposites (10% fiber content) as affected by injection temperature and injection pressure plotted using Tecplot.

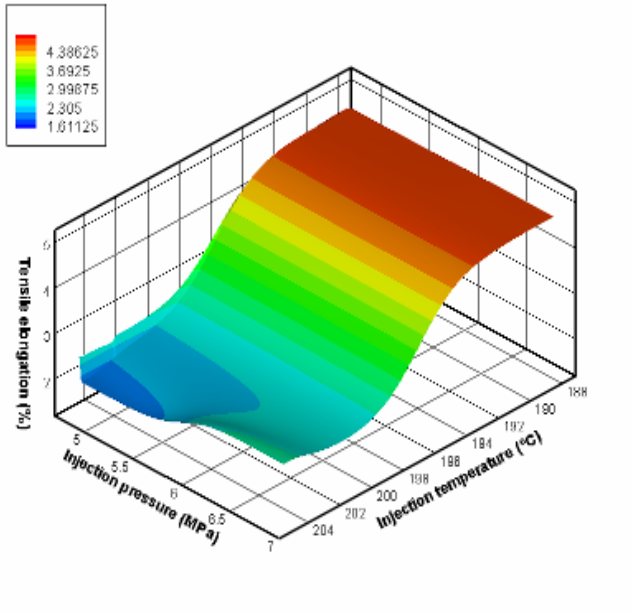

Figure E.7 Tensile elongation of flax fiber-HDPE biocomposites (20% fiber content) as affected by injection temperature and injection pressure plotted using Tecplot.

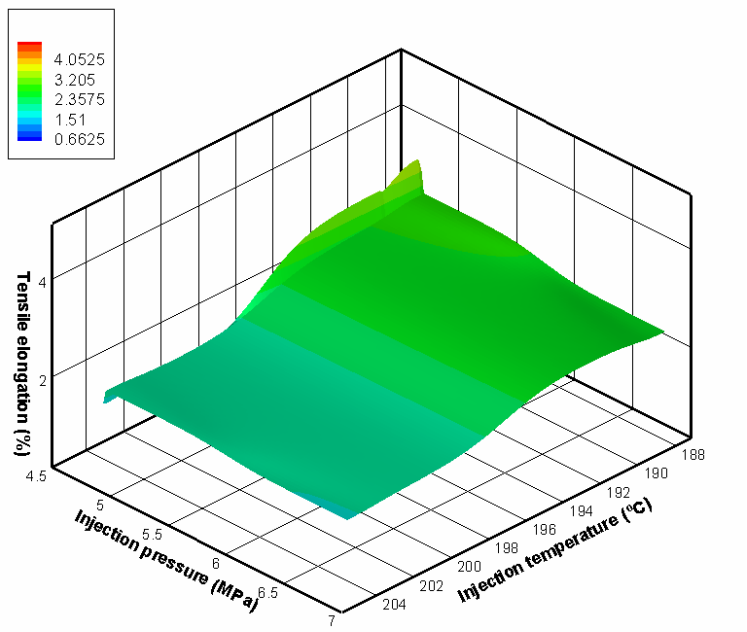

Figure E.8 Tensile elongation of flax fiber-HDPE biocomposites (30% fiber content) as affected by injection temperature and injection pressure plotted using Tecplot.

Table E.5 Coefficient estimates of equation 4.1 obtained by SAS linear regression model.

Source of Variation	Estimated Coefficient	Standard Error	T Value	Sig. (P)
Fiber content (*F*)	2.411	1.345	1.790	0.079
Injection temperature (*T*)	0.111	0.150	0.740	0.463
Injection pressure (*P*)	5.438	5.518	0.990	0.329
$F \times F$	0.004	0.001	2.840	0.007
$T \times T$	0	-	-	-
$P \times P$	0.094	0.877	0.110	0.915
$F \times T$	-0.012	0.007	-1.760	0.085
$F \times P$	-0.360	0.226	-1.590	0.118
$T \times P$	-0.003	0.025	-1.260	0.212
$F \times T \times P$	0.002	0.001	1.540	0.131

Dependent variable: Tensile strength.

Table E.6 Analysis of variance (ANOVA) table of equation 4.1.

Source	Degrees of freedom (DF)	Sum of Squares	Mean Square	F value	Sig. (P)
Model	9	28384.6938	3153.8549	14639.1	< 0.0001
Error	51	10.9875	0.2154		
Total	60	28395.6813			

Dependent variable: Tensile strength.

Predictors: F, T, P, $F \times F$, $P \times P$, $F \times T$, $F \times P$, $T \times P$, $F \times T \times P$.

R Square = 0.9996.

Table E.7 Coefficient estimates of equation 4.2 obtained by SAS linear regression model.

Source of Variation	Estimated Coefficient	Standard Error	T Value	Sig. (P)
Fiber content (F)	26.988	12.498	2.160	0.036
Injection temperature (T)	3.636	1.390	2.620	0.012
Injection pressure (P)	-63.457	51.277	-1.240	0.222
$F \times F$	0.052	0.012	4.370	<0.001
$T \times T$	0	-	-	-
$P \times P$	21.005	8.147	2.580	0.013
$F \times T$	-0.148	0.064	-2.290	0.026
$F \times P$	-7.094	2.101	-3.380	0.001
$T \times P$	-0.916	0.234	-3.920	<0.001
$F \times T \times P$	0.036	0.011	3.920	0.002

Dependent variable: Tensile elongation.

Table E.8 ANOVA table of equation 4.2.

Source	Degrees of freedom (DF)	Sum of Squares	Mean Square	F value	Sig. (P)
Model	9	6539.6018	726.6224	39.05	< 0.0001
Error	51	948.9515	18.6069		
Total	60	7488.5532			

Dependent variable: Tensile elongation.

Predictors: F, T, P, $F \times F$, $P \times P$, $F \times T$, $F \times P$, $T \times P$, $F \times T \times P$.

R Square = 0.8733.

Table E.9 Coefficient estimates of equation 4.3 obtained by SPSS linear regression model.

Source of Variation	Estimated Coefficient	Standard Error	T Value	Sig. (P)
constant	28.9516	2.743	10.553	<0.001
Fiber content (*F*)	0.2531	0.256	0.990	0.327
$F \times F$	0.0049	0.001	3.696	0.001
$T \times T$ *	-0.0002	0.000	-2.980	0.004
$F \times T$	-0.0017	0.001	-1.320	0.192

Dependent Variable: Tensile strength.

* *T* =Injection temperature.

Table E.10 ANOVA table of equation 4.3.

Source	Degrees of freedom (DF)	Sum of Squares	Mean Square	F value	Sig. (P)
Model	4	91.841	22.960	96.096	<0.001
Error	55	13.141	0.239		
Total	59	104.982			

Dependent Variable: Tensile strength.

Predictors: (Constant), *F*, $F \times F$, $T \times T$, $F \times T$.

R Square = 0.8748.

Table E.11 Coefficient estimates of equation 4.4 obtained by SPSS linear regression model.

Source of Variation	Estimated Coefficient	Standard Error	T Value	Sig. (P)
constant	61.5657	15.416	3.994	<0.001
Fiber content (*F*)	-3.6912	1.437	-2.569	0.013
$F \times F$	0.0226	0.008	3.008	0.004
$T \times T$ *	-0.0011	0.000	-2.764	0.008
$F \times T$	0.0126	0.007	1.736	0.088

Dependent Variable: Tensile elongation.

* *T* = Injection temperature.

Table E.12 ANOVA table of equation 4.4.

Source	Degrees of freedom (DF)	Sum of Squares	Mean Square	F value	Sig. (P)
Model	4	646.394	161.599	21.418	<0.001
Error	55	414.966	7.545		
Total	59	1061.361			

Dependent Variable: Tensile elongation.

Predictors: (Constant), F, $F \times F$, $T \times T$, $F \times T$.

R Square = 0.6090.

Table E.13 Homogeneous subsets of flexural strength of biocomposite under SPSS Tukey HSD method.

Trial[#]	N	Subset					
		a	b	c	d	e	f
3	5	26.780					
4	5		28.154				
8	5		28.648				
1	5		28.917				
2	5		29.038	29.038			
7	5		29.216	29.216			
5	5			30.146			
6	5				32.070		
11	5					35.828	
12	5					36.714	
10	5						38.198
9	5						38.361
Sig.		1.000	0.140	0.104	1.000	0.362	1.000

Based on Type III Sum of Squares.

The error term is Mean Square (Error) = 0.313.

Uses Harmonic Mean Sample Size = 5.

[#] The setting of trial refers to Table 3.6.

Means for groups in homogeneous subsets are displayed. The values in same subset mean no significant difference at 5% level.

Table E.14 Homogeneous subsets of flexural modulus of biocomposite under SPSS Tukey HSD method.

Trial[#]	N	Subset							
		a	b	c	d	e	f	g	h
3	5	542.140							
4	5	581.620	581.620						
1	5		613.507	613.507					
2	5		641.202	641.202	641.202				
8	5			661.580	661.580				
5	5				695.480				
7	5				696.640				
6	5					772.280			
11	5						1128.500		
9	5							1215.942	
12	5							1259.800	1259.800
10	5								1284.956
Sig.		0.579	0.075	0.287	0.127	1.000	1.000	0.420	0.962

Based on Type III Sum of Squares.
The error term is Mean Square (Error) = 828.395.
Uses Harmonic Mean Sample Size = 5.
[#] The setting of trial refers to Table 3.6.
Means for groups in homogeneous subsets are displayed. The values in same subset mean no significant difference at 5% level.

Table E.15 SPSS univariate analysis of variance of the effect of fiber content, injection temperature, and injection pressure on the biocomposite flexural stress.

Source	Type III Sum of Squares	df	Mean Square	F	Sig.(P)
Corrected Model	990.932(a)	11	90.085	287.886	<0.001
Intercept	60823.863	1	60823.863	194376.108	<0.001
Fiber_content (*F*)	918.836	2	459.418	1468.172	<0.001
Injection_temperature (*T*)	54.052	1	54.052	172.736	<0.001
Injection_pressure (*P*)	5.324	1	5.324	17.013	<0.001
F × *T*	1.198	2	0.599	1.914	0.159
F × *P*	.423	2	0.211	0.676	0.514
T × *P*	.015	1	0.015	0.048	0.827
F × *T* × *P*	11.084	2	5.542	17.711	<0.001
Error	15.020	48	0.313		
Total	61829.816	60			
Corrected Total	1005.952	59			

Dependent Variable: Flexural stress (MPa).
R Square = 0.985.

Table E.16 SPSS univariate analysis of variance of the effect of fiber content, injection temperature, and injection pressure on the biocomposite flexural modulus.

Source	Type III Sum of Squares	df	Mean Square	F	Sig.(P)
Corrected Model	4614628.583(a)	11	419511.689	205.771	<0.001
Intercept	42450715.025	1	42450715.025	20822.159	<0.001
Fiber_content (*F*)	4483707.876	2	2241853.938	1099.634	<0.001
Injection_temperature (*T*)	51946.104	1	51946.104	25.480	<0.001
Injection_pressure (*P*)	39842.675	1	39842.675	19.543	<0.001
F × *T*	335.182	2	167.591	0.082	0.921
F × *P*	18132.925	2	9066.462	4.447	0.017
T × *P*	594.996	1	594.996	0.292	0.592
F × *T* × *P*	20068.826	2	10034.413	4.922	0.011
Error	97858.938	48	2038.728		
Total	47163202.546	60			
Corrected Total	4712487.521	59			

Dependent Variable: Flexural modulus (MPa).
R Square = 0.979.

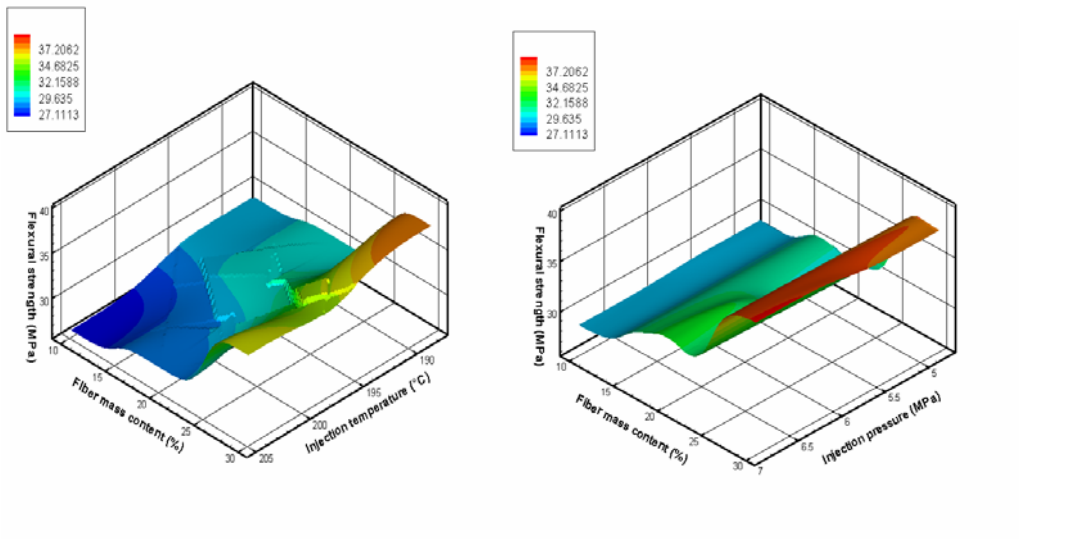

Figure E.9 Flexural strength of flax fiber-HDPE biocomposites as affected by fiber mass content, injection temperature and injection pressure plotted using Tecplot.

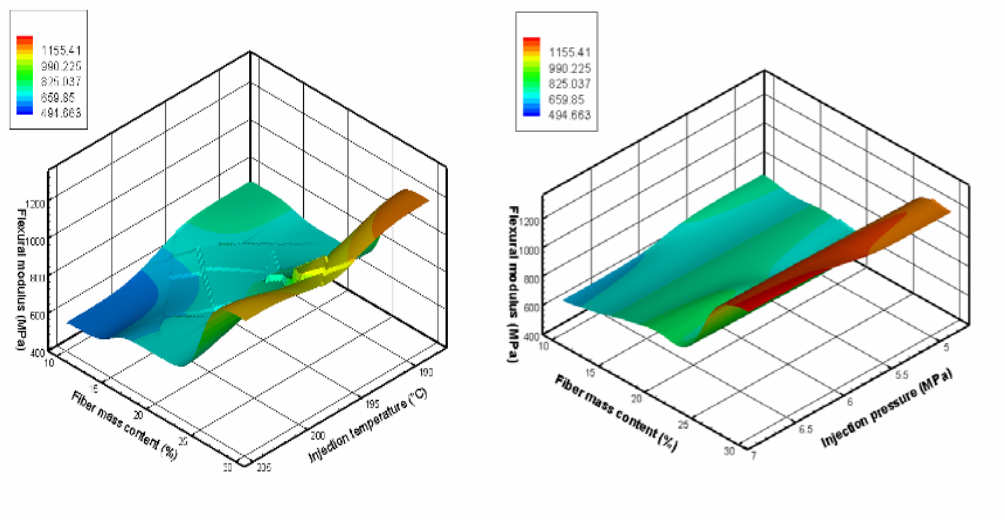

Figure E.10 Flexural modulus of flax fiber-HDPE biocomposites as affected by fiber mass content, injection temperature, and injection pressure plotted using Tecplot.

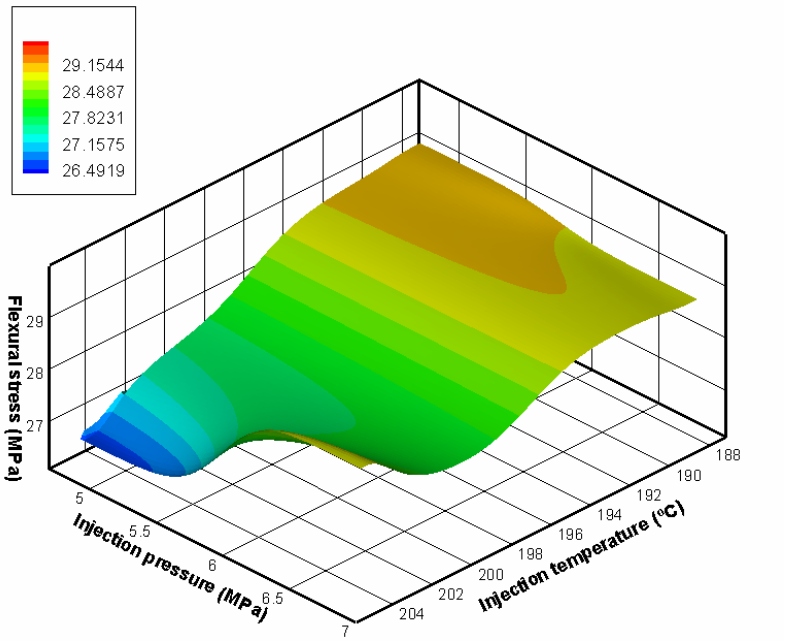

Figure E.11 Flexural strength of flax fiber-HDPE biocomposites (10% fiber content) as affected by injection temperature and injection pressure plotted using Tecplot.

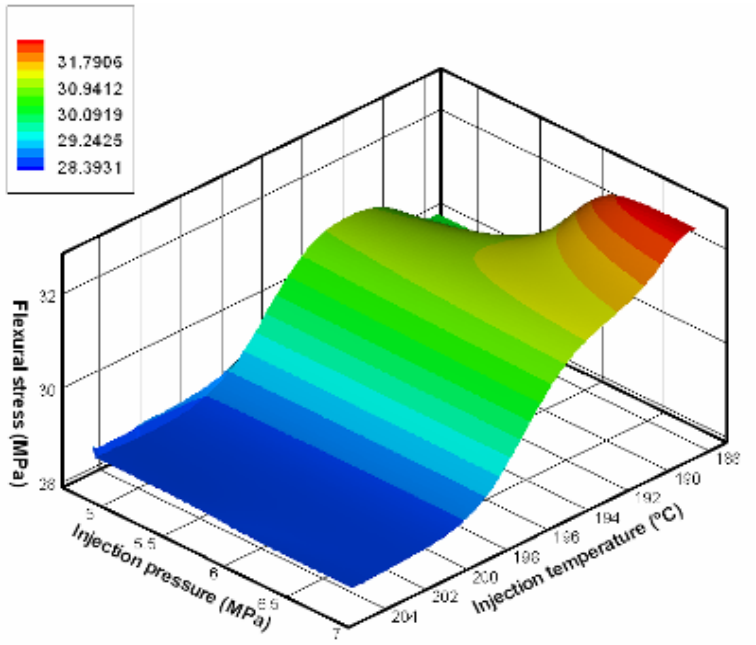

Figure E.12 Flexural strength of flax fiber-HDPE biocomposites (20% fiber content) as affected by injection temperature and injection pressure plotted using Tecplot.

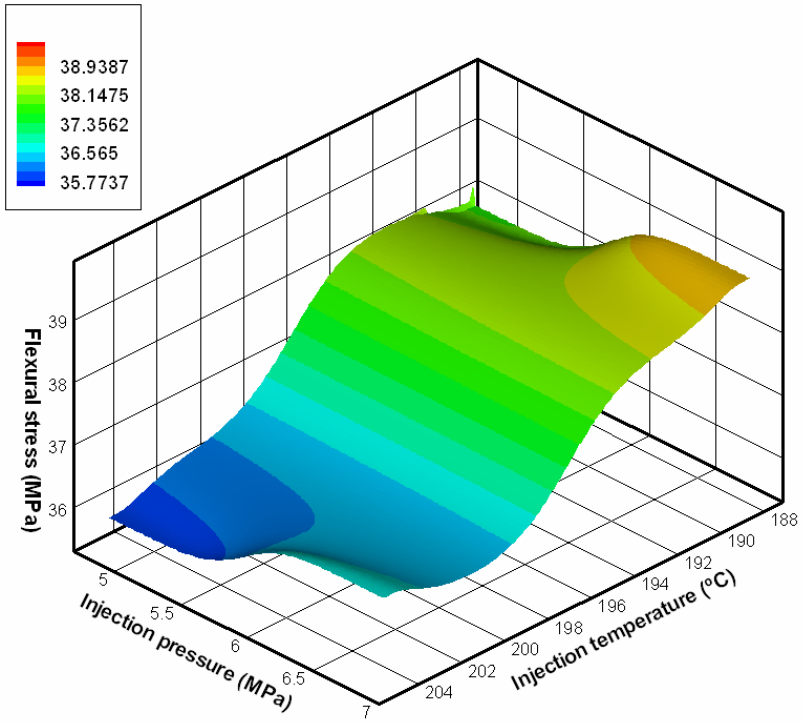

Figure E.13 Flexural strength of flax fiber-HDPE biocomposites (30% fiber content) as affected by injection temperature and injection pressure plotted using Tecplot.

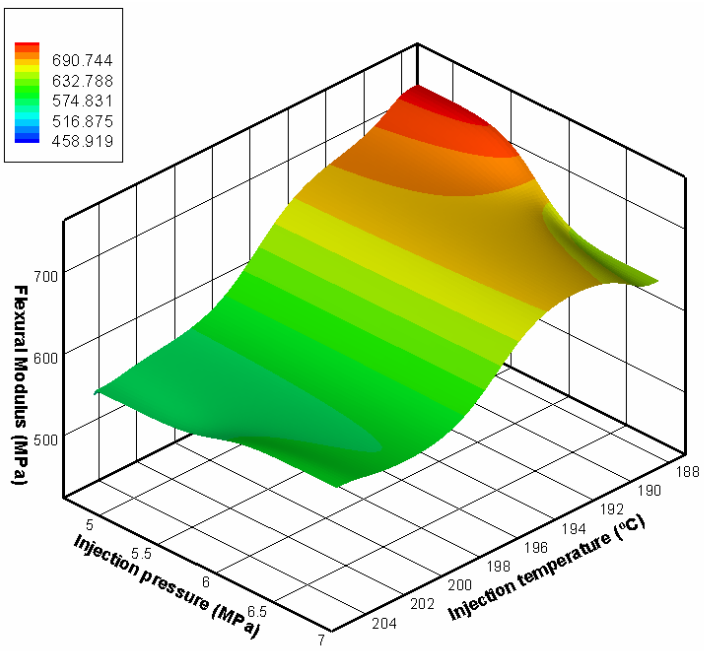

Figure E.14 Flexural modulus of flax fiber-HDPE biocomposites (10% fiber content) as affected by injection temperature and injection pressure plotted using Tecplot.

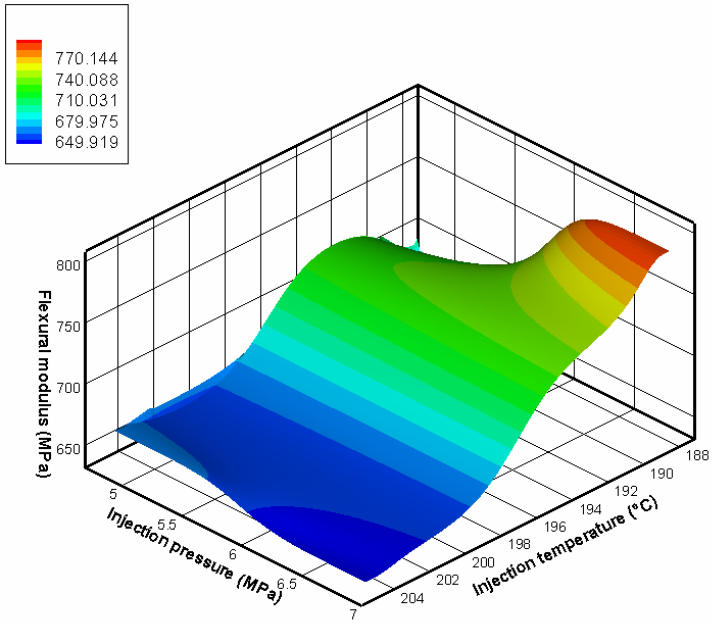

Figure E.15 Flexural modulus of flax fiber-HDPE biocomposites (20% fiber content) as affected by injection temperature and injection pressure plotted using Tecplot.

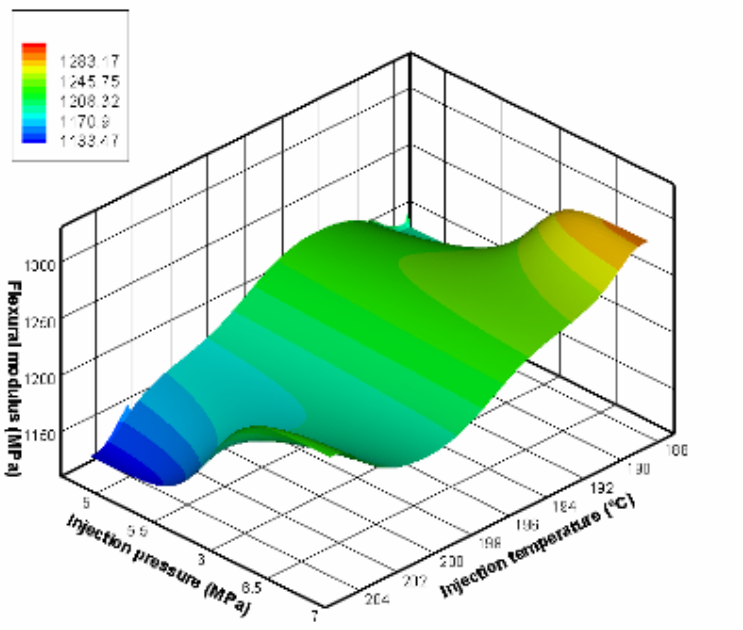

Figure E.16 Flexural modulus of flax fiber-HDPE biocomposites (30% fiber content) as affected by injection temperature and injection pressure plotted using Tecplot.

Table E.17 Coefficient estimates of equation 4.5 obtained by SAS linear regression model.

Source of Variation	Estimated Coefficient	Standard Error	T Value	Sig. (P)
Fiber content (*F*)	-0.643	1.921	-0.330	0.739
Injection temperature (*T*)	-0.237	0.214	-1.110	0.272
Injection pressure (*P*)	22.932	7.883	2.910	0.005
F × *F*	0.027	0.002	15.020	<0.001
T × *T*	0	-	-	-
P × *P*	-2.254	1.252	-1.800	0.078
F × *T*	<0.001	0.010	0.030	0.976
F × *P*	0.070	0.323	0.220	0.831
T × *P*	0.021	0.036	0.570	0.569
F × *T* × *P*	<-0.001	0.002	-0.240	0.808

Dependent Variable: Flexural strength.

Table E.18 ANOVA table of equation 4.5.

Source	Degrees of freedom (DF)	Sum of Squares	Mean Square	F value	Sig. (P)
Model	9	61807.3871	6867.4875	15616.0	< 0.0001
Error	51	22.4285	0.4398		
Total	60	61829.8155			

Dependent Variable: Flexural strength.

Predictors: F, T, P, $F \times F$, $P \times P$, $F \times T$, $F \times P$, $T \times P$, $F \times T \times P$.

R Square = 0.9996.

Table E.19 Coefficient estimates of equation 4.6 obtained by SAS linear regression model.

Source of Variation	Estimated Coefficient	Standard Error	T Value	Sig. (P)
Fiber content (F)	47.625	130.554	0.360	0.717
Injection temperature (T)	3.553	14.520	0.240	0.808
Injection pressure (P)	377.245	535.654	0.700	0.485
$F \times F$	2.020	0.123	16.370	<0.001
$T \times T$	0	-	-	-
$P \times P$	-6.242	85.102	-0.070	0.942
$F \times T$	-0.548	0.672	-0.820	0.419
$F \times P$	-17.853	21.950	-0.810	0.419
$T \times P$	-1.576	2.443	-0.650	0.522
$F \times T \times P$	0.100	0.113	0.890	0.380

Dependent Variable: Flexural modulus.

Table E.20 ANOVA table of equation 4.6.

Source	Degrees of freedom (DF)	Sum of Squares	Mean Square	F value	Sig. (P)
Model	9	47059648.45	5228849.83	2575.19	< 0.0001
Error	51	103554.09	2030.47		
Total	60	47163202.55			

Dependent Variable: Flexural modulus.

Predictors: F, T, P, $F \times F$, $P \times P$, $F \times T$, $F \times P$, $T \times P$, $F \times T \times P$.

R Square = 0.9978.

Table E.21 Coefficient estimates of equation 4.7 obtained by SPSS linear regression model.

Source of Variation	Estimated Coefficient	Standard Error	T Value	Sig. (P)
Constant	43.212	4.311	10.025	<0.001 (a)
Fiber content (*F*)	-0.236	0.402	-0.588	0.559
$F \times F$	0.027	0.002	12.973	<0.001
$T \times T$ *	<-0.001	<0.001	-2.669	0.010
$F \times T$	-0.002	0.002	-1.025	0.310

Dependent Variable: Flexural strength.

* *T* = Injection temperature.

Table E.22 ANOVA table of equation 4.7.

Source	Degrees of freedom (DF)	Sum of Squares	Mean Square	F value	Sig. (P)
Model	4	973.508	243.377	412.575	<0.001
Error	55	32.444	0.590		
Total	59	1005.952			

Dependent Variable: Flexural strength.

Predictors: (Constant), *F*, $F \times F$, $T \times T$, $F \times T$.

R Square = 0.9677.

Table E.23 Coefficient estimates of equation 4.8 obtained by SPSS linear regression model.

Source of Variation	Estimated Coefficient	Standard Error	T Value	Sig. (P)
Constant	1437.0460	260.547	5.515	<0.001
Fiber content (*F*)	-56.8179	24.283	-2.340	0.023
$F \times F$	2.0196	0.127	15.886	<0.001
$T \times T$ *	-0.0146	0.007	-2.145	0.036
$F \times T$	0.0382	0.122	0.313	0.756

Dependent Variable: Flexural modulus.

* *T* = Injection temperature.

Table E.24 ANOVA table of equation 4.8.

Source	Degrees of freedom (DF)	Sum of Squares	Mean Square	F value	Sig. (P)
Model	4	4535864.443	1133966.111	526.193	<0.001
Error	55	118527.078	2155.038		
Total	59	4654391.521			

Dependent Variable: Flexural modulus.

Predictors: (Constant), *F*, *F* × *F*, *T* × *T*, *F* × *T*.

R Square = 0.9745.

Table E.25 Homogeneous subsets of water absorption of biocomposite under SPSS Tukey HSD method.

Trial[#]	N	Subset					
		a	b	c	d	e	f
1	3	0.043					
2	3	0.048					
3	3	0.060					
4	3	0.090	0.090				
5	3		0.155	0.155			
6	3			0.193	0.193		
9	3			0.201	0.201		
10	3				0.237	0.237	
8	3				0.253	0.253	
7	3					0.298	
12	3						0.513
11	3						0.559
Sig.		0.376	0.067	0.402	0.113	0.103	0.400

Based on Type III Sum of Squares.

The error term is Mean Square (Error) = 0.001.

Uses Harmonic Mean Sample Size = 3.

[#] The setting of trial refers to Table 3.6.

Means for groups in homogeneous subsets are displayed. The values in same subset mean no significant difference at 5% level.

Table E.26 SPSS univariate analysis of variance of the effect of fiber content, injection temperature, and injection pressure on the biocomposite water absorption.

Source	Type II Sum of Squares	df	Mean Square	F	Sig.(P)
Corrected Model	0.950(a)	11	0.086	164.944	<0.001
Intercept	1.754	1	1.754	3350.400	<0.001
Fiber content (*F*)	0.604	2	0.302	576.364	<0.001
Injection temperature (*T*)	0.200	1	0.200	382.858	<0.001
Injection pressure (*P*)	<0.001	1	<0.001	0.142	0.709
F × *F*	0.134	2	0.067	128.224	<0.001
T × *T*	0.001	2	<0.001	0.933	0.407
P × *P*	0.005	1	0.005	9.269	0.006
F × *T*	0.006	2	0.003	5.538	0.011
Error	0.013	24	0.001		
Total	2.717	36			
Corrected Total	0.963	35			

Dependent Variable: Water absorption (%).
(a) R Square = 0.987.

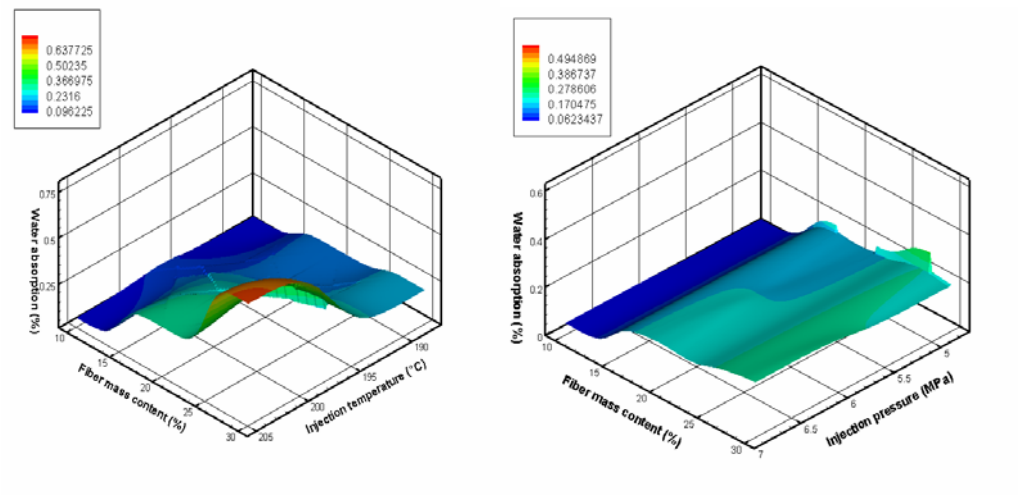

Figure E.17 Water absorption of flax fiber-HDPE biocomposites as affected by fiber mass content, injection temperature and injection pressure plotted using Tecplot.

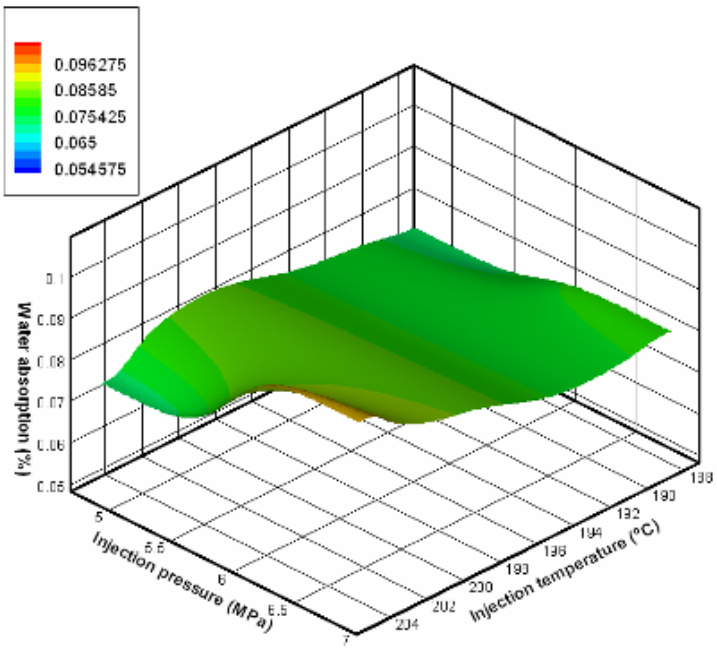

Figure E.18 Water absorption of flax fiber-HDPE biocomposites (10% fiber content) as affected by injection temperature and injection pressure plotted using Tecplot.

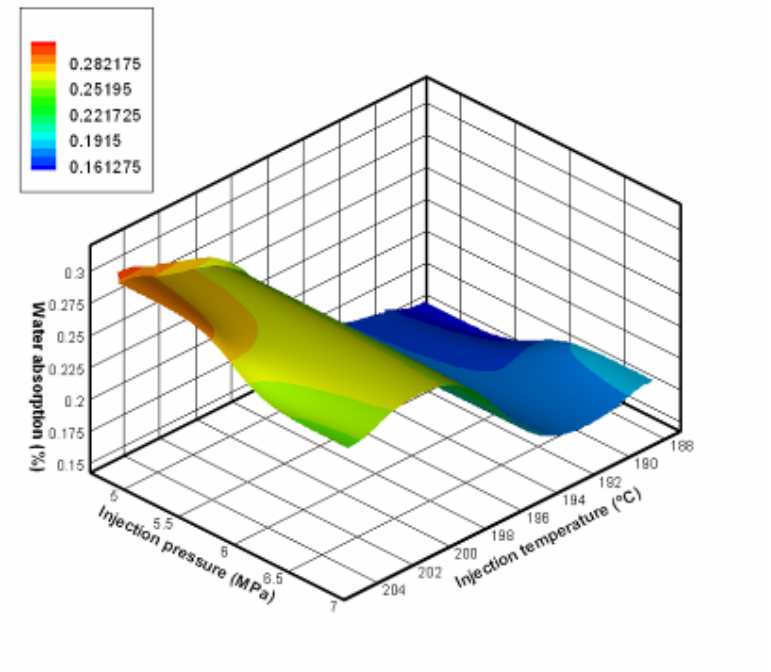

Figure E.19 Water absorption of flax fiber-HDPE biocomposites (20% fiber content) as affected by injection temperature and injection pressure plotted using Tecplot.

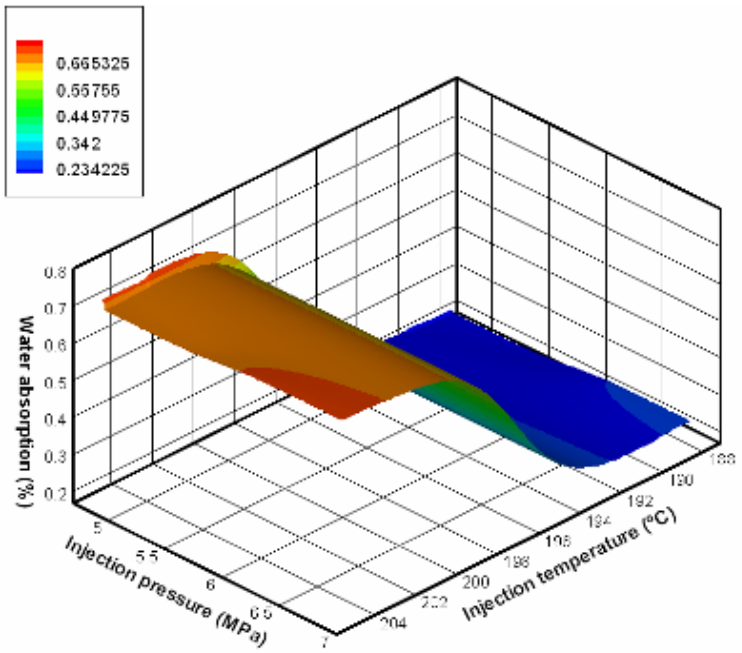

Figure E.20 Water absorption of flax fiber-HDPE biocomposites (30% fiber content) as affected by injection temperature and injection pressure plotted using Tecplot.

Table E.27 Coefficient estimates of equation 4.9 obtained by SAS linear regression model.

Source of Variation	Estimated Coefficient	Standard Error	T Value	Sig. (P)
Fiber content (*F*)	-0.518	0.198	-2.620	0.014
Injection temperature (*T*)	-0.028	0.022	-1.290	0.208
Injection pressure (*P*)	1.755	0.812	2.160	0.040
F × *F*	0.001	<0.001	2.570	0.016
T × *T*	0	-	-	-
P × *P*	-0.167	0.129	-1.290	0.207
F × *T*	0.003	0.001	2.620	0.014
F × *P*	0.025	0.033	0.740	0.467
T × *P*	0.001	0.004	0.280	0.783
F × *T* × *P*	<-0.001	<0.001	-0.740	0.467

Dependent Variable: Water absorption.

Table E.28 ANOVA table of equation 4.9.

Source	Degrees of freedom (DF)	Sum of Squares	Mean Square	F value	Sig. (P)
Model	9	3.9769	0.4419	157.81	< 0.0001
Error	27	0.0756	0.0028		
Total	36	4.0525			

Dependent Variable: Water absorption.

Predictors: *F*, *T*, *P*, *F* × *F*, *P* × *P*, *F* × *T*, *F* × *P*, *T* × *P*, *F* × *T*× *P*.

R Square = 0.9813.

Table E.29 Coefficient estimates of equation 4.10 obtained by SPSS linear regression model.

Source of Variation	Estimated Coefficient	Standard Error	T Value	Sig. (P)
constant	1.003	0.242	4.146	<0.001
Fiber content (*F*)	-0.214	0.023	-9.500	<0.001
F × *F*	-5.598×10-5	<0.001	-0.474	0.639
T × *T* *	-2.969×10-5	<0.001	-4.693	<0.001
F × *T*	0.001	<0.001	10.541	<0.001

Dependent Variable: Water absorption.

* *T* = Injection temperature.

Table E.30 ANOVA table of equation 4.10.

Source	Degrees of freedom (DF)	Sum of Squares	Mean Square	F value	Sig. (P)
Model	4	0.928	0.232	207.959	<0.001
Error	31	0.035	0.001		
Total	35	0.963			

Dependent Variable: Water absorption.

Predictors: (Constant), *F*, *F* × *F*, *T* × *T*, *F* × *T*.

R Square = 0.9641.

APPENDIX F

Shear stress vs. shear rate of HDPE and biocomposites

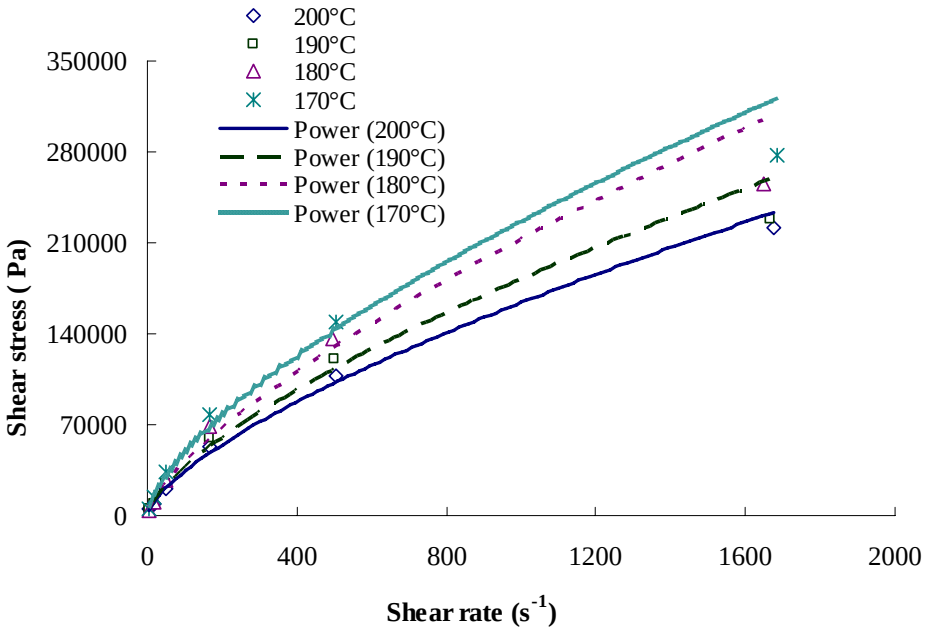

Figure F.1 Shear stress vs. shear rate of HDPE.

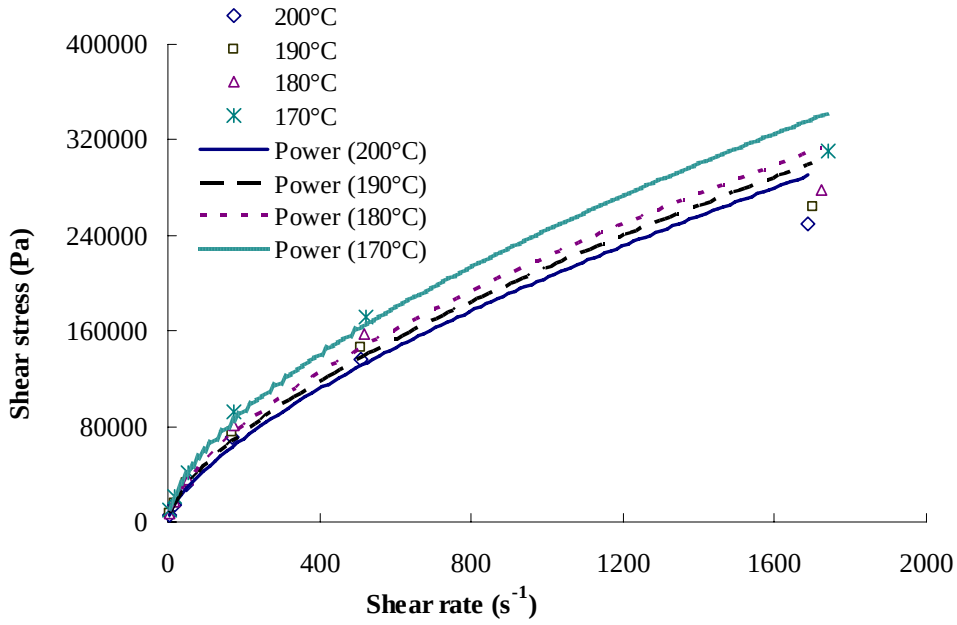

Figure F.2 Shear stress vs. shear rate of biocomposite containing 10% fiber.

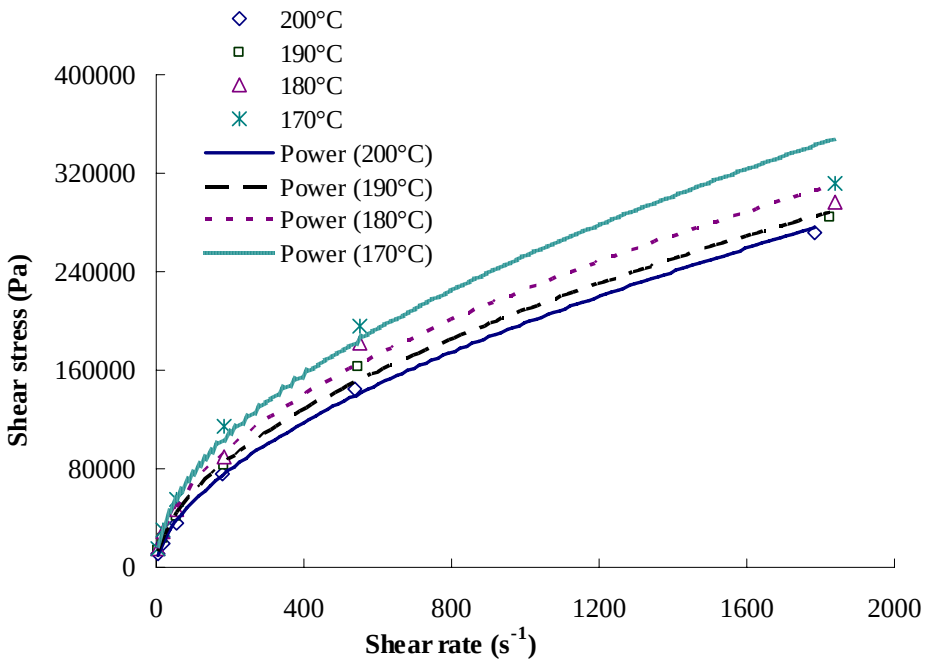

Figure F.3 Shear stress vs. shear rate of biocomposite containing 20% fiber.

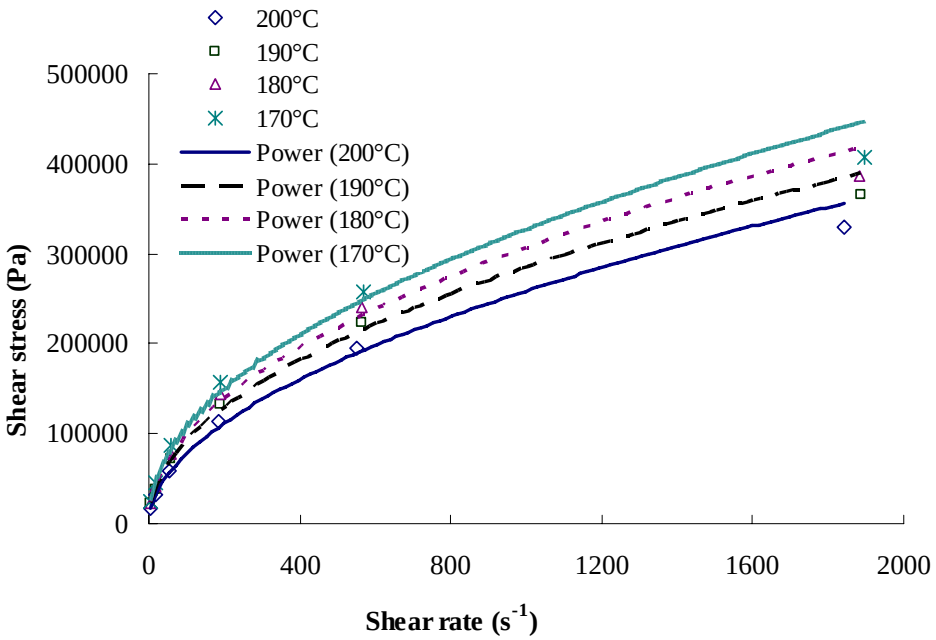

Figure F.4 Shear stress vs. shear rate of biocomposite containing 30% fiber.

APPENDIX G

SPSS and SAS analysis of biocomposite rheological property

Table G.1 ANOVA table of equation 4.11 obtained by SPSS linear regression model.

Source	DF	Sum of Squares	Mean Square	F Value	Sig.(P)
Regression	2	148424763.769	74212381.884	70.577	< 0.0001
Residual	13	13669601.772	1051507.829		
Total	15	162094365.540			

Dependent Variable: *K*.

Predictors: (Constant), Fiber content, Temperature.

R Square = 0.9157.

Table G.2 Coefficient estimates of equation 4.11 obtained by SPSS linear regression model.

Source of Variation	Estimated Coefficient	Standard Error	T Value	Sig.(P)
(Constant)	14854.8775	4263.5597	3.4841	0.0040
Temperature	-75.3220	22.9293	-3.2850	0.0059
Fiber content	261.7995	22.9293	11.4177	< 0.0001

Dependent Variable: *K*.

Table G.3 ANOVA table of equation 4.12 obtained by SPSS linear regression model.

Source	DF	Sum of Squares	Mean Square	F Value	Sig.(P)
Regression	2	0.093	0.047	123.415	< 0.0001
Residual	13	0.005	0.000		
Total	15	0.098			

Dependent Variable: *n*.

Predictors: (Constant), Fiber content, Temperature.

R Square = 0.9500.

Table G.4 Coefficient estimates of equation 4.12 obtained by SPSS linear regression model.

Source of Variation	Estimated Coefficient	Stdandard Error	T Value	Sig.(P)
(Constant)	0.4884	0.0809	6.0383	< 0.0001
Temperature	0.0011	0.0004	2.5359	0.0249
Fiber content	-0.0067	0.0004	-15.5048	< 0.0001

Dependent Variable: *n*.

SAS Program used to develop nonlinear regression model (equation 4.13) is as the following:

```
Data apparent viscosity;
  input temperature fiber rate y;
cards;
170    0    2.677466897   1150.801325
170    0    5.56716877    863.1009937
170    0    10.8573568    671.3007729
170    0    22.57534455     460.32053
170    0    44.02750856   295.3723401
170    0    91.54494904   164.5645895
170    10   5.225328947   1780.329149
170    10   17.41776316    1223.97629
170    10   52.25328947   790.0210599
170    10   174.1776316   529.6479219
170    10   522.5328947   328.2481869
170    10   1741.776316   178.0329149
170    20   5.515003804   2811.362654
170    20   18.38334601   1686.817592
170    20   55.15003804   1001.547945
170    20   183.8334601   622.0139871
170    20   551.5003804    354.934535
170    20   1838.334601   169.7360202
170    30   5.687435766   4429.957383
170    30   18.95811922   2422.845923
170    30   56.87435766   1516.408489
170    30   189.5811922   828.0612647
170    30   568.7435766   453.2187169
170    30   1895.811922   214.6825501
180    0    2.641992867   862.6385601
180    0    5.493408786   646.9789201
180    0    10.71350658   548.951811
180    0    22.27624152   417.5954848
180    0    43.44418363   276.4364477
```

180	0	90.33206072	154.6867782
180	10	5.163268956	1501.439869
180	10	17.21089652	979.6895147
180	10	51.63268956	675.6479411
180	10	172.1089652	470.701399
180	10	516.3268956	305.9183734
180	10	1721.089652	161.5924659
180	20	5.5207181	2632.924419
180	20	18.40239367	1579.754652
180	20	55.207181	860.0886436
180	20	184.0239367	484.4580931
180	20	552.07181	329.9931939
180	20	1840.239367	161.1349745
180	30	5.653250304	4045.353642
180	30	18.84416768	2231.801034
180	30	56.53250304	1364.449788
180	30	188.4416768	766.2174058
180	30	565.3250304	425.1049589
180	30	1884.416768	204.6674681
190	0	2.662016739	929.4458735
190	0	5.535043765	580.9036709
190	0	10.79470509	484.0863924
190	0	22.44507491	360.160276
190	0	43.77345052	240.1068506
190	0	91.01669454	137.0932663
190	10	5.108970407	1251.852767
190	10	17.02990136	887.6774164
190	10	51.08970407	633.5133698
190	10	170.2990136	441.5626123
190	10	510.8970407	286.4087391
190	10	1702.990136	154.7745239
190	20	5.470752608	2479.840021
190	20	18.23584203	1275.346297
190	20	54.70752608	761.6651494
190	20	182.3584203	451.6851468
190	20	547.0752608	297.5808026
190	20	1823.584203	155.6985271
190	30	5.664377289	3934.761091
190	30	18.88125763	2022.125048
190	30	56.64377289	1283.074269
190	30	188.8125763	697.9924022
190	30	566.4377289	393.4761091
190	30	1888.125763	194.0008294
200	0	2.668034269	964.5838942

```
200     0       5.547555818   520.8753029
200     0       10.81910669   405.1252356
200     0       22.49581235   318.3126851
200     0       43.87240109   214.1376245
200     0       91.2224392    132.5338271
200     10      5.068257074   1032.470923
200     10      16.89419025   860.3924358
200     10      50.68257074   604.1866883
200     10      168.9419025   418.7243188
200     10      506.8257074   269.5896299
200     10      1689.419025    147.413904
200     20      5.356331455   1990.068138
200     20      17.85443818   1085.491712
200     20      53.56331455   669.3865555
200     20      178.5443818   423.3417676
200     20      535.6331455   271.3729279
200     20      1785.443818   151.9688396
200     30      5.52893452    2979.546584
200     30      18.42978173   1703.599576
200     30      55.2893452    1076.142119
200     30      184.2978173   618.3435499
200     30      552.893452    354.0402412
200     30      1842.978173   179.2985974
;
proc nlin data=apparent viscosity;
  parameters  b=-5
           c=41 d=5167
           e=-0.4;
  model y = b*temperature + c*fiber + d*(rate)**e;
run;
```

(Note: y = apparent viscosity; b, c, d, and e are the coefficient related to variables of temperature, fiber content, and shear rate.)

Table G.5 Parameter estimate output of SAS NLIN (nonlinear) procedure for equation 4.13.

Parameter	Estimate	Std. Error	Approximate 95% Confidence Limits	
b	-11.1515	2.8941	-16.8995	-5.4035
c	51.5857	4.0437	43.5545	59.6169
d	4231.2	419.1	3398.9	5063.6
e	-0.1754	0.0459	-0.2665	-0.0843

Dependent Variable: apparent viscosity.
Method: Gauss-Newton.

Table G.6 ANOVA table of SAS nonlinear regression model for equation 4.13.

Source	DF	Sum of Squares	Mean Square	F value	Sig. (P)
Regression	4	1.3207E8	33017950	185.24	< 0.0001
Residual	92	16398358	178243		
Uncorrected Total	96	1.4847E8			
Corrected Total	96				

Dependent Variable: apparent viscosity.
R Square = 0.89.

The $(\gamma)^{-0.1754}$ in equation 4.13 ($\mu_a = -11.1515T + 51.5857F + 4231.2(\gamma)^{-0.1754}$) was converted to variable "ratechange". Combined with other variables temperature (T), fiber content (F), Stepwise linear regression method was used in SPSS to determine how variables (temperature, fiber content, and ratechange) influence the apparent viscosity. The results are given in Tables G.7 and G.8.

Table G.7 Variables entered/removed (a,b) in SPSS stepwise linear regression.

Model	Variables Entered	Variables Removed	R Square	Method
1	ratechange	Fiber content, Temperature	0.653	Stepwise (Criteria: Probability-of-F-to-enter <= .050, Probability-of-F-to-remove >= .100).
2	Fiber content	Temperature	0.710	Stepwise (Criteria: Probability-of-F-to-enter <= .050, Probability-of-F-to-remove >= .100).
3	Temperature	.	0.890	Stepwise (Criteria: Probability-of-F-to-enter <= .050, Probability-of-F-to-remove >= .100).

(a) Dependent Variable: Apparent viscosity.
(b) Linear Regression through the Origin.

Table G.8 Coefficients (a,b) of models using stepwise method in SPSS.

Model	Variables Entered	Estimated Coefficient	Standard Error	T Value	Sig.(P)
1	ratechange	1859.115	138.914	13.383	<0.001
2	ratechange	1322.881	179.265	7.379	<0.001
	Fiber content	22.105	5.181	4.266	<0.001
3	ratechange	4231.244	261.140	16.203	<0.001
	Fiber content	51.586	4.007	12.873	<0.001
	Temperature	-11.152	0.906	-12.308	<0.001

(a) Dependent Variable: Apparent viscosity.

(b) Linear Regression through the Origin.

APPENDIX H

Solution of prediction equations of the filling time

The equations related to filling time given in Chapter 4 are:

$$P_1 - a(P_0 - P_1)^{\frac{2}{n}} - b(P_0 - P_1) = 0 \tag{4.14}$$

where

$$a = \left\{ \begin{array}{l} 0.2\left[1.25 - \left(\frac{A_2}{A_1}\right)\right] + \\ \left(\frac{3n+1}{2n+1}\right)\left[\frac{n+3}{2(5n+3)}\left(\frac{A_2}{A_3}\right)^2 - \left(\frac{A_2}{A_3}\right) + \frac{3(3n+1)}{2(5n+3)}\right] \end{array} \right\} \rho \left(\frac{A_1}{A_2}\right)^2 \left(\frac{n}{1+3n}\right)^2 R^{\frac{2}{n}+2} \left(\frac{1}{2KL}\right)^{\frac{2}{n}}$$

$$b = \left(\frac{X}{2L}\right)\left(\frac{A_1}{A_3}\right)^n \left(\frac{R}{h}\right)^{1+n} \left(\frac{2n+1}{1+3n}\right)^n$$

$$t = t_1 + t_3 = \frac{L}{u_1} + \frac{X}{u_3} = cP_0^{-\frac{1}{n}} + dP_0^{-\frac{1}{n}} = (c+d)P_0^{-\frac{1}{n}} \tag{4.20}$$

where $c = L^{\frac{1}{n}+1}\left[\left(\frac{1}{1+b}\right)\frac{1}{2K}\right]^{-\frac{1}{n}}\left(\frac{n}{1+3n}\right)^{-1} R^{-(1+\frac{1}{n})}$

$$d = \frac{1}{0.432} X\left[\left(\frac{1}{1+b}\right)\frac{1}{2KL}\right]^{-\frac{1}{n}}\left(\frac{n}{1+3n}\right)^{-1} R^{-(1+\frac{1}{n})}$$

The values of *a*， *b*， *c,* and *d* in equations 4.14 and 4.20 for HDPE and biocomposites at different temperatures are calculated according to *K* and *n* value and molded material dimensions. The results are listed in Table H.1.

Table H.1 Values of *a*, *b*, *c*, and *d* for HDPE and biocomposites

Sample	Coefficient	Temperature (°C)			
		170	180	190	200
HDPE	a	1.46E-17	5.17E-16	1.21E-16	9.30E-17
	b	0.5182	0.5092	0.5144	0.5159
	c	6.09E+10	9.82E+09	2.08E+10	2.39E+10
	d	7.83E+10	1.26E+10	2.67E+10	3.07E+10
A1*	a	5.57E-20	5.16E-19	3.16E-18	1.24E-17
	b	0.5304	0.5263	0.5225	0.5194
	c	1.07E+12	3.44E+11	1.36E+11	6.75E+10
	d	1.38E+12	4.42E+11	1.75E+11	8.68E+10
A2**	a	6.36E-24	8.18E-24	5.09E-23	2.07E-21
	b	0.5464	0.5467	0.5443	0.5383
	c	1.15E+14	1.01E+14	3.99E+13	5.98E+12
	d	1.48E+14	1.31E+14	5.13E+13	7.69E+12
A3***	a	1.08E-26	4.14E-26	3.92E-26	3.94E-24
	b	0.5540	0.5526	0.5531	0.5471
	c	3.05E+15	1.54E+15	1.59E+15	1.50E+14
	d	3.92E+15	1.98E+15	2.04E+15	1.93E+14

* A1 = Flax fiber-HDPE biocomposite includes 10% fiber by mass content.
** A2 = Flax fiber-HDPE biocomposite includes 20% fiber by mass content.
*** A3 = Flax fiber-HDPE biocomposite includes 30% fiber by mass content.

To solve equation 4.14, Newton's method which is an efficient algorithm for finding approximations to the zeros (or roots) of a real-valued function is used. Equation 4.14 is written as $f(P_1) = (1+b)P_1 - bP_0 - a(P_0 - P_1)^{\frac{2}{n}}$. The Mathcad (MathSoft, Inc. Needham, MA) Program is written to apply Newton's method to solve the equation. Assume P_0 (P) is 5 MPa, X0 is P_1, then the program to solve the value of P_1- NM(X0) for HDPE material at temperature of 170°C is given as following:

$P := 5$

$b := 0.5182$

$a := 1.4627 \cdot 10^{-17}$

$n := 0.6707$

$\frac{2}{n} = 2.982$

$1 + b = 1.518$

$5 \cdot b = 2.591$

$3.982 \cdot a = 0$

$X0 := 4.5$

$F(X0) := 1.5182X0 - 2.591 - 1.4627 \cdot 10^{-17} \cdot (5 - X0)^{2.982}$

$G(X0) := 1.5182 + 5.8244 \cdot 10^{-17} \cdot (5 - X0)^{1.982}$

$\varepsilon \leftarrow 0.00001$

$NM(X0) :=$ | $X1 \leftarrow X0 - G(X0)^{-1} \cdot F(X0)$
| while $|X1 - X0| \leq 0.00000001$
| | $X1 \leftarrow X0 - G(X0)^{-1} \cdot F(X0)$
| | $X0 \leftarrow X1$
| $X1$

$NM(X0) = 1.707$

It takes only one step to solve the equation in Newton's method. This is because *a* value is much smaller than *b* value. It means that $a(P_0 - P_1)^{\frac{2}{n}}$ in equation 4.14 does not influence the output and can be ignored. Because biocompsite A1, A2 and A3 all have smaller *a* value than HDPE, it is concluded that a one step solution can be used to solve the equations for all samples. So equation 4.14 becomes:

$$P_1 - b(P_0 - P_1) = 0 \tag{4.15}$$

APPENDIX I

Development of linear regression model for specific heat (C_p) of biocomposites

Table I.1 Variables entered/removed(a) in SPSS stepwise linear regression.

Model	Variables Entered	Variables Removed	Method
1	Fiber content	Temperature *F2, T2, FT, F3, T3*	Stepwise (Criteria: Probability-of-F-to-enter <= .050, Probability-of-F-to-remove >= .100).
2*	Temperature	*F2, T2, FT, F3, T3*	Stepwise (Criteria: Probability-of-F-to-enter <= .050, Probability-of-F-to-remove >= .100).

(a) Dependent Variable: $C_{p.}$

F2 = (Fiber content)^2; *F3* = (Fiber content)^3;

T2 = (Temperature)^2; *T3* = (Temperature)^3;

FT = Fiber content × Temperature.

*Model 2 is euqaiton 4.26.

Table I.2 ANOVA table of SPSS linear regression for biocomposite specific heat.

Model		Sum of Squares	df	Mean Square	R Square	F Value	Sig.(P)
1	Regression	0.310	1	0.310	0.818	134.430	<0.001 (a)
	Residual	0.069	30	0.002			
	Total	0.379	31				
2*	Regression	0.329	2	0.165	0.869	95.891	<0.001 (b)
	Residual	0.050	29	0.002			
	Total	0.379	31				

Dependent Variable: $C_{p.}$

(a) Predictors: (Constant), Fiber content.

(b) Predictors: (Constant), Fiber content, Temperature.

*Model 2 is euqaiton 4.26.

Table I.3 Coefficient estimates of linear regression models developed by SPSS stepwise method.

Model		Estimated Coefficient	Standard Error	T Value	Sig.(P)
1	(Constant)	2.524	0.014	177.746	<0.001
	Fiber content	-0.009	0.001	-11.594	<0.001
2	(Constant)	2.117	0.122	17.381	<0.001
	Fiber content	-0.009	0.001	-13.435	<0.001
	Temperature	0.002	0.001	3.359	0.002

Dependent Variable: $C_{p.}$

*Model 2 is euqaiton 4.26.

APPENDIX J

Development of linear regression model for thermal diffusivity (α) of biocomposites

Table J.1 Variables entered/removed(a) in stepwise linear regression

Model	Variables Entered	Variables Removed	Method
1	Fiber content	Temperature *F2, T2, FT, F3, T3*	Stepwise (Criteria: Probability-of-F-to-enter <= .050, Probability-of-F-to-remove >= .100).
2*	Temperature	*F2, T2, FT, F3, T3*	Stepwise (Criteria: Probability-of-F-to-enter <= .050, Probability-of-F-to-remove >= .100).

(a) Dependent Variable: Thermal diffusivity.

F2 = (Fiber content)^2; *F3* = (Fiber content)^3;

T2 = (Temperature)^2; *T3* = (Temperature)^3;

FT = Fiber content × Temperature.

*Model 2 is euqaiton 4.28.

Table J.2 ANOVA table of SPSS linear regression for composite thermal diffusivity.

Model		Sum of Squares	df	Mean Square	R Square	F Value	Sig.(P)
1	Regression	3.00E-15	1	2.99E-15	0.969	410.819	<0.001 (a)
	Residual	9.46E-17	13	7.28E-18			
	Total	3.08E-15	14				
2*	Regression	3.02E-15	2	1.51E-15	0.980	293.065	<0.001 (b)
	Residual	6.19E-17	12	5.16E-18			
	Total	3.08E-15	14				

Dependent Variable: Thermal diffusivity.

(a) Predictors: (Constant), Fiber content.

(b) Predictors: (Constant), Fiber content, *F3*

*Model 2 is euqaiton 4.28.

Table J.3 Coefficients of linear regression models developed by SPSS stepwise method

Model		Estimated Coefficient	Standard Error	T Value	Sig.(P)
1	(Constant)	1.80E-07	1.14E-09	158.113	<0.001
	Fiber content	-1.30E-09	6.43E-11	-20.269	<0.001
2*	(Constant)	2.06E-07	1.02E-08	20.147	<0.001
	Fiber content	-1.32E-09	5.46E-11	-24.197	<0.001
	F3	-1.38E-10	5.46E-11	-2.519	0.027

Dependent Variable: Thermal diffusivity.

*Model 2 is euqaiton 4.28.